OSTEOPOROSIS AND THE ROLE OF MUSCLE

EDITED BY: Gordon L. Klein, Marco P. Brotto, Marco Invernizzi and Alex Ireland

PUBLISHED IN: Frontiers in Endocrinology

frontiers Research Topics

ISSN 1664-8714
ISBN 978-2-88976-616-1
DOI 10.3389/978-2-88976-616-1

About Frontiers

Frontiers is more than just an open-access publisher of scholarly articles: it is a pioneering approach to the world of academia, radically improving the way scholarly research is managed. The grand vision of Frontiers is a world where all people have an equal opportunity to seek, share and generate knowledge. Frontiers provides immediate and permanent online open access to all its publications, but this alone is not enough to realize our grand goals.

Frontiers Journal Series

The Frontiers Journal Series is a multi-tier and interdisciplinary set of open-access, online journals, promising a paradigm shift from the current review, selection and dissemination processes in academic publishing. All Frontiers journals are driven by researchers for researchers; therefore, they constitute a service to the scholarly community. At the same time, the Frontiers Journal Series operates on a revolutionary invention, the tiered publishing system, initially addressing specific communities of scholars, and gradually climbing up to broader public understanding, thus serving the interests of the lay society, too.

Dedication to Quality

Each Frontiers article is a landmark of the highest quality, thanks to genuinely collaborative interactions between authors and review editors, who include some of the world's best academicians. Research must be certified by peers before entering a stream of knowledge that may eventually reach the public - and shape society; therefore, Frontiers only applies the most rigorous and unbiased reviews.
Frontiers revolutionizes research publishing by freely delivering the most outstanding research, evaluated with no bias from both the academic and social point of view. By applying the most advanced information technologies, Frontiers is catapulting scholarly publishing into a new generation.

What are Frontiers Research Topics?

Frontiers Research Topics are very popular trademarks of the Frontiers Journals Series: they are collections of at least ten articles, all centered on a particular subject. With their unique mix of varied contributions from Original Research to Review Articles, Frontiers Research Topics unify the most influential researchers, the latest key findings and historical advances in a hot research area! Find out more on how to host your own Frontiers Research Topic or contribute to one as an author by contacting the Frontiers Editorial Office: frontiersin.org/about/contact

OSTEOPOROSIS AND THE ROLE OF MUSCLE

Topic Editors:
Gordon L. Klein, University of Texas Medical Branch at Galveston, United States
Marco P. Brotto, University of Texas at Arlington, United States
Marco Invernizzi, Department of Health Sciences, University of Eastern Piedmont, Italy
Alex Ireland, Manchester Metropolitan University, United Kingdom

Citation: Klein, G. L., Brotto, M. P., Invernizzi, M., Ireland, A., eds. (2022). Osteoporosis and the Role of Muscle. Lausanne: Frontiers Media SA.
doi: 10.3389/978-2-88976-616-1

Table of Contents

frontiers | Frontiers in Endocrinology

EDITORIAL
published: 27 June 2022
doi: 10.3389/fendo.2022.951298

Editorial: Osteoporosis and the Role of Muscle

Marco Brotto[1], *Marco Invernizzi*[2], *Alex Ireland*[3] *and Gordon L. Klein*[4*]

[1] Director of Bone-Muscle Research Center, University of Texas at Arlington, Arlington, TX, United States, [2] Department of Health Sciences, University of Eastern Piedmont, Novara, Italy, [3] Senior Lecturer, Manchester Metropolitan University, Manchester, United Kingdom, [4] Senior Scientist and Adjunct Professor, Department of Orthopaedic Surgery and Rehabilitation, University of Texas Medical Branch, Galveston, TX, United States

Keywords: osteoporosis, muscle, biomechanics, endocrinology, molecular biology, Cell Biology, nutrition, Pharmacology

Editorial on the Research Topic

Osteoporosis and the Role of Muscle

This Research Topic, Osteoporosis and the Role of Muscle, began as an exploration of the effect bone resorption had on muscle wasting and the contribution of the latter to falls and fragility fractures. As contributions began arriving for this topic, it became clear that the subject had many more aspects than was initially conceived. In fact, papers have approached this topic from the standpoints of creation of a new model to study bone and muscle crosstalk, neurologic illnesses and spinal cord injury as a means to understanding the relationships between bone and muscle, genetics, cell biology, biomechanics and nutrition, along with the original translational concept of the biochemical interactions of bone and muscle.

Biguetti et al. developed a mouse model involving surgical injury to the vastus lateralis muscle and the femur in which to study simultaneous healing of muscle and bone in relation to age, sex, and the 5-lipoxygenase pathway, knockout of which demonstrated less inflammation than in wild type animals.

Lin et al. using a weighted gene co-expression analysis of micro RNAs, messenger RNAs and genes that are osteoporosis related to identify a potential micro- and messenger RNA regulatory network. While this study did not specifically mention muscle, if these same bioinformatics techniques were to be used to develop a micro and messenger RNA regulatory network of gene expression in muscle, it might be possible to draw an intriguing comparison of regulatory networks for gene expression in bone and muscle and their relative actions in osteoporosis, as well as other related conditions.

In a slightly different approach to muscle-bone interaction studies, Zhang et al. examined the effect of vitamin D supplementation on hand grip strength in a review and meta-analysis of 13 randomized controlled studies in post-menopausal women. The outcome demonstrated an improvement in handgrip strength, though not in timed Up and Go studies, raising the possibility that vitamin D supplementation may selectively improve only certain muscle function in the elderly.

Studies in biomechanical influences of muscle on bone were reported by Luscher et al. in trained long-distance runners compared to untrained controls using serial peripheral quantitative computed tomography. While the runners had greater bone strength and stiffness in the tibia, they also had lower lateral bending stiffness in the fibula. The authors suggest that this adaptation could improve energy storage during locomotion, implying a novel biomechanical role of the

OPEN ACCESS

Edited and reviewed by:
Jonathan H. Tobias,
University of Bristol, United Kingdom

****Correspondence:***
Gordon L. Klein
gordonklein@ymail.com

Specialty section:
This article was submitted to Bone Research, a section of the journal Frontiers in Endocrinology

Received: *23 May 2022*
Accepted: *30 May 2022*
Published: *27 June 2022*

Citation:
Brotto M, Invernizzi M, Ireland A and Klein GL (2022) Editorial: Osteoporosis and the Role of Muscle. Front. Endocrinol. 13:951298. doi: 10.3389/fendo.2022.951298

skeleton beyond transmitting force and resisting fracture. Nutrition was also examined in high-performing athletes as Heikura et al. demonstrated that a ketogenic diet in elite race walkers impairs biomarkers of bone formation while increasing markers of bone resorption, potentially leading to a low-formation, high-resorption state following exercise, making the case for further study of the biochemical effects of a high fat, low carbohydrate diet on the musculoskeletal system of elite athletes.

Two articles examining cell biologic aspects of muscle and bone metabolism included one by Xu et al. that finds that hypoxia-inducible factor-1 alpha (HIF-1α) in MC3T3 osteoblast-like cells exposed to dexamethasone triggers a pathway *via* pyruvate dehydrogenase kinase-1 (PDK-1) that will phosphorylate the AKT/mTOR anabolic pathway. This pathway is suppressed by dexamethasone exposure. It would not be surprising if this same pathway is active in skeletal muscle as well as glucocorticoid exposure is known to produce oxidative stress in both bone and muscle and result in up-regulation of the FOXO genes that that impair osteoblastogenesis and muscle protein synthesis (1, 2).

A review by Chen et al. examines the role of N^6 methyladenosine (m^6A) in the form of m^6A methyltransferase $METTL_3$, which is involved in the osteogenic versus adipogenic fate of marrow stem cells. Knockdown of $METTL_3$ suppresses expression of runx2 and osterix, which are critical steps in osteoblastogenesis and can also reduce expression of VEGF. M^6A in muscle myoblasts controls their transition to other muscle cell states (3, 4). This is an epigenetic factor that exists in both bone and skeletal muscle and the coordination of actions in both tissues is worth further study.

In manuscripts covering the spinal cord and central nervous system, Iolascon et al. discuss the current treatments available for neuromuscular disease and makes us appreciate the complexity of interactions among muscle, bone, and nerves. It is clear that we have much to learn before we can propose a truly integrated model of muscle, bone and nerve, in the regulation of muscle and bone mass and function. Invernizzi et al. in the meantime review the available treatments for the joint loss of bone and muscle in spinal cord injury. While this review is state of the art, it also leaves us with the need to investigate more thoroughly the relationship between muscle and bone loss in neurologic conditions.

Finally, we return to the original idea in the role of muscle in osteoporosis. That is, that the bone on resorption liberates transforming growth factor beta (TGF-β), as shown by Pin et al. in pediatric burns and by Essex et al. in cisplatin-treated mice. The use of anti-resorptives, pamidronate in the case of pediatric burns and zoledronic acid in the case of cancer-treated mice, protected the bone and muscle mass in each case, demonstrating that is a factor released by bone that contributes to, if not being wholly responsible for, muscle wasting in these conditions. In the case of myoblast studies of Pin et al. the TGF-β released from bone suppressed the phosphorylation of the anabolic AKT/mTor pathway and increased expression of ubiquitin of the catabolic ubiquitin ligase pathway. These findings explain the original report of the characterization of muscle protein preservation with use of bisphosphonates in pediatric burns (5)

This entire collection of articles provides for the first time a focus on a variety of different aspects of muscle and bone interaction in a variety of conditions and with more study of this emerging area we hope that more definitive treatments can be identified that can alter the mechanisms that lead to bone loss and consequent muscle wasting.

AUTHOR CONTRIBUTIONS

All authors listed have made a substantial, direct, and intellectual contribution to the work and approved it for publication.

REFERENCES

1. Almeida M, Han L, Ambrogini E, Weinstein RS, Manolagas SC. Glucocorticoids and Tumor Necrosis Factor α Increase Oxidative Stress and Suppress Wnt Protein Signaling in Osteoblasts. *J Biol Chem* (2011) 286 (52):44326–35. doi: 10.1074/jbc.M111.283481
2. Furukawa K, Kikusato M, Kamizono T, Toyomizu M. Time Course Changes in Muscle Protein Degradation in Heat-Stressed Chickens: Possible Involvement of Corticosterone and Mitochondrial Reactive Oxygen Species Generation in Induction of the Ubiquitin-Proteasome System. *Gen Comp Endocrinol* (2016) 228:105–10. doi: 10.1016/j.ygcen.2016.02.007
3. Gheller BJ, Blum JE, Fong EHH, Malysheva OV, Cosgrove BD, Thalacker-Mercer AE. A Defined N6 Methyladenosine (M^6a) Profile Conferred by METTL3 Regulates Muscle Stem Cell/Myoblast State Transitions. *Cell Death Discov* (2020) 6(1):95. doi: 10.1038/s41420-020-00328-5
4. Zhao T, Zhao R, Yi X, Cai R, Pan W. METTL3 Promotes Proliferation and Myogenic Differentiation Through M^6a RNA Methylation/YTHDF1/2 Signaling Axis in Myoblasts. *Life Sci* (2022) 298:120496. doi: 10.1016/j.lfs.2022.120496
5. Borsheim E, Herndon DN, Hawkins HK, Suman OE, Cotter M, Klein GL. Pamidronate Attenuates Muscle Loss After Pediatric Burn Injury. *J Bone Miner Res* (2014) 29:1369–72. doi: 10.1002/jbmr.2162

Conflict of Interest: The authors declare that the research was conducted in the absence of any commercial or financial relationships that could be construed as a potential conflict of interest.

frontiers in Endocrinology

ORIGINAL RESEARCH
published: 07 August 2019
doi: 10.3389/fendo.2019.00543

Molecular Mechanisms Responsible for the Rescue Effects of Pamidronate on Muscle Atrophy in Pediatric Burn Patients

Fabrizio Pin[1,2], *Andrea Bonetto*[1,2,3,4,5], *Lynda F. Bonewald*[1,2,6] *and Gordon L. Klein*[7]*

[1] Department of Anatomy and Cell Biology, Indiana University School of Medicine, Indianapolis, IN, United States, [2] Indiana Center for Musculoskeletal Health, Indiana University School of Medicine, Indianapolis, IN, United States, [3] Department of Surgery, Indiana University School of Medicine, Indianapolis, IN, United States, [4] Simon Cancer Center, Indiana University School of Medicine, Indianapolis, IN, United States, [5] Department of Otolaryngology—Head and Neck Surgery, Indiana University School of Medicine, Indianapolis, IN, United States, [6] Department of Orthopaedic Surgery, Indiana University School of Medicine, Indianapolis, IN, United States, [7] Department of Orthopaedic Surgery, University of Texas Medical Branch, Galveston, TX, United States

OPEN ACCESS

Edited by:
Giacomina Brunetti, University of Bari Aldo Moro, Italy

Reviewed by:
Shuichi Sato, University of Louisiana at Lafayette, United States
Jawed Akhtar Siddiqui, University of Nebraska Medical Center, United States

***Correspondence:**
Gordon L. Klein
gordonklein@ymail.com

Specialty section:
This article was submitted to Bone Research, a section of the journal Frontiers in Endocrinology

Received: *25 April 2019*
Accepted: *19 July 2019*
Published: *07 August 2019*

Citation:
Pin F, Bonetto A, Bonewald LF and Klein GL (2019) Molecular Mechanisms Responsible for the Rescue Effects of Pamidronate on Muscle Atrophy in Pediatric Burn Patients. Front. Endocrinol. 10:543. doi: 10.3389/fendo.2019.00543

Not only has pamidronate been shown to prevent inflammation associated bone resorption following burn injury, it also reduces protein breakdown in muscle. The aim of this study was to identify the molecular mechanisms responsible for muscle mass rescue in pamidronate treated compared to placebo/standard of care-treated burn patients. Mature myotubes, generated by differentiating murine C2C12 myoblasts, were exposed for 48 h to 1 or 5% serum obtained from 3 groups of children: normal unburned, burned receiving standard of care, and burned receiving standard of care with pamidronate. Exposure to serum from burned patients caused dose-dependent myotube atrophy compared to normal serum as expected based on previous observations of muscle atrophy induced by burn injury in humans and animals. The size of C2C12 myotubes was partially protected upon exposure to the serum from patients treated with pamidronate correlating with the rescue of muscle size previously observed in these patients. At the molecular signaling level, serum from both pamidronate and non-pamidronate-treated burn patients increased pSTAT3/STAT3 and pERK1/2/ERK1/2 compared to normal serum with no significant differences between the two groups of burn patients indicating elevated production of inflammatory cytokines. However, serum from pamidronate-treated patients restored the phosphorylation of AKT and mTOR and reduced protein ubiquitination when compared to burn serum alone, suggesting a prevention of muscle catabolism and a restoration of muscle anabolism. Myotube atrophy induced by burn serum was partially rescued after exposure to a pan anti-TGFβ-1/2/3 antibody, suggesting that this signaling pathway is partially responsible for the atrophy and that bisphosphonate protection of bones from resorption during burn injury prevents the release of muscle pro-catabolic factors such as TGFβ into the circulation.

Keywords: burn, muscle wasting, pamidronate, TGFβ, muscle catabolic factors

INTRODUCTION

Unintentional burn injury in the pediatric population is one of the common causes of mortality and morbidity, representing the fourth cause of death in the United States according to the World Health Organization (1). The total cost of unintentional pediatric burn injuries was estimated at 2.1 billion dollars (2).

Burn injury, in addition to damaging the site of burn, can produce a systemic response, especially when the injured skin surface covers >20% of the total body surface area (3). The extensive thermal injury is accompanied by acute catabolism resulting in lean mass and muscle wasting, negative nitrogen balance, and bone resorption. Other important long-term risks can be growth delay and increased risk of fracture (4, 5).

Among the underlying adaptive responses to burn injury that contribute to this catabolic response are the systemic inflammatory response resulting in increased inflammatory cytokine production, such as interleukin (IL)-1 and IL-6 and the acute stress response, resulting in the increased production of endogenous glucocorticoids (4, 6). Muscle wasting results in a negative muscle protein balance, reduction of muscle mass followed by a functional deficit. This event begins acutely but is sustained over the first year post-burn and can impair rehabilitation compromising the recovery (7). During the acute phase post-burn, the balance between protein synthesis and degradation is impaired, leading to skeletal muscle atrophy (8). This alteration seems to be predominantly mediated by the hyperactivation of the ATP-ubiquitin-proteasome system through the inflammatory response (9). Bone resorption begins on the first day post-burn (10) and continues over the first 2 weeks resulting in a loss of up to 7% lumbar spine bone mineral content and density by 3 weeks post-burn (11). Up to 3% of total body bone mineral content is lost by 6 months post-burn (11). The incidence of post-burn fractures is elevated in children and estimated at 15% (12).

In a previous publication, Klein et al. (11) found that a single administration of the nitrogen-containing bisphosphonate pamidronate within 10 days of the burn injury eliminated resorptive bone loss and preserved bone density in a randomized, double- blinded, placebo-controlled study of severely burned children. Bisphosphonates are anti-resorptive agents which accumulate in bone matrix, and on resorption, are taken up directly by osteoclasts. They inhibit the enzyme farnesyl pyrophosphate synthase (FPS), directly interfering in cholesterol biosynthesis and impairing cell membrane integrity and signal transduction. The result is osteoclast apoptosis and inhibition of bone resorption (13). Przkora et al. (14) found that this rescue effect lasted at least 2 years. In addition, Borsheim et al. (15) described a decrease in muscle protein breakdown, an increase in lower extremity muscle fiber diameter and muscle strength, and a net positive muscle protein balance in burned children who received the single dose of pamidronate compared to a placebo. While the preservation of bone mass was expected due to the affinity of bisphosphonate for bone, the effect of bisphosphonate on muscle protein balance was unanticipated. Therefore, we undertook a study to investigate possible mechanisms by which bisphosphonates may have effected these changes in muscle. A candidate mechanism for investigation is the transforming growth factor (TGF)β production, which has been shown to be elevated in the serum of burned patients (16) and burned animals (17, 18), associated with both hypertrophic scarring (16) and immunosuppression (17, 18). Furthermore, Waning et al. (19) have demonstrated that TGFβ released following bony metastases in breast cancer affects the ryanodine receptor in muscle, causing a calcium leak and cachexia. This effect was inhibited by treatment with bisphosphonates.

MATERIALS AND METHODS

Cell Culture

Murine C2C12 skeletal myoblasts (ATCC, Manassas VA) were grown as described previously (15) in high-glucose DMEM supplemented by 10% FBS, 100 U/ml penicillin, 100 μg/ml streptomycin, 100 μg/ml sodium pyruvate, 2 mmol L-glutamine, and maintained at 37°C in 5% CO_2 in air. Differentiation of myotubes was induced by switching subsonfluent myoblasts to differentiation medium DMEM supplemented by 2% horse serum. The differentiation medium was replaced every other day for up to 5 days. Fully differentiated C2C12 myotubes were exposed for 48 h to 1 or 5% serum from patients enrolled in a randomized controlled trial of pamidronate. In order to determine the effect of transforming growth factor (TGF)-β pan neutralizing antibody on fiber size myotubes were exposed for 48 h to 10 μg/ml of anti-TGFβ-1/2/3, clone 1D11.16.8 (BioXcell West, Lebanon NH) in the presence or absence of burned patients' serum.

Patients

Three different types of serum were used in the study: that from normal, unburned children (N) ($n = 5$), severely burned children given placebo in the randomized trial (B), $n = 5$, and those given a single dose of pamidronate within 10 days of the burn injury (B+P), $n = 5$. Serum samples were de-identified, meaning that there was no way for the investigators to know or to trace any of the samples to their patient source. Additionally, these samples had been frozen at −80°C since the original study was concluded in 2002.The study was carried out in accordance with the recommendations of approved Protocol 92-304G of the University of Texas Medical Branch Institutional Review Board. All samples were obtained during routine care. Consequently, the Institutional Review Board waived the requirement for written informed consent for the usage of the de-identified samples for research purposes. Written informed consent was obtained from all patients as appropriate and all parents of study participants at the time of enrolling in the approved research protocol. Enrolled subjects were burned ≥40% total body surface area, were predominantly males between the ages of 5 and 18 year, and had normal renal function (11, 13). Serum was obtained from these patients at 4 and 6.5–7 week post-burn. All burned patients had excessive urinary cortisol excretion, up to 8 times the upper limits of pediatric normal values (4, 6) as a consequence of the post-burn stress response.

Assessment of Myotube Size

Cell layers were fixed in ice-cold acetone-methanol (50:50) and incubated with an anti-Myosin Heavy Chain antibody (MF20, 1:200, Developmental Studies Hybridoma Bank, Iowa City IA) and an AlexaFluor 488-labeled secondary antibody (Invitrogen, Grand Island NY) as described previously (20). Analysis of myotube size was performed by measuring the average diameter of long, multinucleate fibers (N = 250–350 per condition) avoiding regions of clustered nuclei on a calibrated tissue image using the Image J 1.43 software (21).

Western Blotting

Western blots were essentially performed as described previously (20). Total protein extracts were obtained by lysing cell layers in RIPA buffer (150 mMol NaCl, 1.0% NP-40, 0.5% sodium deoxycholate, 0.1% SDS, and 50 mM Tris, pH 8.0) completed with protease (Roche, Indianapolis IN) and phosphatase (Thermo Scientific, Rockford IL) inhibitor cocktails. Cell debris were removed by centrifugation (15 min 14,000 g) and the supernatant collected and stored at −80°C. Protein concentration was determined using the BCA protein assay method (Thermo Scientific, Rockford IL). Protein extracts (30 μg) then underwent electrophoresis in 4–15% gradient SDS Criterion TGX precast gels (Bio Rad, Hercules CA). Proteins were transferred to nitrocellulose membranes (Bio Rad, Hercules CA). Membranes were blocked with SEA BLOCK blocking reagent (Thermo Scientific, Rockford IL) at room temperature for 1 h, followed by an overnight incubation with SEA BLOCK buffer containing 0.2% Tween-20 at 4°C with gentle shaking. After washing with PBS containing 0.2% Tween-20 (PBST), the membrane was incubated at room temperature for 1 h with either Anti-rabbit IgG (H+L) DyLight 800 or Anti-mouse IgG (H+L) DyLight 600 (Cell Signaling Technologies, Danvers MA). Blots were then visualized with Odyssey Infrared Imaging System (LI-COR Biosciences, Lincoln NE). Optical density measurements were taken using the Gel-Pro analyzer software. Antibodies used were pSTAT3-Y705 (#9145), STAT3 (#8768), pAKT-S473 (#4060), AKT (#9272). pERK1/2 (p-p44/42MAPK, T202/Y204, #4370), ERK1/2(p44/42MAPK, #4695), p-mTOR-S2448(#D9C2), mTOR (#7C10), Ubiquitin (#3933), pSmad2-S465/467/Smad3-S423-425 (#27F4), and Smad2/Smad3 (#D7G7) from Cell Signaling Technologies, Danvers MA, LC3B (#L7543) from Sigma-Aldrich, and α-Tubulin (# 12G10) from Developmental Studies Hybridoma Bank (Iowa City IA).

Statistical Analysis

Results are presented as means ± SD. Significance of the differences was determined by two-way analysis of variance (ANOVA) followed by Tukey's post-test. Differences were considered significant when $p < 0.05$.

RESULTS

Effects of Serum From Burned Patients Receiving Either Standard of Care (B) or Standard of Care Plus Pamidronate (B+P) vs. Serum From Normal Unburned Patients (N) on C2C12 Myotubes

In order to assess the effects of the serum derived from severely burned children on myotube morphology, fully differentiated C2C12 myotubes were exposed to 1% (**Figure 1A**) or 5% (**Figure 1B**) of N, B, or B+P serum. Exposure to B serum caused dose-dependent myotube atrophy compared to N serum (−13%, $p < 0.01$ and −40%, $p < 0.01$, respectively), reproducing the effects of burn injury on muscle atrophy as observed in humans and animals (22, 23). Interestingly, when C2C12 myotubes were exposed to B+P serum, the degree of fiber atrophy was significantly reduced compared to myotubes exposed to B serum (+15%, $p < 0.05$, **Figure 1**). These experiments were repeated two times.

Serum Derived From Burned Patients, B and B+P, Induced Pro-atrophic Signaling in the C2C12 Myotubes

In order to investigate whether the myotube phenotype observed following B or B+P serum exposure was also associated with the modulation of pro-atrophic signaling pathways, the level of proteins associated with protein catabolism was assessed. Interestingly, modulation of several mediators of muscle atrophy were observed using Western blotting analysis performed on whole C2C12 protein extracts. In particular, the activation of the STAT3 signaling pathway (**Figure 2A**) along with the increase in the pERK1/2/ERK1/2 signaling ratio (+91% B vs. N, +140% B vs. N, $p < 0.001$), both STAT3 and ERK differed from normal by $p < 0.001$ in the myotubes exposed to B and B+P serum (**Figure 2B**). Interestingly, a non-significant increase of ubiquitin-labeled peptides characteristic of muscle atrophy in the atrophic myotubes exposed to B serum was significantly less in the myotubes treated with B+P serum (−58% vs. B, $p < 0.05$, **Figure 2C**). This suggests that the partial rescue of myotube size may result from reduced protein catabolism. To investigate the autophagosome-lysosome system, another pathway previously described as being involved in muscle atrophy, the presence of autophagosome accumulation as a marker of autophagy activation was examined. As shown by the ratio of LC3BII/LC3BI protein, no differences in autophagosome accumulation were observed among all three sera (**Figure 2D**). To assess whether the serum derived from burned patients was also able to induce mitochondrial alterations, we analyzed the expression of proteins related to the control of mitrochondrial homeostasis. The expression of proteins related to mitochondrial biogenesis (PGC 1 α and Cytochrome C) or mitochondrial fusion (OPA1) were unchanged in all experimental conditions (**Figure S1**). These experiments were performed once.

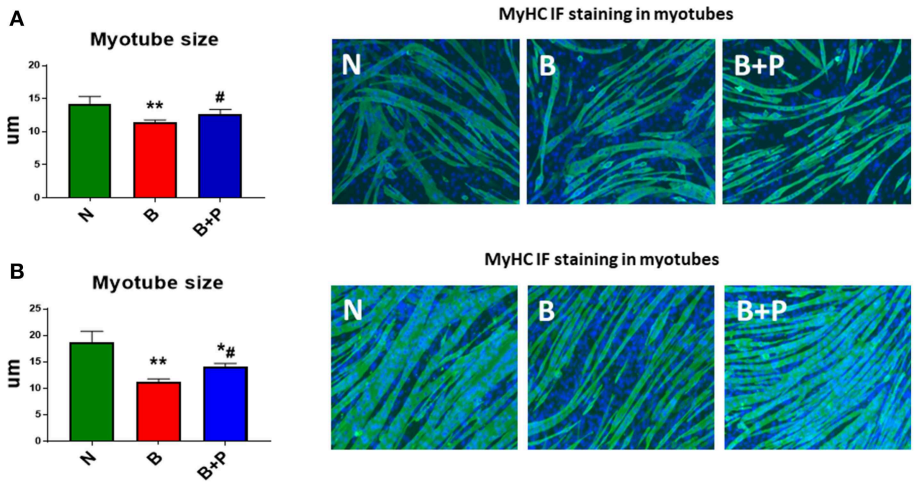

FIGURE 1 | Effects of serum from burned patients receiving standard of care or standard of care and pamidronate on C2C12 myotubes ($N = 5$ per group). Assessment of myofiber size in C2C12 myotube cultures exposed to 1% **(A)** or 5% **(B)** serum for up to 48 h obtained from 3 groups of 5 children: normal unburned (N), burned receiving standard of care after 30 d (B), burned receiving standard of care and pamidronate after 30 d (B+P) ($n = 250$–350 myofibers). Green staining: myosin heavy chain (MyHC). Data (means ± standard deviation) are expressed in micrometers (μm). Significance of the differences: $^{*}p < 0.05$, $^{**}p < 0.01$ vs. N, and $^{\#}p < 0.01$ vs. B. Significance was determined by two-way analysis of variance (ANOVA) followed by Tukey's post-test.

Serum From Burned Patients Receiving Pamidronate Normalized Anabolic Signaling Compared to Serum From Burned Patients

In order to investigate whether B or B+P serum affect protein anabolism in the C2C12 myotubes, the expression of two important markers of anabolism, AKT and mTOR, was quantitated. Myotube atrophy induced by B serum was associated with reduced phosphorylation of AKT (−34% vs. N, $p < 0.05$) and its downstream target mTOR (−51% vs. N, $p < 0.01$), suggesting that muscle anabolism was downregulated through this mechanism (**Figure 3**). B+P serum was able to restore the phosphorylation of AKT (+46% vs. B, $p < 0.05$) and mTOR (+83% vs. B, $p < 0.05$), thus suggesting that protein anabolism was partially restored in this condition. This experiment was performed once.

TGFβ Is Responsible for the Effects of Burn Serum on Myotube Size and Pamidronate Rescues Myotube Size Through a Reduction of TGFβ

Because TGFβ released from bony metastases due to breast cancer has been implicated in cancer-associated cachexia (19), we chose to evaluate whether TGFβ may be responsible for muscle atrophy following burns. A specific pan-neutralizing antibody, TGFβ-1/2/3 was used. When the myotubes were exposed to B+P serum, their size was significantly larger compared to B serum. Treatment with neutralizing antibody TGFβ-1/2/3 was able to partially protect the myotubes from atrophy when exposed to B serum (+35% vs. B, $p < 0.001$) making the myotube size comparable to those exposed to B+P serum (**Figure 4A**). To verify the molecular signaling pathway was due to TGFβ, Western blot analysis of the level of Smad phosphorylation was performed. The levels of p-Smad 2/3 were reduced in myotubes treated with the anti-TGFβ-1/2/3 antibody and exposed to either B or B+P serum. No significant difference in Smad phosphorylation was observed in myotubes exposed to B or B+P serum with or without the anti-TGFβ-1/2/3 antibody (**Figure 4B**). These data suggest that other activators of this pathway may be involved. This experiment was repeated two times.

DISCUSSION

In this study we used an *in vitro* cell line model to begin to identify directly and indirectly the components of burn serum that are potentially responsible for muscle wasting and to determine the effects of bisphosphonate treatment on their signaling in a model of myotube formation. We found that TGFβ in burn serum is responsible for reduced myotube size and that pamidronate reduces TGFβ activity. Other components of burn serum are inferred via the activation of specific signaling pathways. Highly elevated inflammatory molecules are inferred by the dramatic increase in pSTAT3/STAT3 and pERK1/2/ERK1/2 compared to normal serum. This is also in line with previous experimental evidence reporting that burn injury induces severe muscle wasting and cachexia via a marked increase in pro-inflammatory cytokines (4, 19, 24). Pamidronate treatment appeared to have no effect on factors responsible for these signaling pathways. However, pamidronate did rescue the phosphorylation of AKT and mTOR and reduced protein ubiquitination when compared to burn serum from non-treated patients, suggesting that factors present in

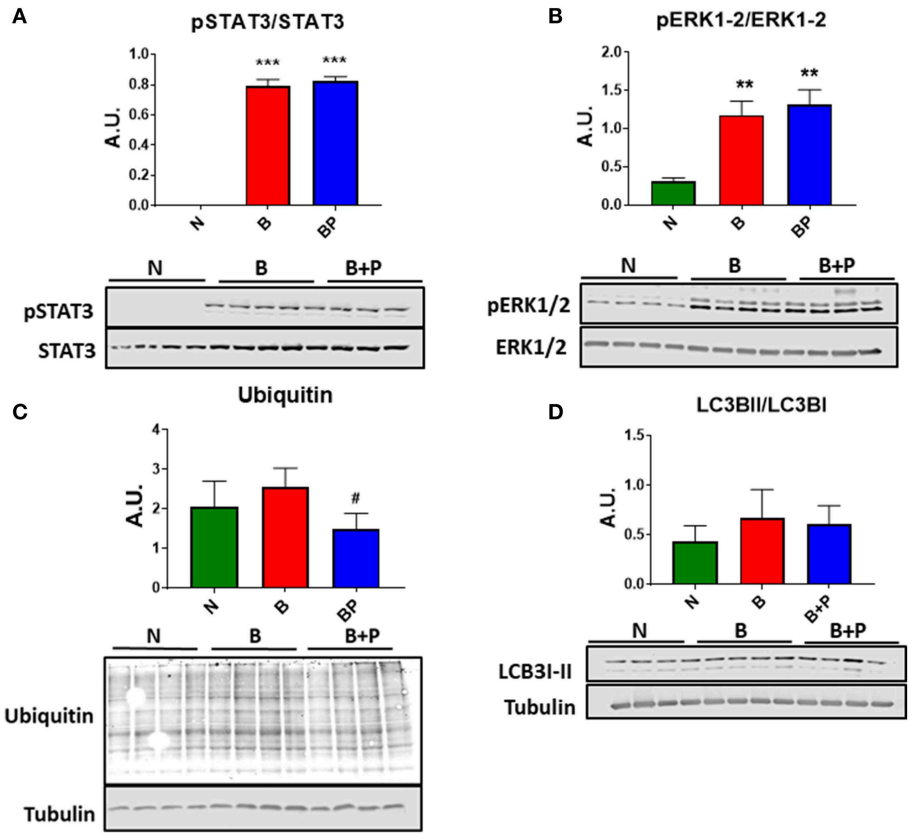

FIGURE 2 | Serum derived from burned patients induced pro-atrophic signaling in the C2C12 myotubes ($N = 4$ per group). Representative Western blotting and quantification of pSTAT3, STAT3 **(A)**, pERK1/2, ERK1/2 **(B)**, Ubiquitin **(C)**, and LC3BII/LC3BI **(D)** in protein extract of C2C12 myotubes exposed for up to 48 h to 5% serum obtained from 3 groups of children: normal unburned (N), burned receiving standard of care after 30 d (B), and burned receiving standard of care and pamidronate after 30 d (B+P). Tubulin was used as a loading control. Data (means ± standard deviation) are expressed as arbitrary units (A.U.). Significance of the differences: $^{**}p < 0.01$, $^{***}p < 0.001$ vs. N, and $^{\#}p < 0.05$ vs. B. Significance was determined by two-way analysis of variance (ANOVA) followed by Tukey's post-test.

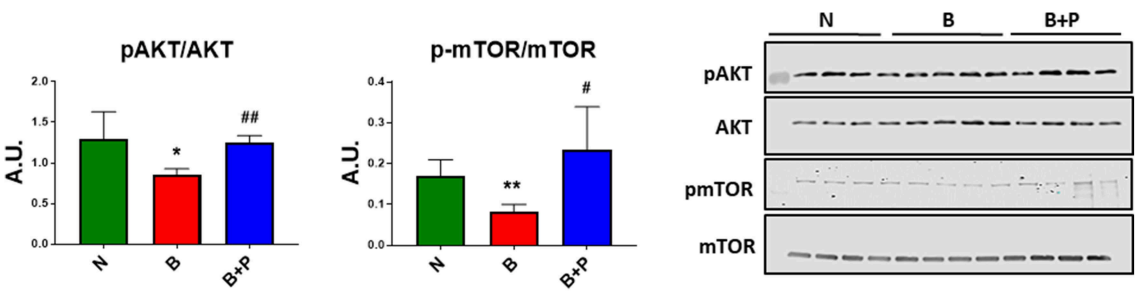

FIGURE 3 | Serum from burn patients receiving pamidronate normalized anabolic signaling compared to serum from burn patients ($N = 4$ per group). Representative Western blotting and quantification of pAKT, AKT, pmTOR, and mTOR in protein extract of murine C2C12 myotubes exposed for up to 48 h to 5% serum obtained from 3 groups of children: normal unburned (N), burned receiving standard of care after 30 d (B), and burned receiving standard of care and pamidronate after 30 d (B+P). Data were normalized to total protein. Data (means ± standard deviation) are expressed as arbitrary units (A.U.). Significance of the differences: $^{*}p < 0.05$, $^{**}p < 0.01$ vs. N and $^{\#}p < 0.05$, $^{\#\#}p < 0.01$ vs. B. Significance was determined by two-way analysis of variance (ANOVA) followed by Tukey's post-test.

burn serum that are responsible for muscle breakdown and catabolism and are prevented from being released by bone due to pamidronate treatment. No effect of pamidronate was observed on the autophagolysosome and mitochondrial gene expression. This *in vitro* study substantiates and extends the initial observations of Borsheim et al. (15) that early use of a bisphosphonate post-burn injury preserves not only bone mass but skeletal muscle mass and strength as well. Moreover, this rescue, initially seen at 4 weeks post-burn, is sustained for at least 6–7 weeks. These data suggest that blocking bone

resorption prevents the release of pro-atrophic factors from the bone.

Serum from burn patients receiving pamidronate normalized anabolic signaling and reduced muscle protein catabolism compared to serum from burn patients not receiving pamidronate. The use of bisphosphonates mitigates the reduction of the AKT/mTOR signaling pathway and blunts the activation of the catabolic ubiquitin-associated pathways. The reactivation of muscle protein synthesis and the down-regulation of muscle protein catabolism contribute to restore a condi of positive muscle protein balance. These data suggest that mitigating bone resorption also reduces the release of factors that can induce muscle protein catabolism and decrease muscle protein anabolism (15).

Extensive burn injury is characterized by a release of pro-inflammatory mediators such as cytokines, glucocorticoids, and reactive oxygen species (24, 25). Altogether, these factors are responsible for local and systemic derangements and can drive the bone and muscle alterations that are frequently observed in burn patients. For example, the strong activation of the STAT3 pathway can result from circulating IL-6 in burn serum, in line with previous observations in an experimental model of burn-induced muscle wasting (24) and in human patients (4). This event, in turn, increases overall catabolism and results in muscle wasting as previously described in models of cancer cachexia (20, 26). Interestingly, exposure of C2C12 myotubes to B+P serum did not prevent the increase in STAT3 phosphorylation. These findings suggest that although pamidronate was able to modulate inflammation in a model of multifocal osteomyelitis (27), overall it did not seem to interfere with the systemic inflammation associated with burn injury.

Muscle atrophy after burn injury is also characterized by the downregulation of anabolic signaling (24). In line with these findings, in the present study we reported a reduction of the AKT and mTOR signaling upon exposure of myotubes to serum from burn patients. Consistent with our results, conditions associated with high inflammatory response showed a negative regulation of protein synthesis through the dysregulation of the mTOR/p70S6K axes (28–31). In particular, the cytokines IL-6 and TNFα were previously shown to be directly involved in the inhibition of AKT/mTOR pathways (30, 31). Pamidronate treatment appears to reduce the effect of cytokines involved in AKT and mTOR signaling

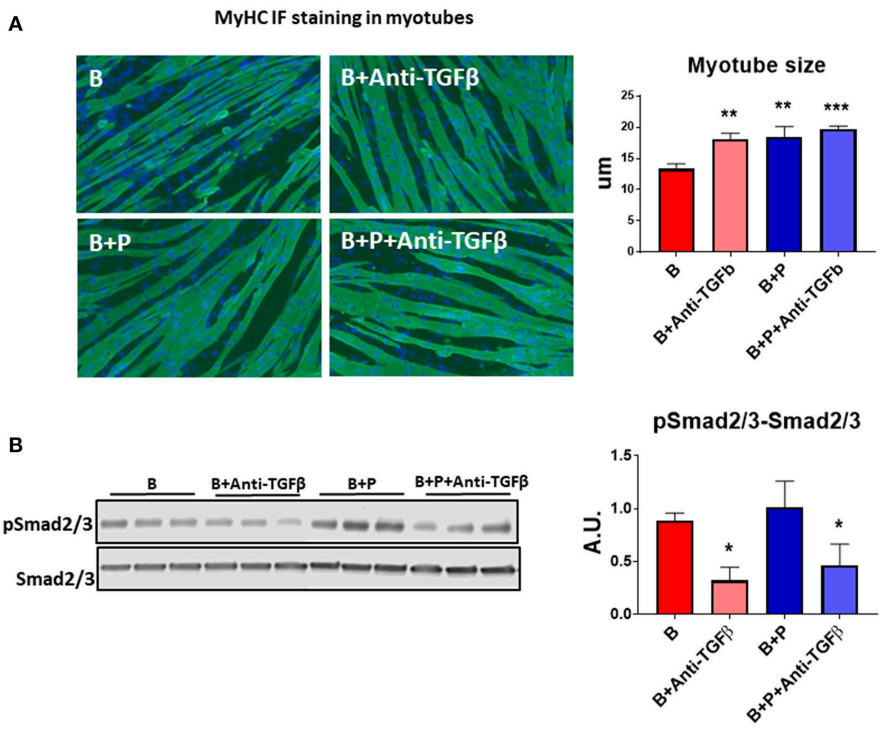

FIGURE 4 | TGFβ is responsible for the effects of burn serum on myotube size ($N = 3$ per group). **(A)** Assessment of myofiber size in C2C12 murine myotube cultures exposed for up to 48 h to 5% serum obtained from 2 groups of children: burned receiving standard of care after 30 d (B), burned receiving standard of care and pamidronate (B+P) after 30 d and co-exposed to a neutralizing antibody, anti-TGFβ-1/2/3. Green staining: myosin heavy chain. Data (means ± standard deviation) are expressed in micrometers (μm). **(B)** Representative Western blotting and quantification of pSMAD 2/3 normalized to total SMAD 2/3 in protein extract of murine C2C12 myotubes exposed for up to 48 h in 5% serum obtained from 2 groups of children: burned receiving standard of care after 30 d (B), and burned receiving standard of care and pamidronate after 30 d (B+P) and co-exposed to a neutralizing antibody anti-TGFβ-1/2/3. Data (means ± standard deviation) are expressed as arbitrary units (A.U.). Significance of the differences: $^{*}p < 0.05$, $^{**}p < 0.01$, and $^{***}p < 0.001$ vs. B. Significance was determined by two-way analysis of variance (ANOVA) followed by Tukey's post-test.

but not STAT3/ERK. We know that pamidronate can reduce inflammatory cytokines and RANKL (32) in bone and thus may reduce not only TGFβ release from bone, but possibly also other muscle catabolic factors. We know also that other mediators belonging to the IL-6 superfamily, including IL-11 and OSM are present in the serum of animals with burn-induced cachexia and can activate the STAT3 signaling system in muscle (24). However, whether pamidronate can modulate these levels remains unknown.

TGFβ blockade of burn serum restored C2C12 myotube size to that of pamidronate treated patients. While no effect was observed using the pan-TGFβ antibody on burn serum from pamidronate treated patients on myotube size, pamidronate treatment partially rescued myotube size compared to burn injury with no pamidronate treatment. The magnitude of the myotube size rescue was similar between the effects of the anti-TGFb antibody and the pamidronate treatment. We interpret these data as consistent with pamidronate prevention of release of TGFβ from bone matrix as shown in a hypothetical diagram in **Figure 5**. Furthermore, we showed that this neutralizing antibody was able to protect the myotubes from undergoing atrophy in the presence of B serum mainly by downregulating the Smad-dependent signaling. However, we could not show a direct connection between the magnitude of Smad signaling and the magnitude of inhibition of myotube formation. Despite the anti-TGFβ-downregulation of Smad phosphorylation, Smad phosphorylation remaining elevated with the pamidronate treated burn serum. A possible explanation for this is that there was still sufficient TGFβ remaining in burned serum to stimulate Smad phosphorylation. Furthermore, we could speculate that other substances present in burn serum, such as myostatin/GDF8 (33) might maintain phosphorylation of Smad. However, we did not measure myostatin in our serum samples. The improvement of myotube size could also be the result of modulation of the AKT/mTOR pathway. Indeed, the myostatin/TGFβ signaling pathway was shown to inhibit the anabolic AKT signaling by means of Smad 2/3 activation, as reviewed by Egerman and Glass (3, 34). Ours is not the first evidence suggesting that blockade of the TGFβ/Smad 2/3 pathways preserves the muscle phenotype in conditions normally associated with muscle wasting. Indeed, administration of ACVR2B/Fc, a synthetic decoy peptide and inhibitor of the signaling downstream of the binding of TGFβ family ligands to the activin receptor type 2B was able to potently preserve muscle mass and prolong survival in a model of cancer cachexia (35). Similarly, we have recently shown that the same inhibitor was able to completely prevent the loss of bone and muscle mass in animals chronically exposed to the chemotherapy regimen Folfiri (36).

Altogether, our results suggest that the anti-resorptive properties of pamidronate prevent the release from the bone of TGFβ-1/2/3 (13) and that the latter may be a catabolic factor that promotes myotube atrophy, thus validating a putative role of TGFβ in promoting muscle atrophy during burn injury. It is unclear whether there are additional muscle catabolic factors within the bone matrix, but the fact that TGFβ is elevated following burns (16–18) and that it has been shown to modulate muscle cachexia in breast cancer patients (19) would suggest that it may at least be one candidate muscle catabolic factor that is liberated from bone following burn injury. The presence of a putative TGFβ mechanism in two such disparate groups of patients as metastatic breast cancer and pediatric burns raises the possibility that this mechanism could be active in a wider range of resorptive bone diseases or may contribute to a cycle of muscle wasting and resorptive bone loss in neuromuscular diseases. The potential role of bisphosphonates or other anti-resorptives should be studied in these situations.

Shortcomings of the Study

Our interpretation of the data has to be tempered by the variable sample size. Studies were conducted depending on the amount of sample required for each experiment and the remaining sample volume available. However, randomization of the original study should have controlled for potential imbalances between the burn

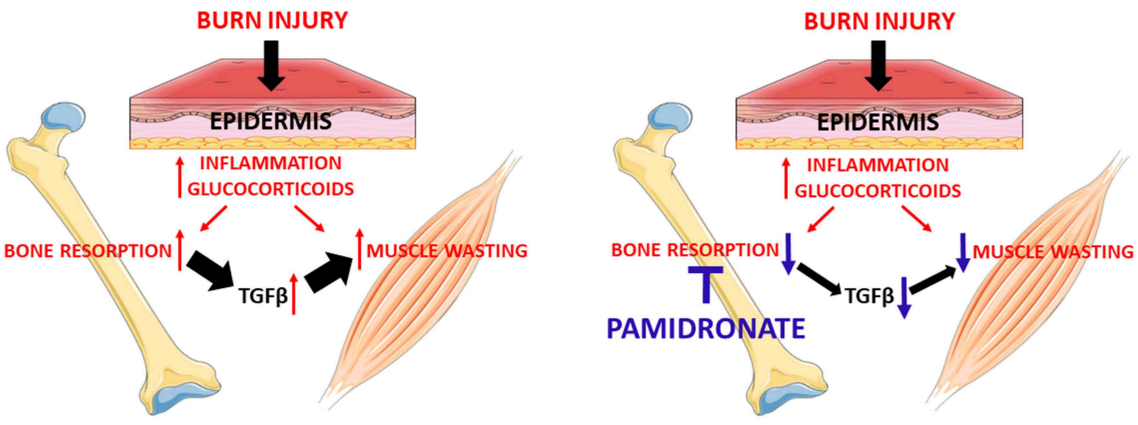

FIGURE 5 | Administration of pamidronate after burn injury through preventing bone resorption hypothetically reduces the release of the TGFβ family members from the bone. The reduction of TGFβ family members seems to be responsible for the partial rescue of myotube atrophy. This signaling appears to be due to the reactivation of the anabolic AKT/mTOR pathway and the reduction of the catabolic ubiquitin-dependent pathway.

groups. Also, both burn groups B and B+P experienced increased endogenous glucocorticoid production as do all severely burned patients (4, 6) which may have contributed to the reduced myotube size as glucocorticoids impact both muscle wasting and bone turnover. However, the significant differences between the two burn groups would indicate that there is still a partial rescue of myotube size with pamidronate treatment. In addition, while we have previously provided evidence that serum concentration of TGFβ increases in burned patients and animals compared to normal unburned controls, we did not measure the concentration of TGFβ in the samples tested in this study.

DATA AVAILABILITY

All datasets generated for this study are included in the manuscript and/or the **Supplementary Files**.

ETHICS STATEMENT

Institutional Review Board of the University of Texas Medical Branch protocol #92-304G. This is the approval of the original randomized controlled double blind prospective study from which the de-identified specimens were obtained for the currently submitted *in vitro* study.

AUTHOR CONTRIBUTIONS

LB conceived and designed the experiments. AB and FP designed the experiments. FP performed the experiments. GK conceived the overall idea for the study. FP, AB, LB, and GK wrote and edited the paper. All authors contributed to the writing and editing of the manuscript.

FUNDING

This work was supported by the V Foundation V2017-021 to AB, NIH NIA 1PO1AG039355 to LB, and Protocol 4 of NIH P50 GM60338 to GK.

ACKNOWLEDGMENTS

This work was presented at the 41st Annual Meeting of the American Society for Bone and Mineral Research, Montreal, Canada, 28 September−1 October 2018. Drs. D. N. Herndon and C. C. Finnerty maintained frozen sera from the randomized controlled trial of GK at Shriners Burns Hospital Galveston. C. L. Nieten provided the frozen de-identified serum samples from this study for analysis. The #MF-20 anti-Myosin Heavy Chain antibody developed by Donald A. Fischman at Cornell University was obtained from the Developmental Studies Hybridoma Bank, created by the NICHD of the NIH and maintained at The University of Iowa, Department of Biology, Iowa City, IA 52242.

SUPPLEMENTARY MATERIAL

The Supplementary Material for this article can be found online at: https://www.frontiersin.org/articles/10.3389/fendo.2019.00543/full#supplementary-material

Figure S1 | Mitochondrial environment is not affected by serum derived from burned patients ($N = 4$ per group). Representative Western blotting and quantification of PGC1α, OPA-1, and Cytochrome C in a protein extract of murine C2C12 myotubes exposed for up to 48 h to 5% serum obtained from 3 groups of children: normal unburned (N), burn receiving standard of care after 30 d (B), and burn receiving standard of care and pamidronate after 30 d (B+P). Tubulin was used as the loading control. Data (means ± standard deviation) are expressed as arbitrary units (A.U.). Significance was determined by two-way analysis of variance (ANOVA) followed by Tukey's post-test. Differences were considered significant when $p < 0.05$.

REFERENCES

1. Lee CJ, Mahendraj K, Houng K, Marano M, Petrone S, Lee R, et al. Pediatric burns: a single institution retrospective review of incidence, etiology and outcomes in 2273 burn patients (1995-2013). *J Burn Care Res.* (2016) 37:e579–85. doi: 10.1097/BCR.0000000000000362
2. Shields BJ, Comstock RD, Fernandez SA, Xiang H, Smith GA. Healthcare resource utilization and epidemiology of pediatric burn-associated hospitalizations, United States 2000. *J Burn Care Res.* (2010) 31:506–7. doi: 10.1097/BCR.0b013e3181db5305
3. Robins EV. Burn shock. *Crit Care Nurs Clin North Am.* (1990) 2:299–307. doi: 10.1016/S0899-5885(18)30830-X
4. Klein GL, Herndon DN, Goodman WG, Langman CB, Phillips WA, Dickson IR, et al. Histomorphometric and biochemical characterization of bone following acute severe burns in children. *Bone.* (1995) 17:455–60. doi: 10.1016/8756-3282(95)00279-1
5. Klein GL, Herndon DN, Langman CB, Rutan TC, Young WE, Pembleton G, et al. Long-term reduction in bone mass after severe burn injury in children. *J Pediatr.* (1995) 126:252–6. doi: 10.1016/S0022-3476(95)70553-8
6. Klein GL, Bi LX, Sherrard DJ, Beavan SR, Ireland D, Compston JE, et al. Evidence supporting a role of glucocorticoids in the short-term bone loss in burned children. *Osteoporos Int.* (2004) 15:468–74. doi: 10.1007/s00198-003-1572-3
7. Hart DW, Wolf SE, Mlcak R, Chinkes DL, Ramzy P, Obeng MK, et al. Persistence of muscle catabolism after severe burn injury. *Surgery.* (2000) 128:312–9. doi: 10.1067/msy.2000.108059
8. Merritt EK, Cross JM, Bamman MM. Inflammatory and protein metabolism signaling responses in human skeletal muscle after burn injury. *J Burn Care Res.* (2012) 33:291–7. doi: 10.1097/BCR.0b013e3182331e4b
9. Rinkinen J, Hwang CD, Agarwal S, Oluwatobi E, Peterson J, Loder S, et al. The systemic effect of burn injury on muscle and bone mass and composition. *Plast Reconst Surg.* (2015) 136:612e−23. doi: 10.1097/PRS.0000000000001723
10. Klein GL, Xie Y, Qin Y-X, Lin L, Hu M, Enkhbaatar P, et al. Preliminary evidence of early bone resorption in a sheep model of acute burn injury: an observational study. *J Bone Miner Metab.* (2014) 32:136–41. doi: 10.1007/s00774-013-0483-4
11. Klein GL, Wimalawansa SJ, Kulkarni G, Sherrard DJ, Sanford AP, Herndon DN. The efficacy of acute administration of pamidronate on the conservation of bone mass following severe burn injury in children: a double-blind, randomized, controlled study. *Osteoporos Int.* (2005) 16:631–5. doi: 10.1007/s00198-004-1731-1
12. Mayes T, Gottschlich MM, Khoury J, Kagan RJ. Investigation of bone health subsequent to vitamin D supplementation in children following burn injury. *Nutr Clin Pract.* (2015) 30:830–7. doi: 10.1177/0884533615587720
13. Russell RGG, Rogers MJ. Bisphosphonates: from the laboratory to the clinic and back again. *Bone.* (1999) 25:97–106. doi: 10.1016/S8756-3282(99)00116-7

14. Przkora R, Herndon DN, Sherrard DJ, Chinkes DL, Klein GL. Pamidronate preserves bone mass for at least 2 years following acute administration for pediatric burn injury. *Bone.* (2007) 41:297–302. doi: 10.1016/j.bone.2007.04.195
15. Borsheim E, Herndon DN, Hawkins HK, Suman OE, Cotter M, Klein GL. Pamidronate attenuates muscle loss after pediatric burn injury. *J Bone Miner Res.* (2014) 29:1369–72. doi: 10.1002/jbmr.2162
16. Tredget E, Shankowsky H, Pannu R, Nedelec B, Iwashima T, Ghahary A, et al. Transforming growth factor-β in thermally injured patients with hypertrophic scars: effects of interferon α2b. *Plastic Reconstr Surg.* (1998) 102:1317–28. doi: 10.1097/00006534-199810000-00001
17. Varedi M, Jeschke MG, Englander EW, Herndon DN, Barrow RE. Serum TGF-beta in thermally injured rats. *Shock.* (2001) 16:380–2. doi: 10.1097/00024382-200116050-00010
18. Meert KL, Ofenstein JP, Genyea C, Sarnaik A, Kaplan J. Elevated transforming growth factor-beta concentration correlates with post-trauma immunosuppression. *J Trauma.* (1996) 40:901–6. doi: 10.1097/00005373-199606000-00007
19. Waning DL, Mohammad KS, Reiken W, Xie DC, Andersson S, John A, et al. Excess TGF beta mediates muscle weakness associated with bone metastases in mice. *Nat Commun.* (2015) 21:1262–71. doi: 10.1038/nm.3961
20. Pin F, Barreto R, Kitase Y, Mitra S, Erne C, Novinger LJ, et al. Growth of ovarian cancer xenografts causes loss of muscle and bone mass: a new model for the study of cancer cachexia. *J Cachexia Sarcopenia Muscle.* (2018) 9:685–700. doi: 10.1002/jcsm.12311
21. Schneider CA, Rasband WS, Eliceiri KW. NIH image to Image J: 25 years of image analysis. *Nat Methods.* (2012) 9:671–5. doi: 10.1038/nmeth.2089
22. Quintana HT, Bortolin JA, da Silva NT, Ribeiro FA, Liberti EA, Ribeiro DA, et al. Temporal study following burn injury in young rats is associated with skeletal muscle atrophy, inflammation, and altered myogenic regulatory factors. *Inflamm Res.* (2015) 64:53–62. doi: 10.1007/s00011-014-0783-8
23. Song J, Saeman MR, De Libero J, Wolf SE. Skeletal muscle loss is associated with TNF-mediated insufficient skeletal myogenic activation after burn. *Shock.* (2015) 44:479–86. doi: 10.1097/SHK.0000000000000444
24. Pedroso FE, Spalding PB, Cheung MC, Yang R, Gutierrez JC, Bonetto A, et al. Inflammation, organomegaly and muscle wasting despite hyperphagia in a mouse model of burn cachexia. *J Cachexia Sarcopenia Muscle.* (2012) 3:199–211. doi: 10.1007/s13539-012-0062-x
25. Miyazaki H, Kinoshita M, Ono S, Seki S, Saitoh D. Burn evoked reactive oxygen species immediately after injury are crucial to restore neutrophil function against postburn infection in mice. *Shock.* (2015) 44:252–7. doi: 10.1097/SHK.0000000000000404
26. Bonetto A, Aydogdu T, Jin X, Zhang Z, Zhan R, Puzis L, et al. JAK/STAT pathway inhibition blocks skeletal muscle wasting downstream of IL-6 and in experimental cancer cachexia. *Am J Physiol Endocrinol Metab.* (2012) 303:E410–21. doi: 10.1152/ajpendo.00039.2012
27. Miettunnen PM, Wei X, Kaura D, Reslan WA, Aguirre AN, Kellner JD. Dramatic pain relief and resolution of bone inflammation following pamidronate in 9 pediatric with persistent chronic recurrent multifocal osteomyelitis (CRMO). *Pediatr Rheumatol Online J.* (2009) 7:2. doi: 10.1186/1546-0096-7-2
28. Corrick KL, Stec MJ, Merritt EK, Windham ST, Thomas SJ, Cross JM, et al. Serum from human burn victims impairs myogenesis and protein synthesis in primary myoblasts. *Front Physiol.* (2015) 6:184. doi: 10.3389/fphys.2015.00184
29. Lang CH, Frost RA, Vary TC. Regulation of muscle protein synthesis during sepsis and inflammation. *Am J Physiol Endocrinol Metab.* (2007) 293:E453–9. doi: 10.1152/ajpendo.00204.2007
30. Frost RA, Lang CH. mTor signaling in skeletal muscle during sepsis and inflammation: where does it all go wrong? *Physiology.* (2011) 26:83–96. doi: 10.1152/physiol.00044.2010
31. Pelosi M, De Rossi M, Barberi L, Musaro A. IL-6 impairs myogenic differentiation by downmodulation of p90RSK/eEF2 and mTOR/p70S6K axes without affecting AKT activity. *Biomed Res Int.* (2014) 2014:206026. doi: 10.1155/2014/206026
32. Tsubaki M, Komai M, Itoh T, Imano M, Sakamoto K, Shimaoka H, et al. Nitrogen-containing bisphosphonates inhbit RANKLand M-CSF induced osteoclast formation through the inhibition of ERK 1/2 and AKT activation. *J Biomed Sci.* (2014) 21:10. doi: 10.1186/1423-0127-21-10
33. Lang CH, Silvis C, Nystrom G, Frost RA. Regulation of myostatin by glucocorticoids after thermal injury. *FASEB J.* (2001) 15:1807–9. doi: 10.1096/fj.00-0849fje
34. Egerman MA, Glass DJ. Signaling pathways controlling skeletal muscle mass. *Crit Rev Biochem Mol Biol.* (2014) 49:59–68. doi: 10.3109/10409238.2013.857291
35. Benny Klimek ME, Aydogdu T, Link MJ, Pons M, Koniaris LG, Zimmers TA. Acute inhibition of myostatin-family proteins preserves skeletal muscle in mouse models of cancer cachexia. *Biochem Biophys Res Commun.* (2010) 391:1548–54. doi: 10.1016/j.bbrc.2009.12.123
36. Barreto R, Kitase Y, Matsumoto T, Pin F, Colston KC, Couch KE, et al. ACVR2B/Fc counteracts chemotherapy induced loss of muscle and bone mass. *Sci Rep.* (2017) 7:14470. doi: 10.1038/s41598-017-15040-1

Conflict of Interest Statement: The authors declare that the research was conducted in the absence of any commercial or financial relationships that could be construed as a potential conflict of interest.

frontiers in Endocrinology

ORIGINAL RESEARCH
published: 19 November 2019
doi: 10.3389/fendo.2019.00809

Bisphosphonate Treatment Ameliorates Chemotherapy-Induced Bone and Muscle Abnormalities in Young Mice

Alyson L. Essex[1†], *Fabrizio Pin*[1†], *Joshua R. Huot*[2], *Lynda F. Bonewald*[1,3,4,5,6], *Lilian I. Plotkin*[1,3] *and Andrea Bonetto*[1,2,3,4,6,7*]

[1] *Department of Anatomy, Cell Biology & Physiology, Indiana University School of Medicine, Indianapolis, IN, United States,* [2] *Department of Surgery, Indiana University School of Medicine, Indianapolis, IN, United States,* [3] *Indiana Center for Musculoskeletal Health, Indiana University School of Medicine, Indianapolis, IN, United States,* [4] *Simon Comprehensive Cancer Center, Indiana University, Indianapolis, IN, United States,* [5] *Department of Orthopaedic Surgery, Indiana University School of Medicine, Indianapolis, IN, United States,* [6] *IUPUI Center for Cachexia Research, Innovation and Therapy, Indiana University School of Medicine, Indianapolis, IN, United States,* [7] *Department of Otolaryngology – Head & Neck Surgery, Indiana University School of Medicine, Indianapolis, IN, United States*

OPEN ACCESS

Edited by:
Marco Invernizzi,
University of Eastern Piedmont, Italy

Reviewed by:
Jan Josef Stepan,
Charles University, Czechia
Natalie A. Sims,
St. Vincents Institute of Medical Research, Australia
Michael Gnant,
Medical University of Vienna, Austria

***Correspondence:**
Andrea Bonetto
abonetto@iu.edu

[†]*These authors have contributed equally to this work*

Specialty section:
This article was submitted to Bone Research, a section of the journal Frontiers in Endocrinology

Received: *24 August 2019*
Accepted: *04 November 2019*
Published: *19 November 2019*

Citation:
Essex AL, Pin F, Huot JR, Bonewald LF, Plotkin LI and Bonetto A (2019) Bisphosphonate Treatment Ameliorates Chemotherapy-Induced Bone and Muscle Abnormalities in Young Mice. Front. Endocrinol. 10:809. doi: 10.3389/fendo.2019.00809

Chemotherapy is frequently accompanied by several side effects, including nausea, diarrhea, anorexia and fatigue. Evidence from ours and other groups suggests that chemotherapy can also play a major role in causing not only cachexia, but also bone loss. This complicates prognosis and survival among cancer patients, affects quality of life, and can increase morbidity and mortality rates. Recent findings suggest that soluble factors released from resorbing bone directly contribute to loss of muscle mass and function secondary to metastatic cancer. However, it remains unknown whether similar mechanisms also take place following treatments with anticancer drugs. In this study, we found that young male CD2F1 mice (8-week old) treated with the chemotherapeutic agent cisplatin (2.5 mg/kg) presented marked loss of muscle and bone mass. Myotubes exposed to bone conditioned medium from cisplatin-treated mice showed severe atrophy (−33%) suggesting a bone to muscle crosstalk. To test this hypothesis, mice were administered cisplatin in combination with an antiresorptive drug to determine if preservation of bone mass has an effect on muscle mass and strength following chemotherapy treatment. Mice received cisplatin alone or combined with zoledronic acid (ZA; 5 μg/kg), a bisphosphonate routinely used for the treatment of osteoporosis. We found that cisplatin resulted in progressive loss of body weight (−25%), in line with reduced fat (−58%) and lean (−17%) mass. As expected, microCT bone histomorphometry analysis revealed significant reduction in bone mass following administration of chemotherapy, in line with reduced trabecular bone volume (BV/TV) and number (Tb.N), as well as increased trabecular separation (Tb.Sp) in the distal femur. Conversely, trabecular bone was protected when cisplatin was administered in combination with ZA. Interestingly, while the animals exposed to chemotherapy presented significant muscle wasting (∼-20% vs. vehicle-treated mice), the administration of ZA in combination with cisplatin resulted

in preservation of muscle mass (+12%) and strength (+42%). Altogether, these observations support our hypothesis of bone factors targeting muscle and suggest that pharmacological preservation of bone mass can benefit muscle mass and function following chemotherapy.

Keywords: muscle, bone, cachexia, chemotherapy, bisphosphonates

INTRODUCTION

Cachexia is experienced by anywhere from 20 to 80% of cancer patients, and is ultimately responsible for poorer outcomes, increased morbidity rates and reduced chance of survival (1–3). Cachexia is frequently accompanied by several complications, such as muscle weakness, fatigue, anorexia, as well as metabolic and energy imbalances (4, 5). All these complications often lead to impaired quality of life in patients affected with cachexia, not to mention the increased economic burden (6). While the loss of lean body mass that follows the development of a tumor is frequently related with reduced responsiveness to and augmented toxicities of anticancer therapies (7, 8), we and others have shown that anticancer therapies alone are able to promote the development of cachexia (9–13).

The multisystemic and multiorgan effects of cancer and its treatments have been well described, although the mechanisms associated with these remain elusive (14). To this end, recent interest has grown in the area of the so-called "muscle-bone crosstalk," primarily based on the idea that bone- and muscle-derived factors are able to reciprocally influence the two tissues beyond their mechanical relationship. In particular, there is mounting interest in exploring the communication between muscle and bone by means of biochemical, circulating factors (15, 16). Bone secretes soluble factors that can signal directly to skeletal muscle (17, 18). For example, Waning et al. elegantly showed that release of TGFβ from the bone matrix in a setting of bone metastases contributes to muscle weakness by decreasing Ca^{2+}-induced muscle force production, thus indicating that bone-derived factors may directly affect muscle function (19).

Pathologic bone loss has been historically well documented in metastatic breast cancers and multiple myeloma and, patients undergoing treatment of a variety of tumors have been reported to be at higher risk of bone loss (20). We and others have provided evidence of a direct link between chemotherapy administration and the appearance of muscle and bone alterations consistent with a cachectic phenotype in experimental animals (13, 21). However, whether anticancer therapies promote disruption of the normal muscle-bone communication and whether preservation of bone mass can have beneficial implications on the preservation of muscle mass and strength is currently unknown.

Several bone-targeted agents, primarily bisphosphonates, were developed to stop osteoclasts from resorbing bone in order to treat pathologic conditions, such as osteoporosis and metastatic bone disruption (22). Bisphosphonates are potent antiresorptive drugs endowed with high selectivity for bone, due to their capacity to directly bind to hydroxyapatite (23). Specifically, zoledronic acid, has been tested as a bone-preserving agent in multiple diseases, including cancer (24–26). In breast cancer, zoledronic acid has been investigated for its anti-bone metastasis effects and for the potential ability to counteract tumor growth within bone (27–29). Additionally, bisphosphonate administration was used to treat skeletal events and hypercalcinemia in prostate cancer, although the potential beneficial effects of such treatment remains to be clarified (30–33). Whether bisphosphonates can also directly target muscle mass and affect muscle function remain unclear.

Interestingly, Yoon et al. showed that administration of the antiresorptive agent pamidronate to dystrophic *mdx* mice revealed positive effects on bone and muscle mass (34), although they did not provide evidence of a direct effect of bisphosphonates on muscle homeostasis. Along the same line, a clinical study showed that pediatric burn patients treated with bisphosphonates to the extent of counteracting bone resorption also present with substantial preservation of muscle mass (35). In line with previous findings (19), we recently showed that one of the mechanisms through which bisphosphonates act is likely by limiting the release of TGFβ from the bone matrix (36). The release of TGFβ prevents the activation of SMAD2/3-dependent pro-atrophy signaling in skeletal muscle, thereby suggesting that bisphosphonate administration may potentially serve as a tool for the maintenance of skeletal muscle mass in various disease states (36). These findings in conjunction with existing clinical applications suggest a potential role for zoledronic acid administration in treatment of cancer-related comorbidities, such as cachexia.

In the present study, we characterized an *in vivo* model of chemotherapy-induced cachexia in young, normal mice (37). Herein, we report the effects associated with bisphosphonate administration on the preservation of bone volume, as well as skeletal muscle mass and strength. These results provide further evidence for muscle-bone crosstalk in the pathogenesis of cachexia induced by anticancer drugs and the therapeutic potential of harnessing this cross-tissue interaction to benefit muscle mass and function following anticancer treatments by bisphosphonate administration.

METHODS

Animals

All animal experiments were conducted with the approval of the Institutional Animal Care and Use Committee at the Indiana University School of Medicine and were in compliance with the National Institutes of Health Guidelines for Use and Care of Laboratory Animals and with the ethical standards laid down in the 1964 Declaration of Helsinki and its later amendments.

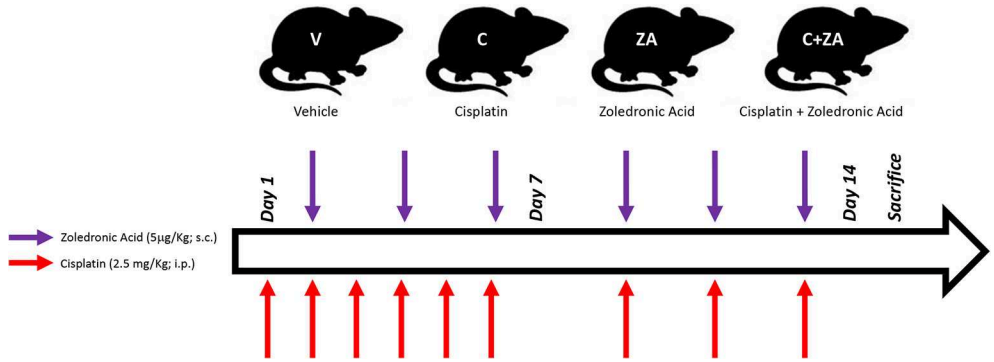

FIGURE 1 | Schematic representation of the *in vivo* model. 8-week old male CD2F1 mice were exposed to i.p. cisplatin injections (C; 2.5 mg/kg), alone or in combination with zoledronic acid (ZA; 5 μg/kg), administered s.c. The control mice received equal volumes of sterile saline (V). The red arrows indicate the day of cisplatin treatment, whereas the purple arrows the day of ZA administration.

All animals were maintained on a regular dark-light cycle (light from 8 a.m. to 8 p.m.), with free access to food and water during the whole experimental period. Briefly, 8-week old CD2F1 male mice (Envigo, Indianapolis, IN) were used (n = 5–8/group). In a first set of experiments, mice were treated with vehicle (sterile saline; V) or cisplatin (2.5 mg/kg, i.p.; C) for up to 2 weeks, similar to what reported in Chen et al. (37). In another set of experiments, mice were randomized into four groups: control mice receiving vehicle alone (V), mice receiving cisplatin (C), mice treated with zoledronate (ZA), and animals receiving the combination cisplatin+ZA (C+ZA). The animals received cisplatin (2.5 mg/kg, i.p.) or ZA (5 μg/kg, s.c.), as shown in **Figure 1** and in line with previously tested dosing schedules (19, 37). The mice were monitored for the entire duration of the experiments. At the time of sacrifice, no animals were excluded from the study. Several tissues were collected, weighed, snap frozen in liquid nitrogen and stored at −80°C for further analyses. The tibialis anterior muscle was frozen in liquid nitrogen-cooled isopentane, mounted in OCT and stored for morphological analyses.

Body Composition Assessment

The quantification of lean (muscle) and fat (adipose) mass was assessed at baseline and the day before sacrifice in physically restrained mice, by means of an EchoMRI-100 (EchoMRI, Houston, USA), as previously shown (38). Data are expressed as variations over the baseline values.

Grip Strength

The evaluation of the whole body strength in mice was assessed as previously described (39). The absolute grip strength (peak force, expressed in grams) was recorded by means of a grip strength meter (Columbus Instruments, Columbus, OH, USA). Five measurements were completed, and the top three measurements were included in the analysis. In order to avoid habituation, the animals were tested for grip strength no more than once weekly.

Micro Computed Tomography (CT) Analysis of Femurs Bone Morphometry

MicroCT scanning was performed to measure morphological indices of metaphyseal regions of femurs. After euthanasia, the left femurs were wrapped in saline-soaked gauze and frozen at −20°C until imaging. Bone samples were rotated around their long axes and images were acquired using a Bruker Skyscan 1176 (Bruker, Kontich, Belgium) with the following parameters: pixel size = 9 μm^3; peak tube potential = 50 kV; X-ray intensity = 500 μA; 0.3° rotation step. Calibration of the grayscale levels was performed using a hydroxyapatite phantom. Based on this calibration and the corresponding standard curve generated, the equivalent minimum calcium hydroxyapatite level was 0.42 g/cm^3. Raw images were reconstructed using the SkyScan reconstruction software (NRecon; Bruker, Kontich, Belgium) to 3-dimensional cross-sectional image data sets using a 3-dimensional cone beam algorithm. Structural indices were calculated on reconstructed images using the Skyscan CT Analyzer software (CTAn; Bruker, Kontich, Belgium). Cortical bone was analyzed by threshold of 160–255 in the femoral mid-shaft. Cortical bone parameters included periosteal perimeter (Ps.Pm), bone area/tissue area (BA/TA), cortical thickness (Ct.Th) and cortical porosity (Ct.Po). Trabecular bone was analyzed between 1.0 and 2.0 mm under the femoral distal growth plate using a threshold of 80–255. Trabecular parameters included bone volume fraction (BV/TV), number (Tb.N), thickness (Tb.Th), separation (Tb.Sp), and pattern factor (Tb.Pf).

Assessment of Muscle Cross Sectional Area (CSA)

Ten μm-thick cryosections of tibialis anterior muscles taken at the mid-belly were processed for immunostaining, as shown in Bonetto et al. (39). Samples were marked with a histology marking pen, blocked in phosphate buffered saline (PBS) containing 8% bovine serum albumin for 1 h at room temperature, and incubated at 4°C overnight with dystrophin primary antibody [Developmental Studies Hybridoma Bank,

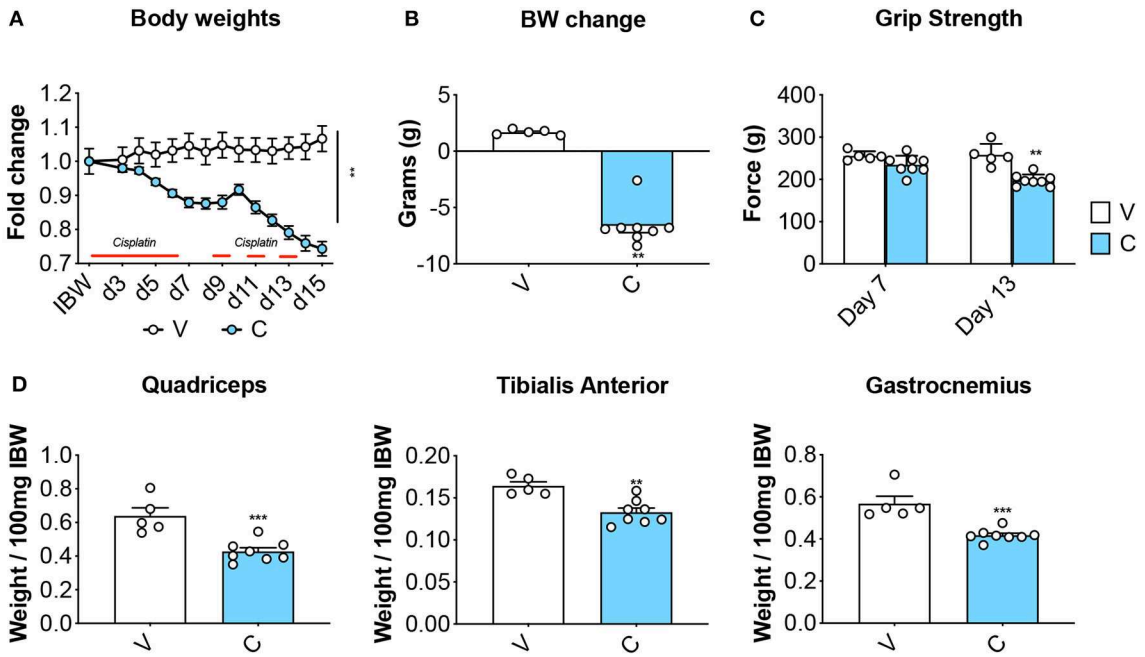

FIGURE 2 | Cisplatin causes body weight loss and muscle depletion. Body weight curves **(A)**, body weight change (i.e., body weight at time of sacrifice vs. initial body weight) **(B)**, whole body grip strength (reported as peak force measured at day 7 and day 13) **(C)** and skeletal muscle weights **(D)** in mice exposed to cisplatin ($n = 8$). Control animals (V; $n = 5$) were administered equal volumes of sterile saline. Muscle weights were normalized to the Initial Body Weight (IBW) and expressed as weight/100 mg IBW. Data (means ± SEM) are expressed in grams. Significance of the differences: $^{**}p < 0.01$, $^{***}p < 0.001$ vs. V.

Iowa City, IA; #MANDRA1(7A10)] diluted in PBS. After the overnight incubation, samples were incubated with a secondary antibody (ThermoFisher Scientific; AlexaFluor 594 # A-11032) for 1 h. Samples were then washed with PBS and mounted with ProLong Antifade mounting medium (ThermoFisher Scientific). For determination of the CSA, the entire muscle section was imaged and quantified by using the Lionheart XL microscope system and the Gen5 software (BioTek, Winooski, VT).

Cell Lines

Murine C2C12 skeletal myoblasts (ATCC, Manassas, VA) were grown in high glucose DMEM supplemented with 10% FBS, 100 U/ml penicillin, 100 mg/ml streptomycin, 100 mg/ml sodium pyruvate, 2 mM L-glutamine, and maintained at 37°C in 5% CO_2, as shown in Pin et al. (40). Myotubes were generated by exposing the myoblasts to DMEM containing 2% horse serum (i.e., differentiation medium, DM), and replacing the medium every other day for 5 days. In order to determine the effects on myotube size dependent on bone-derived factors, myotubes were exposed to 20% bone conditioned medium (CM) for up to 48 h.

Generation of Bone-Derived Conditioned Medium (CM)

Bone-derived CM was generated as shown in Davis et al. (41). Right femur and tibia from vehicle (V)- and cisplatin (C)-treated mice were carefully cleaned of muscle and fibrous tissues, epiphyses cut, and then marrow-flushed multiple times with αMEM. These long bones cortical preparations were then cultured *ex vivo* in 10% FBS and 1% penicillin/streptomycin (P/S)-αMEM for 48 h. CM was collected and stored at −20°C.

Assessment of Myotube Size

C2C12 cell layers were fixed in ice-cold acetone-methanol and incubated with an anti-Myosin Heavy Chain antibody (MF-20, 1:200; Developmental Studies Hybridoma Bank, Iowa City, IA) and an AlexaFluor 488-labeled secondary antibody (Invitrogen, Grand Island, NY), as reported in Pin et al. (40). Analysis of myotube size was performed by measuring the minimum diameter of long, multi-nucleate fibers avoiding regions of clustered nuclei on a calibrated image using the Image J 1.43 software (42). Three biological replicates ($n = 3$) were generated for each experimental condition, and about 250–350 myotubes per replicate were measured. The results of each replicate were then averaged to obtain the final myotube size.

Real-Time Quantitative PCR

Total mRNA from quadriceps muscle was isolated using the miRNeasy Mini Kit (Qiagen, Germantown, MD, USA) and following the protocol provided by the manufacturer. RNA was quantified using a Synergy H1 Spectrophotometer (BioTek Instruments, Winooski, VT, USA). RNA integrity was checked by electrophoresis on a 1.2% agarose gel containing 0.02 M morpholinopropanesulfonic acid and 18% formaldehyde. Total RNA was reverse transcribed to cDNA using the Verso cDNA Kit (Thermo Fisher Scientific). Transcript levels were measured by real-time PCR (Light Cycler 96; Roche), taking

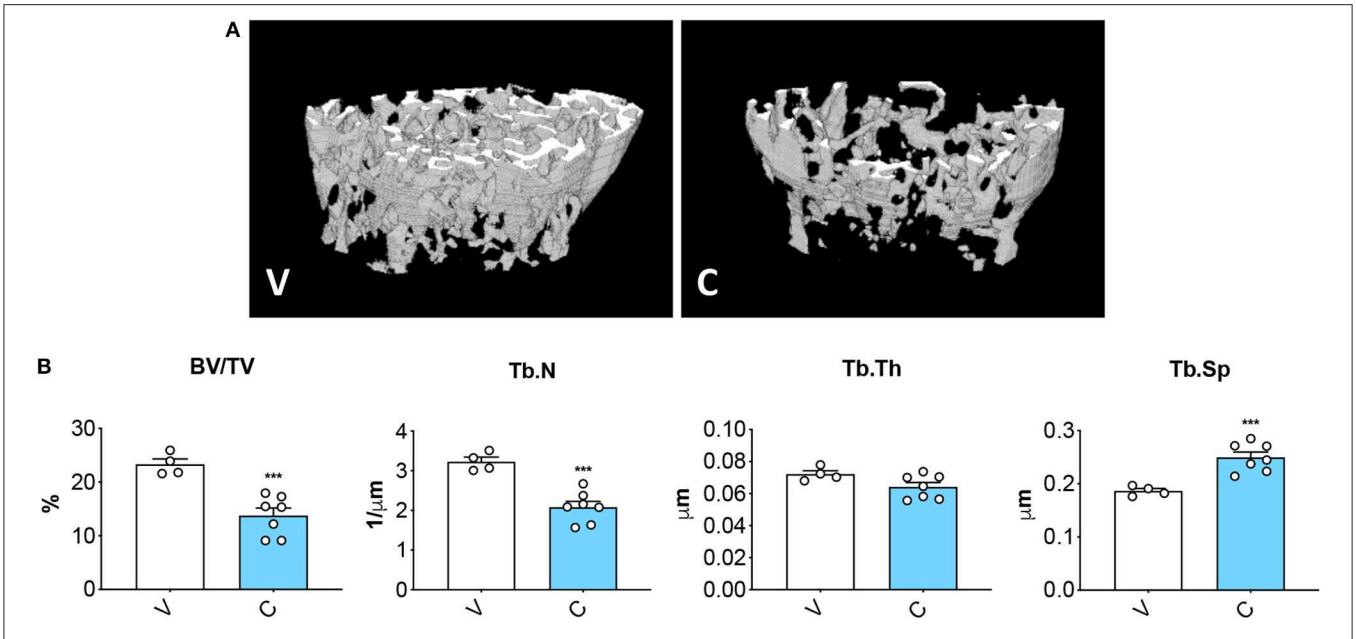

FIGURE 3 | Cisplatin causes severe loss of bone mass. 3D rendering of microCT-based analysis of trabecular bone in femurs from mice receiving V ($n = 4$) or C ($n = 7$) **(A)**. Assessment of trabecular bone volume (BV/TV; expressed as %), trabecular number (Tb.N; expressed as 1/μm), trabecular thickness (Tb.Th; expressed as μm) and trabecular separation (Tb.Sp; expressed as μm) in femoral bones **(B)**. Data are reported as means ± SEM. Significance of the differences: ***$p < 0.001$ vs. V.

advantage of the TaqMan Gene Expression Assay System (Thermo Fisher Scientific). Expression levels for atrogin-1 (Mm00499523_m1) and MuRF-1 (Mm01185221_m1) were quantitated. Gene expression was normalized to TATA-binding protein (TBP; Mm01277042_m1) levels using the standard $2^{-\Delta Ct}$ methods.

Statistical Analysis

Results were presented as means ± SEM. Significance of the differences was determined by unpaired *t*-test when two groups were investigated. When more than two treatments were tested, two-way analysis of variance (ANOVA) followed by Tukey's multiple comparisons test were performed. The interaction *p*-value was reported exclusively when significant. Differences were considered significant when $p < 0.05$.

RESULTS

Cisplatin Treatment Leads to Progressive Body Weight Loss and Muscle Depletion

Eight-week old CD2F1 male mice ($n = 5$) were exposed to daily cisplatin administration (C; 2.5 mg/kg, i.p.) for up to 2 weeks, while control mice (V) received equal volumes of vehicle (i.e., sterile saline). In line with previous findings (37), the animals treated with chemotherapy showed progressive body weight loss (**Figure 2A**), resulting in marked net loss of body weight (−6.6 g vs. initial body weight; $p < 0.01$ vs. V) (**Figure 2B**). In agreement with our published observations (9), the mice receiving cisplatin also showed progressive loss of skeletal muscle strength (−23% vs. V, $p < 0.01$ at day 13) (**Figure 2C**). These effects were consistent with marked depletion of muscle mass, as suggested by the weights of the tibialis anterior, gastrocnemius and quadriceps (**Figure 2D**).

Cisplatin Treatment Leads to Severe Bone Loss

MicroCT assessment of the microarchitecture of femurs excised from mice treated with cisplatin displayed severe loss of cancellous bone (**Figures 3A,B**), as demonstrated by decreased trabecular bone volume ratio (BV/TV; −41%, $p < 0.001$ vs. V) and trabecular number (Tb.N; −36%, $p < 0.001$ vs. V), as well as by the increased trabecular separation (Tb.Sp; +34%, $p < 0.05$ vs. V). The data are consistent with previous evidence supporting the idea that chemotherapy administration associates with impaired bone homeostasis (13, 21).

Myotubes Exposed to Bone Conditioned Medium (CM) From Cisplatin-Treated Mice Display Severe Atrophy

In order to clarify whether cisplatin-induced muscle wasting was triggered by bone-derived soluble factors released upon bone destruction, we exposed fully differentiated C2C12 murine myotubes to 20% bone CM generated by incubating femora and tibiae excised from vehicle (V)- and cisplatin (C)-treated mice in αMEM-containing medium for up to 48 h. The myotubes exposed to 20% C CM displayed severe atrophy compared to V CM, as well as with respect to the myotubes cultured in normal horse serum-containing medium (DM) or unconditioned αMEM-containing (UCM) (**Figure 4**). These observations suggest that mediators released by bone following

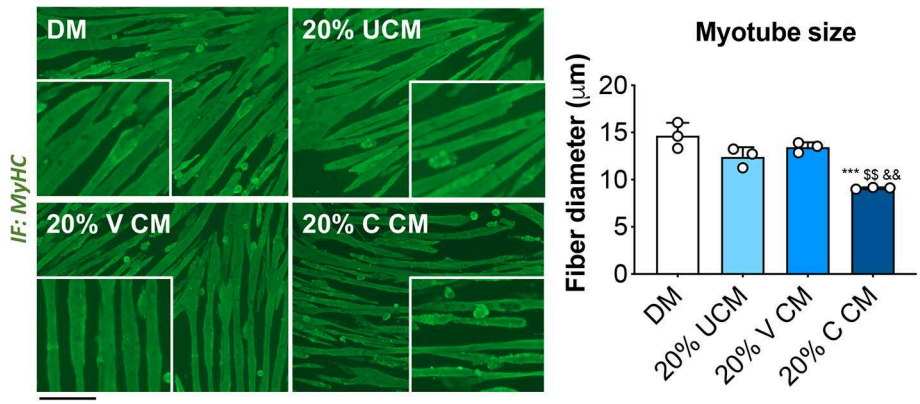

FIGURE 4 | Myotubes exposed to bone conditioned medium from cisplatin-treated mice display severe atrophy. Fully differentiated (5 days) C2C12 myotubes exposed to 20% bone conditioned medium (CM) from animals treated with V or C for up to 48 h. CM was generated by incubating the bones in medium for 48 h. Controls were exposed to either normal horse serum-containing differentiation medium (DM) or 20% αMEM-containing unconditioned medium (UCM). Myotubes were stained for Myosin Heavy Chain (MyHC, green) and myotube size was measured by using the ImageJ software. 250–300 myotubes were measured, $n = 3$. Scale bar: 100 μm. Images were recorded using a 10X magnification (insert: 20X). Data are expressed as means ± SEM. Significance of the differences: $^{***}p < 0.001$ vs. DM; $^{\$\$}p < 0.01$ vs. UCM; $^{\&\&}p < 0.01$ vs. V CM.

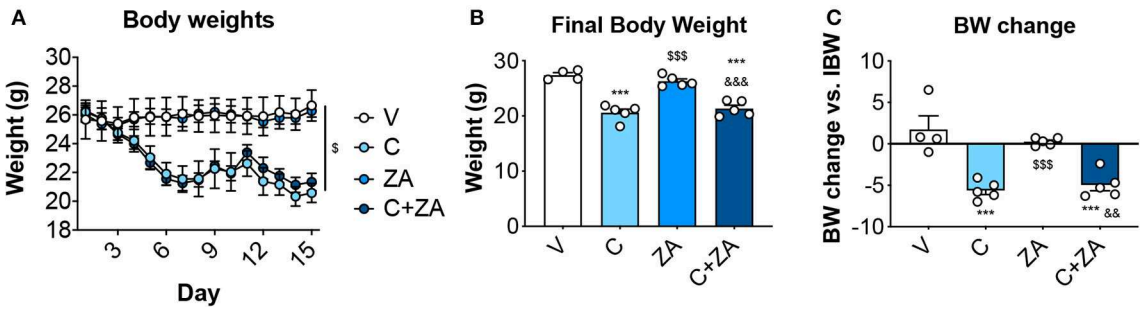

FIGURE 5 | ZA fails to preserve body weight in cisplatin-treated mice. Body weight curves **(A)**, final body weight **(B)** and body weight change (i.e., body weight at time of sacrifice vs. initial body weight) **(C)** in mice exposed to C, alone or in combination with ZA ($n = 4$–5). Control animals (V) were administered equal volumes of sterile saline. Data (means ± SEM) are expressed in grams. Significance of the differences: $^{***}p < 0.001$ vs. V; $^{\$\$\$}p < 0.001$ vs. C; $^{\&\&}p < 0.01$, $^{\&\&\&}p < 0.001$ vs. ZA.

chemotherapy treatment may play a direct role in causing muscle fiber shrinkage.

ZA Administration Is Unable to Counteract Cisplatin Effects on Body Weight

We then investigated whether bone preservation by bisphosphonate treatment also protects skeletal muscle mass in combination with routinely-used chemotherapy regimens. We exposed 8-week old CD2F1 male mice ($n = 5$) to cisplatin (C; 2.5 mg/Kg) (37), alone or in combination with zoledronic acid (ZA; 5 μg/Kg) (19), for up to 2 weeks (**Figure 1**). In line with the observations reported in **Figure 2**, the animals exposed to cisplatin displayed marked and progressive loss of body mass (**Figure 5A**), resulting in significantly reduced body weight (−25%, $p < 0.01$ vs. V) (**Figures 5B,C**). On the other hand, ZA administration was well tolerated and did not show evidence of toxicity, as also suggested by the absence of body weight changes compared to the V group (**Figure 5**). Despite this, ZA administration did not show protective effects on body mass when combined with cisplatin, reporting a body weight change of −4.96 g vs. day 1 in the animals receiving the combined treatment ($p < 0.01$ vs. V). Consistently, body composition assessment by Echo MRI revealed progressive loss of fat content (−58%, $p < 0.001$ vs. V; **Figure 6A**) and lean mass (−16%, $p < 0.001$ vs. V; **Figure 6B**) compared to day 1, whereas ZA did not show any preservation of fat and lean tissue when administered in combination with cisplatin (**Figure 6**). These observations were further corroborated by the observation that the gonadal adipose tissue mass was not preserved in the mice receiving cisplatin and ZA (**Figure S1**).

Trabecular Bone Is Preserved in the Mice Receiving the Combination C+ZA

microCT analysis of femoral bone from animals exposed to cisplatin revealed marked loss of cancellous bone (**Figures 7A,B**). We observed reduced BV/TV (−35%, $p < 0.05$ vs. V) and Tb.N (−28%, $p < 0.05$ vs. V), as well as increased Tb.Sp (+24%, $p < 0.05$ vs. V). ZA treatment alone had a beneficial effect

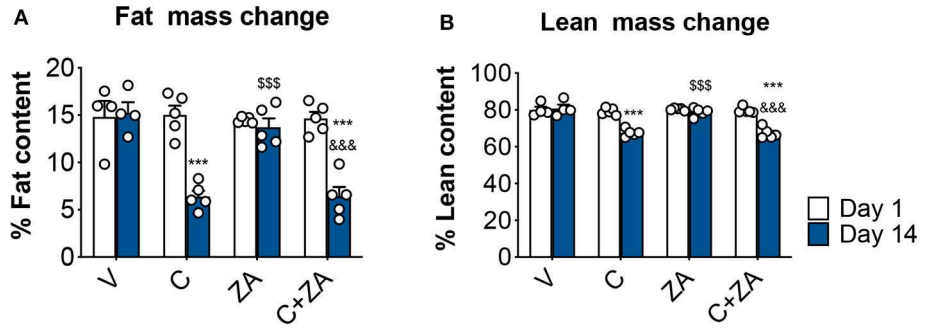

FIGURE 6 | Fat and lean content in chemotherapy-treated mice is not protected by ZA administration. Fat **(A)** and lean **(B)** mass on day 1 and day 14 were assessed in mice exposed to C and/or ZA ($n = 4$–5) by using EchoMRI. Data (means ± SEM) are expressed as percentage of body mass. Significance of the differences: $^{***}p < 0.001$ vs. V; $^{\$\$\$}p < 0.001$ vs. C; $^{\&\&\&}p < 0.001$ vs. ZA (at the respective time point).

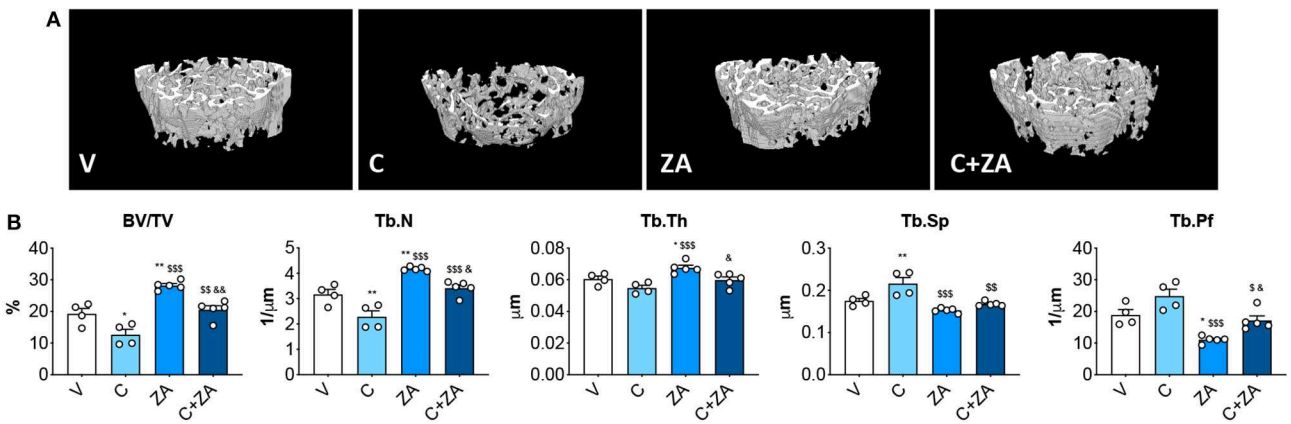

FIGURE 7 | Trabecular bone is preserved in the mice administered the combination C+ZA. 3D reconstruction of microCT-based histomorphometry analysis in femurs from mice receiving V, C, ZA, and C+ZA ($n = 4$–5) **(A)**. Assessment of trabecular bone volume (BV/TV; expressed as %), trabecular thickness (Tb.Th; expressed as μm), trabecular separation (Tb.Sp; expressed as μm), trabecular number (Tb.N; expressed as 1/μm) and trabecular pattern factor (Tb.Pf; expressed as 1/μm) in femoral bones **(B)**. Data are reported as means ± SEM. Significance of the differences: $^{*}p < 0.05$, $^{**}p < 0.01$ vs. V; $^{\$\$}p < 0.01$, $^{\$\$\$}p < 0.001$ vs. C; $^{\&}p < 0.05$, $^{\&\&}p < 0.01$ vs. ZA.

on bone structure, as revealed by significantly elevated BV/TV (+46%, $p < 0.01$ vs. V), trabecular thickness (Tb.Th; +12%, $p < 0.05$ vs. V) and Tb.N (+32%, $p < 0.001$ vs. V), as well as by decreased Tb.Sp (−13%, $p < 0.01$ vs. V) and trabecular pattern factor (Tb.Pf; −42%, $p < 0.01$ vs. V). Interestingly, when combined with cisplatin, ZA was able to preserve bone structure, with BV/TV (+62%, $p < 0.01$ vs. C), Tb.N (+50%, $p < 0.01$ vs. C), Tb.Sp (−22%, $p < 0.01$ vs. C) and Tb.Pf (−31%, $p < 0.05$ vs. C) showing no difference with respect to the V group (**Figure 7**). Further, cisplatin-treated animals displayed reduced cortical thickness (−8%, $p < 0.05$ vs. V), which was substantially preserved following ZA treatment, although no other alterations in cortical bone geometry were detected (**Figure 8**). The loss of trabecular bone appeared milder in the animals receiving C+ZA compared to the animals treated with cisplatin alone (BV/TV: −35% in C vs. V, −27% in C+ZA vs. ZA; Tb.N: −28% in C vs. V, −18% in C+ZA vs. ZA; TB.Sp: +23% in C vs. V, +9% in C+ZA vs. ZA), although no significant interaction was observed between cisplatin and ZA based on the two-way ANOVA analysis (**Figure 7**). Altogether, these observations suggest that ZA does not completely counteract cisplatin-induced bone loss and that bone mass is likely maintained as a result of ZA-derived bone formation.

Bisphosphonates Improve Muscle Size and Function in Cisplatin-Treated Animals

In order to verify whether preservation of bone structure also resulted in protection of muscle mass in animals exposed to chemotherapy, skeletal (tibialis anterior, gastrocnemius and quadriceps) and cardiac muscles were excised from animals administered cisplatin, alone or in combination with ZA (**Figure 9**). In line with previous findings and our initial results (**Figure 2**) (37), cisplatin treatment caused significant loss of skeletal muscle mass (**Figure 9**). Notably, also the heart was significantly smaller in the cisplatin-treated mice (−21%, $p < 0.001$ vs. V) (**Figure 9**). On the other hand, while ZA alone did not show any direct effects on muscle mass, the combination C+ZA revealed improved muscle size, as suggested by the

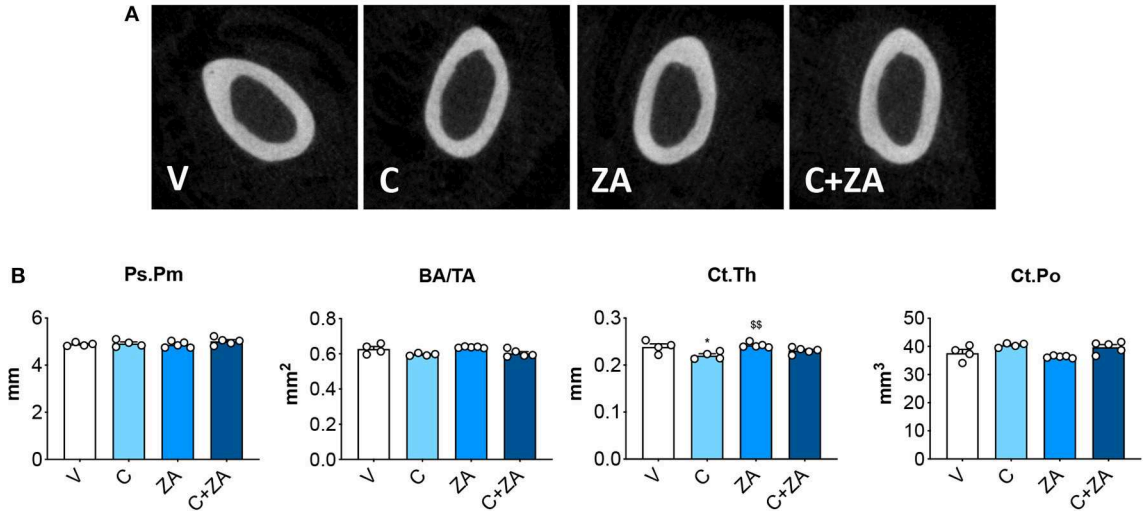

FIGURE 8 | Cortical bone is minimally affected by cisplatin. 2D rendering of microCT-based histomorphometry analysis of cortical bone in femurs from mice receiving V, C, ZA and C+ZA ($n = 4–5$) **(A)**. Assessment of periosteal perimeter (Ps.Pm; expressed as mm), bone area/tissue area (BA/TA; expressed as mm^2), cortical thickness (Ct.Th; expressed as mm) and cortical porosity (Ct.Po; expressed as mm^3) in femoral bones **(B)**. Data are reported as means ± SEM. Significance of the differences: $^{*}p < 0.05$ vs. V; $^{\$\$}p < 0.01$ vs. C.

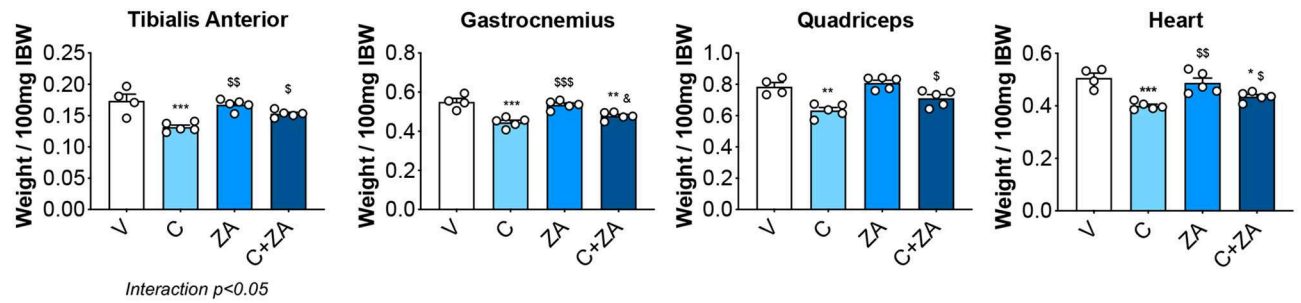

FIGURE 9 | Skeletal muscle mass is partially preserved in the mice treated with C+ZA. Skeletal muscle and heart weights in mice administered C, alone or combined with ZA ($n = 4–5$). Weights were normalized to the Initial Body Weight (IBW) and expressed as weight/100 mg IBW. Data are expressed as means ± SEM. Significance of the differences: $^{*}p < 0.05$, $^{**}p < 0.01$, $^{***}p < 0.001$ vs. V; $^{\$}p < 0.05$, $^{\$\$}p < 0.01$, $^{\$\$\$}p < 0.001$ vs. C; $^{\&}p < 0.05$ vs. ZA.

protection of the tibialis anterior (+16%, $p < 0.01$ vs. C; interaction: $p < 0.05$) and quadriceps (+12%, $p < 0.05$ vs. C), and by the partial preservation of gastrocnemius (+7%, $p < 0.05$ vs. C) and heart weights (+9%, $p < 0.05$ vs. C) (**Figure 9**). Consistent with the effects on muscle mass, muscle fiber size was also partially preserved in the cisplatin-treated animals receiving ZA, as shown by the quantification of the muscle cross-sectional area (+17%, $p < 0.05$ vs. C) (**Figures 10A,B**). Interestingly, the ZA-associated protection of muscle mass was also accompanied by substantially preserved muscle strength in the C+ZA group ($p < 0.001$ vs. C), which was 42% higher than the C-treated animals on day 14 (−25%, $p < 0.01$ vs. V; interaction: $p < 0.01$) (**Figure 10C**). In line with these findings, we investigated the mRNA levels for Atrogin-1 and MuRF-1, ubiquitin ligases normally overexpressed in skeletal muscle during cachexia (40, 43). Atrogin-1 was significantly increased following cisplatin treatment (+54%, $p < 0.05$ vs. V), whereas its expression was returned to control values following ZA administration (**Figure 11**). On the other hand, MuRF-1 muscle levels were reduced in the mice receiving the combination C+ZA (−48%, $p < 0.05$ vs. V), whereas we did not observe changes in the other experimental groups (**Figure 11**).

DISCUSSION

Musculoskeletal derangements are among the most common and most distressing symptoms associated with cancer and its treatment (44, 45), affecting 70–100% of patients receiving chemo-radiation therapies (46–48). Cancer treatments are frequently responsible for a decline of muscle and bone function and the development of muscle weakness and bone frailty, together well-known features of cachexia (49–51). This is a condition frequently observed in upwards of 80% of advanced cancer patients and mainly associated with striking loss of body weight and lean body mass, along with worsening of the quality of life and increased morbidity and mortality rates (52). More importantly, the functional deficits due to muscle weakness have

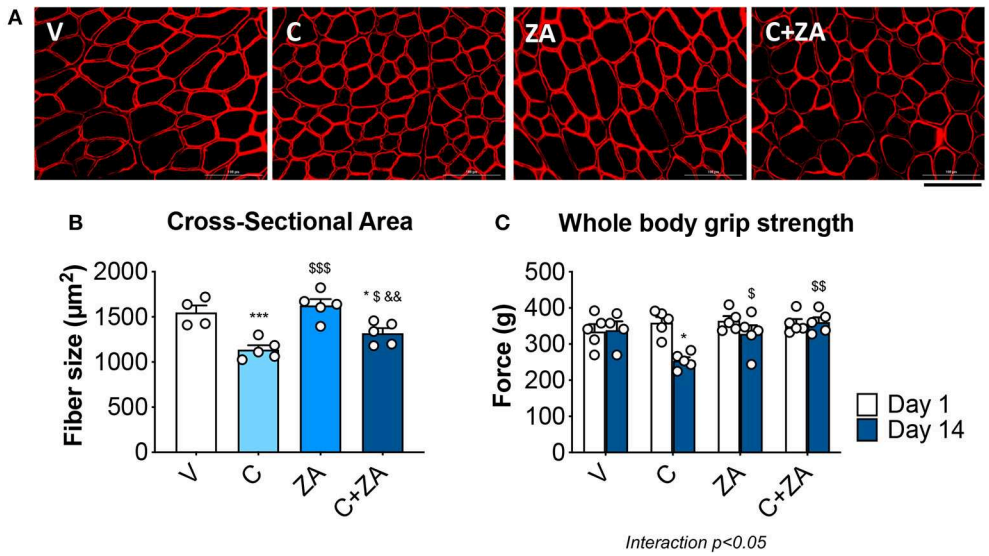

FIGURE 10 | Cisplatin-induced muscle weakness is counteracted by ZA administration. Representative images of immunofluorescence staining for dystrophin **(A)** and quantification of the cross-sectional area **(B)** in the tibialis anterior muscle of mice treated with cisplatin and/or ZA ($n = 4$–5). Scale bar: 100 μm. Whole body grip strength (reported as peak force) was measured at day 1 and day 14 by taking advantage of a grip strength meter and expressed as the average of the three top pulls from each animal **(C)**. Data are shown as means ± SEM. Significance of the differences: $^{*}p < 0.05$, $^{***}p < 0.001$ vs. V; $^{\$}p < 0.05$, $^{\$\$}p < 0.01$ vs. C; $^{\&\&}p < 0.01$ vs. ZA.

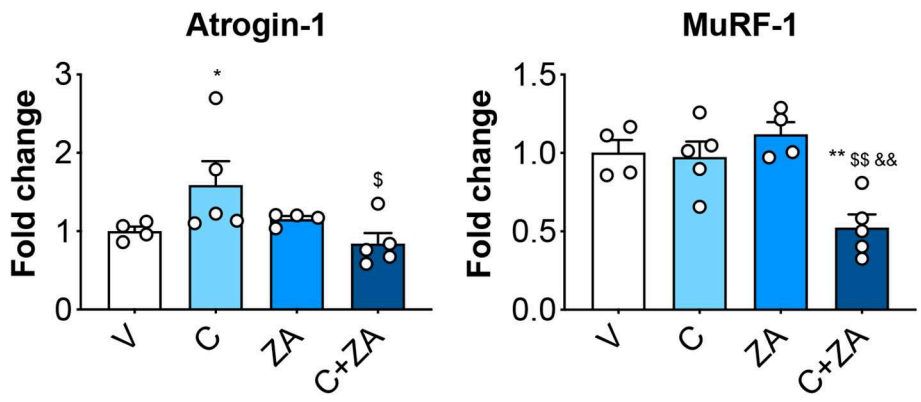

FIGURE 11 | Muscle protein hypercatabolism is counteracted by ZA administration in C-treated mice. mRNA expression for the ubiquitin ligases Atrogin-1 and MuRF-1 in the quadriceps muscle of mice treated with cisplatin and/or ZA ($n = 4$–5). Data are shown as means ± SEM. Significance of the differences: $^{*}p < 0.05$, $^{**}p < 0.01$ vs. V; $^{\$}p < 0.05$, $^{\$\$}p < 0.01$ vs. C; $^{\&\&}p < 0.01$ vs. ZA.

been shown to persist for months to years following remission (53–56), thereby causing a significant worsening of the quality of life (57). Unfortunately, cancer-related muscle weakness is further intensified with the aggressiveness of chemotherapy, and no treatments have been shown to relieve such conditions thus far (58, 59).

In line with data from Chen et al. (37), here we showed that cisplatin, a platinum-based alkylating agent usually prescribed for the treatment of solid tumors, leads to severe musculoskeletal deficits in growing mice. Consistent with previous findings (60), our observations generated in an *in vitro* model also suggest that chemotherapy-dependent effects on muscle fiber size are triggered by circulating factors, likely released upon bone destruction. We previously reported that chronic administration of Folfiri, a chemotherapy regimen often prescribed for the treatment of solid tumors, participates in the pathogenesis of cachexia by affecting muscle mass and function and by causing dramatic loss of trabecular bone (9, 13). In line with our observations, Hain et al. (21) recently showed that treatment with another platinum-based agent, carboplatin, despite being effective in counteracting tumor dissemination in a model of metastatic breast cancer, contributes to significant muscle atrophy and weakness, also accompanied by loss of trabecular bone.

The correlation between chemotherapy treatment and decreases in bone mass primarily due to the negative effects of anticancer drugs on bone remodeling has been investigated for quite some time (61, 62). For example, imatinib, used for the treatment of gastrointestinal tumors and leukemias, was found to directly target platelet-derived growth factor (PDGF) receptor, among others (63). Similarly, taxanes were shown to cause myelosuppression and, in turn, bone loss and increased levels of inflammatory mediators (64). Methotrexate, routinely prescribed for the treatment of several solid tumors, was reported to directly target bone tissue and promote bone degeneration by increasing the expression of IL-6 and IL-11 (65). Further, corticosteroids, frequently used in combination with anticancer agents, were shown to directly affect bone mass by reducing osteoblast differentiation and by increasing osteoclast-dependent bone resorption (66). At the same time, chemotherapy was also reported to cause bone damage by impinging on indirect systemic effects involving gonadal suppression. Indeed, cytotoxic chemotherapy was recently associated with significant gonadal damage (67, 68). Similarly, ovarian failure resulting from chemotherapy treatments in premenopausal women with breast cancer was shown to promote rapid bone loss (69). Interestingly, hypogonadism in patients receiving anticancer treatments was also linked to the occurrence of musculoskeletal abnormalities (70, 71). Nevertheless, the mechanism(s) responsible for changes in bone mass and relationship to changes in muscle homeostasis, especially in a setting of chemotherapy treatment, is not completely understood.

In the present study, we administered cisplatin in combination with zoledronic acid, a bone-targeted drug used to preserve bone mass in osteoporosis, to investigate whether the treatment with antiresorptive drugs was able to preserve bone mass, as well as muscle size and strength following chemotherapy administration. As shown in our experimental results, zoledronic acid was able to completely preserve cancellous and cortical bone loss in mice receiving cisplatin, without apparent signs of toxicity. Notably, zoledronic acid proved effective in partially preserving muscle mass and strength, thereby supporting the concept that bone-derived factors play a role in the muscle deficits in cachexia induced by chemotherapy. We can speculate that the absence of a complete protective effect of zoledronic acid on muscle mass may be due to the combined action of other non-bone derived mediators, and/or direct toxicity of chemotherapy on the muscle fibers. However, whether zoledronic acid is also able to affect the levels of bone-derived factors remains unknown.

Of note, the improvement in muscle mass and muscle strength was also accompanied by a normalization of the levels of Atrogin-1, a ubiquitin ligase normally upregulated in conditions characterized by skeletal muscle atrophy (43), also suggesting that enhanced muscle hypercatabolism could play a role in cisplatin-induced muscle wasting. On the other hand, MuRF-1, previously shown significantly elevated in the skeletal muscle of cachectic mice (40), was significantly downregulated in the animals receiving the combination treatment with respect to the control, consistent with data reporting protection of muscle mass in MuRF-1 knock-out mice exposed to the pro-catabolic drug dexamethasone (72). On the other hand, cisplatin alone did not cause any upregulation, at least at the performed time point. In this regard, our observation that zoledronic acid was unable to alter skeletal muscle wet weights in normal conditions, but rather only in combination with chemotherapy, further supports the concept that abnormal muscle-bone interactions may play a role in the pathogenesis of cachexia.

Recently, major interest has grown toward understanding the so-called "muscle-bone crosstalk." According to this concept, muscle tissue represents a storehouse of "myokines," known to affect bone mass by regulating bone destruction and bone formation (16). Conversely, bone-secreted factors would seem to influence skeletal muscle beyond the mechanical relationship in loading and primarily through the release of soluble mediators (known as "osteokines") (73, 74). These are now known to directly influence muscle mass by contributing to regulation of size and contractility (15–18). Exacerbated loss of bone along with increased osteolysis are well-documented in breast cancers and multiple myeloma, along with formation of metastases to bone (19, 75). In particular, Waning *et al.* previously suggested that enhanced bone resorption associated with cancer dissemination results in release of TGFβ from the bone matrix, which in turn causes modulation of muscle regulatory pathways and contributes to muscle weakness (19). Similarly, investigative efforts from our group have shown that bone loss also occurs in the absence of bone metastases and frequently associates with changes of muscle homeostasis and function (38, 76), although the causative mechanism(s) responsible for such abnormalities have not been completely elucidated.

In this regard, pro-inflammatory cytokines, such as TGFβ-family ligands, are known to play a role in the regulation of skeletal muscle mass (77). These cytokines were shown to be released from the mineralized matrix in conditions associated with bone destruction, including cachexia (19, 36, 78, 79). This is also in line with previous evidence from our group, showing that administration of an activin receptor type-2B (ACVR2B) antagonist, previously shown to improve muscle mass and prolong survival in tumor-bearing mice (80), was able to completely restore muscle and bone mass in animals chronically administered Folfiri (13). Therefore, our results suggest that cessation of basal homeostatic skeletal turnover alone is not directly involved in the regulation of skeletal muscle mass, whereas bisphosphonate-induced correction of abnormal bone resorption in cachexia may be sufficient to ameliorate skeletal muscle atrophy *per se*.

Interestingly, Børsheim et al. (35) previously reported that children affected with unintentional burn-injury not only show preservation of bone mass upon treatment with bisphosphonates, but also significant improvements in muscle mass. In a recent collaborative investigation, we provided evidence supporting the idea that TGFβ plays a pivotal role in causing muscle atrophy in burn children, usually characterized by dramatic loss of bone and muscle mass, whereas administration of the bone-protecting agent pamidronate would seem to improve muscle size by counteracting the TGFβ-dependent signaling and restoring the proper muscle anabolism (36). However, it remains unclear whether similar mechanisms also participate in causing bone loss

and muscle wasting and whether preservation of bone mass effectively improves muscle size and function following chemotherapy administration.

The idea that bone and muscle communicate at a biochemical level by exchanging soluble mediators also provides new avenues for direct pharmacological interventions aimed at targeting these factors, as reviewed by Brotto and Bonewald (16). In particular, bone-targeted agents, primarily bisphosphonates, are potent antiresorptive drugs, routinely used in the clinic for the treatment of post-menopausal osteoporosis and bone frailty associated with chronic conditions or metastatic cancers (22). These drugs were originally designed to counteract osteoclast activity and bone resorption, and subsequently shown to prevent the release of pro-inflammatory cytokines and other signaling molecules, including TGFβ, BMP2, and IGF-1, from the bone matrix (78, 79, 81, 82). In adult individuals, altered bone "coupling," i.e., the physiologic coordination of bone resorption with bone formation (83), often occurs with increases in osteoclast activity with little to no change in osteoblast-driven bone formation. This results in an imbalance in bone remodeling and leads to decreased bone mass, increased risk for fractures and worsened survival rates (84). We and others have provided evidence of bone loss in both cancer- and chemotherapy-induced cachexia, likely suggesting an imbalance in osteoclast vs. osteoblast activity in association with loss of muscle mass and strength (13, 21, 36, 38, 76).

Notably, bone is now often referred to as an endocrine organ, secreting osteogenic factors (i.e., osteokines), which can be released during resorption (16). Originally, all these factors were thought to mainly take part to the regulation of bone mass, although it is becoming clear that these osteokines can also affect muscle homeostasis (85). For example, while components of the Wnt/®β-catenin pathway are important regulators of bone mass, it has been shown that Wnts also affect muscle by supporting myogenesis and muscle function (86). In a similar manner, receptor activator of nuclear factor kappa-B ligand (RANKL) and its natural decoy receptor osteoprotegerin (OPG) are mainly produced by bone cells and are critical for the activation of osteoclasts and the regulation of bone resorption (87). Interestingly, the receptor for RANKL, known as RANK, is also expressed in skeletal muscle, where it appears to regulate muscle contractility (88), whereas anti-RANKL antibodies and OPG-Fc have been shown to improve muscle size and function in dystrophic *mdx* mice (89). Another example is provided by osteocalcin, mainly produced by mature osteoblasts and osteocytes. Osteocalcin not only was shown to regulate glucose and energy metabolism, as well as fertility in male mice and ectopic calcification, but also appears to affect muscle mass, based on the evidence that supplementation with osteocalcin restores reduced exercise capacity in mice and improves muscle strength (90). Moreover, elevated levels of the osteocyte-derived fibroblast growth factor 23 (FGF23) were also shown to negatively impact cardiac muscle by increasing the risk of heart disease, left ventricular hypertrophy, vascular calcification, although no effects were conclusively described in skeletal muscle (91). The osteocyte factor prostaglandin E2 (PGE2), normally released in response to fluid flow shear stress, was also shown to affect muscle growth and function by acting as a potent stimulator of myogenic differentiation in primary myoblasts/myotubes (92). Interestingly, osteoclasts were shown to secrete soluble factors endowed with muscle-protective properties. This is the case of cardiotrophin-1 (CT-1) and sphingosine-1-phosphate (S1P) (93). Specifically, CT-1, an IL-6 superfamily member signaling through binding to the leukemia inhibitory factor (LIF) receptor, was described as an osteoclast-derived factor critically involved in bone remodeling (94). However, recent observations suggest that CT-1 may also directly affect muscle tissue. Indeed, CT-1 was shown to exert cardioprotective effects and to stimulate myogenic and vascular remodeling of the heart, as well as to increase extraocular muscle mass and strength in experimental animal models (95–97). Similarly, S1P, a bioactive lipid that acts via G protein-coupled receptors previously implicated in several osteogenesis-related processes, including differentiation and survival of osteoblasts and their subsequent coupling with osteoclasts (98), was also shown to positively impact muscle tissue, through the regulation of skeletal myoblast proliferation (99), as well as in the control of normal cardiac development (100) and of smooth muscle cell proliferation, migration and contraction (101). In our study we did not assess the levels of these factors, although the evidence that muscle mass was improved by administration of an anti-resorptive agent, such as zoledronate, appears to suggest that some of these osteokines, normally released from the bone matrix upon activation of bone resorption, may well play a role in the regulation of muscle mass in cachexia induced by chemotherapy.

A strength of our approach is that we did circumvent the lack of muscle targeted therapeutics and, instead, aimed at repurposing existing, FDA-approved drugs for alternate uses. While the long-term side effects of bisphosphonate treatment have been previously characterized (102), whether bisphosphonates also promote long-term toxicities on skeletal muscle, especially in subjects treated with chemotherapy, remain to be clarified, along with the impact that these drugs may have on efficacy and tolerability of anticancer drugs. Our data may appear in disagreement with previous studies reporting no effects or moderate toxicities associated with long-term (>3 years) bisphosphonate administration on skeletal muscle mass in post-menopausal osteoporotic women, showing bone and muscle defects at time of first treatment (18, 103). However, our experimental model, using normal, healthy animals exposed to chemotherapy and treated with bisphosphonates for the entire duration of the experiment (i.e., since day 1) is not directly comparable with such studies. Taking into account also the results reported by Børsheim et al. (35), showing beneficial effects on muscle mass in pediatric patients administered pamidronate shortly after burn injury, our observations support the idea that bisphosphonates, rather than rescue muscle mass once musculoskeletal complications are already established, may instead contribute to preserve skeletal muscle in conditions normally associated with pro-cachectic stimuli. Moreover, it is important to point out that our studies were conducted in young, skeletally immature growing animals, therefore

characterized by elevated rates of bone formation, as also supported by the analysis of the bone histomorphometry data. At this time, we cannot exclude that different outcomes might occur by using the same therapeutic approach in adult or aged animals, in accordance with evidence suggesting that bisphosphonates concomitantly impair bone formation in adult individuals, thus increasing the likelihood of long-term adverse events (104).

Nonetheless, the use of bisphosphonates as anticancer agents has recently been investigated due to their beneficial properties in counteracting the formation of bone metastases and preventing adverse skeletal events in cancer (24, 25, 33). In this study, we did not take into examination animals bearing cancers plus chemotherapy. Although this choice may represent a limitation of our study, in this pre-clinical investigation we decided to focus on establishing mechanisms responsible for chemotherapy induced muscle wasting. In this regard, the findings described here corroborate the idea that chemotherapy-associated toxicities negatively impact bone and muscle mass, thus leading to phenotypes consistent with cachexia.

In this study we focused on investigating the musculoskeletal abnormalities that occur following chemotherapy treatment, with the ultimate goal of determining whether anti-resorptive drugs could contribute to preserve both bone and muscle in a setting of anticancer treatment. In this regard, we have to keep in mind that the dosing for cisplatin and zoledronate used in our experimental model, tested in previous studies (37, 60), does not necessarily compare to the one usually prescribed for humans. Indeed, by converting the animal dosing to the human equivalent dose, calculated following the guidelines reported in Nair and Jacob (105), our animals may appear underdosed, especially if compared to the clinical setting (106, 107). However, it is important to note that as patients are normally treated with either drugs once every 2-to-4 weeks, on the contrary our experimental animals received multiple treatments over 2 weeks.

In conclusion, in the present study we provide evidence that bone-protecting agents, such as bisphosphonates, may be combined with routinely used anticancer drugs to the extent of reducing their associated toxicities and, ultimately, mitigating the occurrence of chemotherapy-associated musculoskeletal abnormalities. Moreover, our experimental data corroborate the possibility that bisphosphonates are administered in combination with chemotherapeutics since first treatment in order to maximize their efficacy in preserving muscle and bone. Overall, we expect our findings will pave the way to major investigations on the use of bisphosphonates in oncology care and encourage future studies aimed at defining zoledronic acid as a new anti-cachexia treatment in combination with traditional chemotherapy or cancer.

DATA AVAILABILITY STATEMENT

The datasets generated for this study are available on request to the corresponding author.

ETHICS STATEMENT

The animal study was reviewed and approved by Institutional Animal Care and Use Committee at Indiana University School of Medicine.

AUTHOR CONTRIBUTIONS

AE, FP, and AB conceived and designed the experiments. AE, FP, JH, and AB performed the *in vitro* and *in vivo* experiments, the body composition assessment, the muscle function analysis, the microCT analysis of the bone, and the molecular characterization of cachexia. LB and LP provided support for the bone studies. AE, FP, LB, LP, and AB wrote and edited the paper.

FUNDING

This study was supported by the Department of Surgery and the Department of Otolaryngology – Head & Neck Surgery at Indiana University, and by grants from the V Foundation for Cancer Research (V2017-021), the American Cancer Society (132013-RSG-18-010-01-CCG), and the Showalter Research Trust to AB. AE was supported by a T32 Institutional Training Grant from NIH (AR065971).

ACKNOWLEDGMENTS

The #MF-20 anti-Myosin Heavy Chain antibody (developed by Donald A. Fischman at Cornell University) and the #MANDRA1(7A10) anti-Dystrophin monoclonal antibody (developed by Morris GE at NE Wales Institute) were obtained from the Developmental Studies Hybridoma Bank, created by the NICHD of the NIH and maintained at The University of Iowa, Department of Biology, Iowa City, IA. The authors thank John Spence, Ph.D. for his contribution in editing the manuscript, Teresa A. Zimmers, Ph.D. for allowing access to the equipment for *in vivo* characterization of cachexia, as well as Joseph Wallace, Ph.D. and Matthew R. Allen, Ph.D. for helping with the discussion of the microCT data.

SUPPLEMENTARY MATERIAL

The Supplementary Material for this article can be found online at: https://www.frontiersin.org/articles/10.3389/fendo.2019.00809/full#supplementary-material

REFERENCES

1. Arthur ST, Van Doren BA, Roy D, Noone JM, Zacherle E, Blanchette CM. Cachexia among US cancer patients. *J Med Econ*. (2016) 19:874–80. doi: 10.1080/13696998.2016.1181640

2. Anker MS, Holcomb R, Muscaritoli M, von Haehling S, Haverkamp W, Jatoi A, et al. Orphan disease status of cancer cachexia in the USA and in the European Union: a systematic review. *J Cachexia Sarcopenia Muscle*. (2019) 10:22–34. doi: 10.1002/jcsm.12402

3. von Haehling S, Anker SD. Cachexia as a major underestimated and unmet medical need: facts and numbers. *J Cachexia Sarcopenia Muscle*. (2010) 1:1–5. doi: 10.1007/s13539-010-0002-6
4. Fearon K, Strasser F, Anker SD, Bosaeus I, Bruera E, Fainsinger RL, et al. Definition and classification of cancer cachexia: an international consensus. *Lancet Oncol*. (2011) 12:489–95. doi: 10.1016/S1470-2045(10)70218-7
5. Fearon K, Arends J, Baracos V. Understanding the mechanisms and treatment options in cancer cachexia. *Nat Rev Clin Oncol*. (2012) 10:90. doi: 10.1038/nrclinonc.2012.209
6. von Haehling S, Anker SD. Prevalence, incidence and clinical impact of cachexia: facts and numbers-update 2014. *J Cachexia Sarcopenia Muscle*. (2014) 5:261–3. doi: 10.1007/s13539-014-0164-8
7. Antoun S, Baracos VE, Birdsell L, Escudier B, Sawyer MB. Low body mass index and sarcopenia associated with dose-limiting toxicity of sorafenib in patients with renal cell carcinoma. *Ann Oncol*. (2010) 21:1594–8. doi: 10.1093/annonc/mdp605
8. Prado CM, Antoun S, Sawyer MB, Baracos VE. Two faces of drug therapy in cancer: drug-related lean tissue loss and its adverse consequences to survival and toxicity. *Curr Opin Clin Nutr Metab Care*. (2011) 14:250–4. doi: 10.1097/MCO.0b013e3283455d45
9. Barreto R, Waning DL, Gao H, Liu Y, Zimmers TA, Bonetto A. Chemotherapy-related cachexia is associated with mitochondrial depletion and the activation of ERK1/2 and p38 MAPKs. *Oncotarget*. (2016) 7:43442–60. doi: 10.18632/oncotarget.9779
10. Damrauer JS, Stadler ME, Acharyya S, Baldwin AS, Couch ME, Guttridge DC. Chemotherapy-induced muscle wasting: association with NF-κB and cancer cachexia. *Eur J Transl Myol*. (2018) 28:7590. doi: 10.4081/ejtm.2018.7590
11. Huot RJ, Essex LA, Gutierrez M, Barreto R, Wang M, Waning LD, et al. Chronic treatment with multi-kinase inhibitors causes differential toxicities on skeletal and cardiac muscles. *Cancers*. (2019) 11:E571. doi: 10.3390/cancers11040571
12. Barreto R, Mandili G, Witzmann FA, Novelli F, Zimmers TA, Bonetto A. Cancer and chemotherapy contribute to muscle loss by activating common signaling pathways. *Front Physiol*. (2016) 7:472. doi: 10.3389/fphys.2016.00472
13. Barreto R, Kitase Y, Matsumoto T, Pin F, Colston KC, Couch KE, et al. ACVR2B/Fc counteracts chemotherapy-induced loss of muscle and bone mass. *Sci Rep*. (2017) 7:14470. doi: 10.1038/s41598-017-15040-1
14. Porporato PE. Understanding cachexia as a cancer metabolism syndrome. *Oncogenesis*. (2016) 5:e200. doi: 10.1038/oncsis.2016.3
15. Bonewald L. Use it or lose it to age: a review of bone and muscle communication. *Bone*. (2019) 120:212–8. doi: 10.1016/j.bone.2018.11.002
16. Brotto M, Bonewald L. Bone and muscle: interactions beyond mechanical. *Bone*. (2015) 80:109–14. doi: 10.1016/j.bone.2015.02.010
17. Mo C, Romero-Suarez S, Bonewald L, Johnson M, Brotto M. Prostaglandin E2: from clinical applications to its potential role in bone- muscle crosstalk and myogenic differentiation. *Recent Pat Biotechnol*. (2012) 6:223–9. doi: 10.2174/1872208311206030223
18. Bonnet N, Bourgoin L, Biver E, Douni E, Ferrari S. RANKL inhibition improves muscle strength and insulin sensitivity and restores bone mass. *J Clin Invest*. (2019) 129:3214–23. doi: 10.1172/JCI125915
19. Waning DL, Mohammad KS, Reiken S, Xie W, Andersson DC, John S, et al. Excess TGF-beta mediates muscle weakness associated with bone metastases in mice. *Nat Med*. (2015) 21:1262–71. doi: 10.1038/nm.3961
20. Brown SA, Guise TA. Cancer-associated bone disease. *Curr Osteoporos Rep*. (2007) 5:120–7. doi: 10.1007/s11914-007-0027-8
21. Hain BA, Xu H, Wilcox JR, Mutua D, Waning DL. Chemotherapy-induced loss of bone and muscle mass in a mouse model of breast cancer bone metastases and cachexia. *JCSM Rapid Commun*. (2019) 2:e00075. doi: 10.1002/j.2617-1619.2019.tb00011.x
22. Lewiecki EM. Bisphosphonates for the treatment of osteoporosis: insights for clinicians. *Ther Adv Chronic Dis*. (2010) 1:115–28. doi: 10.1177/2040622310374783
23. Cole LE, Vargo-Gogola T, Roeder RK. Targeted delivery to bone and mineral deposits using bisphosphonate ligands. *Adv Drug Deliv Rev*. (2016) 99:12–27. doi: 10.1016/j.addr.2015.10.005
24. Agarwala S, Vijayvargiya M. Single dose therapy of zoledronic acid for the treatment of transient osteoporosis of hip. *Ann Rehabil Med*. (2019) 43:314–20. doi: 10.5535/arm.2019.43.3.314
25. O'Carrigan B, Wong MH, Willson ML, Stockler MR, Pavlakis N, Goodwin A. Bisphosphonates and other bone agents for breast cancer. *Cochrane Database Syst Rev*. (2017) 10:CD003474-CD. doi: 10.1002/14651858.CD003474.pub4
26. von Moos R, Costa L, Gonzalez-Suarez E, Terpos E, Niepel D, Body JJ. Management of bone health in solid tumours: from bisphosphonates to a monoclonal antibody. *Cancer Treat Rev*. (2019) 76:57–67. doi: 10.1016/j.ctrv.2019.05.003
27. Dhesy-Thind S, Fletcher GG, Blanchette PS, Clemons MJ, Dillmon MS, Frank ES, et al. Use of adjuvant bisphosphonates and other bone-modifying agents in breast cancer: a cancer care ontario and American society of clinical oncology clinical practice guideline. *J Clin Oncol*. (2017) 35:2062–81. doi: 10.1200/JCO.2016.70.7257
28. Aft R, Naughton M, Trinkaus K, Watson M, Ylagan L, Chavez-MacGregor M, et al. Effect of zoledronic acid on disseminated tumour cells in women with locally advanced breast cancer: an open label, randomised, phase 2 trial. *Lancet Oncol*. (2010) 11:421–8. doi: 10.1016/S1470-2045(10)70054-1
29. Biskup E, Cai F, Vetter M. Bone targeted therapies in advanced breast cancer. *Swiss Med Wkly*. (2017) 147:w14440. doi: 10.4414/smw.2017.14440
30. Body JJ, von Moos R, Niepel D, Tombal B. Hypocalcaemia in patients with prostate cancer treated with a bisphosphonate or denosumab: prevention supports treatment completion. *BMC Urol*. (2018) 18:81. doi: 10.1186/s12894-018-0393-9
31. Vale CL, Burdett S, Rydzewska LHM, Albiges L, Clarke NW, Fisher D, et al. Addition of docetaxel or bisphosphonates to standard of care in men with localised or metastatic, hormone-sensitive prostate cancer: a systematic review and meta-analyses of aggregate data. *Lancet Oncol*. (2016) 17:243–56. doi: 10.1016/S1470-2045(15)00489-1
32. Finianos A, Aragon-Ching JB. Zoledronic acid for the treatment of prostate cancer. *Expert Opin Pharmacother*. (2019) 20:657–66. doi: 10.1080/14656566.2019.1574754
33. Macherey S, Monsef I, Jahn F, Jordan K, Yuen KK, Heidenreich A, et al. Bisphosphonates for advanced prostate cancer. *Cochrane Database Syst Rev*. (2017) 12:CD006250-CD. doi: 10.1002/14651858.CD006250.pub2
34. Yoon SH, Sugamori KS, Grynpas MD, Mitchell J. Positive effects of bisphosphonates on bone and muscle in a mouse model of Duchenne muscular dystrophy. *Neuromuscul Disord*. (2016) 26:73–84. doi: 10.1016/j.nmd.2015.09.015
35. Borsheim E, Herndon DN, Hawkins HK, Suman OE, Cotter M, Klein GL. Pamidronate attenuates muscle loss after pediatric burn injury. *J Bone Miner Res*. (2014) 29:1369–72. doi: 10.1002/jbmr.2162
36. Pin F, Bonetto A, Bonewald LF, Klein GL. Molecular mechanisms responsible for the rescue effects of pamidronate on muscle atrophy in pediatric burn patients. *Front Endocrinol*. (2019) 10:543. doi: 10.3389/fendo.2019.00543
37. Chen JA, Splenser A, Guillory B, Luo J, Mendiratta M, Belinova B, et al. Ghrelin prevents tumour- and cisplatin-induced muscle wasting: characterization of multiple mechanisms involved. *J Cachexia Sarcopenia Muscle*. (2015) 6:132–43. doi: 10.1002/jcsm.12023
38. Pin F, Barreto R, Kitase Y, Mitra S, Erne CE, Novinger LJ, et al. Growth of ovarian cancer xenografts causes loss of muscle and bone mass: a new model for the study of cancer cachexia. *J Cachexia Sarcopenia Muscle*. (2018) 9:685–700. doi: 10.1002/jcsm.12311
39. Bonetto A, Andersson DC, Waning DL. Assessment of muscle mass and strength in mice. *Bonekey Rep*. (2015) 4:732. doi: 10.1038/bonekey.2015.101
40. Pin F, Novinger LJ, Huot JR, Harris RA, Couch ME, O'Connell TM, et al. PDK4 drives metabolic alterations and muscle atrophy in cancer cachexia. *FASEB J*. (2019) 33:7778–90. doi: 10.1096/fj.201802799R
41. Davis HM, Essex AL, Valdez S, Deosthale PJ, Aref MW, Allen MR, et al. Short-term pharmacologic RAGE inhibition differentially affects bone and skeletal muscle in middle-aged mice. *Bone*. (2019) 124:89–102. doi: 10.1016/j.bone.2019.04.012
42. Schneider CA, Rasband WS, Eliceiri KW. NIH Image to ImageJ: 25 years of image analysis. *Nat Methods*. (2012) 9:671–5. doi: 10.1038/nmeth.2089
43. Lecker SH, Jagoe RT, Gilbert A, Gomes M, Baracos V, Bailey J, et al. Multiple types of skeletal muscle atrophy involve a common program of changes in gene expression. *FASEB J*. (2004) 18:39–51. doi: 10.1096/fj.03-0610com

44. Curt GA, Breitbart W, Cella D, Groopman JE, Horning SJ, Itri LM, et al. Impact of cancer-related fatigue on the lives of patients: new findings from the Fatigue Coalition. *Oncologist*. (2000) 5:353–60. doi: 10.1634/theoncologist.5-5-353
45. Glaus A. Assessment of fatigue in cancer and non-cancer patients and in healthy individuals. *Support Care Cancer*. (1993) 1:305–15. doi: 10.1007/BF00364968
46. Ahlberg K, Ekman T, Gaston-Johansson F, Mock V. Assessment and management of cancer-related fatigue in adults. *Lancet*. (2003) 362:640–50. doi: 10.1016/S0140-6736(03)14186-4
47. Stasi R, Abriani L, Beccaglia P, Terzoli E, Amadori S. Cancer-related fatigue: evolving concepts in evaluation and treatment. *Cancer*. (2003) 98:1786–801. doi: 10.1002/cncr.11742
48. Neefjes ECW, van den Hurk RM, Blauwhoff-Buskermolen S, van der Vorst M, Becker-Commissaris A, de van der Schueren MAE, et al. Muscle mass as a target to reduce fatigue in patients with advanced cancer. *J Cachexia Sarcopenia Muscle*. (2017) 8:623–9. doi: 10.1002/jcsm.12199
49. Patrick DL, Ferketich SL, Frame PS, Harris JJ, Hendricks CB, Levin B, et al. National institutes of health state-of-the-science conference statement: symptom management in cancer: pain, depression, and fatigue, July 15-17, 2002. *J Natl Cancer Inst Monogr*. (2004) 95:9–16. doi: 10.1093/jncimonographs/djg014
50. Aubier M, Banzett RB, Bellemare F, Braun NMT, Cherniack NS, Clanton TL, et al. NHLBI Workshop summary. Respiratory muscle fatigue. Report of the Respiratory Muscle Fatigue Workshop Group. *Am Rev Respir Dis*. (1990) 142:474–80. doi: 10.1164/ajrccm/142.2.474
51. Guise TA. Bone loss and fracture risk associated with cancer therapy. *Oncologist*. (2006) 11:1121–31. doi: 10.1634/theoncologist.11-10-1121
52. Fearon KC, Moses AG. Cancer cachexia. *Int J Cardiol*. (2002) 85:73–81. doi: 10.1016/S0167-5273(02)00235-8
53. Knobel H, Havard Loge J, Lund MB, Forfang K, Nome O, Kaasa S. Late medical complications and fatigue in Hodgkin's disease survivors. *J Clin Oncol*. (2001) 19:3226–33. doi: 10.1200/JCO.2001.19.13.3226
54. Luctkar-Flude M, Groll D, Woodend K, Tranmer J. Fatigue and physical activity in older patients with cancer: a six-month follow-up study. *Oncol Nurs Forum*. (2009) 36:194–202. doi: 10.1188/09.ONF.194-202
55. Meeske K, Smith AW, Alfano CM, McGregor BA, McTiernan A, Baumgartner KB, et al. Fatigue in breast cancer survivors two to five years post diagnosis: a HEAL study report. *Qual Life Res*. (2007) 16:947–60. doi: 10.1007/s11136-007-9215-3
56. Goedendorp MM, Andrykowski MA, Donovan KA, Jim HS, Phillips KM, Small BJ, et al. Prolonged impact of chemotherapy on fatigue in breast cancer survivors: a longitudinal comparison with radiotherapy-treated breast cancer survivors and noncancer controls. *Cancer*. (2012) 118:3833–41. doi: 10.1002/cncr.26226
57. Montazeri A. Quality of life data as prognostic indicators of survival in cancer patients: an overview of the literature from 1982 to 2008. *Health Qual Life Outcomes*. (2009) 7:102. doi: 10.1186/1477-7525-7-102
58. Jacobsen PB, Donovan KA, Small BJ, Jim HS, Munster PN, Andrykowski MA. Fatigue after treatment for early stage breast cancer: a controlled comparison. *Cancer*. (2007) 110:1851–9. doi: 10.1002/cncr.22993
59. Prue G, Allen J, Gracey J, Rankin J, Cramp F. Fatigue in gynecological cancer patients during and after anticancer treatment. *J Pain Symptom Manage*. (2010) 39:197–210. doi: 10.1016/j.jpainsymman.2009.06.011
60. Waning DL, Guise TA. Cancer-associated muscle weakness: What's bone got to do with it? *Bonekey Rep*. (2015) 4:691. doi: 10.1038/bonekey.2015.59
61. Baylink DJ. Glucocorticoid-induced osteoporosis. *N Engl J Med*. (1983) 309:306–8. doi: 10.1056/NEJM198308043090509
62. Fisher DE, Bickel WH. Corticosteroid-induced avascular necrosis. A clinical study of seventy-seven patients. *J Bone Joint Surg Am*. (1971) 53:859–73. doi: 10.2106/00004623-197153050-00002
63. Kubo T, Piperdi S, Rosenblum J, Antonescu CR, Chen W, Kim HS, et al. Platelet-derived growth factor receptor as a prognostic marker and a therapeutic target for imatinib mesylate therapy in osteosarcoma. *Cancer*. (2008) 112:2119–29. doi: 10.1002/cncr.23437
64. Quach JM, Askmyr M, Jovic T, Baker EK, Walsh NC, Harrison SJ, et al. Myelosuppressive therapies significantly increase pro-inflammatory cytokines and directly cause bone loss. *J Bone Miner Res*. (2015) 30:886–97. doi: 10.1002/jbmr.2415
65. Shandala T, Shen Ng Y, Hopwood B, Yip YC, Foster BK, Xian CJ. The role of osteocyte apoptosis in cancer chemotherapy-induced bone loss. *J Cell Physiol*. (2012) 227:2889–97. doi: 10.1002/jcp.23034
66. Canalis E, Delany AM. Mechanisms of glucocorticoid action in bone. *Ann N Y Acad Sci*. (2002) 966:73–81. doi: 10.1111/j.1749-6632.2002.tb04204.x
67. Chovanec M, Abu Zaid M, Hanna N, El-Kouri N, Einhorn LH, Albany C. Long-term toxicity of cisplatin in germ-cell tumor survivors. *Ann Oncol*. (2017) 28:2670–9. doi: 10.1093/annonc/mdx360
68. Marques P, Van Huellen H, Fitzpatrick A, Druce M. Late endocrine effects of cancer and cancer therapies in survivors of childhood malignancies. *Minerva Endocrinol*. (2016) 41:78—104.
69. Saarto T, Blomqvist C, Valimaki M, Makela P, Sarna S, Elomaa I. Chemical castration induced by adjuvant cyclophosphamide, methotrexate, and fluorouracil chemotherapy causes rapid bone loss that is reduced by clodronate: a randomized study in premenopausal breast cancer patients. *J Clin Oncol*. (1997) 15:1341–7. doi: 10.1200/JCO.1997.15.4.1341
70. Willemse PM, Hamdy NA, de Kam ML, Burggraaf J, Osanto S. Changes in bone mineral density in newly diagnosed testicular cancer patients after anticancer treatment. *J Clin Endocrinol Metab*. (2014) 99:4101–8. doi: 10.1210/jc.2014-1722
71. Cameron DA, Douglas S, Brown JE, Anderson RA. Bone mineral density loss during adjuvant chemotherapy in pre-menopausal women with early breast cancer: is it dependent on oestrogen deficiency? *Breast Cancer Res Treat*. (2010) 123:805–14. doi: 10.1007/s10549-010-0899-7
72. Baehr LM, Furlow JD, Bodine SC. Muscle sparing in muscle RING finger 1 null mice: response to synthetic glucocorticoids. *J Physiol*. (2011) 589:4759–76. doi: 10.1113/jphysiol.2011.212845
73. Karsenty G, Ferron M. The contribution of bone to whole-organism physiology. *Nature*. (2012) 481:314–20. doi: 10.1038/nature10763
74. Dallas SL, Prideaux M, Bonewald LF. The osteocyte: an endocrine cell ... and more. *Endocr Rev*. (2013) 34:658–90. doi: 10.1210/er.2012-1026
75. Terpos E, Ntanasis-Stathopoulos I, Gavriatopoulou M, Dimopoulos MA. Pathogenesis of bone disease in multiple myeloma: from bench to bedside. *Blood Cancer J*. (2018) 8:7. doi: 10.1038/s41408-017-0037-4
76. Bonetto A, Kays JK, Parker VA, Matthews RR, Barreto R, Puppa MJ, et al. Differential bone loss in mouse models of colon cancer cachexia. *Front Physiol*. (2017) 7:679. doi: 10.3389/fphys.2016.00679
77. Guttridge DC. A TGF-beta pathway associated with cancer cachexia. *Nat Med*. (2015) 21:1248–9. doi: 10.1038/nm.3988
78. Regan JN, Trivedi T, Guise TA, Waning DL. The role of TGFβ in bone-muscle crosstalk. *Curr Osteoporos Rep*. (2017) 15:18–23. doi: 10.1007/s11914-017-0344-5
79. Wildemann B, Kadow-Romacker A, Haas NP, Schmidmaier G. Quantification of various growth factors in different demineralized bone matrix preparations. *J Biomed Mater Res A*. (2007) 81:437–42. doi: 10.1002/jbm.a.31085
80. Benny Klimek ME, Aydogdu T, Link MJ, Pons M, Koniaris LG, Zimmers TA. Acute inhibition of myostatin-family proteins preserves skeletal muscle in mouse models of cancer cachexia. *Biochem Biophys Res Commun*. (2010) 391:1548–54. doi: 10.1016/j.bbrc.2009.12.123
81. Sartori R, Schirwis E, Blaauw B, Bortolanza S, Zhao J, Enzo E, et al. BMP signaling controls muscle mass. *Nat Genet*. (2013) 45:1309–18. doi: 10.1038/ng.2772
82. Levinger I, Scott D, Nicholson GC, Stuart AL, Duque G, McCorquodale T, et al. Undercarboxylated osteocalcin, muscle strength and indices of bone health in older women. *Bone*. (2014) 64:8–12. doi: 10.1016/j.bone.2014.03.008
83. Hattner R, Epker BN, Frost HM. Suggested sequential mode of control of changes in cell behaviour in adult bone remodelling. *Nature*. (1965) 206:489–90. doi: 10.1038/206489a0
84. Agri F, Bourgeat M, Becce F, Moerenhout K, Pasquier M, Borens O, et al. Association of pelvic fracture patterns, pelvic binder use and arterial angio-embolization with transfusion requirements and mortality rates; a 7-year retrospective cohort study. *BMC Surg*. (2017) 17:104. doi: 10.1186/s12893-017-0299-6

85. Bonetto A, Bonewald LF. Chapter: Bone and Muscle. *Basic and Applied Bone Biology*, 2nd Ed. London: Academic Press; Elsevier (2019). p. 317–32. doi: 10.1016/B978-0-12-813259-3.00016-6
86. Rudnicki MA, Williams BO. Wnt signaling in bone and muscle. *Bone*. (2015) 80:60–6. doi: 10.1016/j.bone.2015.02.009
87. Fuller K, Wong B, Fox S, Choi Y, Chambers TJ. TRANCE is necessary and sufficient for osteoblast-mediated activation of bone resorption in osteoclasts. *J Exp Med*. (1998) 188:997–1001. doi: 10.1084/jem.188.5.997
88. Dufresne SS, Dumont NA, Boulanger-Piette A, Fajardo VA, Gamu D, Kake-Guena SA, et al. Muscle RANK is a key regulator of Ca2+ storage, SERCA activity, and function of fast-twitch skeletal muscles. *Am J Physiol Cell Physiol*. (2016) 310:C663-72. doi: 10.1152/ajpcell.00285.2015
89. Dufresne SS, Boulanger-Piette A, Bosse S, Argaw A, Hamoudi D, Marcadet L, et al. Genetic deletion of muscle RANK or selective inhibition of RANKL is not as effective as full-length OPG-fc in mitigating muscular dystrophy. *Acta Neuropathol Commun*. (2018) 6:31. doi: 10.1186/s40478-018-0533-1
90. Mera P, Laue K, Wei J, Berger JM, Karsenty G. Osteocalcin is necessary and sufficient to maintain muscle mass in older mice. *Mol Metab*. (2016) 5:1042–7. doi: 10.1016/j.molmet.2016.07.002
91. Touchberry CD, Green TM, Tchikrizov V, Mannix JE, Mao TF, Carney BW, et al. FGF23 is a novel regulator of intracellular calcium and cardiac contractility in addition to cardiac hypertrophy. *Am J Physiol Endocrinol Metab*. (2013) 304:E863–73. doi: 10.1152/ajpendo.00596.2012
92. Ho ATV, Palla AR, Blake MR, Yucel ND, Wang YX, Magnusson KEG, et al. Prostaglandin E2 is essential for efficacious skeletal muscle stem-cell function, augmenting regeneration and strength. *Proc Nat Acad Sci USA*. (2017) 114:6675–84.
93. Sims NA, Martin TJ. Coupling the activities of bone formation and resorption: a multitude of signals within the basic multicellular unit. *Bonekey Rep*. (2014) 3:481. doi: 10.1038/bonekey.2013.215
94. Walker EC, McGregor NE, Poulton IJ, Pompolo S, Allan EH, Quinn JM, et al. Cardiotrophin-1 is an osteoclast-derived stimulus of bone formation required for normal bone remodeling. *J Bone Miner Res*. (2008) 23:2025–32. doi: 10.1359/jbmr.080706
95. Ruixing Y, Jinzhen W, Dezhai Y, Jiaquan L. Cardioprotective role of cardiotrophin-1 gene transfer in a murine model of myocardial infarction. *Growth Factors*. (2007) 25:286–94. doi: 10.1080/08977190701781289
96. Li T, Wiggins LM, von Bartheld CS. Insulin-like growth factor-1 and cardiotrophin 1 increase strength and mass of extraocular muscle in juvenile chicken. *Invest Ophthalmol Vis Sci*. (2010) 51:2479–86. doi: 10.1167/iovs.09-4414
97. Abdul-Ghani M, Suen C, Jiang B, Deng Y, Weldrick JJ, Putinski C, et al. Cardiotrophin 1 stimulates beneficial myogenic and vascular remodeling of the heart. *Cell Res*. (2017) 27:1195–215. doi: 10.1038/cr.2017.87
98. Sartawi Z, Schipani E, Ryan KB, Waeber C. Sphingosine 1-phosphate (S1P) signalling: Role in bone biology and potential therapeutic target for bone repair. *Pharmacol Res*. (2017) 125(Pt B):232–45. doi: 10.1016/j.phrs.2017.08.013
99. Sassoli C, Frati A, Tani A, Anderloni G, Pierucci F, Matteini F, et al. Mesenchymal stromal cell secreted sphingosine 1-phosphate (S1P) exerts a stimulatory effect on skeletal myoblast proliferation. *PLoS ONE*. (2014) 9:e108662. doi: 10.1371/journal.pone.0108662
100. Clay H, Wilsbacher LD, Wilson SJ, Duong DN, McDonald M, Lam I, et al. Sphingosine 1-phosphate receptor-1 in cardiomyocytes is required for normal cardiac development. *Dev Biol*. (2016) 418:157–65. doi: 10.1016/j.ydbio.2016.06.024
101. Liu L, Zhai C, Pan Y, Zhu Y, Shi W, Wang J, et al. Sphingosine-1-phosphate induces airway smooth muscle cell proliferation, migration, and contraction by modulating Hippo signaling effector YAP. *Am J Physiol Lung Cell Mol Physiol*. (2018) 315:L609–21. doi: 10.1152/ajplung.00554.2017
102. Kennel KA, Drake MT. Adverse effects of bisphosphonates: implications for osteoporosis management. *Mayo Clin Proc*. (2009) 84:632–7. doi: 10.1016/S0025-6196(11)60752-0
103. Uchiyama S, Ikegami S, Kamimura M, Mukaiyama K, Nakamura Y, Nonaka K, et al. The skeletal muscle cross sectional area in long-term bisphosphonate users is smaller than that of bone mineral density-matched controls with increased serum pentosidine concentrations. *Bone*. (2015) 75:84–7. doi: 10.1016/j.bone.2015.02.018
104. Reyes C, Hitz M, Prieto-Alhambra D, Abrahamsen B. Risks and benefits of bisphosphonate therapies. *J Cell Biochem*. (2016) 117:20–8. doi: 10.1002/jcb.25266
105. Nair AB, Jacob S. A simple practice guide for dose conversion between animals and human. *J Basic Clin Pharm*. (2016) 7:27–31. doi: 10.4103/0976-0105.177703
106. Morse RT, Ganju RG, TenNapel MJ, Neupane P, Kakarala K, Shnayder Y, et al. Weekly cisplatin chemotherapy dosing vs. triweekly chemotherapy with concurrent radiation for head and neck squamous cell carcinoma. *Head Neck*. (2019) 41:2492–9. doi: 10.1002/hed.25717
107. Hortobagyi GN, Van Poznak C, Harker WG, Gradishar WJ, Chew H, Dakhil SR, et al. Continued treatment effect of zoledronic acid dosing every 12 vs. 4 weeks in women with breast cancer metastatic to bone: the OPTIMIZE-2 randomized clinical trial. *JAMA Oncol*. (2017) 3:906–12. doi: 10.1001/jamaoncol.2016.6316

Conflict of Interest: The authors declare that the research was conducted in the absence of any commercial or financial relationships that could be construed as a potential conflict of interest.

frontiers in Endocrinology

REVIEW
published: 22 November 2019
doi: 10.3389/fendo.2019.00794

Neuromuscular Diseases and Bone

Giovanni Iolascon, Marco Paoletta, Sara Liguori, Claudio Curci and Antimo Moretti*

Department of Medical and Surgical Specialties and Dentistry, University of Campania "Luigi Vanvitelli", Naples, Italy

Neuromuscular diseases (NMDs) are inherited or acquired conditions affecting skeletal muscles, motor nerves, or neuromuscular junctions. Most of them are characterized by a progressive damage of muscle fibers with reduced muscle strength, disability, and poor health-related quality of life of affected patients. In this scenario, skeletal health is usually compromised as a consequence of modified bone–muscle cross-talk including biomechanical and bio-humoral issues, resulting in increased risk of bone fragility and fractures. In addition, NMD patients frequently face nutritional issues, including malnutrition due to feeding disorders and swallowing problems that might affect bone health. Moreover, in these patients, low levels of physical activity or immobility are common and might lead to overweight or obesity that can also interfere with bone strength features. Also, vitamin D deficiency could play a critical role both in the pathogenesis and in the clinical scenario of many NMDs, suggesting that its correction could be useful in maintaining or enhancing bone health, especially in the early phases of NMDs. Last but not least, specific disease-modifying drugs, available for some NMDs, are frequently burdened with adverse effects on bone tissue. For example, glucocorticoid therapy, standard of care for many muscular dystrophies, prolongs long-term survival in treated patients; nevertheless, high dose and/or chronic use of these drugs are a common cause of secondary osteoporosis. This review addresses the current state of knowledge about the factors that play a role in determining bone alterations reported in NMDs, how these factors can modify the biological pathways underlying bone health, and which are the available interventions to manage bone involvement in patients affected by NMDs. Considering the complexity of care of these patients, an interdisciplinary and multimodal management strategy based on both pharmacological and non-pharmacological interventions is recommended, particularly targeting musculoskeletal issues that are closely related to functional independence as well as social implications.

Keywords: neuromuscular diseases, osteoporosis, fractures, physical activity, vitamin D, glucocorticoids, rehabilitation

OPEN ACCESS

Edited by:
Gordon L. Klein,
University of Texas Medical Branch at Galveston, United States

Reviewed by:
William A. Bauman,
James J. Peters VA Medical Center, United States
David R. Weber,
University of Rochester, United States

****Correspondence:***
Giovanni Iolascon
giovanni.iolascon@gmail.com

Specialty section:
This article was submitted to Bone Research, a section of the journal Frontiers in Endocrinology

Received: *11 September 2019*
Accepted: *30 October 2019*
Published: *22 November 2019*

Citation:
Iolascon G, Paoletta M, Liguori S, Curci C and Moretti A (2019) Neuromuscular Diseases and Bone. Front. Endocrinol. 10:794. doi: 10.3389/fendo.2019.00794

DEFINITIONS AND PATHOPHYSIOLOGICAL ISSUES

Neuromuscular disease (NMD) is an umbrella term encompassing different categories of disorders affecting anterior horn cells, peripheral nerves, neuromuscular junctions, and skeletal muscles (**Table 1**). If we exclude diabetic neuropathy, when considered individually, NMDs are rare diseases, although overall involve a considerable population.

TABLE 1 | Neuroanatomical classification of neuromuscular diseases.

Lesion level	Hereditary	Acquired	Abbreviation
Anterior horn	Spinal muscular atrophy		SMA
	Amyotrophic lateral sclerosis		ALS
		Post-polio syndrome	PPS
Nerve	Charcot–Marie–Tooth disease		CMT
		Guillain–Barre syndrome	GBS
		Chronic inflammatory demyelinating polyneuropathy	CIDP
		Neuropathy with monoclonal gammopathy of unknown significance	MGUS
Neuromuscular junction		Myasthenia gravis	MG
		Lambert–Eaton myasthenic syndrome	LEMS
Muscle	Duchenne muscular dystrophy		DMD
	Becker muscular dystrophy		BMD
	Facioscapulohumeral dystrophy		FSHD
	Limb–Girdle muscular dystrophies		LGMD
	Emery–Dreifuss dystrophy		EDD
	Oculopharyngeal muscular dystrophy		OPMD
	Myotonic dystrophy		DM
	Pompe's disease		PD
		Polymyositis	PM
		Dermatomyositis	DM
	Inclusion body myositis		IBM

Even if muscle weakness is a typical finding in several NMDs, a heterogeneous clinical scenario characterizes these conditions involving different organs and systems. Moreover, severe functional implications occur, forcing affected patients to be wheelchair-bound in advanced stages. As a consequence, both the pathology itself and the complex clinical management lead to a huge economic and social impact, also because in most of cases NMDs affect young people.

Although muscle impairment represents the main determinant, bone damage could play a role in the functional prognosis and consequently in the level of quality of life. From both physiological and pathological points of view, muscle and bone are connected by various pathways and mechanisms. The bone–muscle cross-talk includes several biological factors that could affect bone metabolism in NMDs independently of mechanical load.

Muscle tissue releases specific molecules, called myokines, that could interact with bone through different pathways. Myostatin, a transforming growth factor-beta (TGF-β) superfamily member, is a growth and differentiation factor highly expressed in muscle in pathological conditions leading to muscle atrophy. At the same time, myostatin modulates bone metabolism, promoting osteoclast differentiation and inducing bone loss (1).

On the other hand, muscle contraction promotes the release of bone protective molecules, including irisin, which stimulates osteoblasts and inhibits osteoclast activities through the NFkB signaling pathway, increasing cortical bone thickness and reducing the risk of fragility fractures in osteoporotic women (2, 3).

In this scenario, other players have been identified, such as β-aminoisobutyric acid (BAIBA) and musclin, which might improve bone accrual and prevent bone loss by activating osteoblast precursors and by inhibiting osteoclastogenesis (4, 5). Interestingly, the complexity of the biological interaction between muscle and bone is further supported by the evidence that about 50% of patients with inclusion body myositis caused by valosin-containing protein (VCP) gene mutation develop Paget's disease of bone (6).

Indeed, the VCP protein is implicated in membrane trafficking to facilitate the ubiquitin proteasome system in its function to eliminate aberrant proteins, and it also has a role in autophagy-mediated protein aggregation with its dysfunction leading to pathological aggregates in bone, muscle, and brain. These findings suggest a putative genetic susceptibility to bone metabolic disorders in NMDs (6).

Karasik et al. (7) identified three main periods, where this link occurs, including embryonic life, the postnatal period (allometric growth), and adult life (homeostatic relationship). This conceptual model will guide our review addressing the relationship between muscle and bone in the most common NMDs. However, in this review, we cannot include diabetic neuropathy because of the complexity of the pathophysiological mechanisms underneath bone damage in diabetic disease that is beyond the scope of this review.

EPIDEMIOLOGY

NMDs are rare diseases (prevalence $< 1/2000$) that require challenging management strategies in terms of diagnostic and therapeutic approaches to address several clinical and functional issues (8).

Although our knowledge and the diagnostic tools in NMDs have been improved during the last decades, the prevalence of these conditions has not significantly increased compared with the past (9). However, myotonic dystrophy (MD) has doubled its prevalence, probably due to the use of more accurate genetic tests. The age distribution of NMDs is quite variable. Some of these diseases have early onset in childhood, such as Duchenne muscular dystrophy (DMD) and congenital muscular dystrophies, while amyotrophic lateral sclerosis (ALS), post-polio syndrome (PPS), Lambert–Eaton myasthenic syndrome (LEMS), and inclusion body myositis (IBM) have an onset in adulthood. However, some NMDs are characterized by a uniform age distribution, namely, Charcot–Marie–Tooth disease (CMT), Guillain–Barré syndrome (GBS), myasthenia gravis (MG), facioscapulohumeral dystrophy (FSHD), and MD. Regarding gender distribution, most NMDs equally affect men and women. Nevertheless, ALS, chronic inflammatory demyelinating polyneuropathy (CIDP), GBS, LEMS, DMD and Becker muscular

dystrophies (BMD), and FSHD are more prevalent in males, whereas MG, polymyositis (PM), and dermatomyositis (DM) are more prevalent in females (10).

Although the prevalence of each NMD is very low worldwide, the early onset, the longer survival rates related to new available therapies, and the progressive worsening of the clinical conditions and physical performance impose a heavy social and economic burden. The costs of NMDs include medical expense, costs for the caregiver, and use of medical or external devices such as ventilators, orthoses, and wheelchairs for improving the clinical condition and the quality of life of affected individuals.

Per-patient medical costs for NMDs are more than double the estimated mean all-cause disability-associated healthcare expenditures (11) in particular, the costs are two times higher for DMD (12). The increase in healthcare costs depends not only on cardiorespiratory complications but also on bone damage along with a dramatic rise in costs related to fractures, particularly for patients affected by DMD who lose the ability to ambulate independently (13). The progressive loss of muscle power and strength and of the ability to stand up are associated with poor bone health and increased risk of falls, leading to higher rate of fragility fractures. For instance, in patients with spinal muscular atrophy (SMA), the prevalence of these fractures ranges from 9.3 to 46%, and they commonly occur at the distal femur (14). However, epidemiological data about fragility fractures are widely variable in various NMDs due to different patterns of disease progression. Indeed, in DMD patients, the prevalence of vertebral fractures (VFs), often undiagnosed, is estimated up to 30% commonly occurring in older, non-ambulatory patients, whereas limb fragility fractures (femur or tibia) affect from 20 to 60% of younger, ambulatory patients (15). However, VFs are strictly related to glucocorticoids (GCs) use considering that these drugs mainly affect the trabecular bone.

NMDs INVOLVING ANTERIOR HORN CELLS

SMA is a typical and clarifying example of anterior horn cells disease. This condition is an autosomal recessive disorder due to absence or low level of survival motor neuron protein codified by survival motor neuron genes (SMN 1 and 2) located on long arm chromosome 5. Homozygous deletion of SMN1 is diagnostic of SMA and the clinical variability depends on the SMN2 copy number that defines the level of protein produced (16).

Considering the embryonic period in the bone–muscle cross-talk, SMA genotypes characterized by deletions or point mutations regarding exons 6 and 7 of the SMN genes showed enhanced production of cytokines that stimulate the formation and activation of osteoclasts, resulting in increased bone resorption (17, 18). In the $Smn^{-/-}$SMN2 mouse model, a notable decrease of bone mineral density (BMD) and caudal vertebra alterations along with pelvic fractures compared to wild types were reported. Similarly, prenatal SMA 0 patients showed a phenotype characterized by reduced bone mass mainly due to decreased load on the fetal skeleton through reduction of fetal movement (19). However, also in the postnatal and adult period of bone–muscle cross-talk, skeletal involvement in SMA is strongly correlated to the severity of the muscular impairment [**Table 2**; (14, 19–22)].

Wassermann et al. reported low BMD in SMA patients, including one to three subtypes. In particular, patients affected by SMA 1, despite an initial improvement of lateral distal femur (LDF) BMD from 3 to 10 years old, exhibited BMD *Z*-scores declining during adolescence and, however, normal BMD values are never reached. On the contrary, patients affected by SMA 3 show a reduction of LDF-BMD later, as weight bearing declines. Furthermore, significantly increased fracture risk is reported in all subtypes, particularly for SMA 1, typically affecting lower limbs (14). A recent 36-month study investigating bone health in prepubertal SMA type 2 and 3 population showed low serum 25-OH vitamin D3 [25(OH)D], high serum parathyroid hormone (PTH), and bone resorption markers [C-terminal telopeptide (CTx)] with bone formation markers [bone-specific alkaline phosphatase (BSAP)] within normal ranges. Furthermore, low lumbar spine (LS) BMD and increased asymptomatic VFs were reported (21). In particular, Baranello et al. claimed that, in SMA patients, bone loss occurred regardless of muscle wasting, suggesting a multifactorial mechanism of bone involvement in this population.

Further studies are needed to define both the causes and the rate of progression of bone impairment in all subtypes of SMA patients. It would be interesting to investigate the efficacy of drugs (e.g., nusinersen) and gene therapy in improving bone density and preventing fragility fractures.

Beyond classic SMN1-related SMA, "SMA plus" or atypical SMA phenotypes, characterized by a distinct pattern of weakness and specific gene mutations, other than SMN, have been recently described. SMA plus includes some variants of antenatal SMA associated with skeletal abnormalities, in which arthrogryposis, osteopenia, and multiple fractures are typically present at birth associated with severe hypotonia (23). Fetal akinesia predisposes to multiple congenital contractures and contributes to abnormal intrauterine neuromuscular development (24).

For example, a premature variant of SMA with a mutation in two genes encoding part of activating signal cointegrator 1 (ASC-1) complex, a regulator of neuromuscular unit and probably of the adjacent bony structures, is responsible for congenital bone fractures (25).

NMDs INVOLVING PERIPHERAL NERVE

A typical peripheral nervous system disease that can potentially involve bone at various stages of life is the hereditary motor and sensor neuropathy or CMT.

This condition, occurring early in the first to third decade, is characterized by alterations of proteins involved in the structure and function of the peripheral nervous system; it includes axonal, demyelinating, and dominant intermediate variants, with a homogeneous clinical phenotype (26). Patients with CMT manifest symmetric, distal motor neuropathy associated with muscle weakness and atrophy, areflexia, and distal sensory loss. For CMT, there are no existing data reporting its role in bone health during fetal development. Indeed, CMT typically begins in childhood, and lower limbs are more affected, making walking

TABLE 2 | Classification of clinical variant of SMA.

Type	SNM2 Copy Number	Onset	Life Survival	Motor Milestones	Peculiar Findings	Bone Involvement
SMA 0	1	Prenatal	Weeks	None achieved	Severe hypotonia Respiratory distress at birth	Generalized osteopenia Bone deformities
SMA I (Werdnig–Hoffmann disease) 45% of cases	2–3	0–6 months	Death prior to age 2	Sit with support	Bell-shaped deformity of the chest "Frog-leg" lower limb posture Feeding problems (suck and/or swallowing)	Lowest aBMD *Z*-scores at all skeletal sites Higher fracture risk Osteoporosis*
SMA II 20% of cases	3	<18 months	70% alive at age 25 years	Independent sitting achieved by 9 months or delayed Never stand or walk independently	Postural tremor of fingers (minipolymyoclonus)	Increased bone resorption markers Low aBMD *Z*-scores at the LS and the LDF Fragility vertebral fractures
SMA III (Kugelberg–Welander disease) 30% of cases	3–4	IIIa 18 months−3 years IIIb 3–30 years	Normal	Independent ambulation	No available data	Increased bone resorption markers Low aBMD *Z*-scores at the LDF Asymptomatic vertebral fractures
SMA IV Less than 5% of cases	4 or more	Adulthood	Normal	Normal	No available data	No available data

**According to 2015 ISCD pediatric criteria; aBMD, areal bone mineral density; LS, lumbar spine; LDF, lateral distal femur.*

increasingly difficult. Beside the sensory-motor component, in CMT patients, several bone deformities (i.e., hip dysplasia and/or cavovarus foot) occur as well as a balance impairment resulting in increased risk of falls and fractures (27). There is little evidence of a role of CMT mutated genes during embryonic and postnatal periods. Therefore, children affected by CMT seem not predisposed to secondary osteoporosis, despite the muscle weakness, and to fragility fractures although bone deformities and balance impairment occur. On the other hand, in adult CMT patients, an increased fracture risk of 1.5-fold has been reported. Also, in this population, the increased risk of fractures mainly affects distal limbs and not the sites of major osteoporotic fractures (spine, hip, proximal humerus, and wrist). Nevertheless, fractures in adults with CMT are not considered depending on low BMD and are interpreted as high-energy trauma injury, occurring in the first year after diagnosis in uncommon osteoporotic sites (i.e., ankle, hand, foot) (28). Therefore, it is likely that even for adults with CMT, primary and secondary bone damage is not a determining factor for fracture risk, while muscle weakness and sensorial alterations are likely to affect gait performance and consequent increased risk of falls. Finally, no data are reported on the alteration of bone turnover and BMD during the time span of the disease.

NMDs INVOLVING NEUROMUSCULAR JUNCTION

Myasthenia gravis is an autoimmune NMD caused by autoantibodies against the acetylcholine receptor (AChR), and less frequently to MuSK protein (muscle-specific kinase) or the LRP4 (lipoprotein related protein 4), located on post-synaptic membrane of the skeletal muscles (29). Myasthenia gravis is characterized by an unexpected fluctuating clinical scenario with variable weakness distribution involving the ocular, bulbar, limb, and respiratory muscles (30). Considering the age of onset of clinical manifestation, MG is classified into juvenile MG (pre and post pubertal) and adult MG (early and late onset).

A significantly increased risk of osteoporosis in patients affected by MG has been demonstrated, with an HR of 1.52 in corticosteroid-naïve patients, whereas the corticosteroid-treated group had an HR of 2.37 (31).

Danikowski et al. hypothesized that enhanced bone resorption and myogenic proliferation inhibition in MG patients might be related to dysfunction of T-regulatory cells (Tregs) and overexpression of cytokines and chemokines, such as tumor necrosis factor-α (TNF-α), interleukin-6 (IL-6), and 10 (IL-10) (32, 33). Also genetic variants could be involved in the pathophysiological mechanisms of MG, resulting in heterogeneous phenotypes. A recent genome-wide association study of MG demonstrates the relationship between TNFRSF11A gene and MG. This gene encodes the receptor activator of nuclear factor-κ B (RANK) involved in both immune surveillance and osteoclastogenesis. In particular, mutations in TNFRSF11A are responsible for inherited forms of osteopetrosis and Paget's disease of bone and seem to be related to late-onset MG patients (34).

These data allow us to speculate on the primary bone damage that has been observed in the late-onset variant of MG associated with TNFRSF11A mutation. However, bone damage is associated with GC use in MG patients as well. Furthermore,

in this population, a high incidence of vitamin D deficiency and increased serum levels of bone resorption markers (i.e., CTx) were reported (35).

While bone involvement in MG is well described in adults, particularly in GC users, two variants of MG characterized by bone damage occurring in embryonic and postnatal periods, such as congenital and neonatal myasthenia (NM), have been identified: congenital myasthenia is an autosomal recessive inherited disorder of the childhood, resulting from choline acetyltransferase (ChAT) deficiency and postsynaptic anomalies.

Neonatal myasthenia affects newborn of women with MG due to the passive transfer of maternal autoantibodies, which recognize fetal acetylcholine receptors. Neonatal myasthenia is transitory and symptoms disappear after a maximum of a few weeks when the antibody titer decreases (36).

Sometimes, newborns affected by NM could manifest arthrogryposis multiplex congenita (AMC) caused by lack of fetal movement *in utero* with consequent multiple joint contractures and growth retardation. Ultrasonography evaluation of long bones in fetuses with AMC shows a hypomineralization and hypoechogenicity of long bones with osteopenia to support the role of muscle hypotonia on bone development (37).

NMDs INVOLVING SKELETAL MUSCLE STRUCTURE

A representative NMD involving skeletal muscle, characterized by genetic etiology and early disease onset, is DMD.

Duchenne muscular dystrophy is an X-linked disease caused by a mutation in the DMD gene that encodes dystrophin protein. Becker muscular dystrophy is an allelic X-linked variant of muscular dystrophy that leads to a reduction in dystrophin expression and a milder clinical phenotype (38).

In DMD, muscular impairment is symmetric and proximal, involving pelvic girdle that causes the classic clinical sign, Gower's maneuver, that indicates proximal lower limbs weakness (39).

Also, for DMD, the reduced biomechanical muscle strength and loss of independent ambulation cause bone alterations and secondary osteoporosis. In particular, structural changes at the myotendinous junctions, due to dystrophin complex alteration, are responsible for reduced force transmission and mechanical stimuli on bone tissue during muscular contraction with a detrimental effect on bone health (40). The main clinical consequences are bone fragility and higher risk of fracture. Because muscle weakness usually occurs at about 3–6 years old, in DMD patients, it is very likely that no bone damage is present at birth. Thus, we can believe that this disease interferes with muscle–bone cross-talk preferentially in the phase of allometric growth (41).

From a functional point of view, DMD children might not achieve or maintain the motor development milestones, and are compelled to use wheelchair in a few years. During the progression of disease, they became wheelchair-dependent usually at the age of 13 years with worsening of bone deformities and onset of scoliosis (42).

In association with mobility limitation, secondary osteoporosis in DMD patients is due to the prolonged use of GCs. This therapy is usually initiated at approximately 5 years of age, which has resulted in a significant improvement in the clinical and functional status, delaying the loss of independent ambulation. However, the use of deflazacort or prednisone at the dose of maximum 36 and 30 mg/day, respectively (0.75 mg/kg/day; 0.9 mg/kg/day), leads to a further worsening of bone health in terms of BMD and bone quality, through its direct and indirect effects (38). As a direct effect, GCs suppress bone formation by reducing osteoblast proliferation, differentiation, and function. GCs also influence the activity of osteocytes, mechanosensors of the bone, inducing apoptosis. Moreover, GCs increase the osteoclast activity and enhance the production of pro-inflammatory cytokines, such as IL-6. As an indirect effect, GCs inhibit gastrointestinal calcium absorption with a resultant fall in the ionized calcium concentration and the subsequent rise in serum PTH concentration. Finally, GCs play a role in the GH/IGF I axis and sex hormone axis, reducing IGF I and estrogen expression, respectively (43).

Fragility fracture risk in patients with DMD is significantly higher (44), with a fracture prevalence 5-fold higher compared with age-matched healthy young people (48 vs. 9%) with lower limb fractures (femur and tibia) more frequent in DMD. Most of the long-bone fractures in DMD patients are caused by low-energy trauma (i.e., fall from a standing position), an extremely rare condition in healthy young people. Long-bone fractures substantially contribute to functional and postural impairments, accelerating the transition to a wheelchair (45). Moreover, increased fracture risk of 75% (all skeletal sites) after 3 months of full wheelchair use has also been demonstrated (46). Finally, in GC-treated DMD patients, a moderate prevalence of symptomatic VFs (up to 40%) has been reported (47).

Joseph et al. showed a mean latency of 2.3 years to incur in symptomatic VFs after the beginning of the treatment (48). However, painful VFs are present in less than half of DMD patients, with these lesions frequently detected as asymptomatic incidental findings. Therefore, adequate follow-ups by performing spine radiograph are mandatory to have an early identification of the first fracture, as well as to monitor and prevent the occurrence of multiple VFs ("cascade fracturative"). Healthy children with VFs might show a spontaneous growing-mediated phenomenon, called vertebral reshaping, a vertebral restoration in height and width due to physiological bone remodeling. In children affected by several chronic illnesses such as DMD, the child's self-correcting reshaping mechanism fails to occur, but the administration of intravenous bisphosphonates (BPs) has been demonstrated to restore this process; therefore, when the fracture appears, antiresorptive drug treatment should start as early as possible (9, 49).

Further side effects of GC treatment are the impaired growth and delayed puberty due to hypogonadism caused by reduced testosterone serum level that compromises bone health (50). The role of testosterone on bone health is well established; direct and indirect mechanisms are mainly involved (51). First, low level of androgens causes muscle weakness that reduces mechanical stimulation on bones (52). Secondly, reduced activation of bone

androgen receptor by testosterone has a negative impact on the expression and function of the all three lines of bone-related cells (osteoblast, osteoclast, and osteocyte), resulting in an overall bone loss. Testosterone is also partially converted via aromatase into estrogens that play a crucial role in peak bone mass acquisition and in periosteal bone expansion during puberty in men (53).

NMDs INVOLVING SKELETAL MUSCLE METABOLISM

In the context of metabolic myopathies, Pompe's disease (PD) is an inherited NMD associated with low BMD and increased risk of fracture.

Pompe's disease is an autosomal recessive lysosomal storage disorder (LSD) due to mutations that cause reduction or absence of acid α-glucosidase (GAA gene on chromosome 17). This enzyme is ubiquitous in the body, and its reduction in activity leads to a progressive accumulation of glycogen within the lysosomes, and later between myofibrils, contributing to the clinical phenotype of skeletal, cardiac, and respiratory muscle involvement (54, 55). Two main forms of PD are described: infantile onset (IOPD, classic and non-classic variants) and late onset (LOPD), different in terms of organ involvement and the rate of progression. Severe muscle weakness and cardiac involvement characterize IOPD; on the contrary, a slow progression of limb–girdle muscle weakness and a respiratory dysfunction are typical of LOPD (56).

In both the PD variants, bone health is largely compromised, predisposing to an increased risk of osteoporosis or low bone mass for chronological age, strongly correlated to reduction of muscle strength (57).

In IOPD, severe muscle wasting negatively influences bone health in early phases of skeletal development, particularly at cortical sites, and consequently is associated with a higher risk of long-bone fractures (58). On the other hand, evidence of a higher prevalence of fragility fractures in LOPD patients is limited.

Exact pathogenetic mechanisms underneath muscle and bone relationship in LOPD patients are still unknown. These patients have different patterns of muscle involvement, commonly characterized by weakness of paravertebral, hip flexor, and knee extensor muscles that results in poor mechanical load applied to the spine and the proximal femur (59). The clinical phenotype of muscle impairment might explain the site-specific BMD loss (i.e., at LS and/or femoral neck). van den Berg showed a decreased BMD particularly in non-ambulatory and ventilator-dependent patients (54 vs. 15% in ambulant subjects) (58). The authors found a statistically significant positive mild-to-moderate correlation between total body less head (TBLH) BMD and proximal muscle strength of both the upper ($r = 0.37$) and lower extremities ($r = 0.43$). Moreover, this study suggested a putative role of prolonged inactivity and immobilization as risk factors for bone loss in these patients (58). These data were confirmed by Khan et al. who analyzed bone microarchitecture using high-resolution peripheral computed tomography (HR-pQCT) at two standard skeletal sites, distal radius and distal tibia (60).

Bertoldo et al. showed that asymptomatic and atraumatic VFs occur frequently in LOPD patients. However, the authors did not find any relationship between muscle function [assessed by Medical Research Council Scale (MRC), 6-min walking test (6MWT), and Gait, Stairs, Gower and Chair score (GSGC)] and BMD or biochemical markers of bone metabolism. No difference in muscle function, respiratory parameters, and serum 25(OH)D between patients with or without morphometric VF was also reported. Therefore, the authors conclude that bone involvement seems to be independent from muscular phenotype and vitamin D status in patients with LOPD (61).

With the introduction of the enzyme replacement therapy (ERT), the course of disease has been strongly modified, in particular for the IOPD variant, improving both muscle and respiratory functions. Otherwise, tangible effects of ERT in terms of improving bone health are poorly supported (62, 63).

To date, bone damage in PD is considered a consequence of muscle atrophy and reduction of weight bearing and load; furthermore, taking into account the severity of bone involvement in IOPD, a potential intrinsic bone mechanism directly linked to metabolic degeneration itself or to lysosome storage alteration is suggested.

BONE HEALTH ASSESSMENT IN NMDs

In the multidisciplinary and comprehensive management of patients affected by NMDs, the assessment of bone health status through clinical, instrumental, and laboratory testing should be integrated as a mandatory component in the evaluation of muscle impairment and functional independence.

Bone health screening in NMDs should include:

- Laboratory exams of bone metabolism such as serum and urinary calcium and phosphorus, serum parathyroid hormone (PTH), 25(OH)D, and alkaline phosphatase (ALP) (at the diagnosis and every 12 months);

- Imaging: lateral thoracolumbar spine radiographs at least every 12–36 months, taking into account drug therapy with detrimental effects on bone health (i.e., GCs), which require closer follow-ups. However, in case of referred low back pain, history of recent trauma, or spine BMD *Z*-score decline >0.5 SD in serial follow-ups, lateral thoracolumbar spine x-ray should be taken, to assess VFs.

- Dual-Energy X-ray Absorptiometry (DXA) to measure BMD and bone mineral content (BMC) considered as *Z*-score for children and *T*-score for adults over 50 years old and postmenopausal women (at the diagnosis and at least every 12 months). According to the International Society for Clinical Densitometry (ISCD), skeletal health assessment in children (between 5 and 19 years old) consists of DXA evaluation including posterior–anterior (PA) spine and total body less head (TBLH) scans for BMC and BMD measurements. However, these skeletal sites may not be suitable for densitometric assessment for all children affected by clinical conditions adversely involving bone health. Therefore, in recent ISCD Official Positions, additional DXA scans (proximal femur, PF, LDF, and distal forearm, DF) as well as the role of vertebral fracture assessment

(VFA) were thoroughly evaluated for utility, applicability, and ability to assess skeletal health and to predict fragility fractures in selected pediatric patients (44). Indeed, for many children with NMDs with poor ambulatory status and at risk of bone damage, these additional DXA scans are useful when TBLH or LS scans are not feasible (i.e., positioning issues, severe scoliosis).

Moreover, the occurrence and identification of spine fractures remain critical issues for skeletal health in individuals at risk of poor bone strength, including NMD patients. However, the most recent generation of DXA scanners provides a better resolution of lateral spine imaging compared to the past, thus allowing a safer bone health monitoring, by minimizing radiation exposure of children affected by NMDs.

The presence of at least one vertebral fragility fracture is sufficient for definition of osteoporosis in children. Moreover, an alternative diagnostic criterion in the same population includes densitometric assessment, namely, BMD *Z*-score ≤ -2.0 SD, combined with a clinically significant history of fracture (two or more long-bone fractures by 10 years of age and/or three or more long-bone fractures up to 19 years); BMD *Z*-score ≤ -2.0 SD without a history of fractures should be defined as low BMD for age and gender (64, 65). In men younger than 50 years or premenopausal women, the ISCD recommends the use of *Z*-scores; diagnosis of low BMD in this population is defined by a *Z*-score of ≤ -2.0 SD (the term "osteoporosis" should be avoided in these cases) (66, 67). In postmenopausal women and in men aged 50 years and older, osteoporosis may be appropriately diagnosed when LS, total hip, or femoral neck *T*-score is $\leq$-2.5 SD (BMD that lies -2.5 SD or more below the average value for young healthy individuals) (68).

Diagnosis of osteopenia includes LS, total hip, or femoral neck BMD *T*-score between -1.0 and -2.5 SD (**Table 3**) (69–73).

For the assessment of bone health in NMDs, nutritional assessment is advised, in particular for the pediatric population (74).

Nutrient requirement is different during the course of life, and monitoring their intake is useful also to better prevent underfeeding or overfeeding. Nutritional calcium intake, through specific questionnaires available online (https://www.iofbonehealth.org/calcium-calculator), is mandatory for bone health assessment, especially in NMDs.

Finally, sunlight exposure of a patient affected by NMD should be investigated, considering that 80% of vitamin D is produced by the skin under sunlight irradiation.

THERAPEUTIC OPPORTUNITIES

Non-pharmacological Therapies

Therapeutic management of patients affected by NMDs should take into account many clinical features that occur during the disease. Novel therapies available and better clinical approach to these patients lead to longer survival, allowing the observation of additional clinical issues previously poorly reported, in particular the progressive decline of bone health. Therefore, a tailored approach has to be implemented in terms of prevention and treatment of bone complications. Of prime importance, patients with NMDs should adopt a healthy lifestyle from as early an age as possible with the objective to optimally preserve musculoskeletal health. In this context, healthy lifestyle includes nutrition, sun exposure, and physical activity.

Nutrition has a pivotal role in musculoskeletal metabolism. In several NMD conditions, overnutrition is a major issue caused by an excess of caloric intake. The use of some drugs, such as corticosteroids (e.g., DMD patients), leads to an increased appetite, and the compassionate attitude of the caregiver could significantly contribute to weight gain (74). On the other hand, undernutrition is more common in severe and advanced stages of different NMDs due to dysphagia, delayed gastric emptying, prolonged mealtime, and constipation, all of them related to progressive muscle weakness (75). Therefore, an adequate caloric intake is mandatory in each stage of NMDs taking into account the proper proportion between protein and complex carbohydrates (76). A calcium-rich diet based on dairy products is strongly suggested, with a calcium intake of at least 1300 mg/day in patients aged 9–18 years, and 1000 mg day between 19 and 50 years old. The recommended dose of vitamin D for infants and children aged 0–1 year is at least 400 IU/day, while in children aged 1–18 years and in adults, the recommended dose is 600 IU/day (77). When patients do not reach the suggested intakes, it is necessary to consider calcium and vitamin D supplementations. Vitamin D status that requires supplementation in children is still debated; the Institute of Medicine (IOM) suggests serum 25(OH)D $<$20 ng/ml as threshold to start treatment, which is also the same recommendation to initiate treatment for adults (78).

Vitamin D supplementation is usually provided by cholecalciferol administration. However, in obese patients, particularly those treated with corticosteroids, higher doses of vitamin D are needed because of low bioavailability (79). Moreover, NMD patients usually receive other drugs metabolized in the liver by the CYP system involved in the hydroxylation of native vitamin D (e.g., corticosteroids and β-blockers); therefore, the use of calcifediol, a hydroxylated metabolite of vitamin D3 with higher bioavailability that does not require hepatic activation, should be considered. Furthermore, calcifediol is usually recommended in patients with malabsorption or hepatic disease, and when a rapid increase in serum 25(OH)D is required.

In patients affected by DMD, calcifediol administration at the dose of 0.8 mcg/kg daily per os plus adjustment of the dietary calcium intake, at least 1,000 mg/day, demonstrates a statistically significant increase of BMC and BMD in over 65% of patients and normalization of bone turnover markers (BTMs) in most patients (78.8%) (80). Therefore, periodic screening of the serum 25(OH)D is strongly suggested to monitor and, if indicated, adjust the supplementation of vitamin D. At the same time, it is possible to suggest a main role of vitamin D supplementation in the management of bone metabolism disorders in other NMDs. Moreover, considering the detrimental effects of vitamin D deficiency on muscle performance (81) as well as the encouraging data supporting calcifediol use for improving muscle function in different populations (82), a putative beneficial role of vitamin D administration on skeletal muscle in NMDs has been hypothesized. Indeed, Karam et al.

TABLE 3 | Bone health assessment in NMDs.

	NMDs	Bone turnover markers	DXA	Lateral toracolumbar spine radiograph
SMA (types 1–4)	Sitters	At the diagnosis and every 12 months	At the diagnosis and every 12 months	*If symptomatic
	Non-sitters			
CMT		At the diagnosis and every 12 months	At the diagnosis and eventually every 24 months	Not required
MG	On GC	At the diagnosis and every 12 months	At the diagnosis and every 12 months	*If symptomatic
	Not on GC		At the diagnosis and eventually every 24 months	
DMD	On GC	At the diagnosis and every 12 months	At the diagnosis and every 12 months	Every 1–2 years
	Not on GC			Every 2–3 years
PD	IOPD	At the diagnosis and every 12 months	At the diagnosis and every 12 months	*If symptomatic
	LOPD			

Presence of back pain or suspected vertebral fractures.

found an improvement of functional parameter in patients with ALS treated with high dose of cholecalciferol (83), although these results are not confirmed by a successive study (84).

Physical activity (PA) should be considered a cornerstone for the prevention and treatment of bone alterations in patients affected by NMDs. Despite the lack of evidence about the role of exercise on improving bone health in NMDs, the benefits of a tailored exercise program can be assumed.

Physical activity has a role in stimulating osteoblast bone formation and reducing osteoclast-mediated bone resorption through biological pathways modulated by mechanical loading (85). In particular, PA enhances attaining peak bone mass in childhood and adolescence, and contributes to bone turnover in adulthood (86). According to the WHO recommendation, children should perform PA for at least 60 min each day (87); however, most of NMD patients, even in the early ambulatory stages, do not reach these levels of PA (88).

Starting adequate PA as early as possible, considered as more than 3,000 accelerometer movement counts per minute (89) (about 5 metabolic equivalents, METs, corresponding to normal walking speed in children) (90), results in an improvement of 7 and 5% for the spine, and 6 and 4% for hip at 3 and 6 years, respectively, in terms of BMC (91). In patients with NMDs, dynamic low-moderate intensity weight-bearing exercises (i.e., walking) that result in greater gains in bone tissue compared to static activities are strongly recommended (92). There is no evidence that performing high-intensity exercise provides greater benefit than performing moderate-intensity exercise; on the contrary, NMD patients should avoid heavy exercises to prevent fatigue (93). In DMD patients, strengthening exercises, such arms and legs cycle in 30-min sessions (15 min for arms and 15 min for legs), 5 days per week, reduce muscle disuse atrophy and excessive functional loss (94).

Moreover, balance disorders are frequently reported in patients with NMDs. In particular, it has been demonstrated that patients with proximal muscle weakness (i.e., DMD) show more difficulties in static balance, while patients with primarily distal muscle involvement (i.e., CMT) show more difficulties in dynamic balance. Exercises to maintain muscle strength that improve balance when performing both static and dynamic activities reduce the risk of fall (95).

Pharmacological Therapies

Bisphosphonates

In association with a proper lifestyle, with the aim to improve bone strength and reduce the risk of fractures, the use of pharmacological treatment is advisable. Anti-osteoporotic drugs, such as BPs, are widely used in postmenopausal and GC-induced osteoporosis (GIO). Bisphosphonates have a high affinity to bone tissue, and they are capable of inhibiting bone resorption in humans, mainly leading to osteoclast apoptosis with different mechanisms of action (96). The use of antiresorptive drugs has been already investigated in children; in particular, BPs have been demonstrated to have efficacy and safety in patients affected by other rare diseases, such as Paget disease of bone (97, 98), osteogenesis imperfecta (OI) (99), β-thalassemia (100), and overall secondary osteoporosis in children (101). Limited evidence supports the use of BPs in NMDs. To date, an abstract recently presented at the 101st Annual Meeting of the Endocrine Society including four children affected by SMA on intravenous BPs therapy (102) showed no significant change in BMD at 1 year follow-up; the authors also reported some mild adverse events and one atypical femur fracture. In MG, the use of oral alendronate (70 mg/week) in a patient under GC treatment improved the LS BMD of 3.4% after 12 months without side effects (103). However, caution should be paid for possible exacerbation of MG symptoms, such as muscle weakness and extreme fatigue, after drug administration (104).

In a case report of an osteoporotic patient, symptoms of MG were exacerbated by the administration of risedronate (105);

however, the exact mechanism underneath this pathological condition remains unclear.

Recent care recommendations endorse the use of intravenous BPs as first-line therapy for the treatment of osteoporosis in DMD patients with fragility fractures of the spine or long bones (72, 106). Moreover, the administration of oral alendronate or risedronate (107) and intravenous pamidronate or zoledronic acid (106) seems to reduce back pain in patients affected by VF. The role of BPs for primary prevention of fragility fractures in DMD as for the other NMDs is still debated.

Denosumab

Denosumab (Dmab), a fully human IgG2 monoclonal antibody that neutralizes the receptor activator of nuclear factor kappa-B ligand (RANKL), is the most potent antiresorptive agent available in clinical practice. It blocks the interaction between the cytokine and its receptor (RANK), inhibiting osteoclast-mediated bone resorption. Approved by the FDA for postmenopausal osteoporotic women at high risk of fracture, Dmab reduces the risk of vertebral and non-vertebral fractures compared to placebo (108) and improves BMD compared to BPs (109).

To the best of our knowledge, few anecdotal studies demonstrate the effectiveness of Dmab in NMDs.

A case report in a 14-year-old patient affected by SMA II showed an improvement of LS BMD of 19% after 6 months of 60 mg s.c. of Dmab without adverse effects (110). The same dosage of Dmab increased significantly LS BMD (about 16%) at 12 months in a 13-year-old boy with DMD and GIO (111).

Teriparatide

Teriparatide is a recombinant human parathyroid hormone 1–34 (rhPTH 1–34) stimulating bone formation. It is widely used in postmenopausal women at high risk of fracture and in GIO (112). Despite its potential benefits, in particular on trabecular bone in NMD patients with VF on GC therapy, its use is reserved for selected patients. In particular, the safety of teriparatide has not been established in pediatric patients due to the high risk of osteosarcoma (113). However, to date, a single case report shows improvement of the LS *Z*-score BMD, back pain, and quality of life in a DMD patient with multiple VFs in GC treatment after the administration of 20 mcg once daily of s.c. teriparatide (114).

CONCLUSIONS

NMDs are a group of disorders characterized by skeletal muscle wasting that usually affect different organs and systems, including bone. Muscle–bone cross-talk plays a key role in the pathophysiological mechanisms that result in predictable clinical phenotypes. However, this relationship is often underestimated until a fracture occurs. Instead, it is essential that the biological and functional link between muscle and bone is investigated across the three phases of bone development, including the embryonic life, the postnatal period, and the adult life. Physicians who treat adult patients with NMDs with chronic GCs should consider the administration of anti-osteoporotic medications to prevent fragility fractures, although no such formal recommendation currently exists for pediatric patients.

AUTHOR CONTRIBUTIONS

GI and AM contributed to conception and design of the review. MP, SL, and CC wrote the first draft of the manuscript. All authors wrote sections of the manuscript, contributed to manuscript revision, and read and approved the submitted version.

ACKNOWLEDGMENTS

The authors would like to acknowledge VAnviteLli pEr la RicErca (VALERE) program for the allocation of funding that aims to publish University of Campania "Luigi Vanvitelli" research products.

REFERENCES

1. Qin Y, Peng Y, Zhao W, Pan J, Ksiezak-Reding H, Cardozo C, et al. Myostatin inhibits osteoblastic differentiation by suppressing osteocyte-derived exosomal microRNA-218: a novel mechanism in muscle-bone communication. *J Biol Chem.* (2017) 292:11021–11033. doi: 10.1074/jbc.M116.770941
2. Colaianni G, Mongelli T, Cuscito C, Pignataro P, Lippo L, Spiro G, et al. Irisin prevents and restores bone loss and muscle atrophy in hind-limb suspended mice. *Sci Rep.* (2017) 7:2811. doi: 10.1038/s41598-017-02557-8
3. Colaianni G, Cuscito C, Mongelli T, Pignataro P, Buccoliero C, Liu P, et al. The myokine irisin increases cortical bone mass. *Proc Natl Acad Sci USA.* (2015) 112:12157–62. doi: 10.1073/pnas.1516622112
4. Kitase Y, Vallejo JA, Gutheil W, Vemula H, Jähn K, Yi J, et al. β-aminoisobutyric Acid, l-BAIBA, is a muscle-derived osteocyte survival factor. *Cell Rep.* (2018) 22:1531–44. doi: 10.1016/j.celrep.2018.01.041
5. Subbotina E, Sierra A, Zhu Z, Gao Z, Koganti SR, Reyes S, et al. Musclin is an activity-stimulated myokine that enhances physical endurance. *Proc Natl Acad Sci USA.* (2015) 112:16042–7. doi: 10.1073/pnas.1514250112
6. Kimonis V. Inclusion body myopathy with paget disease of bone and/or frontotemporal Dementia. In: Adam MP, Ardinger HH, Pagon RA, Wallace SE, Bean LJH, Stephens K, Amemiya A, editors. *GeneReviews®*. Seattle, WA: University of Ashington (2007). p. 1993–2019.
7. Karasik D, Kiel DP. Genetics of the musculoskeletal system: a pleiotropic approach. *J Bone Miner Res.* (2008) 23:788–802. doi: 10.1359/jbmr.080218
8. Feldman EL, Callaghan BC, Pop-Busui R, Zochodne DW, Wright DE, Bennett DL, et al. Diabetic neuropathy. *Nat Rev Dis Primers.* (2019) 5:41. doi: 10.1038/s41572-019-0092-1
9. Emery AE. Population frequencies of inherited neuromuscular diseases–a world survey. *Neuromuscul Disord.* (1991) 1:19–29. doi: 10.1016/0960-8966(91)90039-U
10. Deenen JC, Horlings CG, Verschuuren JJ, Verbeek AL, van Engelen BG. The epidemiology of neuromuscular disorders: a comprehensive overview of the literature. *J Neuromuscul Dis.* (2015) 2:73–85. doi: 10.3233/JND-140045
11. Larkindale J, Yang W, Hogan PF, Simon CJ, Zhang Y, Jain A, et al. Cost of illness for neuromuscular diseases in the United States. *Muscle Nerve.* (2014) 49:431–8 doi: 10.1002/mus.23942
12. Available online at: https://www.cdc.gov/ncbddd/disabilityandhealth/data-highlights.html
13. Ryder S, Leadley RM, Armstrong N, Westwood M, de Kock S, Butt T, et al. The burden, epidemiology, costs and treatment for Duchenne muscular dystrophy: an evidence review. *Orphanet J Rare Dis.* (2017) 12:79. doi: 10.1186/s13023-017-0631-3

14. Wasserman HM, Hornung LN, Stenger PJ, Rutter MM, Wong BL, Rybalsky I, et al. Low bone mineral density and fractures are highly prevalent in pediatric patients with spinal muscular atrophy regardless of disease severity. *Neuromuscul Disord*. (2017) 27:331–7. doi: 10.1016/j.nmd.2017.01.019
15. Ma J, McMillan HJ, Karagüzel G, Goodin C, Wasson J, Matzinger MA, et al. The time to and determinants of first fractures in boys with Duchenne muscular dystrophy. *Osteoporos Int*. (2017) 28:597–608. doi: 10.1007/s00198-016-3774-5
16. Arnold WD, Kassar D, Kissel JT. Spinal muscular atrophy: diagnosis and management in a new therapeutic era. *Muscle Nerve.* (2015) 51:157–67. doi: 10.1002/mus.24497
17. Kurihara N, Menaa C, Maeda H, Haile DJ, Reddy SV. Osteoclast-stimulating factor interacts with the spinal muscular atrophy gene product to stimulate osteoclast formation, *J Biol Chem.* (2001) 276:41035–9. doi: 10.1074/jbc.M100233200
18. Shanmugarajan S. Congenital bone fractures in spinal muscular atrophy: functional role for SMN protein in bone remodeling. *J Child Neurol.* (2007) 22:967–73. doi: 10.1177/0883073807305664
19. Prior TW, Finanger E. Spinal muscular atrophy. In: Adam MP, Ardinger, HH, Pagon RA, Wallace SE, Bean LJH, Stephens K, Amemiya A, editors. *GeneReviews*®. Seattle, WA: University of Washington (2000). p. 1993–2019.
20. Singh A, Dalal P, Singh J, Tripathi P. Type 0 spinal muscular atrophy in rare association with congenital contracture and generalized osteopenia. *Iran J Child Neurol.* (2018) 12:105–8.
21. Baranello G, Vai S, Broggi F, Masson R, Arnoldi MT, Zanin R, et al. Evolution of bone mineral density, bone metabolism and fragility fractures in Spinal Muscular Atrophy (SMA) types 2 and 3. *Neuromuscul Disord*. (2019) 29:525–32. doi: 10.1016/j.nmd.2019.06.001
22. Vai S, Bianchi ML, Moroni I, Mastella C, Broggi F, Morandi L, et al. Bone and spinal muscular atrophy. *Bone*. (2015) 79:116–20. doi: 10.1016/j.bone.2015.05.039
23. Teoh HL, Carey K, Sampaio H, Mowat D, Roscioli T, Farrar M. Inherited paediatric motor neuron disorders: beyond spinal muscular atrophy. *Neural Plast*. (2017) 2017:6509493. doi: 10.1155/2017/6509493
24. Bamshad M, Van Heest AE, Pleasure D. Arthrogryposis: a review and update. *J Bone Joint Surg Am.* (2009) 91(Suppl. 4):40–6. doi: 10.2106/JBJS.I.00281
25. Knierim E, Hirata H, Wolf NI, Morales-Gonzalez S, Schottmann G, Tanaka Y, et al. Mutations in subunits of the activating signal cointegrator 1 complex are associated with prenatal spinal muscular atrophy and congenital bone fractures. *Am J Hum Genet.* (2016) 98: 473–89. doi: 10.1016/j.ajhg.2016.01.006
26. Vallat JM, Mathis S, Funalot B. The various Charcot-Marie-Tooth diseases. *Curr Opin Neurol.* (2013) 26:473–80. doi: 10.1097/WCO.0b013e328364c04b
27. Bird TD. Charcot-Marie-Tooth (CMT) hereditary neuropathy overview. In: Adam MP, Ardinger HH, Pagon RA, Wallace SE, Bean LJH, Stephens K, Amemiya A, editors. *GeneReviews*®. (1998).
28. Pouwels S, de Boer A, Leufkens HG, Weber WE, Cooper C, de Vries F, Risk of fracture in patients with Charcot-Marie-Tooth disease, *Muscle Nerve.* (2014) 50:919–24. doi: 10.1002/mus.24240
29. Gilhus NE, Verschuuren JJ. Myasthenia gravis: subgroup classification and therapeutic strategies. *Lancet Neurol.* (2015) 14:1023–36. doi: 10.1016/S1474-4422(15)00145-3
30. Berrih-Aknin S, Frenkian-Cuvelier M, Eymard B. Diagnostic and clinical classification of autoimmune myasthenia gravis. *J Autoimmun*. (2014) 48–49:143–8. doi: 10.1016/j.jaut.2014.01.003
31. Yeh JH, Chen HJ, Chen YK, Chiu HC, Kao CH. Increased risk of osteoporosis in patients with myasthenia gravis: a population-based cohort study. *Neurology*. (2014) 83:1075–9. doi: 10.1212/WNL.0000000000000804
32. Danikowski KM, Jayaraman S, Prabhakar BS. Regulatory T cells in multiple sclerosis and myasthenia gravis. *Neuroinflammation*. (2017) 14:117. doi: 10.1186/s12974-017-0892-8
33. Meyer SU, Krebs S, Thirion C, Blum H, Krause S, Pfaffl MW. Tumor necrosis factor alpha and insulin-like growth factor 1 induced modifications of the gene expression kinetics of differentiating skeletal muscle cells. *PLoS ONE*. (2015) 10:e0139520 doi: 10.1371/journal.pone.0139520
34. Renton AE, Pliner HA, Provenzano C, Evoli A, Ricciardi R, Nalls MA, et al. A genome-wide association study of myasthenia gravis. *JAMA Neurol.* (2015) 72:396–404. doi: 10.1001/jamaneurol.2014.4103
35. Guan Y, Lv F, Meng Y, Ma D, Xu X, Song,Y, et al. Association between bone mineral density, muscle strength, and vitamin D status in patients with myasthenia gravis: a cross-sectional study. *Osteoporosis Int*. (2017) 28:2383–90. doi: 10.1007/s00198-017-4041-0
36. Peragallo JH. Pediatric Myasthenia Gravis. *Sem Pediatr Neurol.* (2017) 24:116–21. doi: 10.1016/j.spen.2017.04.003
37. Murphy JC, Neale D, Bromley B, Benacerra BR, Copel JA. Hypoechogenicity of fetal long bones: a new ultrasound marker for arthrogryposis. *Prenat Diagn*. (2002) 22:1219–22. doi: 10.1002/pd.492
38. Darras BT, Urion DK, Ghosh PS. Dystrophinopathies, dystrophinopathies. In: Adam MP, Ardinger HH, Pagon RA, Wallace SE, Bean LJH, Stephens K, Amemiya A, editors. *GeneReviews*® (2000).
39. Guzmán ORC, García ALC, Cruz MR. Muscular dystrophies at different ages: metabolic and endocrine alterations. *Int J Endocrinol*. (2012) 2012:485376. doi: 10.1155/2012/485376
40. Welser JV, Rooney JE, Cohen NC, Gurpur PB, Singer CA, Evans RA, et al. Myotendinous junction defects and reduced force transmission in mice that lack alpha7 integrin and utrophin. *Am J Pathol.* (2009) 175:1545–54. doi: 10.2353/ajpath.2009.090052
41. Sarrazin E, von der Hagen M, Schara U, von Au K, Kaindl AM. Growth and psycomotor development of patients with Duchenne muscular dystrophy. *Eur J Pediatr Neurol.* (2014) 18:38–44. doi: 10.1016/j.ejpn.2013.08.008
42. Perera N, Farrar M. Bone health in children with duchenne muscular dystrophy: a review. *Pediat Therapeut.* (2015) 5:252. doi: 10.4172/2161-0665.1000252
43. Canalis E, Mazziotti G, Giustina A, Bilezikian JP. Glucocorticoid-induced osteoporosis: pathophysiology and therapy. *Osteoporos Int.* (2007) 18:1319–28. doi: 10.1007/s00198-007-0394-0
44. Weber DR, Boyce A, Gordon C, Högler W, Kecskemethy HH, Misra M, et al. The utility of DXA assessment at the forearm, proximal femur, and lateral distal femur, and vertebral fracture assessment in the pediatric population: the 2019 official pediatric positions of the ISCD. *J Clin Densitom*. (2019). doi: 10.1016/j.jocd.2019.07.002. [Epub ahead of print].
45. Ness K, Apkon SD. Bone health in children with neuromuscular disorders. *J Pediatr Rehabil Med*. (2014) 7:133–42. doi: 10.3233/PRM-140282
46. James KA, Cunniff C, Apkon SD, Mathews K, Lu Z, Holtzer C, et al. Risk factors for first fractures among males with duchenne or becker muscular dystrophy. *J Pediatr Orthopaed.* 35:640–44. doi: 10.1097/BPO.0000000000000348
47. Buckner JL, Bowden SA, Mahan JD. optimizing bone health in duchenne muscular dystrophy. *Int J Endocrinol*. (2015) 2015:928385 doi: 10.1155/2015/928385
48. Joseph S, Wang C, Di Marco M, Horrocks I, Abu-Arafeh I, Baxter A, et al. Fractures and bone health monitoring in boys with Duchenne muscular dystrophy managed within the Scottish Muscle Network. *Neuromuscul Disord.* (2019) 29:59–66 doi: 10.1016/j.nmd.2018.09.005
49. Petty R, Laxer RM, Lindsley CB, Wedderburn LR (eds.). *Textbook of Pediatric Rheumatology, 7th edn*. Philadelphia: Elsevier (2016).
50. Birnkrant DJ, Bushby K, Bann CM, Apkon SD, Blackwell A, Brumbaugh D, et al. DMD Care Considerations Working Group, Diagnosis and management of Duchenne muscular dystrophy, part 1: diagnosis, and neuromuscular, rehabilitation, endocrine, and gastrointestinal and nutritional management. *Lancet Neurol.* (2018) 17:251–67. doi: 10.1016/S1474-4422(18)30024-3
51. Golds G, Houdek D, Arnason T. Male hypogonadism and osteoporosis: the effects, clinical consequences, and treatment of testosterone deficiency in bone health. *Int J Endocrinol.* (2017) 2017:4602129. doi: 10.1155/2017/4602129
52. Kao KT, Joseph S, Capaldi N, Brown S, Di Marco M, Dunne J, et al. Skeletal disproportion in glucocorticoid-treated boys with Duchenne muscular dystrophy. *Eur J Pediatr.* (2019) 178:633–40. doi: 10.1007/s00431-019-03336-5

53. Vanderschueren D, Laurent MR, Claessens F, Gielen E, Lagerquist MK, Vandenput L, et al. Sex steroid actions in male bone. Endocr Rev. (2014) 35:906–60. doi: 10.1210/er.2014-1024
54. Hirschhorn R., Reuser A. Glycogen storage disease type II: acid alphaglucosidase (acid maltase) deficiency. In: Scriver C, Beaudet A, Sly W, Valle D, editors. *The Metabolic and Molecular Bases of Inherited Disease.* 8th ed. New York, NY: McGraw-Hill (2001). p. 3389–420.
55. Kishnani PS, Steiner RD, Bali D, Berger K, Byrne BJ, Case LE, et al. Pompe disease diagnosis and management guideline. *Genet Med.* (2006) 8:267–88. doi: 10.1097/01.gim.0000218152.87434.f3
56. Katzin LW, Amato AA. Pompe disease: a review of the current diagnosis and treatment recommendations in the Era of enzyme replacement therapy. *J Clin Neuromusc Dis.* (2008) 9:421–31. doi: 10.1097/CND.0b013e318176dbe4
57. van den Berg LE, Zandbergen AA, van Capelle CI, de Vries JM, Hop WC, van den Hout JM, et al. Low bone mass in Pompe disease: muscular strength as a predictor of bone mineral density. *Bone.* (2010) 47:643–9. doi: 10.1016/j.bone.2010.06.021
58. van den Berg LEM. *The Musculoskeletal System in Pompe Disease: Pathology, Consequences and Treatment Options*. Erasmus University Rotterdam (2014). Available online at: http://hdl.handle.net/1765/51599
59. Case LE, Kishnani PS. Physical therapy management of Pompe disease. *Genet Med.* (2006) 8 318–27. doi: 10.1097/01.gim.0000217789.14470.c5
60. Khan A, Weinstein Z, Hanley DA, Casey R, McNeil C, Ramage B, et al. *In vivo* bone architecture in Pompe disease using high-resolution peripheral computed tomography. *JIMD Rep*. (2013) 7:81–8. doi: 10.1007/8904_2012_146
61. Bertoldo F, Zappini F, Brigo M, Moggio M, Lucchini V, Angelini C, et al. Prevalence of asymptomatic vertebral fractures in late-onset pompe disease. *J Clin Endocrinol Metab.* (2015) 100:401–6. doi: 10.1210/jc.2014-2763
62. Papadimas G, Terzis G, Papadopoulos C, Areovimata A, Spengos K, Kavouras S, et al. Bone density in patients with late onset pompe disease. *Int J Endocrinol Metab.* (2012) 10:599–603. doi: 10.5812/ijem.4967
63. Sheng B, Chu YP, Wong WT, Yau EKC, Chen SPL, Luk WH. Improvement of bone mineral density after enzyme replacement therapy in Chinese late-onset Pompe disease patients. *BMC Res Notes.* (2017) 10:351. doi: 10.1186/s13104-017-2681-y
64. Gordon CM, Leonard MB, Zemel BS. 2013 Pediatric Position Development Conference: executive summary and reflections. *J Clin Densitom.* (2014) 17:219–24. doi: 10.1016/j.jocd.2014.01.007
65. Yasar E, Adigüzel E, Arslan M, Matthews DJ. Basics of bone metabolism and osteoporosis in common pediatric neuromuscular disabilities. *Eur J Paediatr Neurol.* (2018) 22:17–26. doi: 10.1016/j.ejpn.2017.08.001
66. Papaioannou A, Morin S, Cheung AM, Atkinson S, Brown JP, Feldman S, et al. Scientific Advisory Council of Osteoporosis Canada; 2010 clinical practice guidelines for the diagnosis and management of osteoporosis in Canada: summary. *CMAJ.* (2010) 182:1864–73. doi: 10.1503/cmaj.100771
67. Shepherd JA, Schousboe JT, Broy SB, Engelke K, Leslie WD. Executive summary of the 2015 ISCD position development conference on advanced measures From DXA and QCT: fracture prediction beyond BMD. *J Clin Densitom.* (2015) 18:274–86. doi: 10.1016/j.jocd.2015.06.013
68. Jeremiah MP, Unwin BK, Greenawald MH, Casiano VE. Diagnosis and management of osteoporosis. *Am Fam Physician.* (2015) 92:261–8.
69. World Health Organization (WHO). *WHO Scientific Group on the Assessment of Osteoporosis at Primary Health Care Level: Summary Meeting Report*. (2019). Available online at: http://www.who.int/chp/topics/Osteoporosis.pdf (accessed August 25, 2019).
70. Mercuri E, Finkel RS, Muntoni F, Wirth B, Montes J, Main M, et al. SMA Care Group, Diagnosis and management of spinal muscular atrophy: Part 1: recommendations for diagnosis, rehabilitation, orthopedic and nutritional care. *Neuromuscul Disord.* (2018) 28:103–15. doi: 10.1016/j.nmd.2017.11.005
71. Ilias I, Zoumakis E, Ghayee H. An overview of glucocorticoid induced osteoporosis. In: Feingold KR, Anawalt B, Boyce A, Chrousos G, Dungan K, Grossman A, Hershman JM, Kaltsas G, Koch C, Kopp P, Korbonits M, McLachlan R, Morley JE, New M, Perreault L, Purnell J, Rebar R, Singer F, Trence DL, Vinik A, Wilson DP, editors. *Endotext* (2018).
72. Birnkrant DJ, Bushby K, Bann CM. Diagnosis and management of Duchenne muscular dystrophy, part 2: respiratory, cardiac, bone health, and orthopaedic management. *Lancet Neurol.* (2018) 17:347–61. doi: 10.1016/S1474-4422(18)30025-5
73. Cupler EJ, Berger KI, Leshner RT, Wolfe GI, Han JJ, Barohn RJ, et al. the AANEM consensus committee on late-onset pompe disease, consensus treatment recommendations for late-onset pompe disease. *Muscle Nerve.* (2012) 45:319–33. doi: 10.1002/mus.22329
74. Salera S, Menni F, Moggio M, Guez S, Sciacco M, Esposito S. Nutritional challenges in duchenne muscular dystrophy. *Nutrients*. (2017) 9:594. doi: 10.3390/nu9060594
75. Messina S, Pane M, De Rose P, Vasta I, Sorleti D, Aloysius A, et al. Feeding problems and malnutrition in spinal muscular atrophy type II. *Neuromuscul. Disord.* (2008) 18:389–93. doi: 10.1016/j.nmd.2008.02.008
76. Bianchi ML, Biggar D, Bushby K, Rogol AD, Rutter MM, Tseng B. Endocrine aspect of Duchenne muscular dystrophy. *Neuromuscul Disord*. (2011) 21:298–303. doi: 10.1016/j.nmd.2011.02.006
77. Holick MF, Binkley NC, Bischoff-Ferrari HA, Gordon CM, Hanley DA, Heaney RP, et al. Endocrine society. evaluation, treatment, and prevention of vitamin d deficiency: an endocrine society clinical practice guideline. *Clin Endocrinol Metab*. (2011) 96:1911–30. *J Clin Endocrinol Metab.* (2011) 96:3908. doi: 10.1210/jc.2011-0385
78. Institute of Medicine (US). Committee to Review Dietary Reference Intakes for Vitamin D and Calcium. In: Ross AC, Taylor CL, Yaktine AL, Del Valle HB, editors. *Dietary Reference Intakes for Calcium and Vitamin D*. Washington, DC: National Academies Press (2011). p. 365–402.
79. Bian Q, McAdam L, Grynpas M, Mitchell J, Harrington J. Increased rates of Vitamin D insufficiency in boys with duchenne muscular dystrophy despite higher Vitamin D3 supplementation. *Glob Pediatr Health*. (2019) 6:2333794X19835661. doi: 10.1177/2333794X19835661
80. Bianchi ML, Morandi L, Andreucci E, Vai S, Frasunkiewicz J, Cottafava R. Low bone density and bone metabolism alterations in Duchenne muscular dystrophy: response to calcium and vitamin D treatment. *Osteoporos Int*. (2011) 22:529–39. doi: 10.1007/s00198-010-1275-5
81. Iolascon G, Mauro GL, Fiore P, Cisari C, Benedetti MG, Panella L, et al. Can vitamin D deficiency influence muscle performance in postmenopausal women? A multicenter retrospective study. *Eur J Phys Rehabil Med*. (2018) 54:676–82. doi: 10.23736/S1973-9087.17.04533-6
82. Iolascon G, Moretti A, de Sire A, Calafiore D, Gimigliano F. Effectiveness of calcifediol in improving muscle function in post-menopausal women: a prospective cohort study. *Adv Ther*. (2017) 34:744–52. doi: 10.1007/s12325-017-0492-0
83. Karam C, Barrett MJ, Imperato T, MacGowan DJ, Scelsa S. Vitamin D deficiency and its supplementation in patients with amyotrophic lateral sclerosis. *J Clin Neurosci*. (2013) 20:1550–3. doi: 10.1016/j.jocn.2013.01.011
84. Libonati L, Onesti E, Gori M.C, Ceccanti M, Cambieri C, Fabbri A, et al. VitaminD in amyotrophic lateral sclerosis. *Funct. Neurol*. (2017) 32:35–40. doi: 10.11138/FNeur/2017.32.1.035
85. Takata S, Yasui N. Disuse osteoporosis. *J Med Investig.* (2001) 48:147–56. doi: 10.1016/s0140-6736(63)91031-6
86. Weaver CM, Gordon CM, Janz KF, Kalkwarf HJ, Lappe JM, Lewis R, et al. The National Osteoporosis Foundation's position statement on peak bone mass development and lifestyle factors: a systematic review and implementation recommendations. *Osteoporos Int.* (2016) 27:1281–386. doi: 10.1007/s00198-015-3440-3
87. World Health Organization. *Global Recommendations on Physical Activity for Health.* Geneva: WHO (2010).
88. Heutinck L, Kampen NV, Jansen M, Groot IJ. Physical activity in boys with duchenne muscular dystrophy is lower and less demanding compared to healthy boys. *J Child Neurol.* (2017) 32:450–7. doi: 10.1177/0883073816685506
89. Pulsford RM, Cortina-Borja M, Rich C, Kinnafick FE, Dezateux C, Griffiths LJ. Actigraph accelerometer-defined boundaries for sedentary behaviour and physical activity intensities in 7 year old children. *PLoS ONE.* (2011) 6:e21822 doi: 10.1371/journal.pone.0021822
90. Evenson KR, Catellier DJ, Gill K, Ondrak KS, McMurray RG. Calibration of two objective measures of physical activity for children. *J Sports Sci*. (2008) 26:1557–65. doi: 10.1080/02640410802334196

91. Janz KF, Letuchy EM, Eichenberger Gilmore JM, Burns TL, Torner JC, Willing MC, et al. Early physical activity provides sustained bone health benefits later in childhood. *Med Sci Sports Exerc.* (2010) 42:1072–8. doi: 10.1249/MSS.0b013e3181c619b2
92. Bell JM, Shields MD, Watters J, Hamilton A, Beringer T, Elliott M, et al. Interventions to prevent and treat corticosteroid-induced osteoporosis and prevent osteoporotic fractures in Duchenne muscular dystrophy. *Cochrane Database Syst Rev.* (2017) 1:CD010899. doi: 10.1002/14651858.CD010899.pub2
93. Abresch RT, Carter GT, Han J, McDonald CM. Exercise in neuromuscular diseases. *Phys Med Rehabil Clin N Am.* (2012) 23:653–73. doi: 10.1016/j.pmr.2012.06.001
94. Jansen M, de Groot IJ, van Alfen N, Geurts ACh. Physical training in boys with Duchenne muscular dystrophy: the protocol of the No Use is Disuse study. *BMC Pediatr.* (2010) 10:55. doi: 10.1186/1471-2431-10-55
95. Kaya P, Alemdaroglu I, Yilmaz Ö, Karaduman A, Topaloglu H. Effect of muscle weakness distribution on balance in neuromuscular disease. *Pediatr Int.* (2015) 57:92–7. doi: 10.1111/ped.12428
96. Russell RG, Watts NB, Ebetino FH, Rogers MJ Mechanisms of action of bisphosphonates: similarities and differences and their potential influence on clinical efficacy. *Osteoporos Int*. (2008) 19:733–59. doi: 10.1007/s00198-007-0540-8
97. Merlotti D, Rendina D, Gennari L, Mossetti G, Gianfrancesco F, Martini G, et al. Comparison of intravenous and intramuscular neridronate regimens for the treatment of Paget disease of bone. *J Bone Miner Res.* (2011) 26:512–8. doi: 10.1002/jbmr.237
98. Merlotti D, Gennari L, Martini G, Valleggi F, De Paola V, Avanzati A, et al. Comparison of different intravenous bisphosphonate regimens for Paget's disease of bone. *J Bone Miner Res.* (2007) 22:1510–7. doi: 10.1359/jbmr.070704
99. Dwan K, Phillipi CA, Steiner RD, Basel D. Bisphosphonate therapy for osteogenesis imperfecta. *Cochrane Database Syst Rev.* (2016) 10:CD005088. doi: 10.1002/14651858.CD005088.pub4
100. Bhardwaj A, Swe KM, Sinha NK, Osunkwo I. Treatment for osteoporosis in people with ß-thalassaemia. *Cochrane Database Syst Rev.* (2016) 3:CD010429. doi: 10.1002/14651858.CD010429.pub2
101. Ward L, Tricco AC, Phuong P, Cranney A, Barrowman N, Gaboury I, et al. Bisphosphonate therapy for children and adolescents with secondary osteoporosis. *Cochrane Database Syst Rev.* (2007) 4:CD005324. doi: 10.1002/14651858.CD005324.pub2
102. Nasomyont, N, Hornung L, Wasserman H. Intravenous bisphosphonate therapy in children with spinal muscular atrophy. *J Endocr Soc.* (2019) 3(Suppl 1): SAT-LB052. doi: 10.1210/js.2019-SAT-LB052
103. Lv F, Guan Y, Ma D, Xu X, Song Y, Li L, et al. Effects of alendronate and alfacalcidol on bone in patients with MG initiating glucocorticoids treatment. *Clin Endocrinol.* (2018) 88:380–7. doi: 10.1111/cen.13537
104. Kesikburun S, Güzelküçük U, Alay S, Yavuz F, Tan AK. Exacerbation of myasthenia gravis by alendronate. *Osteoporos Int.* (2014) 25:2319–20. doi: 10.1007/s00198-014-2768-4
105. Raja V, Sandanshiv P, Neugebauer M. Risedronate induced transient ocular myasthenia. *J Postgrad Med.* (2007) 53:274–5. doi: 10.4103/0022-3859.37525
106. Sbrocchi AM, Rauch F, Jacob P, McCormick A, McMillan HJ, Matzinger MA, et al. The use of intravenous bisphosphonate therapy to treat vertebral fractures due to osteoporosis among boys with Duchenne muscular dystrophy. *Osteoporos Int*. (2012) 23:2703–11. doi: 10.1007/s00198-012-1911-3
107. Wood CL, Bettolo CM, Bushby K, Straub V, Rawlings D, Sarkozy A, et al. Bisphosphonate use in Duchenne Muscular Dystrophy – why, when to start and when to stop? *Expert Opinion on Orphan Drugs.* (2016) 4:407–16. doi: 10.1517/21678707.2016.1148596
108. Cummings SR, San Martin J, McClung MR, Siris ES, Eastell R, Reid IR, et al. Denosumab for prevention of fractures in postmenopausal women with osteoporosis. *N Engl J Med*. (2009) 361:756–65. doi: 10.1056/NEJMoa0809493
109. Beaudoin C, Jean S, Bessette L, Ste-Marie LG, Moore L, Brown JP, Denosumab compared to other treatments to prevent or treat osteoporosis in individuals at risk of fracture: a systematic review and meta-analysis. *Osteoporos Int.* (2016) 27:2835–44. doi: 10.1007/s00198-016-3607-6
110. Kutilek S. denosumab treatment of severe disuse osteoporosis in a boy with spinal muscular atrophy. *Acta Med Iran.* (2017) 55:658–60.
111. Kumaki D, Nakamura Y, Sakai N, Kosho T, Nakamura A, Hirabayashi S, et al. Efficacy of denosumab for glucocorticoid-induced osteoporosis in an adolescent patient with duchenne muscular dystrophy: a case report. *JBJS Case Connect.* (2018) 8:e22. doi: 10.2106/JBJS.CC.17.00190
112. Zhang D, Potty A, Vyas P, Lane J. The role of recombinant PTH in human fracture healing: a systematic review. *J Orthop Trauma*. (2014) 28:57–62. doi: 10.1097/BOT.0b013e31828e13fe
113. Saraff V, Högler W. ENDOCRINOLOGY AND ADOLESCENCE: osteoporosis in children: diagnosis and management. *Eur J End*. (2015) 173:R185–97. doi: 10.1530/EJE-14-0865
114. Catalano A, Vita GL, Russo M, Vita G, Lasco A, Morabito N, et al. Effects of teriparatide on bone mineral density and quality of life in Duchenne muscular dystrophy related osteoporosis: a case report. *Osteoporos Int.* (2016) 27:3655–9. doi: 10.1007/s00198-016-3761-x

Conflict of Interest: The authors declare that the research was conducted in the absence of any commercial or financial relationships that could be construed as a potential conflict of interest.

frontiers in Endocrinology

ORIGINAL RESEARCH
published: 27 November 2019
doi: 10.3389/fendo.2019.00833

Differences in the Cortical Structure of the Whole Fibula and Tibia Between Long-Distance Runners and Untrained Controls. Toward a Wider Conception of the Biomechanical Regulation of Cortical Bone Structure

Sergio H. Lüscher[1], Laura M. Nocciolino[1,2], Nicolás Pilot[2], Leonardo Pisani[2], Alex Ireland[3], Jörn Rittweger[4,5], José L. Ferretti[1], Gustavo R. Cointry[1] and Ricardo F. Capozza[1]*

[1] Center for P-Ca Metabolism Studies (CEMFoC), National University of Rosario, Rosario, Argentina, [2] Unity of Musculoskeletal Biomechanical Studies (UDEBOM), Universidad del Gran Rosario, Rosario, Argentina, [3] School of Healthcare Science, Manchester Metropolitan University, Manchester, United Kingdom, [4] Institute of Aerospace Medicine, German Aerospace Center (DLR), Cologne, Germany, [5] Department of Pediatrics and Adolescent Medicine, University of Cologne, Cologne, Germany

OPEN ACCESS

Edited by:
Elizabeth Mary Curtis, MRC Lifecourse Epidemiology Unit (MRC), United Kingdom

Reviewed by:
Hannah Rice, University of Exeter, United Kingdom
Camille Parsons, MRC Lifecourse Epidemiology Unit (MRC), United Kingdom

***Correspondence:**
Alex Ireland
a.ireland@mmu.ac.uk

Specialty section:
This article was submitted to Bone Research, a section of the journal Frontiers in Endocrinology

Received: *11 September 2019*
Accepted: *14 November 2019*
Published: *27 November 2019*

Citation:
Lüscher SH, Nocciolino LM, Pilot N, Pisani L, Ireland A, Rittweger J, Ferretti JL, Cointry GR and Capozza RF (2019) Differences in the Cortical Structure of the Whole Fibula and Tibia Between Long-Distance Runners and Untrained Controls. Toward a Wider Conception of the Biomechanical Regulation of Cortical Bone Structure. Front. Endocrinol. 10:833. doi: 10.3389/fendo.2019.00833

The cortical structure of human fibula varies widely throughout the bone suggesting a more selective adaptation to different mechanical environments with respect to the adjacent tibia. To test this hypothesis, serial-pQCT scans of the dominant fibulae and tibiae of 15/15 men/women chronically trained in long-distance running were compared with those of 15/15 untrained controls. When compared to controls, the fibulae of trained individuals had similar (distally) or lower (proximally) cortical area, similar moments of inertia (MI) for anterior-posterior bending (xMI) and lower for lateral bending (yMI) with a lower "shape-index" (yMI/xMI ratio) throughout, and higher resistance to buckling distally. These group differences were more evident in men and independent of group differences in bone mass. These results contrast with those observed in the tibia, where, as expected, structural indicators of bone strength were greater in trained than untrained individuals. Proximally, the larger lateral flexibility of runners' fibulae could improve the ability to store energy, and thereby contribute to fast-running optimization. Distally, the greater lateral fibular flexibility could reduce bending strength. The latter appears to have been compensated by a higher buckling strength. Assuming that these differences could be ascribed to training effects, this suggests that usage-derived strains in some bones may modify their relative structural resistance to different kinds of deformation in different regions, not only regarding strength, but also concerning other physiological roles of the skeleton.

Keywords: fibula, bone biomechanics, pQCT, running, bone mechanostat, exercise and bone

INTRODUCTION

The human tibia and fibula, despite being spatially close, experience substantially different loading environments during locomotion (1–5). The fibula's contribution to axial shank loading varies substantially with magnitude and position, from <5% of low-magnitude axial loads in ankle *varus* to about 19% during high-magnitude loading in dorsiflexion (6, 7). In addition, large differences were reported in structural behavior and stiffness/strain distribution along the human fibula subjected to varying loading configurations (8), and little is known about the transmission of bending and torsional forces in the shank. In fact, forces are transmitted in part through the tibiofibular and other ligaments (6) and the interosseous membrane, a mechanical contribution which has been scarcely investigated.

Bones generally adapt to increased loads by slowly increasing in mass and/or by optimizing the distribution of the mass to increase the architectural efficiency of their design in the predominant directions determined by the history of their customary mechanical usage. Accordingly with the mechanostat Theory (9), the mechanism chronically involved in the bone response to loading is chiefly bone modeling (i.e., bone formation and destruction in different sites of the structure; **Figure 1**). As a result, the structure and strength of bones should reflect both their morphogenetical determination and mechanical environment (10, 11). Recent studies suggest that tibia and fibula, in addition to differing substantially in cortical structure, respond differently to the same kind of mechanical stimulation. In the human *tibia*, we have shown that (1) the cortical structure is highly adapted to compression stresses throughout the bone, with a smoothly variable adaptation to bending and torsion which reaches maximum effectiveness at the mid diaphysis (2), and (2) in long-distance runners, the pQCT-assessed cortical mass and diaphyseal design and strength indicators were all significantly larger than those of untrained controls, proportionally to the uniform variation of compression, bending and torsion stresses supported throughout the bone (3). In contrast, along the *fibula* shaft we have described no less than five different tomographic regions with varying structural features, suggesting that the adaptation of fibula structure to bending and torsion follows a non-uniform pattern along the shaft (5).

To note, the fibula appears to be little affected by long-term disuse, except in the epiphyseal sites (12, 13). This contrasts with the large deficits in mineralized mass and differences in distal diaphysis geometry evident in the adjacent tibia. It was also observed that the age-related decrease in muscle mass/strength in healthy men was associated to reduced tibia but not fibula cortical mass (14). In addition, the cross-sectional design of the normal human fibula diaphysis suggests to be more irregularly influenced along the bone by bending and torsional forces (as revealed by the distribution of the corresponding cross-sectional moments of inertia values) than by compressive loads (as revealed by the distribution of cortical area values) (5). Furthermore, conflicting findings about the structural responses of the fibula to exercise have been reported in the few studies to date (1, 15–18). The fibula was shown to be irresponsive to 9-month resistive exercise with whole-body vibration in postmenopausal women (15) and was structurally reinforced in torsion by only high-impact exercise loading in premenopausal women (1). In men trained in high-impact sprinting in whom only the site at the fibula mid diaphysis was scanned, no differences attributable to training on fibula structure or volumetric BMD distribution were reported (16). However, hockey players (who accelerate and turn with substantial dorsiflexion and eversion of the foot) had greater fibular strength than runners (17), and footballers showed a more robust cortical structure of the fibula in the supporting than in the kicking leg (18).

These observations suggest that, oppositely to the tibia, the adaptability of cortical fibula structure to mechanical environment could vary in magnitude, type, and even in direction, and may show either positive or negative responses to similar kinds of mechanical stimulation along the bone, with high site specificity, and perhaps in an unpredictable way in some instances (19). Cristofolini et al. (8) showed different structural responses of the fibula and other leg bones to opposite regimens of stimulation which could not be explained by the theory of elasticity, and proposed that bone tissue could show a non-symmetric behavior in some instances, perhaps defying some aspects of Wolff's Law and mechanostat Theory (9). Others' observations (20–24) would be in consonance with that view. In fact, some fibula adaptations to different kinds of mechanical stimulation could have both positive and negative impact on the function. For example, a fibula that was more compliant to lateral bending could be somewhat weaker, but also more efficient at storing energy from muscle contractions for jumping (25). The question seems to be, how much fibular deformability should be allowed in order to favor the biomechanical performance of the bone without substantially increasing the risk of fracture.

The few (cross-sectional) available studies of exercise effects on the *fibula* have investigated only one or no more than 4 sites or only one sex. No study has described the responses to exercise throughout the male and female fibula, allowing comparison of regions which biomechanical and tomographic descriptions would suggest experience substantially different mechanical loading. To partially fill this gap, this study (also cross-sectional) aimed to describe differences in fibula structure as assessed by pQCT in trained long-distance runners and untrained controls of both sexes and compare them with those observed in the adjacent tibiae. The working hypothesis was that, in contrast with the tibia, the runners' fibula structure should show some regional differences with respect to that of the untrained individuals which could be more related with the functional behavior of the bone in running (with a high selective relevance) than with an improvement in bone strength.

MATERIALS AND METHODS

The Study Participants

The studied individuals were 60 healthy, freely active, young white adults (30/30 men/women), residents of the urban area of Rosario City, Argentina. None of them had a history of fractures or diseases, smoking or drinking, or treatments affecting the skeleton, and none of the women had a history of menstrual disorders.

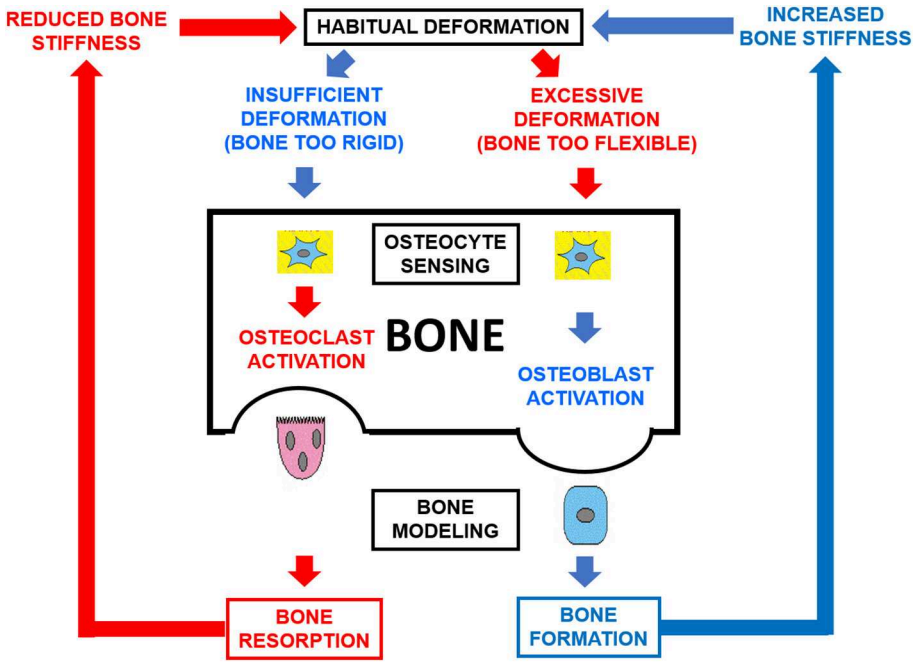

FIGURE 1 | Schematic representation of the double-loop feedback system [bone mechanostat (8)] which controls the structural stiffness of bones as a function of the mechanical usage of the skeleton. Osteocytes sense the magnitude of the induced strains and modulate bone formation and destruction by osteoblasts and clasts (OB, OC) directionally in their environment. As a result, bone modeling is oriented tending to compensate for any directional inadequacy of bone structural stiffness.

TABLE 1 | Means and SDs of age, body weight, body height, body/mass index, tibia length, and tibia length/body height ratio of the studied groups, and ANOVA tests of the differences in these variables between sedentary and runner individuals within each sex.

	Men			Women		
	Untrained	**Runner**	**ANOVA, *p***	**Untrained**	**Runner**	**ANOVA, *p***
Age, year	30.8 ± 3.0	32.7 ± 3.0	0.382 (ns)	30.4 ± 2.9	30.8 ± 3.4	0.173 (ns)
Weight, kg	78.1 ± 6.3	74.3 ± 5.	0.589 (ns)	57.6 ± 5.7	54.1 ± 4.1	0.262 (ns)
Height (h), cm	173.9 ± 3.3	173.2 ± 3.1	0.400 (ns)	163.5 ± 3.1	161.0 ± 4.1	0.200 (ns)
Body/mass index	26.8 ± 4.2	26.4 ± 1.4	0.748 (ns)	21.8 ± 0.8	22.3 ± 1.2	0.180 (ns)
Tibia length, mm	39.8 ± 1.8	39.2 ± 2.1	0.401 (ns)	37.2 ± 2.3	36.5 ± 2.1	0.199 (ns)
Tibia length/h ratio	0.22 ± 0.01	0.23 ± 0.0	0.503 (ns)	0.23 ± 0.01	0.22 ± 0.01	0.161 (ns)

From that selected group, 30 individuals (15/15 men/women) aged 25–38 years had been engaged as a single, voluntary and self-controlled group in regular long-distance running comprising 3–5 sessions per week, 10–16 km per session, for 8–11 years, at an average velocity of 11.2 ± 0.7 km/h for men and 10.3 ± 0.7 km/h for women (runners group) until the time of the study. In a unique, cross-sectional observation, they were compared with a control group of 15/15 men/women of comparable age. The latter were selected from a freely recruited sample of voluntary participants after a public announcement made in the ambit of the UGR (i.e., within the same social environment as that of the runners), avoiding inclusion of those with excessive large or small weight and stature within sexes with respect to the corresponding means and SDs of the trained groups in order to minimize the influence of allometric associations of the assessed variables which could have been difficult to neutralize by the adjusting procedures applied. All individuals studied performed a similar, regular pattern of daily activities concerning activity at work, travel to and from places of work, and recreational activities which was equivalent to the "moderate" level of activity established by the *Global Physical Activity Questionnaire (GPAQ)* (26). The control groups had never been trained in running or in any other discipline involving a specific use of the legs; hence, they were regarded as active (non-sedentary) untrained individuals. The age and anthropometric data of the samples and their tibia length (as assessed for the tomographic studies—see below) and tibia length/body height ratio are given in **Table 1.** The statistical significance of the inter-group differences within sexes in all the above variables is also indicated as a measure of the degree of homogeneity achieved for the respective samples.

Informed consent was obtained by every individual before inclusion in the study. The study was approved by the Hospital's Ethics Committee (*Comité de Ética, Hospital Provincial del Centenario*, Rosario, Argentina).

pQCT Measurements

An *XCT-2000* scanner *(Stratec, Germany),* software version 5.0, was used to scan the entire dominant leg of each individual. The radiation dose was about 0.9 μSV per scan (<20 μSv for the whole study). The slices were 2.5 mm thick, and the in-plane pixel size was 0.5 mm. A previously reported, computer-aided procedure to serially scan the whole tibia (2) was used to analyze the corresponding length of the adjacent fibula. Leg scans were obtained at every 5% of the leg length from the projection of the tibia-talar joint line to the articular line of the knee. Scans were numbered from S5 (5% site, located 5% of the scanned length proximal to the tibia-talar joint) to S95 (95% site, located 95% of the scanned length proximal to the tibia-talar joint). The device allows for no more than 9 slices per session. Thus, each half of the scanned length of the leg had to be studied separately and the scan at S50 (starting point for scanning the proximal segment of the leg) could not be obtained. The distal end of the fibula (analogously to the tibia malleolus as a distal landmark) could not be scanned below the S5 because the field size did not allow for introduction of the foot. Therefore, a total of 18 scans were obtained per each fibula and tibia, and hitherto any reference to the studied bones applies to the described length taken proximally from S10 to S80 (i.e., 14 scans per individual) in merit of accuracy and reliability of the measurements or calculations. Threshold values for total and cortical bone were selected at 180.0 and 710.0 mg/cm^3, respectively, using the parameters *contmode* 2, *peelmode* 2, and *cortmode* 1. The following indicators were obtained as allowed in every site studied.

Cortical Perimeters and Thickness

- *Periosteal perimeter*, in mm.
- *Endocortical perimeter*, in mm.
- *Cortical thickness:* average thickness of the bone cortex automatically given by the machine, in mm.

These indicators describe the most elementary geometric parameters which are directly affected by bone modeling.

Bone "Mass" Indicator

- *Cortical bone area*, in mm^2.

This indicator reflects the amount of available cortical tissue in the bone section. It was studied as such and was also normalized by body mass (27) to evaluate the influence of allometric factors in the determination of the observed differences.

Bone Tissue Mineralization [and Intrinsic Stiffness (28)] Indicator

- *Volumetric cortical mineral density (cortical vBMD) = cortical BMC (mg/mm of scan thickness)/cortical area*, in mg/cm^3 [data shown for only the S15-S75 range of bone sites as allowed by the cortical thickness (29)].

This indicator assesses the degree of mineralization of bone tissue, which is regarded as an indirect indicator of its intrinsic stiffness (elastic modulus) (28).

Indicators of the Architectural Efficiency of Cortical Tissue Distribution Within the Bone Section

- *Cross-sectional moments of inertia (MI's)*: The reference axes for MI calculation were the ML (x) axis (AP bending MI, xMI), and the AP (y) axis (ML bending MI, yMI), in mm^4. Total sums of products of the area of every cortical pixel by its squared perpendicular distance to the x and y axes of the image center of mass were obtained, after rotating the axis system until achieving a maximal "y" value of the AP axis. The xMI and yMI values are proportional to the stiffness of bone shafts in AP and ML bending, respectively. All MI values were studied after being normalized by the product of body weight times the bone length (bw*L) (27) to minimize their allometric associations.
- *Fibula/tibia MI ratio.* The yMI was also expressed as the ratio between its fibula and tibia values as a further, allometrically-free comparison of yMI values between the two bones.
- *yMI/xMI ratio ["shape index"* (30), dimensionless]: relationship between the yMI and xMI values determined at each bone site. This index is regarded as a *body size-unrelated* indicator of the relative development of the yMI with respect to that of the xMI in the same bone sites or regions.
- *Buckling ratio (BR) = R/CtTh* (dimensionless), being R the mean diaphyseal cross-sectional radius, and CtTh the average cortical thickness. This indicator is proportional to the *risk* of the diaphysis to fail in buckling.
- *Buckling Resistance Index (BRI)* = 1/BR (dimensionless). In this study, this index is regarded as an indicator of the *resistance* of the diaphysis to fail in buckling (31).

Statistical Analyses

Statistica (StatSoft Inc., USA, 2008) software was used. Means and SEs were calculated for each indicator separately in men and women and in runners and controls within each sex and plotted by scanned site for each bone. The distribution of all the pQCT indicators throughout the fibula was examined in order to define site-specific differences throughout the bone, and to compare them with those observed for the tibia. Factorial ANOVA of the evolution of the studied indicators in men and women in every site throughout the two bones ("site-effect") evaluated the higher-order interactive effects of all the studied groups ("sex effect" and "training effect"). The procedure automatically detected any group of successive sites within which the "training effect" showed significant global differences between trained and untrained individuals within each sex. No statistically significant differences were detected for single, isolated sites in any instance. Thus, continuous segments of bone diaphyses showing significant results could be objectively defined for each sex and selected for further comparisons.

The numbers of individuals per group were all larger than those which were analyzed in all our 4 previously published studies employing the same analytical model (2–5). The potency of the method for comparisons between runner and untrained

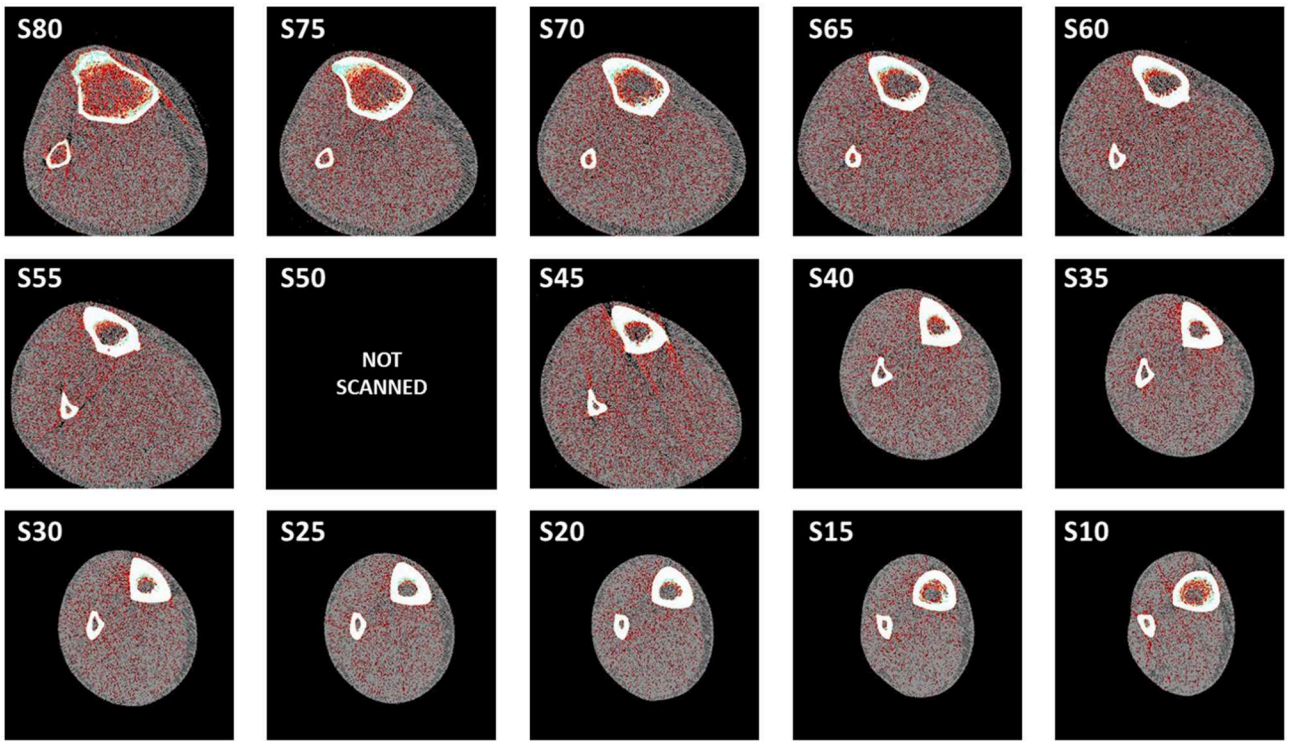

FIGURE 2 | Examples of the 14 selected scans corresponding to the leg of one of the untrained individuals, taken from the most proximal site (S80) to the most distal one (S10), as described in Materials and Methods.

individuals within each sex for $\alpha = 0.05$ ranged from 0.84 for a defined significant segment containing a minimum of 3 consecutive sites to a minimum of 0.99 when 7 or more consecutive sites were included in the selected segment.

RESULTS

Table 1 shows the relative homogeneity of the trained and untrained samples concerning age and some of the more relevant anthropometric features to the biological determination of all bone parameters studied.

Figure 2 shows the complete series of 14 selected scans taken from the leg of one of the untrained individuals, from the most proximal (S80) to the most distal (S10) site.

The comparison of runner vs. control data differed from tibia to fibula indicators. The differences observed were generally more evident in men than in women and exhibited some bone-site specificity in several cases, as described below.

Bone Mass Indicator (Cortical Bone Area—Figure 3A)

In the tibiae (left), cortical area was significantly higher in runners than controls throughout the bone in men and along the central-proximal region in women, while in the fibulae (right), cortical area was lower in runners than controls in the proximal (men) or central-proximal regions (women). Adjustment of the data to body mass (not shown) did not affect the intra- or inter-group behavior of the data.

Bone Mineralization and Tissue Stiffness (28) Indicator (Cortical vBMD—Figure 3B)

In the tibiae, cortical vBMD was slightly but significantly lower proximally (−1% to −3%) in runner men and women and higher distally (+1 to +4%) in runner men with respect to controls. In the fibulae, cortical vBMD was significantly higher (+2 to +5%) in runner men (only) than in controls below S70.

Cortical Perimeters and Thickness (Figure 4)

In running men only, periosteal perimeter was significantly larger at the central-proximal region of the tibia and slightly but significantly smaller toward the distal end of the fibula with respect to untrained controls (**Figure 4A**). These differences were largely reduced or neutralized after adjustment by body weight (not shown). The endo-cortical perimeter was significantly smaller in runners than in control men and women in the distal tibiae and in the central-distal fibulae only in the men (**Figure 4B**). The balance of these differences led to a significantly higher cortical thickness in runners than controls all along the tibiae in both sexes but only in the central-distal fibulae in men's bones (**Figure 4C**).

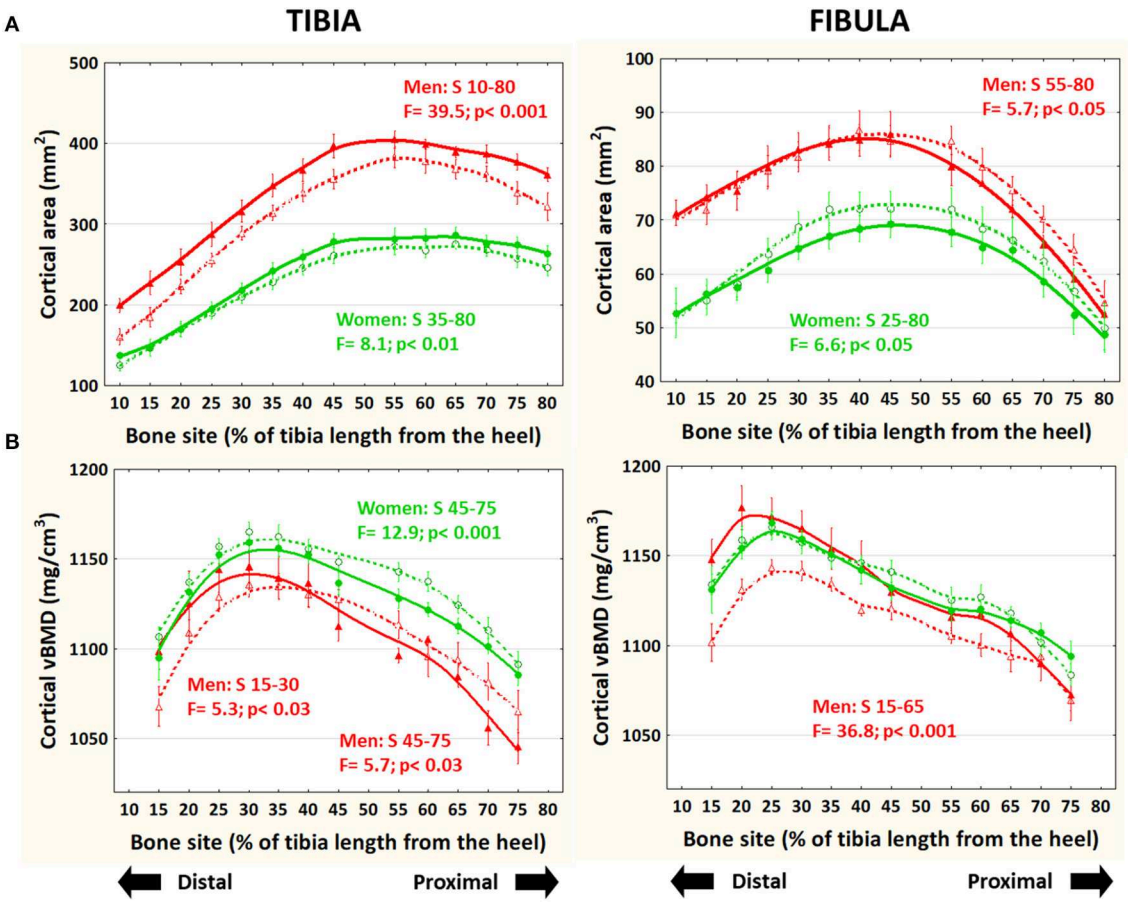

FIGURE 3 | Distribution of means and S.E. of the cortical bone cross-sectional area **(A)** and volumetric mineral density **(B)** of the tibia (left graphs) and fibula (right graphs) of runner (continuous lines) and untrained (dashed lines) men (red curves) and women (green curves) in all studied sites along the bones. Statistical significances of the factorial-ANOVA assessed differences between runners and untrained individuals within each sex and the corresponding, automatically defined site intervals showing significant results are indicated. Outside the indicated sites these differences were non-significant.

Bone Cross-Sectional Design Indicators (MIs, "Shape Index," BRI—Figures 5, 6)

In the tibiae, both [bw*L]-adjusted MIs were progressively larger in runners than in controls, proximally to S30 in men and to S10 in the women. In contrast, in the fibulae, the adjusted yMI and xMI varied differently. While the yMI was significantly *lower* in runner than in control men and women virtually throughout the bone (**Figure 5A**), the xMI showed no significant differences (**Figure 5B**).

The body-size unrelated "shape index" (unadjusted yMI/xMI ratio; **Figure 6A**) showed virtually no variation in the tibiae in all groups throughout. Instead, in the fibulae, it was generally higher in men than in women in the central-proximal region, and significantly lower in runners than controls all through (average −18% in men and −8% in women).

The ratio between fibula and tibia yMIs (unrelated to body size) was lower in all runners than controls throughout the bones (**Figure 6B**).

The BRI (also unrelated to body size) was significantly higher in runner than control men (central-distally in both bones) and women (only in the distal fibula) (**Figure 7**).

DISCUSSION

The aim of this cross-sectional study was to describe differences in fibula cortical bone structure between trained runners and controls throughout the bone's length, and to compare these differences with those observed in the neighboring tibia of the same individuals. We observed site-specific differences in several cortical bone parameters of the fibula, with values in trained individuals being generally similar to or lower than those observed in controls with the exception of higher resistance to buckling distally. These results contrast with those observed in the tibia, where structural indicators of bone strength were generally greater in trained individuals.

It is widely accepted that the long-term mechanical stimulation of any mobile bone strengthens rather than weakening its structure, and *vice-versa* (32). In this study, the

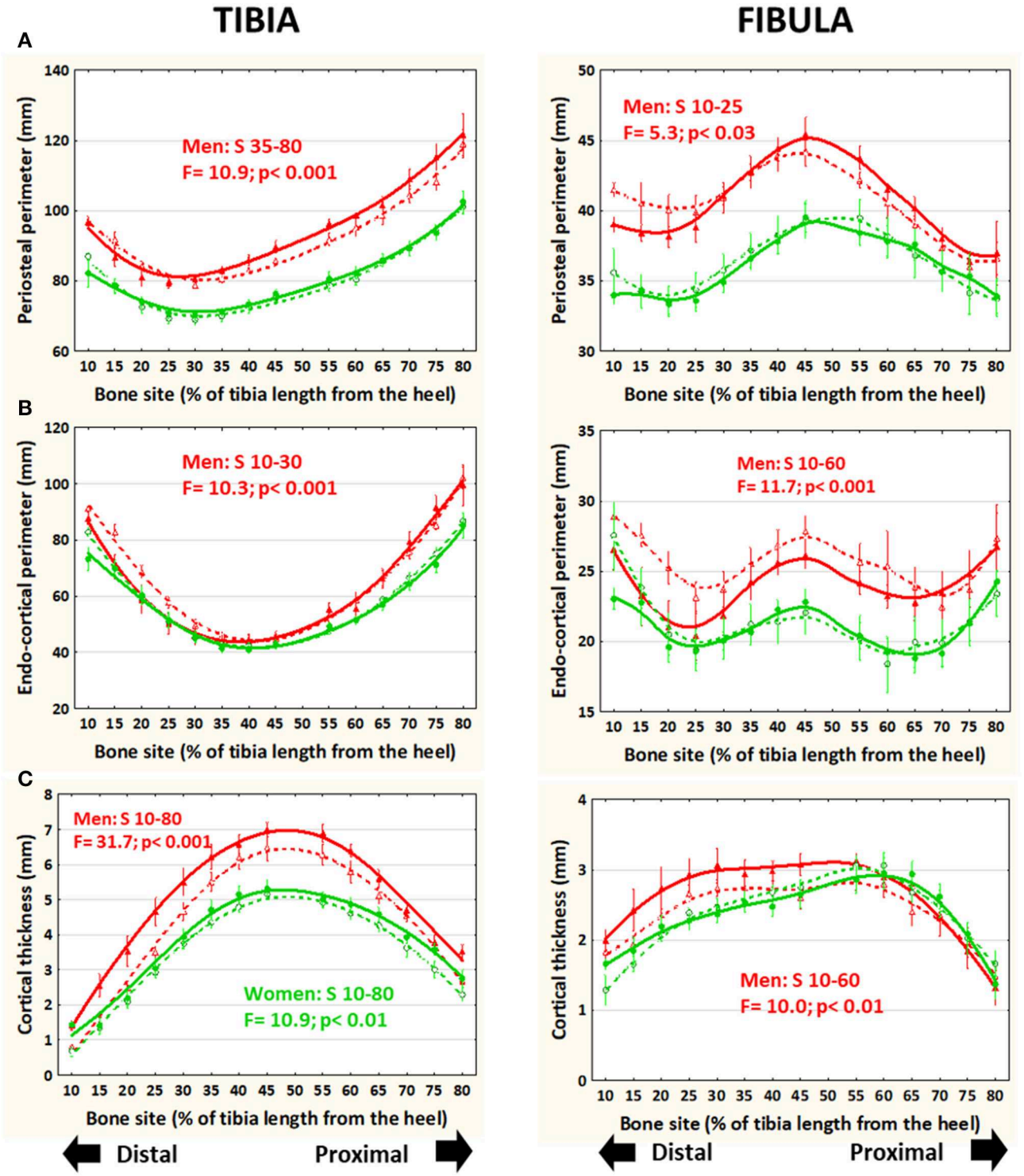

FIGURE 4 | Distribution of means and S.E. of the cross-sectional periosteal **(A)** and endocortical **(B)** perimeters and cortical thickness **(C)** of the tibia (left graphs) and fibula (right graphs) of runner (continuous lines) and untrained (dashed lines) men (red curves) and women (green curves) in all studied sites along the bones. Statistical significances of the factorial-ANOVA assessed differences between runners and untrained individuals within each sex and the corresponding, automatically defined site intervals showing significant results are indicated. Outside the indicated sites these differences were non-significant.

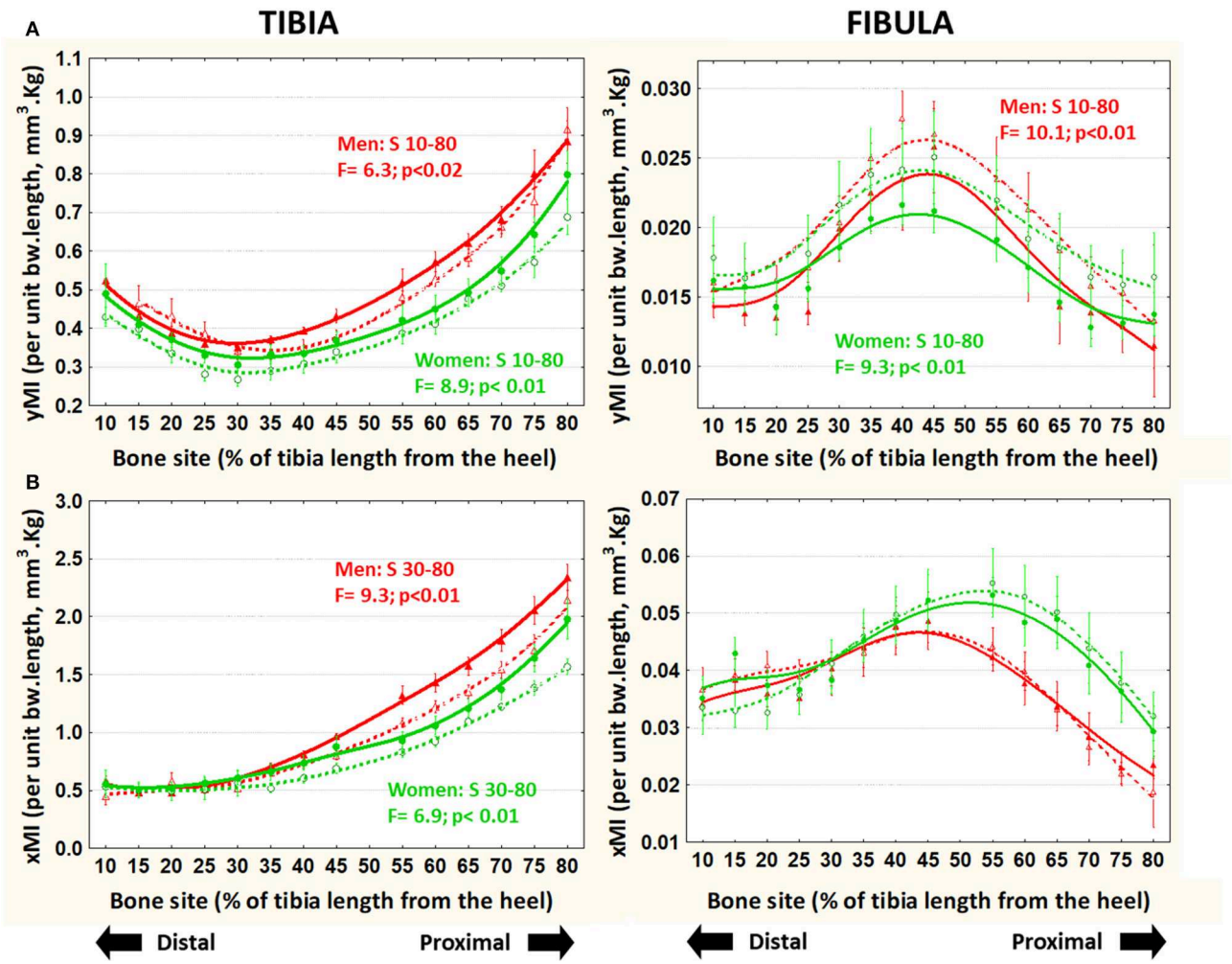

FIGURE 5 | Means and S.E. of the [bw*L]-adjusted cross-sectional moments of inertia for ML bending (yMI, **A**) and AP bending (xMI, **B**) of the tibia (left graphs) and fibula (right graphs) of runner (continuous lines) and untrained (dashed lines) men (red curves) and women (green curves) in all studied sites along the bones. Statistical significances of the factorial-ANOVA assessed differences between runners and untrained individuals within each sex and the corresponding, automatically defined site intervals showing significant results are indicated. Outside the indicated sites these differences were non-significant.

differences observed between the runners' tibiae were congruent with that idea, as expected after a previous observation (3). However, the fibula data revealed (1) a different behavior of medio-lateral and A-P bending stiffness indicators, yMI and xMI, in runners than in controls, and (2) a different behavior of the inter-group differences in yMI (decrease in runners) and BRI (increase in runners) toward the distal end of the bone. These differences were generally more evident in men's than in women's bones, possibly because of the differences in muscle force and hormonal status which may exert direct effects on bones that are known to show some skeletal-envelope and site specificity (33–36).

The distribution of the observed inter-group differences throughout each bone was also contrasting. In fact, in the runners' tibiae, the differences in the indicators of bone AP and ML bending stresses (xMI, yMI) increased consistently in parallel in the proximal direction, progressively improving the ability of the cross-sectional design to resist the natural, training-induced stresses in bending and torsion with respect to untrained controls, as previously described (3). In contrast, in the runners fibulae, each of the two MIs and also the BRI changed differently through the bone, suggesting that, in individuals subjected to the same training, the fibula can show either a higher or a lower bone stiffness than that of untrained individuals, depending on the bone region and kind of stress considered (ML or AP bending, buckling).

In addition, whatever the nature of the underlying mechanisms involved, the differences in fibula indicators between runners and controls were associated to some apparent incongruence between the differences observed in fibula mass/density and in design/strength indicators, chiefly derived from regional differences in the periosteal and endosteal perimeters. In fact, in the central-distal region of runner's fibulae, despite that bone mass was similar, cortical thickness was greater

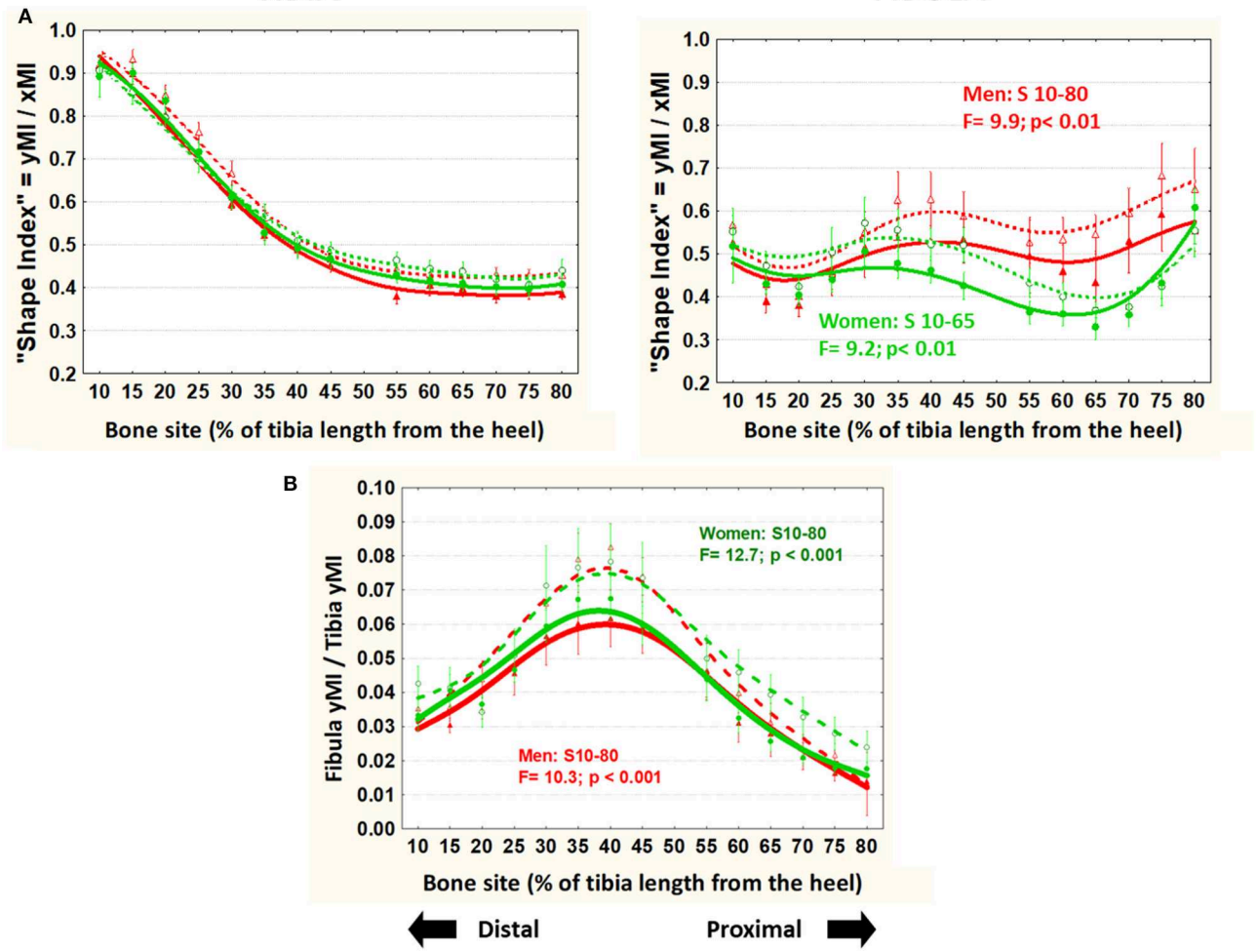

FIGURE 6 | Means and S.E. of the "shape index" (unadjusted yMI/xMI ratio) of the tibia (left graph) and fibula (right graph) **(A)** and the fibula/tibia yMI ratio **(B)** of runner (continuous lines) and untrained (dashed lines) men (red curves) and women (green curves) in all studied sites along the bones. Statistical significances of the factorial-ANOVA assessed differences between runners and untrained individuals within each sex and the corresponding, automatically defined site intervals showing significant results are indicated. Outside the indicated sites these differences were non-significant.

than in controls. Furthermore, the ML bending stiffness (as assessed by the yMI) was lower than controls throughout the bone, while the A-P bending stiffness (as assessed by the xMI) was similar in both groups, independently from the regional differences in bone mass. This contrasts with the generally higher values of all mass and design/strength indicators observed in the tibiae of the same individuals in this and in a similar, previously studied sample (3). Therefore, the observed differences in fibula MIs development should have reflected *differences in proximal and distal behavior* of bone modeling and/or remodeling.

The larger resistance to buckling (BRI) observed distally in runners' fibulae than in controls' can be also related to differences in all bone mass, design and mineralization. In fact, both the BRI (proportional to cortical thickness) and cortical vBMD (a general correlate of bone tissue stiffness) were higher in the runners in that region. There is some evidence that these differences, biomechanically opposite to the negative differences observed in ML bending stiffness (yMI), may be explained by a larger sensitivity to mechanical loading in the endocortical than in the periosteal surface (37) as determined by systemic (non-directional) factors (the "*anti-mechanostat*") (38).

The above proposals to explain the contrasting behavior of different indicators in our runners' fibulae [in agreement with the striking structural differences between bones which were already observed by us in chronically immobilized legs (13)] are congruent with our description of five morphologically different regions throughout the human fibula in which some structural indicators varied widely between sites (5). This suggests that the bone could respond differently to different kinds of strains with large site specificity. The observation of different responses to exercise of structural indicators of bones situated in the same limb or in different regions of the same bones is not new (20, 23).

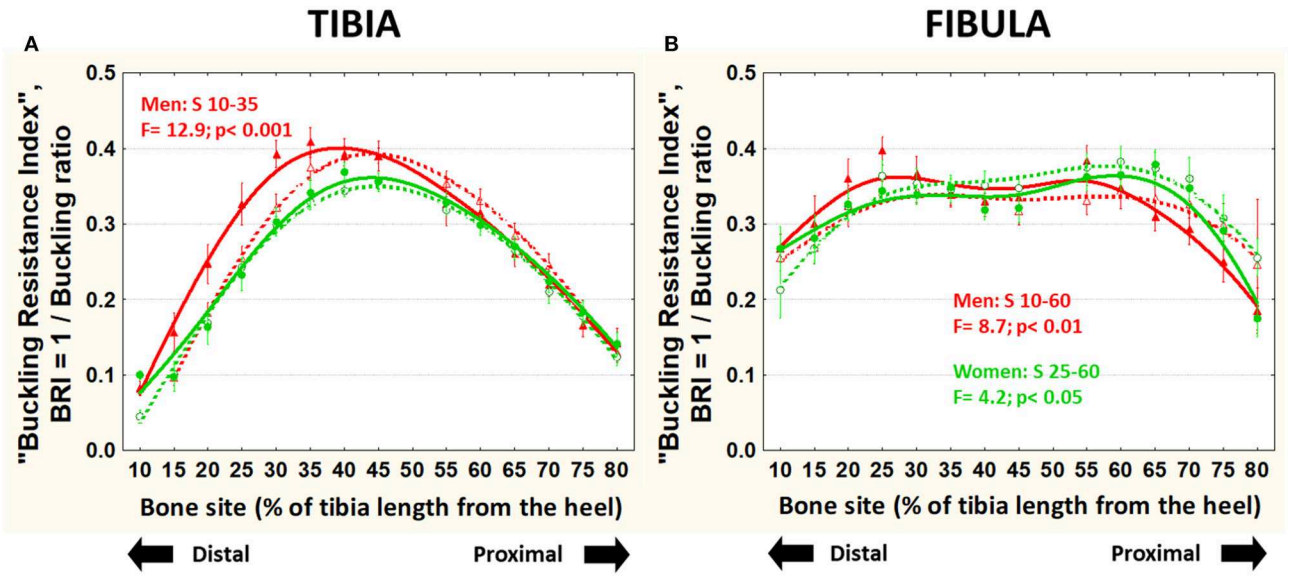

FIGURE 7 | Means and S.E. of the "buckling resistance index," BRI = 1/buckling ratio) of the tibia (left graph) **(A)** and fibula **(B)** (right graph) of runner (continuous lines) and untrained (dashed lines) men (red curves) and women (green curves) in all studied sites along the bones. Statistical significances of the factorial-ANOVA assessed differences between runners and untrained individuals within each sex and the corresponding, automatically defined site intervals showing significant results are indicated. Outside the indicated sites these differences were non-significant.

The nature of some exercise-induced changes has been shown to be negative in some instances, with a possible association with a locally reduced osteoblast generation or activity (22, 39).

At any rate, these findings are congruent with the current conception that the "customary strain level" to which bone tissue seems to be adapted is not constant, but varies by skeletal location, type of strain, strain gradient, and loading history (19, 33, 34, 40–43). In the fibula, running could have induced repetitive loads in AP and ML bending (17, 44) and many factors (not assessed in this study) could have affected the type of strain induced to the fibulae by long-distance running, including the behavior of the ankle joint and the distal tibiofibular syndesmosis, and the stiffness of the interosseous membrane (6, 45).

If the above assumptions are right, then our results would also suggest that the behavior of the fibula in our chronically trained runners would lay beyond our traditional knowledge about bone responses to mechanical environment as managed by the bone *mechanostat* (9). In consonance with this interpretation, cross-sectional studies in animals showed that loading-induced bone growth may not be directionally related to the induced local strains in every instance (24, 46).

The above interpretations are congruent with some phylogenetical observations. In fact, the evolutionary pathways of the fibula oscillate from region-specific robustness or slenderness according to survival needs even in taxonomically close species, including hominoids (17, 45). Following that idea, in can be proposed that, in our runners' fibulae, the generally larger compliance to ML bending with respect to controls might conveniently improve the ability of the bone to store elastic energy during the contraction of the locally inserted muscles which act on the foot during running/jumping (25, 47–49). On the other hand, the weakening of the proximal and distal design of the fibula concerning ML bending could increase the risk of ML-bending fractures. However, this apparent inconvenience could be at least partially overcome by the distal enhancement of buckling strength which was also observed. This could reduce the risk of most common (buckling) fractures at the most critical [distal (50)] region of the bone.

Therefore, in congruence with our hypothesis, our findings could be more easily explained if the fibula *could respond distinctly to different types of strains in different regions*, as observed in the ulna (19, 51) and in *in-vitro* studies at the cellular level of biological organization (52). As stressed by Ruff (19), (1) "strain distributions in bones that are less specialized for cursorial locomotion more closely match traditional expectations of greater bone strength in directions of higher strain, especially during vigorous movement" (51), and (2) "some degree of bending could actually be beneficial to bone tissue by maintaining strains within the 'optimum customary' window (53) avoiding potentially catastrophic strains in 'unusual' orientations," as observed in this study. Thus, *bone structure may be genetically designed in some cases to confine strains to more predictable patterns rather than strictly to minimize strains* (48, 53, 54).

In other words, our results would suggest that the fibula could be regarded as a "less predictable" bone than the tibia, the reasons for the difference being as much phylogenetic as mechanical (19). This interpretation is congruent with the assumption that, *rather than mathematical optimization rules for bone architecture, there seems to be just a biological process which adapts bone structure to mechanical demands, adequate for evolutionary endurance* (55, 56).

LIMITATIONS OF THE STUDY

The cross-sectional nature of the study precludes any reference to "improvements" or "impairments" of the studied indicators as directly derived from training, thus restricting the discussion of the observed effects to simple comparisons between the bone features of the studied groups. In fact, results could, at least partly, be explained by self-selection bias, given that the athletes chose their disciplines by their own volition. However, the observed anthropometric homogeneity of the samples, the MI adjustments to body weight and bone length, the behavior of the size-unrelated "shape index," and the comparisons made between fibula and tibia MI data of the same individuals should have minimized any interference from allometric correlates with the described inter-group differences. Therefore, the different behavior of cortical bone mass distribution in tibia and fibula between runners and controls could be reasonably regarded as a "training effect." Nevertheless, we think that further, specifically designed longitudinal studies will be needed to confirm our findings and conclusions.

The number of individuals per group (15), although being somewhat larger than those selected for our previous, similar studies (1–5), could be regarded as relatively small. However, the acceptable potency of the study and the statistical strength of most of the differences observed would support our interpretation of the reported results. At any rate, further studies with larger number of individuals (and wider ranges of ages) will be needed to support our interpretation of the present findings.

The studied sample comprised only healthy, active (not sedentary) adult men and pre-menopausal women that were either untrained or trained in long-distance running for several years. Thus, the conclusions should be restricted to these specific experimental conditions.

The study model was restricted to determinations of bone features which can be assessed by pQCT, i.e., to only those which are strictly derived from and affected by changes in bone mineralization and geometry of the studied bones.

CONCLUSIONS

This study affords some original evidence of a striking, "non-canonical" behavior of the human fibula concerning its structural response to mechanical environment as compared to the adjacent tibia. In the tibia, runners were found to have generally bigger, stronger diaphyses. In the fibula, however, runners exhibited diaphyses which were somewhat smaller in size and lower in structural strength compared to non-runners.

Those differences, more evident in men than in women, could have enhanced the ability of the fibula to contribute to fast-running optimization, in spite of a general weakening of the bone in lateral bending and independently of the differences observed in bone mass. However, the buckling strength of the bones seemed to have been conveniently improved at its distal end, which is the site most prone to fracture.

These findings support the idea that bone functional adaptation is complex and not easy to predict based on our current understanding of the process. The study suggests that mechanical loading may affect different bones in distinct ways, beyond the scope currently proposed by the mechanostat Theory, not only regarding resistance to fracture, but also concerning other bone features which may show some selective connotations.

DATA AVAILABILITY STATEMENT

The datasets generated for this study are available on request to the corresponding author.

ETHICS STATEMENT

The studies involving human participants were reviewed and approved by Comité de Ética, Hospital Provincial del Centenario, Rosario, Argentina. The patients/participants provided their written informed consent to participate in this study.

AUTHOR CONTRIBUTIONS

RC, GC, and JF contributed to conception and design of the study. LP and NP were responsible for data collection. SL and LN were responsible for data and statistical analysis. JF wrote the first draft of the manuscript. JR, AI, and JF provided interpretation of the results. JF and AI wrote sections of the manuscript. All authors contributed to manuscript revision, read and approved the submitted version.

FUNDING

This study was supported by a grant (PIP 0435/2015) from the Consejo de Investigaciones Científicas y Técnicas (CONICET, Argentina). NP and LP were fellows of the UGR. LN was a fellow of the CONICET.

REFERENCES

1. Rantalainen T, Nikander R, Heinonen A, Suominen H, Sievänen H. Direction-specific diaphyseal geometry and mineral mass distribution of tibia and fibula: a pQCT study of female athletes representing different exercise loading types. *Calcif Tissue Int*. (2010) 86:447–54. doi: 10.1007/s00223-010-9358-z
2. Capozza RF, Feldman S, Mortarino P, Reina PS, Schiessl H, Rittweger J, et al. Structural analysis of the human tibia by tomographic (pQCT) serial scans. *J Anat*. (2010) 216:470–81. doi: 10.1111/j.1469-7580.2009.01201.x
3. Feldman S, Capozza RF, Mortarino PA, Reina AS, Ferretti JL, Rittweger J, et al. Site and sex effects on tibia structure in distance runners and untrained people. *Med Sci Sports Exerc*. (2012) 44:1580–8. doi: 10.1249/MSS.0b013e31824e10b6
4. Capozza RF, Rittweger J, Reina PS, Mortarino P, Nocciolino LM, Feldman S, et al. pQCT-assessed relationships between diaphyseal design and cortical bone mass and density in the tibiae of healthy sedentary and trained men and women. *J Musculoskelet Neuronal Interact*. (2013) 13:195–205.
5. Cointry GR, Nocciolino L, Ireland A, Hall NM, Kriechbaumer A, Ferretti JL, et al. Structural differences in cortical shell properties between upper and

lower human fibula as described by pQCT serial scans. A biomechanical interpretation. *Bone*. (2016) 90:185–94. doi: 10.1016/j.bone.2016.06.007
6. Wang Q, Whittle M, Cunningham J, Kenwright J. Fibula and its ligaments in load transmission and ankle joint stability. *Clin Orthop Relat Res*. (1996) 330:261–70. doi: 10.1097/00003086-199609000-00034
7. Funk JR, Rudd RW, Kerrigan JR, Crandall JR. The line of action in the tibia during axial compression of the leg. *J Biomech*. (2007) 40:2277–82. doi: 10.1016/j.jbiomech.2006.10.012
8. Cristofolini L, Conti G, Juszczyk M, Cremonini S, Van Sint Jan S, Viceconti M. Structural behavior and strain distribution of the long bones of the human lower limbs. *J Biomech*. (2010) 43:826–35. doi: 10.1016/j.jbiomech.2009.11.022
9. Frost HM, editor. *The Utah Paradigm of Skeletal Physiology*, Vol I. *Bone and Bones*. Athens: ISMNI (2002).
10. Carter DR, Wong M, Orr TE. Musculoskeletal ontogeny, phylogeny, and functional adaptation. *J Biomech*. (1991) 24 (Suppl. 1):3–16. doi: 10.1016/0021-9290(91)90373-U
11. Cristofolini L. *In vitro* evidence of the structural optimization of the human skeletal bones. *J Biomech*. (2015) 48:787–96. doi: 10.1016/j.jbiomech.2014.12.010
12. Dudley-Javoroski S, Shields RK. Regional cortical and trabecular bone loss after spinal cord injury. *J Rehabil Res Dev*. (2012) 49:1365–76. doi: 10.1682/JRRD.2011.12.0245
13. Ireland A, Capozza RF, Cointry RG, Nocciolino L, Ferretti JL, Rittweger J. Meagre effects of disuse on the human fibula are not explained by bone size or geometry. *Osteoporos Int*. (2017) 28:633–41. doi: 10.1007/s00198-016-3779-0
14. McNeil CJ, Raymer GH, Doherty TJ, Marsh GD, Rice CL. Geometry of a weight-bearing and non-weight-bearing bone in the legs of young, old, and very old men. *Calcif Tissue Int*. (2009) 85:22–30. doi: 10.1007/s00223-009-9261-7
15. Stolzenberg N, Belavý DL, Beller G, Ambrecht G, Semler J, Felsenberg D. Bone strength and density via pQCT in post-menopausal osteopenic women after 9 months resistive exercise with whole body vibration or proprioceptive exercise. *J Musculoskelet Neuronal Interact*. (2013) 13:66–76.
16. Rantalainen T, Duckhem RL, Suominen H, Heinonen A, Alén M, Korhonen MT. Tibial and fibular mid-shaft bone traits in young and older sprinters and non-athletic men. *Calcif Tissue Int*. (2014) 95:132–40. doi: 10.1007/s00223-014-9881-4
17. Marchi D, Shaw CN. Variation on fibular robusticity reflects variation in mobility patterns. *J Hum Evol*. (2011) 61:609–16. doi: 10.1016/j.jhevol.2011.08.005
18. Hart NH, Newton RU, Weber J, Spiteri T, Rantalainen T, Dobbin M, et al. Functional basis of asymmetrical lower-body skeletal morphology in professional Australian rules footballers. *J Strength Cond Res*. (2018). doi: 10.1519/JSC.0000000000002841. [Epub ahead of print].
19. Ruff CB, Holt B, Trinkaus E. Who's afraid of the Big Bad Wolff?: "Wolff's Law" and bone functional adaptation. *Am J Phys Anthropol*. (2006) 129:484–98. doi: 10.1002/ajpa.20371
20. Li K-C, Zernicke RF, Barnard RJ, Li F-Y. Differential response of rat limb bones to strenuous exercise. *J Appl Physiol*. (1991) 70:554–60. doi: 10.1152/jappl.1991.70.2.554
21. Matsuda JJ, Zernicke RF, Vailas AC, Pedrini VA, Pedrini-Mille A, Maynard JA. Structural and mechanical adaptation of immature bone to strenous exercise. *J Appl Physiol*. (1986) 60:2028–34. doi: 10.1152/jappl.1986.60.6.2028
22. Lieberman DE, Polk JD, Demes B. Predicting long bone loading from cross-sectional geometry, *Am J Phys Anthropol*. (2004) 123:156–71. doi: 10.1002/ajpa.10316
23. Main RP. Ontogenetic relationships between *in vivo* strain environment, bone histomorphometry and growth in the goat radius. *J Anat*. (2007) 210:272–93. doi: 10.1111/j.1469-7580.2007.00696.x
24. Wallace IJ, Demes B, Mongle C, Pearson OM, Polk JD, Lieberman DE. Exercise-induced bone formation is poorly linked to local strain magnitude in the sheep tibia. *PLoS ONE*. (2014) 9:e99108 doi: 10.1371/journal.pone.0099108
25. Ryan TM, Shaw CN. Gracility of the modern *Homo sapiens* skeleton is the result of decreased biomechanical loading. *Proc Natl Acad Sci USA*. (2015) 112:372–7. doi: 10.1073/pnas.1418646112
26. Bull FC, Maslin TS, Armstrong T. Global physical activity questionnaire (GPAQ): nine country reliability and validity study. *J Phys Act Health*. (2009) 6:790–804. doi: 10.1123/jpah.6.6.790
27. Ruff CB. Body size, body shape, and long bone strength in modern humans. *J Hum Evol*. (2000) 38:269–90. doi: 10.1006/jhev.1999.0322
28. Currey JD. Incompatible mechanical properties in compact bone. *J Theor Biol*. (2004) 231:569–80. doi: 10.1016/j.jtbi.2004.07.013
29. Louis O, Willnecker J, Soykens S, Van der Winkel P, Osteaux M. Cortical thickness assessment by peripheral quantitative computed tomography: accuracy evaluated on radius specimens. *Osteoporos Int*. (1995) 5:446–9. doi: 10.1007/BF01626606
30. Ruff CB, Hayes WC. Cross-sectional geometry of Pecos Pueblo femora and tibiae - a biomechanical investigation. II. Sex, age, and side differences. *Am J Phys Anthropol*. (1983) 60:383–400. doi: 10.1002/ajpa.1330600309
31. Pecina M, Ruszkowsky I, Muftic O, Anticevic D. The fibula in clinical and experimental evaluation of the theory of functional adaptation of the bone. *Coll Antropol (Zagreb)*. (1982) 6:197–206.
32. Boyde A. The real response of bone to exercise. *J Anat*. (2003) 203:173–89. doi: 10.1046/j.1469-7580.2003.00213.x
33. Lorentzon M, Swanson C, Andersson N, Mellström D, Ohlsson C. Free testosterone is a positive, whereas free estradiol is a negative, predictor of cortical bone size in young Swedish men: the GOOD study. *J Bone Miner Res*. (2005) 20:1334–41. doi: 10.1359/JBMR.050404
34. Paschalis EP, Gamsjaeger S, Hassler N, Klaushofer K, Burr D. Ovarian hormone depletion affects cortical bone quality differently on different skeletal envelopes. *Bone*. (2017) 95:55–64 doi: 10.1016/j.bone.2016.10.029
35. Riggs BL, Melton J III, Robb RA, Camp JJ, Atkinson EJ, Peterson JM, et al. Population-based study of age and sex differences in bone volumetric density, size, geometry, and structure at different skeletal sites. *J Bone Miner Res*. (2004) 19:1945–54. doi: 10.1359/jbmr.040916
36. Ruff CB, Hayes WC. Sex differences on age-related remodeling of the femur and tibia. *J Orthop Res*. (1988) 6:886–96. doi: 10.1002/jor.1100060613
37. Birkchold AI, Razi H, Duda GN, Weinkamer R, Checa S, Willie BM. The periosteal bone surface is less mechano-responsive than the endocortical. *Nat Sci Rep*. (2016) 6:23480. doi: 10.1038/srep23480.
38. Saxon LK, Turner CH. Estrogen receptor β: the antimechanostat? *Bone*. (2005) 36:185–92. doi: 10.1016/j.bone.2004.08.003
39. Wallace IJ, Pagnotti GM, Rubin-Sigler J, Naeher M, Copes LE, Judex S, et al. Focal enhancement of the skeleton to exercise correlates with responsivity of bone marrow mesenchymal stem cells rather than peak external forces. *J Exp Biol*. (2015) 218:3002–9. doi: 10.1242/jeb.118729
40. Turner CH. Three rules for bone adaptation to mechanical stimuli. *Bone*. (1998) 23:399–407. doi: 10.1016/S8756-3282(98)00118-5
41. Hsieh IF, Robling AG, Ambrosius WT, Burr DB, Turner CH. Mechanical loading of diaphyseal bone in vivo: the strain threshold for an osteogenic response varies with location. *J Bone Miner Res*. (2001) 16:2291–7. doi: 10.1359/jbmr.2001.16.12.2291
42. Currey JD, editor. *Bones: Structure and Mechanics*. Princeton: Princeton University Press (2002).
43. Judex S, Gross TS, Zernicke RF. Strain gradients correlate with sites of exercise-induced bone-forming surfaces in the adult skeleton. *J Bone Miner Res*. (1997) 12:1737–45. doi: 10.1359/jbmr.1997.12.10.1737
44. Sparacello VS, Marchi D, Shaw CN. The importance of considering fibular robusticity when inferring the mobility patterns of past populations. In: Carlson KJ, Marchi D, editors. *Reconstructing Mobility: Environmental, Behavioral, and Morphological Determinants*. New York, NY: Springer (2014). doi: 10.1007/978-1-4899-7460-0_6
45. Barnett CH, Napier JR. The rotatory mobility of the fibula in eutherian mammals. *J Anat*. (1953) 87:11–21.
46. Demes B, Quin Y-X, Stern JT, Larson SG, Rubin CT. Patterns of strain in the macaque tibia during functional activity. *Am J Phys Anthropol*. (2001) 116:257–65 doi: 10.1002/ajpa.1122
47. Bramble DM, Lieberman DE. Endurance running and the evolution of Homo. *Nature*. (2004) 432:345–52. doi: 10.1038/nature03052
48. Lieberman DE, Bramble DM. The evolution of marathon running: capabilities in humans. *Sports Med*. (2007) 37:288–90. doi: 10.2165/00007256-200737040-00004

49. Hudgins B, Scharfenberg J, Triplett NT, McBride JM. Relationship between jumping ability and running performance in events of varying distance. *J Strength Condition Res*. (2013) 27:563–7. doi: 10.1519/JSC.0b013e31827e136f
50. Sherbondy PS, Sebastianelli WJ. Stress fractures of the medial malleolus and distal fibula. *Clin Sports Med.* (2006) 25:129–37. doi: 10.1016/j.csm.2005.08.006
51. Schaffler MB, Burr DB, Jungers WL, Ruff CB. Structural and mechanical indicators of limb specialization in primates. *Folia Primatol (Basel)*. (1985) 45:61–75. doi: 10.1159/000156218
52. Vatsa A, Breuls RG, Semeins CM, Salmon PL, Smit TH, Klein-Nulend J. Osteocyte morphology in fibula and calvaria - Is there a role for mechanosensing? *Bone*. (2008) 43:452–8. doi: 10.1016/j.bone.2008.01.030
53. Lanyon LE, Rubin CT. Functional adaptation in skeletal structures. In: Hildebrand M, Bramble DM, Liem KF, Wake DB, editors. *Functional Vertebrate Morphology*. Cambridge, MA: Belknap Press (1985). p. 1–25. doi: 10.4159/harvard.9780674184404.c1
54. Huiskes R. If bone is the answer, then what is the question? *J Anat.* (2000) 197:145–56. doi: 10.1046/j.1469-7580.2000.19720145.x
55. Bertram JE, Biewener AA. Bone curvature: sacrificing strength for load predictability? *J Theor Biol.* (1988) 131:75–92. doi: 10.1016/S0022-5193(88)80122-X
56. Pearson OM, Lieberman DE. The aging of Wolff's "Law": ontogeny and responses to mechanical loading in cortical bone. *Yearb Phys Anthropol.* (2004) 47:63–69. doi: 10.1002/ajpa.20155

Conflict of Interest: The authors declare that the research was conducted in the absence of any commercial or financial relationships that could be construed as a potential conflict of interest.

frontiers in Endocrinology

REVIEW
published: 10 January 2020
doi: 10.3389/fendo.2019.00911

Regulatory Role of RNA N^6-Methyladenosine Modification in Bone Biology and Osteoporosis

Xuejiao Chen[1†], *Wenfeng Hua*[2†], *Xin Huang*[1], *Yuming Chen*[3], *Junguo Zhang*[1] *and Guowei Li*[1,4*]

[1] Center for Clinical Epidemiology and Methodology (CCEM), Guangdong Second Provincial General Hospital, Guangzhou, China, [2] Department of Laboratory Medicine and Central Laboratories, Guangdong Second Provincial General Hospital, Guangzhou, China, [3] Department of Medical Statistics and Epidemiology, School of Public Health, Sun Yat-sen University, Guangzhou, China, [4] Department of Health Research Methods, Evidence, and Impact (HEI), McMaster University, Hamilton, ON, Canada

Osteoporosis is a metabolic skeletal disorder in which bone mass is depleted and bone structure is destroyed to the degree that bone becomes fragile and prone to fractures. Emerging evidence suggests that N^6-methyladenosine (m^{6}A) modification, a novel epitranscriptomic marker, has a significant role in bone development and metabolism. M^{6}A modification not only participates in bone development, but also plays important roles as writers and erasers in the osteoporosis. M^{6}A methyltransferase METTL3 and demethyltransferase FTO involves in the delicate process between adipogenesis differentiation and osteogenic differentiation, which is important for the pathological development of osteoporosis. Conditional knockdown of the METTL3 in bone marrow stem cells (BMSCs) could suppress PI3K-Akt signaling, limit the expression of bone formation-related genes (such as Runx2 and Osterix), restrain the expression of vascular endothelial growth factor (VEGF) and down-regulate the decreased translation efficiency of parathyroid hormone receptor-1 mRNA. Meanwhile, knockdown of the METTL3 significantly promoted the adipogenesis process and janus kinase 1 (JAK1) protein expression via an m^{6}A-dependent way. Specifically, there was a negative correlation between METTL3 expression and porcine BMSCs adipogenesis. The evidence above suggested that the relationship between METTL3 expression and adipogenesis was inverse, and osteogenesis was positive, respectively. Similarly, FTO regulated for BMSCs fate determination during osteoporosis through the GDF11-FTO-PPARγ axis, prompting the shift of MSC lineage commitment to adipocyte and inhibiting bone formation during osteoporosis. In this systematic review, we summarize the most up-to-date evidence of m^{6}A RNA modification in osteoporosis and highlight the potential role of m^{6}A in prevention, treatment, and management of osteoporosis.

Keywords: RNA N^6-methyladenosine modification, m^{6}A writers, m^{6}A erasers, bone development, osteoporosis

OPEN ACCESS

Edited by:
Marco Invernizzi,
University of Eastern Piedmont, Italy

Reviewed by:
Stefano Pagano,
University of Perugia, Italy
Alessandro de Sire,
University of Eastern Piedmont, Italy

***Correspondence:**
Guowei Li
lig28@mcmaster.ca

[†]These authors have contributed equally to this work

Specialty section:
This article was submitted to Bone Research, a section of the journal Frontiers in Endocrinology

Received: *09 September 2019*
Accepted: *13 December 2019*
Published: *10 January 2020*

Citation:
Chen X, Hua W, Huang X, Chen Y, Zhang J and Li G (2020) Regulatory Role of RNA N^6-Methyladenosine Modification in Bone Biology and Osteoporosis. Front. Endocrinol. 10:911. doi: 10.3389/fendo.2019.00911

INTRODUCTION

Osteoporosis is a systemic skeletal disease characterized by decrease in bone mineral density (BMD) and deterioration in bone microarchitecture (1, 2). It is a complex multifactorial disorder due to an interaction between genetic and environmental factors, dietary habits, and lifestyle. Patients suffer from chronic pain and decreased quality of life (3). Osteoporotic fractures increase disability,

mortality, and health-care cost, especially among elder peoples (4). For example, the cumulative mortality after 1 year of an osteoporotic hip fracture occurrence varies between 20 and 40% (5). Due to its silent nature, osteoporosis is often under-diagnosed and under-managed, which needs immediate attention.

Epigenetics is the study of heritable changes in gene expression that do not involve alterations in the DNA/RNA sequence, including DNA methylation, histone modification, and RNA modification (6, 7). As a consequence of gene–environment interactions, various environmental factors could trigger different epigenetic processes which regulate gene transcription (8, 9). Among them, DNA methylation and demethylation are the most extensively studied, especially alteration in the methylation of cytosine nucleotides in CpG islands located in the promoter region of genes. Hypomethylation of the cytosine bases of the DNA promoter sequence in CpG islands activates gene expression, and hypermethylation silences gene expression (8, 10). Aberrant DNA methylation patterns can result in developmental disorders (11). Modification of histone molecules within chromatin plays important roles in regulating gene expression. Enzymes, including histone acetyltransferases (HAT), histone methyltransferases (HMT), histone deacetylases (HDAC), histone demethylases (HDM), and others, could modify histones to alter gene expression by regulating promoter activity, chromatin structure, dosage compensation, and epigenetic memory, without changes in the nucleic acid sequences (8, 12). Moreover, epigenetic factors are also involved in bone biology and osteoporosis, which play a bridging role between individual genetic aspects and environmental influences (13).

RNA modification is another important post-transcriptional regulation, among which N^6-methyladenosine (m^{6}A) modification of mRNA is one of the most highly abundant (14, 15). First reported in 1970s, m^{6}A modification was found to have a broad functional influence on stabilizing homeostasis closely correlated to post-transcriptional gene expression regulation, growth and development (14, 16–20). It regulates the metabolic processes of most RNAs, including the pre-mRNA splicing, mRNA export, turnover, and translation of mRNA (18, 21–23). M^{6}A modification is tightly closely correlated to fundamental biological processes such as adipogenesis (24–26), mammalian spermatogenesis development (27), RNA dynamics of T cells (28), pluripotency differentiation (29–35), and response to heat shock (36, 37). Moreover, it was found to get involved in the etiology of various diseases including cancers (36, 38, 39), systemic lupus erythematosus (40), rheumatoid arthritis (16), and coronary artery disease (41). It was revealed that m^{6}A modification commonly occurred at the consensus motif RRACH (R = A, G; H = A, C, U) (14, 40). The process is catalyzed by the orchestrated action of highly conserved methyltransferase (m^{6}A writers) and demethylase (m^{6}A erasers) enzymes (42). M^{6}A writer is composed of a METTL3 (methyltransferase-like3)-METTL14 (methyltransferase-like 14)-WTAP (Wilm's tumor–associated protein) complex (43–45). Two members of the Fe(II)- and 2-oxoglutarate-dependent oxygenase superfamily, FTO and ALKBH5, act as m^{6}A erasers (46). N6-methyladenosine (m^{6}A) reader proteins of the YTH family serve as recognition elements for the effector proteins. YTHDF1/3 enhance translation efficiency of methylated mRNAs, while YTHDF2 promotes mRNA decay (6) (**Figure 1**). Recently, it is demonstrated that the DNA demethylase ALKBH1 play an unexpected role in modulating hypoxia-induced genes in human glioblastoma. M^{6}A modification of DNA modification is markedly upregulated and highly associated with the

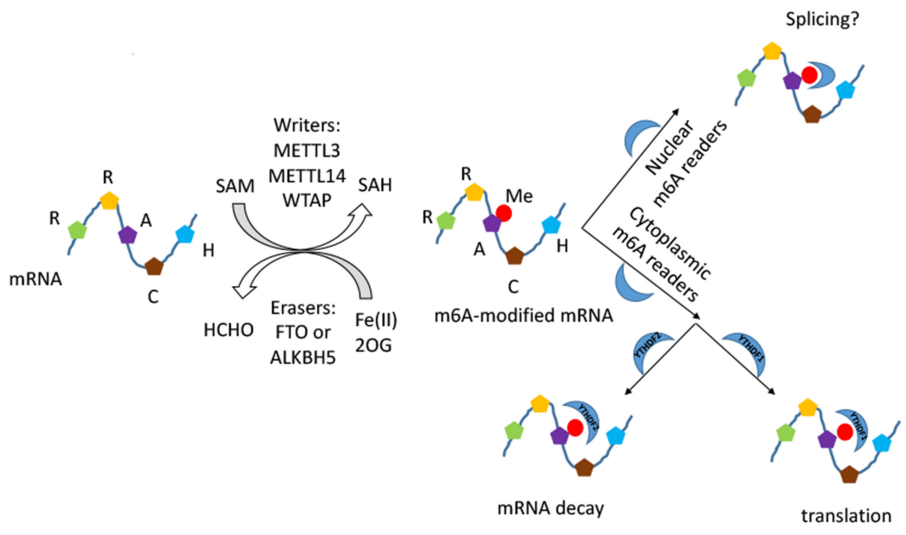

FIGURE 1 | The schematic diagram of m^{6}A RNA modification. The process is composed of installation, removal, and identification performed by writers, erasers, and readers. The METTL3–METTL14–WTAP methyltransferase complex catalyses a methyl group transfered from SAM into the N6 position, and the demethylases FTO and ALKBH5 catalyse the oxidative demethylation from methylated adenosine. The methyl group introduced is marked in red. The readers of the YTH domain family are effectors that decode the m6A methylation code and transform it into a functional signal in nucleus and cytoplasm.

TABLE 1 | Summary of included studies about the regulatory role of m^{6}A mRNA modification in osteoporosis.

References	Country	Key findings	Study type	Summarized role of m^{6}A in osteoporosis
Tian et al. (54)	China	METTL3 regulates osteogenic differentiation and alternative splicing of Vegfa in bone marrow mesenchymal stem cells.	Experimental study	Bone development; Differentiation of adipocyte and osteoblast.
Yao et al. (55)	China	METTL3 inhibits BMSC adipogenic differentiation by targeting the JAK1/STAT5/C/EBPbeta pathway via an m^{6}A-YTHDF2–dependent manner.	Experimental study	Bone development; Differentiation of adipocyte and osteoblast.
Wu et al. (53)	China	METTL3-mediated m(6)A RNA methylation regulates the fate of bone marrow mesenchymal stem cells and osteoporosis.	Experimental study	Bone development; m^{6}A writer in osteoporosis; Differentiation of adipocyte and osteoblast.
Tran et al. (56)	Australia	Association between fat-mass-and-obesity-associated (FTO) gene and hip fracture susceptibility.	The candidate gene association study	m^{6}A-associated SNPs for bone mineral density or osteoporosis.
Guo et al. (57)	China	The fat mass and obesity associated gene, FTO, is also associated with osteoporosis phenotypes.	The candidate gene association study	m^{6}A eraser in osteoporosis; m^{6}A-associated SNPs for bone mineral density or osteoporosis; Differentiation of adipocyte and osteoblast.
Shen et al. (51)	China	The GDF11-FTO-PPARgamma axis controls the shift of osteoporotic MSC fate to adipocyte and inhibits bone formation during osteoporosis.	Experimental study	Bone development; m^{6}A eraser in osteoporosis.
Mo et al. (52)	China	Genome-wide identification of m(6)A-associated SNPs as potential functional variants for bone mineral density.	Genome-wide association study	m^{6}A-associated SNPs for bone mineral density or osteoporosis.
Sachse et al. (58)	UK	FTO demethylase activity is essential for normal bone growth and bone mineralization in mice.	Experimental study	m^{6}A eraser in osteoporosis.
McMurray et al. (59)	UK	Pharmacological inhibition of FTO.	Experimental study	m^{6}A eraser in osteoporosis.

H3K9me3 heterochromatin histone modification in human glioblastoma (47).

It has been shown that DNA methylation and posttranslational histone modification participant in gene expression of bone cells (48, 49). These epigenetic programs are essential for physiological and pathological process, such as bone remodeling and bone metabolic disorders (6, 50). Besides, there is growing evidence that m^{6}A modification is a potential pathogenesis mechanism in osteoporosis (51–53). We systematically searched PubMed and EMBASE (up to July 2019) using keywords "(mRNA modifications OR epitranscriptomics OR N6-methyladenosine modification OR m^{6}A modification OR m^{6}A OR FTO OR Mettl3) AND (bone OR osteoporosis OR bone marrow stem cells OR BMSCs OR bone mineral density OR BMD)" to decipher the role of m^{6}A modification in osteoporosis, which might help further understand the pathogenesis of osteoporosis and provide theoretical basis for potential epigenetic-based therapeutics of osteoporosis. The inclusion criteria was: (1) to evaluate the association between RNA N6-methyladenosine modification in bone biology and osteoporosis; (2) full-text articles; (3) sufficient data on the regulatory mechanism. We identified 223 and 103 citations in PubMed and EMBASE, respectively. After removing 32 duplicates, 294 citations remained for title and abstract screening, from which nine articles were retrieved for full text screening (**Table 1**). Studies excluded due to not associated with RNA N6-methyladenosine modification in bone biology and osteoporosis ($n = 247$), reviews ($n = 26$), meta-analysis ($n = 2$), letters ($n = 1$), case reports ($n = 2$), meeting abstracts ($n = 4$), protocol ($n = 1$), and clinical trials ($n = 2$). Of the nine relevant studies, six were experimental studies, two were the candidate gene association studies and one was genome-wide association study. Based on the nine included studies, we discussed five parts below in detail related to m^{6}A modification and osteoporosis in this systematic review.

M^{6}A MODIFICATION REGULATES BONE DEVELOPMENT

M^{6}A modification of mRNAs has been discovered as a reversible RNA methylation and is widely conserved in mammalian cells (15, 42, 60). It is the most prevalent and internal modification that is tightly related to fundamental biological processes (**Figure 1**). M^{6}A has recently been reported to play a part in pluripotency differentiation and development of the cell lineage (29, 30, 32, 33), including osteogenic differentiation of bone marrow stem cells (BMSCs) (51, 53, 54). The human skeleton is a metabolically active tissue that undergoes continuous turnover and remodeling throughout life (48). Under homeostatic conditions, there is a delicate balance between osteoblast-mediated bone regeneration and osteoclast-mediated bone resorption (61, 62). Abnormalities of this process can produce a variety of skeletal disorders (63). BMSCs, also known as bone marrow-derived mesenchymal stem cells, are multipotent stromal cells with the ability of differentiating into osteoblast, chondrocyte, and adipocyte both *in vitro* and *in vivo* (64). In normal conditions, that would be a

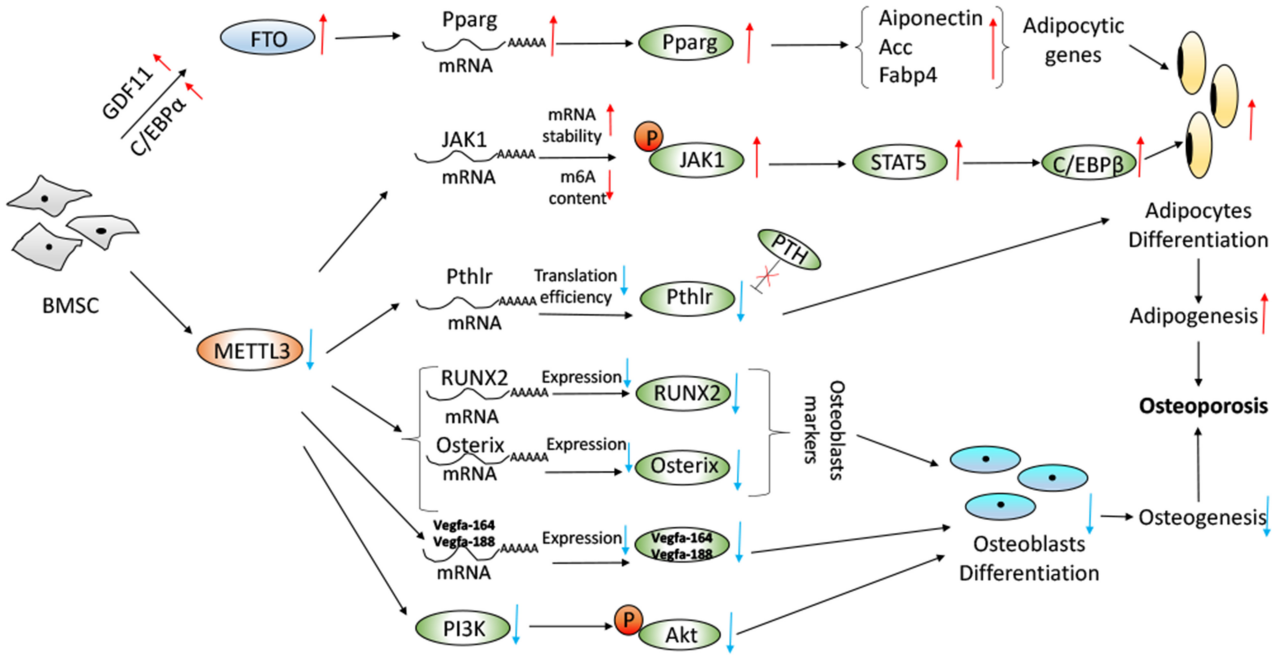

FIGURE 2 | Proposed model depicting regulation and role of METTL3 and FTO in BMSC adipogenesis and osteogenesis with regard to osteoporosis. Working model of the mechanism of METTL3 knockdown increased JAK1/STAT5/C/EBPb pathway, decreased PTH/Pth1r signaling axis, decreased expression of RUNX2, Osterix, and Vegfa and decreased PI3K-Akt signaling pathway. Overexpression of FTO in a GDF11-C/EBPα-dependent mechanism resulted in increase of the Pparg mRNA and the promotion of adipogenesis.

dynamic equilibrium for their differentiation of adipocytes and osteoblasts (65).

Recently, Yao et al. found that METTL3 plays an important role in BMSCs differentiation and adipogenesis. There was a negative correlation between METTL3 expression and porcine BMSCs (pBMSCs) adipogenesis (55). Specifically, METTL3 inhibited pBMSCs adipogenic differentiation by targeting the JAK1/STAT5/C/EBPβ pathway *via* an m^{6}A-YTHDF2–dependent manner. It was demonstrated that the deletion of METTL3 significantly promoted the pBMSCs adipogenesis process and janus kinase 1 (JAK1) protein expression *via* an m^{6}A-dependent way (55) (**Figure 2**). Similarly, in Tian's study, it was shown that METTL3 was highly expressed in osteogenically differentiated BMSCs (54). METTL3 knockdown limited the expression of vascular endothelial growth factor (VEGF) and its bone formation-related splice variants (Vegfa-164 and Vegfa188) in osteoblast-induced BMSCs, which was implicated in the maturation of osteoblasts, ossification and bone turnover. METTL3 knockdown decreased the expression of bone formation-related genes (such as Runx2 and Osterix), Akt phosphorylation, the alkaline phosphatase activity and the formation of mineralized nodules. PI3K-Akt signaling was suppressed by METTL3 knockdown in BMSCs during the osteogenic differentiation process (54) (**Figure 2**). Furthermore, METTL3 had a functional role in osteoarthritis progression by regulating NF-kB signaling and extracellular matrix synthesis in chondrocytes (66). RNA demethylase AlkB Homolog 5 (ALKBH5) was amplified in sarcomas and its expression was highly elevated in osteosarcoma patients. Silencing of ALKBH5 inhibited the osteosarcoma growth and migration without affecting the viability of normal human fetal osteoblast cells by sensitizing osteosarcoma cells to DNA damaging agents (67). Moreover, METTL3 promoted osteosarcoma cell progression by regulating the m^{6}A level of lymphoid enhancer-binding factor 1and activating Wnt/b-catenin signaling pathway (68).

M^{6}A WRITERS IN OSTEOPOROSIS

Wu et al. reported that METTL3-mediated m^{6}A RNA methylation could regulate the fate of bone marrow mesenchymal stem cells and osteoporosis (53). Conditional knockout of the m^{6}A methyltransferase METTL3 in BMSCs induced pathological features of osteoporosis in mice and resulted in impaired bone formation, incompetent osteogenic differentiation potential, and increased marrow adiposity. Conversely, METTL3 overexpression in BMSCs protected the mice from estrogen deficiency-induced osteoporosis. METTL3 depletion resulted in the decreased translation efficiency of parathyroid hormone receptor-1 mRNA. M^{6}A affected both osteogenic and adipogenic differentiation of MSCs through PTH (parathyroid hormone)/Pth1r (parathyroid hormone receptor-1) signaling axis. METTL3 knockout reduced the translation efficiency of MSCs lineage allocator Pth1r, leading to reduction of the global methylation level of m^{6}A and disruption of the PTH-induced osteogenic and adipogenic responses. PTH, bone-promoting molecule, stimulates bone formation by activating the

HSP90-dependent PERK-EIF2α-ATF4 signaling pathway (69) and increasing the receptor activator of nuclear factor κ-B ligand (RANKL)/osteoprotegerin (OPG) ratio through its receptor (70). M^{6}A modification was required for Pth1r translation. Loss of METTL3 changed Pth1r mRNA from the polysome fractions to the sub-polysome fractions (71), leading to slowing down the protein synthesis of Pth1r and blocking the downstream signaling pathways of Pth1r responsive to PTH treatment (53). The regulatory mechanism was shown in **Figure 2**.

M^{6}A ERASERS IN OSTEOPOROSIS

As an m^{6}A eraser, FTO was associated with osteoporosis phenotypes (57). It was founded that the whole body FTO knockout mice appeared as immediate postnatal growth retardation with shorter body length, lower body weight, and lower bone mineral density (BMD) (72). As Sachse et al. showed that FTO catalytic was essential for normal bone growth and mineralization but was not required for normal body composition except for normal body size and viability (58). They found both BMD and BMC (bone mineral content) were reduced in FTO knockout mice, which was comparable to that seen in osteoporosis. It was indicated that a relatively small amount of catalytic activity, roughly 20–50%, was sufficient to rescue the bone phenotype (58).

Moreover, Shen et al. have reported that FTO was a regulator for BMSCs fate determination during osteoporosis, with a rise in bone marrow in a growth-differentiation factor 11 (GDF11)-C/EBPα-dependent mechanism. Increased serum GDF11 concentration was associated with a high prevalence of osteoporosis by stimulating osteoclastogenesis and inhibiting osteoblast through inducing Smad2/3 phosphorylation (73–75). Peroxisome proliferator-activated receptor gamma (PPARγ) promoted the adipocyte differentiation and inhibited osteoblast differentiation from BMSCs (76, 77). The GDF11-FTO-PPARγ axis prompted the shift of MSC lineage commitment to adipocyte and inhibited bone formation during osteoporosis, as a result of the imbalance between bone mass and fat. FTO expression resulted in the increase of the serum concentration of GDF11 in the bone, which was a key risk for osteoporosis. The GDF11-FTO signaling regulated the adipocyte and osteoblast differentiation of MSC by targeting PPARγ dependent of the m^{6}A demethylase activity of FTO. Knock down the expression of FTO by means of lentivirus-mediated shRNA in BMSCs blocked the function of GDF11 and reduced the cells to differentiate to adipocytes. FTO knockout repressed the development of osteopenia *in vivo* through upregulation of adipocytic and down-regulation of an osteoblastic gene. FTO could regulate the m^{6}A level of the transcriptional factor PPARγ mRNA. Aging and osteopenia were associated with a decline in m^{6}A content in total RNA, which was consistent with the up-regulation of FTO expression (51). McMurray et al. conducted an evaluation to examine the effect of FTO demethylase function, and they found that pharmacologically inhibition FTO with IOX3 did significantly reduce BMD, BMC, and alter adipose tissue distribution. The level of alkaline phosphatase, an indicator of osteoblast function (61), was increased after use of IOX3 in mice compared with the controls (59). The process was revealed in **Figure 2**.

IDENTIFICATION OF M^{6}A-ASSOCIATED SNPS FOR BONE MINERAL DENSITY OR OSTEOPOROSIS

FTO polymorphisms are associated with elevated body mass index and increased risk for obesity (78, 79). Based on the candidate gene association study, FTO gene was found to be associated with hip fracture susceptibility (57). Specifically, researchers analyzed six single nucleotide polymorphisms (rs1421085, rs1558902, rs1121980, rs17817449, rs9939609, and rs9930506) of the FTO gene and found that female carriers of rs1121980 AA genotype had significantly higher risk of hip fracture with a hazard ratio of 2.06 (95% CI 1.17–3.62) than the female carriers of the wild-type. It was reported that ∼17% of the variability in hip fracture risk was attributable to SNP rs1121980. The FTO gene might be a new candidate for BMD variation and osteoporosis in Chinese population, as a candidate genetic marker for peak bone mass acquisition (56). In Zhang's study, it was demonstrated that osteoblast expression of FTO was required for normal bone formation and maintenance of bone mass in mature mice. The results identified an epigenetic pathway in which FTO normally functioned in bone to enhance the stability of mRNA-encoding proteins that protected osteoblasts from genotoxic damage (80). Utilizing the Mendelian randomization analysis, it was founded that the FTO-BMI polymorphism (rs9939609), as an instrument, was significantly associated with total hip and femoral neck BMD but was not correlated with total spine BMD (81). In aggregate, it was revealed that FTO SNPs were not only associated with obesity and type 2 diabetes but also with the BMD at the hip (57, 79).

Currently, based on genome-wide association study, plenty of m^{6}A-associated SNPs were identified as potential functional variants for BMD (52). Mo et al. found that 138, 125, and 993 m^{6}A-SNPs were associated with the BMD of femoral neck, lumbar spine, and quantitative heel ultrasounds, respectively. Among them, the association between two genes (MIR196A2 and ESPL1) and BMD of lumbar spine reached the genome-wide significant level [rs11614913 ($P = 8.92 \times 10^{-10}$) and rs1110720 ($P = 2.05 \times 10^{-10}$), respectively] (52). Furthermore, expression quantitative trait locus analyses indicated that 47 of these BMD-associated m^{6}A-SNPs were related with expressions of the 46 corresponding local genes. Besides, 24 m^{6}A-SNPs were founded to be significantly associated with quantitative heel ultrasounds ($P < 5.0 \times 10^{-8}$) (52). This study provided new clues for further understanding of functional mechanism underlying the associations between SNPs and osteoporosis.

M^{6}A MODIFICATION IN THE DIFFERENTIATION OF ADIPOCYTE AND OSTEOBLAST

Obesity and osteoporosis are closely correlated genetically (82–87). BMSCs is the same progenitor for adipocytes and osteoblasts and osteoblasts can also differentiate into adipocytes (87). Candidate genes, such as RANK (88), SP7 (89), and SOX6 (90), are all associated with obesity and osteoporosis. FTO

affected not only obesity phenotypes, but also osteoporosis phenotypes, like BMD (57). FTO-knockout mice showed a significant reduction in adipose tissue and body lean mass (91), and in turn, reduced lean mass is associated with weaken femur bone strength (92). METTL3-mediated m^{6}A RNA methylation also participated in the delicate process between pBMSCs adipogenesis differentiation and osteogenic differentiation (53–55, 66). BMI might be the causative role in osteoporosis the same as osteoarthritis on the effect of FTO variation (93). Recently, using a Mendelian randomization approach, Kemp et al. found that fat mass/BMI was strongly positively related to increased bone mineral density of the limbs, pelvis, and spine, but not the skull. In contrast, they reported that no evidence showed BMD could causally affect BMI or measures of adiposity (94). Taken together, m^{6}A modification was closely related to the differentiation of adipocyte and osteoblast, which was important for the pathological development of osteoporosis.

CONCLUDING REMARKS

Osteoporosis is a major public health concern with growing prevalence. Studies have indicated the important role of m^{6}A modification in prevention, treatment and management of osteoporosis; however, more endeavors are needed to further understand the mechanism and clarify the relationship between m^{6}A modification and osteoporosis.

AUTHOR CONTRIBUTIONS

All authors listed have made a substantial, direct and intellectual contribution to the work, and approved it for publication.

FUNDING

Research grant from the Science Foundation of Guangdong Second Provincial General Hospital (YY2018-002).

REFERENCES

1. Gosch M, Kammerlander C, Neuerburg C. Osteoporosis-epidemiology and quality of care. *Z Gerontol Geriatr*. (2019) 52:408–13. doi: 10.1007/s00391-019-01559-7
2. Wicklein S, Gosch M. Osteoporosis and multimorbidity. *Z Gerontol Geriatr*. (2019) 52:433–9. doi: 10.1007/s00391-019-01569-5
3. Wang J, Lu HX, Wang J. Cannabinoid receptors in osteoporosis and osteoporotic pain: a narrative update of review. *J Pharm Pharmacol*. (2019) 71:1469–74. doi: 10.1111/jphp.13135
4. Cho H, Byun JH, Song I, Kim HY, Ha YC, Kim TY, et al. Effect of improved medication adherence on health care costs in osteoporosis patients. *Medicine*. (2018) 30:e11470. doi: 10.1097/MD.0000000000011470
5. Guzon-Illescas O, Perez Fernandez E, Crespi Villarias N, Quiros Donate FJ, Pena M, Alonso-Blas C. Mortality after osteoporotic hip fracture: incidence, trends, and associated factors. *J Orthop Surg Res*. (2019) 1:203. doi: 10.1186/s13018-019-1226-6
6. Arguello AE, Leach RW, Kleiner RE. *In vitro* selection with a site-specifically modified RNA library reveals the binding preferences of N(6)-methyladenosine (m^{6}A) reader proteins. *Biochemistry*. (2019) 31:3386–95. doi: 10.1021/acs.biochem.9b00485
7. McGee SL, Hargreaves M. Epigenetics and exercise. *Trends Endocrinol Metab*. (2019) doi: 10.1016/j.tem.2019.06.002
8. Goyal D,Limesand SW and Goyal R. Epigenetic responses and the developmental origins of health and disease. *J Endocrinol*. (2019) 1:T105–19. doi: 10.1530/JOE-19-0009
9. Perera BPU, Faulk C, Svoboda LK, Goodrich JM, Dolinoy DC. The role of environmental exposures and the epigenome in health and disease. *Environ Mol Mutagen*. (2019). doi: 10.1002/em.22311. [Epub ahead of print].
10. Zeng Y, Chen T. DNA methylation reprogramming during mammalian development. *Genes*. (2019) 4:E257. doi: 10.3390/genes10040257
11. Hamidi T, Singh AK, Chen T. Genetic alterations of DNA methylation machinery in human diseases. *Epigenomics*. (2015) 2:247–65. doi: 10.2217/epi.14.80
12. Martin C, Zhang Y. The diverse functions of histone lysine methylation. *Nat Rev Mol Cell Biol*. (2005) 11:838–49. doi: 10.1038/nrm1761
13. Marini F, Cianferotti L, Brandi ML. Epigenetic mechanisms in bone biology and osteoporosis: can they drive therapeutic choices? *Int J Mol Sci*. (2016) 8:E1329. doi: 10.3390/ijms17081329
14. Roundtree IA, He C. RNA epigenetics–chemical messages for posttranscriptional gene regulation. *Curr Opin Chem Biol*. (2016) 30:46–51. doi: 10.1016/j.cbpa.2015.10.024
15. Pan T. N6-methyl-adenosine modification in messenger and long non-coding RNA. *Trends Biochem Sci*. (2013) 4:204–9. doi: 10.1016/j.tibs.2012.12.006
16. Mo XB, Zhang YH, Lei SF. Genome-wide identification of N(6)-Methyladenosine (m^{6}A) SNPs associated with rheumatoid arthritis. *Front Genet*. (2018) 9:299. doi: 10.3389/fgene.2018.00299
17. Hsu PJ, Shi H, He C. Epitranscriptomic influences on development and disease. *Genome Biol*. (2017) 1:197. doi: 10.1186/s13059-017-1336-6
18. Wei W, Ji X, Guo X, Ji S. Regulatory role of N(6) -methyladenosine (m^{6}A) methylation in RNA processing and human diseases. *J Cell Biochem*. (2017) 9:2534–43. doi: 10.1002/jcb.25967
19. Chandola U, Das R, Panda B. Role of the N6-methyladenosine RNA mark in gene regulation and its implications on development and disease. *Brief Funct Genomics*. (2015) 3:169–79. doi: 10.1093/bfgp/elu039
20. Dominissini D, Moshitch-Moshkovitz S, Schwartz S, Salmon-Divon M, Ungar L, Osenberg S, et al. Topology of the human and mouse m6A RNA methylomes revealed by m6A-seq. *Nature*. (2012) 7397:201–6. doi: 10.1038/nature11112
21. Maity A, Das B. N6-methyladenosine modification in mRNA: machinery, function and implications for health and diseases. *FEBS J*. (2016) 9:1607–30. doi: 10.1111/febs.13614
22. Edupuganti RR, Geiger S, Lindeboom RGH, Shi H, Hsu PJ, Lu Z, et al. N(6)-methyladenosine (m^{6}A) recruits and repels proteins to regulate mRNA homeostasis. *Nat Struct Mol Biol*. (2017) 10:870–8. doi: 10.1038/nsmb.3462
23. Saletore Y, Meyer K, Korlach J, Vilfan ID, Jaffrey S, Mason CE. The birth of the Epitranscriptome: deciphering the function of RNA modifications. *Genome Biol*. (2012) 10:175. doi: 10.1186/gb-2012-13-10-175
24. Zhang M, Zhang Y, Ma J, Guo F, Cao Q, Zhang Y, et al. The demethylase activity of FTO (fat mass and obesity associated protein) is required for preadipocyte differentiation. *PLoS ONE*. (2015) 7:e0133788 doi: 10.1371/journal.pone.0133788
25. Zhao X, Yang Y, Sun BF, Shi Y, Yang X, Xiao W, et al. FTO-dependent demethylation of N6-methyladenosine regulates mRNA splicing and is required for adipogenesis. *Cell Res*. (2014) 12:1403–19. doi: 10.1038/cr.2014.151
26. Wang X, Sun B, Jiang Q, Wu R, Cai M, Yao Y, et al. mRNA m(6)A plays opposite role in regulating UCP2 and PNPLA2 protein expression in adipocytes. *Int J Obes*. (2018) 11:1912–24. doi: 10.1038/s41366-018-0027-z
27. Lin Z, Tong MH. m(6)A mRNA modification regulates mammalian spermatogenesis. *Biochim Biophys Acta Gene Regul Mech*. (2019) 3:403–11. doi: 10.1016/j.bbagrm.2018.10.016
28. Furlan M, Galeota E, de Pretis S, Caselle M, Pelizzola M. m6A-dependent RNA dynamics in T cell differentiation. *Genes*. (2019) 10:E28. doi: 10.3390/genes10010028

29. Geula S, Moshitch-Moshkovitz S, Dominissini D, Mansour AA, Kol N, Salmon-Divon M, et al. Stem cells. m6A mRNA methylation facilitates resolution of naive pluripotency toward differentiation. *Science*. (2015) 6225:1002–6. doi: 10.1126/science.1261417
30. Ji P, Wang X, Xie N, Li Y. N6-methyladenosine in RNA and DNA: an epitranscriptomic and epigenetic player implicated in determination of stem cell fate. *Stem Cells Int*. (2018) 2018:3256524. doi: 10.1155/2018/3256524
31. Kudou K, Komatsu T, Nogami J, Maehara K, Harada A, Saeki H, et al. The requirement of Mettl3-promoted MyoD mRNA maintenance in proliferative myoblasts for skeletal muscle differentiation. *Open Biol.* (2017) 9:170119. doi: 10.1098/rsob.170119
32. Zhao BS, He C. Fate by RNA methylation: m6A steers stem cell pluripotency. *Genome Biol.* (2015) 16:43. doi: 10.1186/s13059-015-0609-1
33. Batista PJ, Molinie B, Wang J, Qu K, Zhang J, Li L, et al. m(6)A RNA modification controls cell fate transition in mammalian embryonic stem cells. *Cell Stem Cell*. (2014) 6:707–19. doi: 10.1016/j.stem.2014.09.019
34. Frye M, Blanco S. Post-transcriptional modifications in development and stem cells. *Development*. (2016) 21:3871–81. doi: 10.1242/dev.136556
35. Chen T, Hao YJ, Zhang Y, Li MM, Wang M, Han W, et al. m(6)A RNA methylation is regulated by microRNAs and promotes reprogramming to pluripotency. *Cell Stem Cell*. (2015) 3:289–301. doi: 10.1016/j.stem.2015.02.011
36. Wang S, Chai P, Jia R, Jia R. Novel insights on m(6)A RNA methylation in tumorigenesis: a double-edged sword. *Mol Cancer*. (2018) 1:101. doi: 10.1186/s12943-018-0847-4
37. Yu J, Li Y, Wang T, Zhong X. Modification of N6-methyladenosine RNA methylation on heat shock protein expression. *PLoS ONE*. (2018) 6:e0198604. doi: 10.1371/journal.pone.0198604
38. Chen J, Du B. Novel positioning from obesity to cancer: FTO, an m(6)A RNA demethylase, regulates tumour progression. *J Cancer Res Clin Oncol*. (2019) 1:19–29. doi: 10.1007/s00432-018-2796-0
39. Li Z, Weng H, Su R, Weng X, Zuo Z, Li C, et al. FTO plays an oncogenic role in acute myeloid leukemia as a N(6)-methyladenosine RNA demethylase. *Cancer Cell*. (2017) 1:127–41. doi: 10.1016/j.ccell.2016.11.017
40. Li LJ, Fan YG, Leng RX, Pan HF, Ye DQ. Potential link between m(6)A modification and systemic lupus erythematosus. *Mol Immunol*. (2018) 93:55–63. doi: 10.1016/j.molimm.2017.11.009
41. Mo XB, Lei SF, Zhang YH, Zhang H. Detection of m(6)A-associated SNPs as potential functional variants for coronary artery disease. *Epigenomics*. (2018) 10:1279–87. doi: 10.2217/epi-2018-0007
42. Jia G, Fu Y, He C. Reversible RNA adenosine methylation in biological regulation. *Trends Genet*. (2013) 2:108–15. doi: 10.1016/j.tig.2012.11.003
43. Meyer KD, Jaffrey SR. Rethinking m(6)A readers, writers, and erasers. *Annu Rev Cell Dev Biol*. (2017) 33:319–42. doi: 10.1146/annurev-cellbio-100616-060758
44. Balacco DL, Soller M. The m(6)A writer: rise of a machine for growing tasks. *Biochemistry*. (2019) 5:363–78. doi: 10.1021/acs.biochem.8b01166
45. Scholler E, Weichmann F, Treiber T, Ringle S, Treiber N, Flatley A, et al. Interactions, localization, and phosphorylation of the m(6)A generating METTL3-METTL14-WTAP complex. *RNA*. (2018) 4:499–512. doi: 10.1261/rna.064063.117
46. Romano G, Veneziano D, Nigita G, Nana-Sinkam SP. RNA methylation in ncRNA: classes, detection, and molecular associations. *Front Genet*. (2018) 9:243. doi: 10.3389/fgene.2018.00243
47. Xie Q, Wu TP, Gimple RC, Li Z, Prager BC, Wu Q, et al. N(6)-methyladenine DNA modification in glioblastoma. *Cell*. (2018) 5:1228–43.e20. doi: 10.1016/j.cell.2018.10.006
48. Vrtacnik P, Marc J, Ostanek B. Epigenetic mechanisms in bone. *Clin Chem Lab Med*. (2014) 5:589–608. doi: 10.1515/cclm-2013-0770
49. Huang T, Peng X, Li Z, Zhou Q, Huang S, Wang Y, et al. Epigenetics and bone diseases. *Genet Res*. (2018) 100:e6. doi: 10.1017/S0016672318000034
50. Shin Y, Ghate NB, Moon B, Park K, Lu W, An W. DNMT and HDAC inhibitors modulate MMP-9-dependent H3 N-terminal tail proteolysis and osteoclastogenesis. *Epigenetics Chromatin*. (2019) 1:25. doi: 10.1186/s13072-019-0270-0
51. Shen GS, Zhou HB, Zhang H, Chen B, Liu ZP, Yuan Y, et al. The GDF11-FTO-PPARgamma axis controls the shift of osteoporotic MSC fate to adipocyte and inhibits bone formation during osteoporosis. *Biochim Biophys Acta Mol Basis Dis*. (2018) 12:3644–54. doi: 10.1016/j.bbadis.2018.09.015
52. Mo XB, Zhang YH, Lei SF. Genome-wide identification of m(6)A-associated SNPs as potential functional variants for bone mineral density. *Osteoporos Int*. (2018) 9:2029–39. doi: 10.1007/s00198-018-4573-y
53. Wu Y, Xie L, Wang M, Xiong Q, Guo Y, Liang Y, et al. Mettl3-mediated m(6)A RNA methylation regulates the fate of bone marrow mesenchymal stem cells and osteoporosis. (2018) 1:4772. doi: 10.1038/s41467-018-06898-4
54. Tian C, Huang Y, Li Q. Mettl3 regulates osteogenic differentiation and alternative splicing of vegfa in bone marrow mesenchymal stem cells. *Int J Mol Sci*. (2019) 3:E551. doi: 10.3390/ijms20030551
55. Yao Y, Bi Z, Wu R, Zhao Y, Liu Y, Liu Q, et al. METTL3 inhibits BMSC adipogenic differentiation by targeting the JAK1/STAT5/C/EBPbeta pathway via an m(6)A-YTHDF2-dependent manner. *FASEB J*. (2019) 6:7529–44. doi: 10.1096/fj.201802644R
56. Tran B, Nguyen ND, Center JR, Eisman JA, Nguyen TV. Association between fat-mass-and-obesity-associated (FTO) gene and hip fracture susceptibility. *Clin Endocrinol*. (2014) 2:210–7. doi: 10.1111/cen.12335
57. Guo Y, Liu H, Yang TL, Li SM, Li SK, Tian Q, et al. The fat mass and obesity associated gene, FTO, is also associated with osteoporosis phenotypes. *PLoS ONE*. (2011) 11:e27312. doi: 10.1371/journal.pone.0027312
58. Sachse G, Church C, Stewart M, Cater H, Teboul L, Cox RD, et al. FTO demethylase activity is essential for normal bone growth and bone mineralization in mice. *Biochim Biophys Acta Mol Basis Dis*. (2018) 3:843–50. doi: 10.1016/j.bbadis.2017.11.027
59. McMurray F, Demetriades M, Aik W, Merkestein M, Kramer H, Andrew DS, et al. Pharmacological inhibition of FTO. *PLoS ONE*. (2015) 4:e0121829. doi: 10.1371/journal.pone.0121829
60. Meyer KD, Saletore Y, Zumbo P, Elemento O, Mason CE, Jaffrey SR. Comprehensive analysis of mRNA methylation reveals enrichment in 3' UTRs and near stop codons. *Cell*. (2012) 7:1635–46. doi: 10.1016/j.cell.2012.05.003
61. Feng X, McDonald JM. Disorders of bone remodeling. *Annu Rev Pathol*. (2011) 6:121–45. doi: 10.1146/annurev-pathol-011110-130203
62. Yang S, Duan X. Epigenetics, bone remodeling and osteoporosis. *Curr Stem Cell Res Ther*. (in press).
63. Raisz LG. Physiology and pathophysiology of bone remodeling. *Clin Chem*. (1999) 8(Pt 2):1353–8.
64. Caplan AI. Mesenchymal stem cells: time to change the name! *Stem Cells Transl Med*. (2017) 6:1445–51. doi: 10.1002/sctm.17-0051
65. Chen Q, Shou P. Fate decision of mesenchymal stem cells: adipocytes or osteoblasts? (2016) 23:1128–39. doi: 10.1038/cdd.2015.168
66. Both J, Wu T, Bras J, Schaap GR, Baas F, Hulsebos TJ. Identification of novel candidate oncogenes in chromosome region 17p11.2-p12 in human osteosarcoma. *PLoS ONE*. (2012) 1:e30907. doi: 10.1371/journal.pone.0030907
67. Yadav P, Subbarayalu P, Abdelfattah N, Eedunuri VK, Chen Y, Rao MK. Methyladenosine RNA demethylase ALKBH5 as a novel therapeutic target for osteosarcoma. *Cancer Res*. (2018) 13(Suppl.):4146. doi: 10.1158/1538-7445.AM2018-4146
68. Miao W, Chen J, Jia L, Ma J, Song D. The m6A methyltransferase METTL3 promotes osteosarcoma progression by regulating the m6A level of LEF1. *Biochem Biophys Res Commun*. (2019) 516:719–25. doi: 10.1016/j.bbrc.2019.06.128
69. Zhang K, Wang M, Li Y, Li C, Tang S, Qu X, et al. The PERK-EIF2alpha-ATF4 signaling branch regulates osteoblast differentiation and proliferation by PTH. *Am J Physiol Endocrinol Metab*. (2019) 4:E590–604. doi: 10.1152/ajpendo.00371.2018
70. Silva BC, Bilezikian JP. Parathyroid hormone: anabolic and catabolic actions on the skeleton. *Curr Opin Pharmacol*. (2015) 22:41–50. doi: 10.1016/j.coph.2015.03.005
71. Poria DK, Ray PS. Polysome analysis. *Bio Protoc*. (2017) 6:e2192. doi: 10.21769/BioProtoc.2192
72. Gao X, Shin YH, Li M, Wang F, Tong Q, Zhang P. The fat mass and obesity associated gene FTO functions in the brain to regulate postnatal growth in mice. *PLoS ONE*. (2010) 11:e14005. doi: 10.1371/journal.pone.0014005
73. Jin M, Song S, Guo L, Jiang T, Lin ZY. Increased serum GDF11 concentration is associated with a high prevalence of osteoporosis in elderly

native Chinese women. *Clin Exp Pharmacol Physiol*. (2016) 11:1145–7. doi: 10.1111/1440-1681.12651
74. Lu Q, Tu ML, Li CJ, Zhang L, Jiang TJ, Liu T, et al. GDF11 inhibits bone formation by activating Smad2/3 in bone marrow mesenchymal stem cells. *Calcif Tissue Int*. (2016) 5:500–9. doi: 10.1007/s00223-016-0173-z
75. Liu W, Zhou L, Zhou C, Zhang S, Jing J, Xie L, et al. GDF11 decreases bone mass by stimulating osteoclastogenesis and inhibiting osteoblast differentiation. *Nat Commun*. (2016) 7:12794. doi: 10.1038/ncomms12794
76. Xu C, Wang J, Zhu T, Shen Y, Tang X, Fang L, et al. Cross-talking between PPAR and WNT signaling and its regulation in mesenchymal stem cell differentiation. *Curr Stem Cell Res Ther*. (2016) 3:247–54. doi: 10.2174/1574888X10666150723145707
77. Yuan Z, Li Q, Luo S, Liu Z, Luo D, Zhang B, et al. PPARγ and Wnt signaling in adipogenic and osteogenic differentiation of mesenchymal stem cells. *Curr Stem Cell Res Ther*. (2016) 3:216–25. doi: 10.2174/1574888X10666150519093429
78. Fawcett KA, Barroso I. The genetics of obesity: FTO leads the way. *Trends Genet*. (2010) 6:266–74. doi: 10.1016/j.tig.2010.02.006
79. Scuteri A, Sanna S, Chen WM, Uda M, Albai G, Strait J, et al. Genome-wide association scan shows genetic variants in the FTO gene are associated with obesity-related traits. *PLoS Genet*. (2007) 7:e115. doi: 10.1371/journal.pgen.0030115
80. Zhang Q, Riddle RC, Yang Q, Rosen CR, Guttridge DC, Dirckx N, et al. The RNA demethylase FTO is required for maintenance of bone mass and functions to protect osteoblasts from genotoxic damage. *Proc Natl Acad Sci USA*. (2019) 36:17980–9. doi: 10.1073/pnas.1905489116
81. Warodomwichit D, Sritara C, Thakkinstian A, Chailurkit LO, Yamwong S, Ratanachaiwong W, et al. Causal inference of the effect of adiposity on bone mineral density in adults. *Clin Endocrinol*. (2013) 5:694–9. doi: 10.1111/cen.12061
82. Toth E, Ferenc V, Meszaros S, Csupor E, Horvath C. [Effects of body mass index on bone mineral density in men]. *Orv Hetil*. (2005) 28:1489–93.
83. Rosen CJ, Bouxsein ML. Mechanisms of disease: is osteoporosis the obesity of bone? *Nat Clin Pract Rheumatol*. (2006) 1:35–43. doi: 10.1038/ncprheum0070
84. Albala C, Yanez M, Devoto E, Sostin C, Zeballos L, Santos JL. Obesity as a protective factor for postmenopausal osteoporosis. *Int J Obes Relat Metab Disord*. (1996) 11:1027–32.
85. Zhao LJ, Liu YJ, Liu PY, Hamilton J, Recker RR, Deng HW. Relationship of obesity with osteoporosis. *J Clin Endocrinol Metab*. (2007) 5:1640–6. doi: 10.1210/jc.2006-0572
86. Choi YJ, Song I, Jin Y, Jin HS, Ji HM, Jeong SY, et al. Transcriptional profiling of human femoral mesenchymal stem cells in osteoporosis and its association with adipogenesis. *Gene*. (2017) 632:7–15. doi: 10.1016/j.gene.2017.08.015
87. Gimble JM, Robinson CE, Wu X, Kelly KA. The function of adipocytes in the bone marrow stroma: an update. *Bone*. (1996) 5:421–8. doi: 10.1016/S8756-3282(96)00258-X
88. Zhao LJ, Guo YF, Xiong DH, Xiao P, Recker RR, Deng HW. Is a gene important for bone resorption a candidate for obesity? An association and linkage study on the RANK (receptor activator of nuclear factor-kappaB) gene in a large Caucasian sample. *Hum Genet*. (2006) 4:561–70. doi: 10.1007/s00439-006-0243-9
89. Zhao J, Bradfield JP, Li M, Zhang H, Mentch FD, Wang K, et al. BMD-associated variation at the *Osterix locus* is correlated with childhood obesity in females. *Obesity*. (2011) 6:1311–4. doi: 10.1038/oby.2010.324
90. Liu YZ, Pei YF, Liu JF, Yang F, Guo Y, Zhang L, et al. Powerful bivariate genome-wide association analyses suggest the SOX6 gene influencing both obesity and osteoporosis phenotypes in males. *PLoS ONE*. (2009) 8:e6827. doi: 10.1371/journal.pone.0006827
91. Fischer J, Koch L, Emmerling C, Vierkotten J, Peters T, Bruning JC, et al. Inactivation of the Fto gene protects from obesity. *Nature*. (2009) 7240:894–8. doi: 10.1038/nature07848
92. Travison TG, Araujo AB, Esche GR, Beck TJ, McKinlay JB. Lean mass and not fat mass is associated with male proximal femur strength. *J Bone Miner Res*. (2008) 2:189–98. doi: 10.1359/jbmr.071016
93. Panoutsopoulou K, Metrustry S, Doherty SA, Laslett LL, Maciewicz RA, Hart DJ, et al. The effect of FTO variation on increased osteoarthritis risk is mediated through body mass index: a Mendelian randomisation study. *Ann Rheum Dis*. (2014) 12:2082–6. doi: 10.1136/annrheumdis-2013-203772
94. Kemp JP, Sayers A, Smith GD, Tobias JH, Evans DM. Using Mendelian randomization to investigate a possible causal relationship between adiposity and increased bone mineral density at different skeletal sites in children. *Int J Epidemiol*. (2016) 5:1560–72. doi: 10.1093/ije/dyw079

Conflict of Interest: The authors declare that the research was conducted in the absence of any commercial or financial relationships that could be construed as a potential conflict of interest.

frontiers in Endocrinology

ORIGINAL RESEARCH
published: 21 January 2020
doi: 10.3389/fendo.2019.00880

A Short-Term Ketogenic Diet Impairs Markers of Bone Health in Response to Exercise

Ida A. Heikura[1,2†], Louise M. Burke[1,2†], John A. Hawley[2], Megan L. Ross[1,2], Laura Garvican-Lewis[1,2], Avish P. Sharma[1,3], Alannah K. A. McKay[1,4], Jill J. Leckey[2], Marijke Welvaert[1,5,6], Lauren McCall[7] and Kathryn E. Ackerman[7,8]*

[1] Australian Institute of Sport, Canberra, ACT, Australia, [2] Exercise and Nutrition Research Program, Mary MacKillop Institute for Health Research, Australian Catholic University, Melbourne, VIC, Australia, [3] Griffith Sports Physiology and Performance, School of Allied Health Sciences, Griffith University, Gold Coast, QLD, Australia, [4] School of Human Sciences (Exercise and Sport Science), The University of Western Australia, Crawley, WA, Australia, [5] University of Canberra Research Institute for Sport and Exercise, Canberra, ACT, Australia, [6] Statistical Consulting Unit, Australian National University, Canberra, ACT, Australia, [7] Division of Sports Medicine, Boston Children's Hospital, Boston, MA, United States, [8] Neuroendocrine Unit, Massachusetts General Hospital and Harvard Medical School, Boston, MA, United States

OPEN ACCESS

Edited by:
Gordon L. Klein,
University of Texas Medical Branch at Galveston, United States

Reviewed by:
Peter Ebeling,
Monash University, Australia
Hasmik Jasmine Samvelyan,
Edinburgh Napier University, United Kingdom
Craig Sale,
Nottingham Trent University, United Kingdom
Gustavo A. Nader,
Pennsylvania State University (PSU), United States

***Correspondence:**
Louise M. Burke
louise.burke@ausport.gov.au

[†]These authors have contributed equally to this work

Specialty section:
This article was submitted to Bone Research, a section of the journal Frontiers in Endocrinology

Received: 04 September 2019
Accepted: 02 December 2019
Published: 21 January 2020

Citation:
Heikura IA, Burke LM, Hawley JA, Ross ML, Garvican-Lewis L, Sharma AP, McKay AKA, Leckey JJ, Welvaert M, McCall L and Ackerman KE (2020) A Short-Term Ketogenic Diet Impairs Markers of Bone Health in Response to Exercise. Front. Endocrinol. 10:880. doi: 10.3389/fendo.2019.00880

Objectives: To investigate diet-exercise interactions related to bone markers in elite endurance athletes after a 3.5-week ketogenic low-carbohydrate, high-fat (LCHF) diet and subsequent restoration of carbohydrate (CHO) feeding.

Methods: World-class race walkers (25 male, 5 female) completed 3.5-weeks of energy-matched (220 kJ·kg·d^{-1}) high CHO (HCHO; 8.6 g·kg·d^{-1} CHO, 2.1 g·kg·d^{-1} protein, 1.2 g·kg·d^{-1} fat) or LCHF (0.5 g·kg·d^{-1} CHO, 2.1 g·kg·d^{-1} protein, 75–80% of energy from fat) diet followed by acute CHO restoration. Serum markers of bone breakdown (cross-linked C-terminal telopeptide of type I collagen, CTX), formation (procollagen 1 N-terminal propeptide, P1NP) and metabolism (osteocalcin, OC) were assessed at rest (fasting and 2 h post meal) and after exercise (0 and 3 h) at Baseline, after the 3.5-week intervention (Adaptation) and after acute CHO feeding (Restoration).

Results: After Adaptation, LCHF increased fasting CTX concentrations above Baseline ($p = 0.007$, Cohen's $d = 0.69$), while P1NP ($p < 0.001$, $d = 0.99$) and OC ($p < 0.001$, $d = 1.39$) levels decreased. Post-exercise, LCHF increased CTX concentrations above Baseline ($p = 0.001$, $d = 1.67$) and above HCHO ($p < 0.001$, $d = 0.62$), while P1NP ($p < 0.001$, $d = 0.85$) and OC concentrations decreased ($p < 0.001$, $d = 0.99$) during exercise. Exercise-related area under curve (AUC) for CTX was increased by LCHF after Adaptation ($p = 0.001$, $d = 1.52$), with decreases in P1NP ($p < 0.001$, $d = 1.27$) and OC ($p < 0.001$, $d = 2.0$). CHO restoration recovered post-exercise CTX and CTX exercise-related AUC, while concentrations and exercise-related AUC for P1NP and OC remained suppressed for LCHF ($p = 1.000$ compared to Adaptation).

Conclusion: Markers of bone modeling/remodeling were impaired after short-term LCHF diet, and only a marker of resorption recovered after acute CHO restoration. Long-term studies of the effects of LCHF on bone health are warranted.

Keywords: ketogenic diet, bone health, exercise, nutrition, endurance athletes

INTRODUCTION

Despite the generally positive effects of exercise in promoting bone health, bone injuries represent a challenge to consistent training and competition in high performance sport (1). This, in part, is due to the interaction of dietary factors (e.g., low energy availability, poor vitamin D status, inadequate calcium intake) with unique features of the exercise program [e.g., minimal or excessive bone loading associated with weight- and non-weight-bearing sports, poor biomechanics (1, 2)]. Low energy availability (a mismatch between energy intake and the energy cost of exercise) occurs in both female and male athletes (2) and impairs bone health via direct (uncoupled bone turnover with increased resorption rates) and indirect (mediation by reproductive and metabolic hormones) mechanisms (1). In addition, carbohydrate (CHO) availability may also play a role in bone health. Indeed, results from several studies show that commencing endurance exercise with low compared to normal or high glycogen availability stimulates the release of the cytokine interleukin-6 (IL-6) from the exercising muscles (3, 4). Among its range of effects, IL-6 has been hypothesized to lead to enhanced activity of the receptor activator of the nuclear factor K B-ligand, which controls bone turnover by increasing osteoclastic activity (thereby increasing bone breakdown) (5). In support of this contention, bone resorption is acutely increased when CHO is restricted before (6), during (7), and after (8) prolonged (1–2 h) endurance (running) exercise, and may be linked to concomitant increases in IL-6 concentrations (7). However, a recent study has reported that acute reductions in CHO availability around exercise mediated an increase in markers of bone resorption that are independent of energy availability and circulating IL-6 (9). Apparent effects on other markers of bone metabolism, such as osteocalcin (OC) and the bone formation marker procollagen 1 N-terminal propeptide (P1NP) in these models have been small (6–9), although a 24 h fast has been reported to reduce blood OC concentrations in lightweight rowers (10).

Whether these changes in markers of bone metabolism persist (or are amplified) after chronic exposure to low CHO availability around exercise remains unknown, but is of relevance in view of the promotion of a ketogenic low CHO-high fat (LCHF) diet to athletes and its putative benefits for endurance performance (11). To date, no studies have examined the effects of longer-term restriction of CHO at rest or in relation to exercise, although in animal models and children with intractable epilepsy, chronic adaptation to a ketogenic LCHF diet is associated with poor bone health (12–16). In view of our recent observations of increased post-exercise IL-6 concentrations in elite race walkers following a 3.5-week adaptation to a LCHF diet (17), we investigated the interaction of this diet and strenuous exercise on markers of bone modeling/remodeling as secondary outcomes of our larger study.

METHODS

Participants

Thirty world-class athletes (25 male, 5 female race walkers; ages 27.7 ± 3.4 yr, BMI 20.6 ± 1.7 kg/m^2) were recruited over three separate training camps during preparation for the 2016 Summer Olympic Games and the 2017 World Championships, and provided written informed consent in accordance with the Human Ethics Committee of the Australian Institute of Sport (ethics approval no. 20150802 and 20161201). Six male participants undertook two camps, however two of these data sets were incomplete due to insufficient tissue samples, resulting in 4 participants who had completed two camps being included in the final analysis. In addition, two additional (male) data sets were excluded from the final analysis due to their inability to complete one of the experimental trials due to injury (unrelated to bone). Therefore, our final data set provided a total of 32 trials (n = 28 participants, 23 males, 5 females) with data for pre- (*Baseline*) and post-treatment (*Adaptation*), of which 18 trials (13 males, 5 females) also contributed to data from acute restoration to a HCHO diet (*Restoration*). Participants and elite coaches contributed to the concept and implementation of the research camps, helping to prioritize the themes of interest and contributing to the design of the training program and test protocols.

Study Overview

Participants completed a 3.5-week block of intensified training and laboratory and field testing, supported by either a high-CHO (HCHO) or an isoenergetic LCHF diet (**Figure 1**, **Table 1**), consumed under strict dietary control (18). Upon completion of the 3.5-week dietary intervention, a subset of participants (n = 18) completed a further testing block under conditions of acute high CHO availability. Markers of bone metabolism were measured after an overnight fast, in response to an energy-matched meal of nutrient composition matching the intervention diet, and in response to a bout of strenuous exercise (19), at Baseline, Adaptation, and Restoration (**Figure 1**).

Dietary Control

Details of dietary control are described briefly here; more details are described in prior work (18). Participants were allocated into HCHO and LCHF groups based on preference. Both diets were isocaloric (**Table 1**), however dietary CHO and fat intakes differed between groups during intervention. Study diets were designed and individualized for each athlete by trained members of the research team including registered sports dietitians, a professional chef, and exercise physiologists. All meals were weighed (food scales accurate to 2 g) and provided for athletes at set meal times. In addition, a collection of snacks per individual meal plans were provided to the athletes each day. Any unconsumed items or changes made to menu plans were weighed and recorded for final analysis of dietary intakes. Compliance to the meal plans was assessed daily. Meal plans were designed and final dietary analysis of actual intakes was conducted using FoodWorks 8 Professional Program (Xyris Software Australia Pty Ltd, Australia). Further analysis of intakes was completed using Microsoft Excel.

Experimental Design

Testing at Baseline, Adaptation, and Restoration involved a hybrid laboratory/field test of 25 km (males) or 19 km (females)

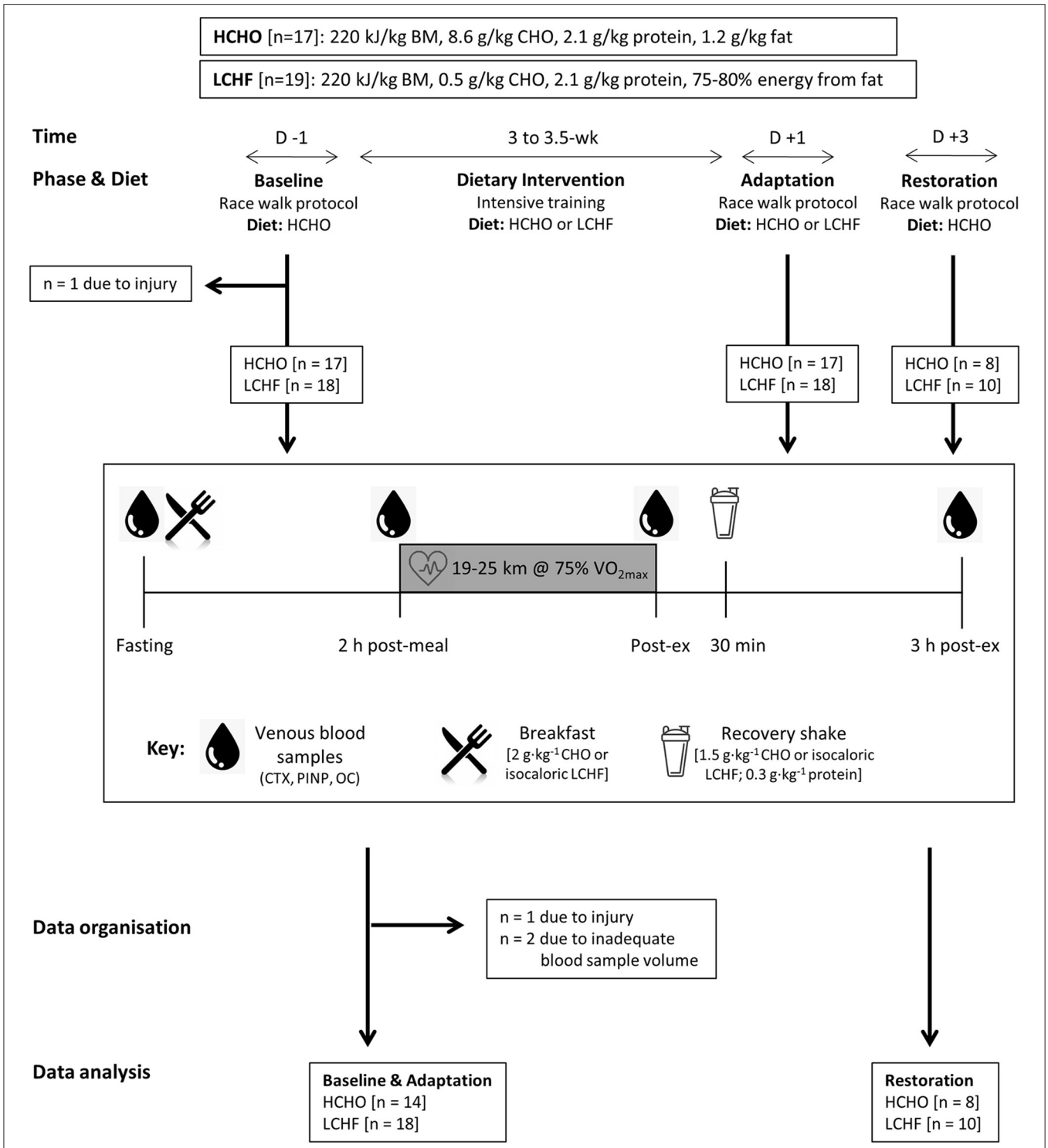

FIGURE 1 | Study flowchart and overview. Thirty-two data sets were gathered from 30 participants who participated in one or more training camps. After Baseline testing on a carbohydrate-rich (HCHO) diet, they elected to follow a 3.5-week energy-matched dietary intervention of either HCHO or ketogenic low carbohydrate-high fat (LCHF) principles. After Adaptation, the participants underwent an acute period of Restoration of high carbohydrate availability. At Baseline and at the end (Adaptation) of this intervention, as well as after acute carbohydrate reintroduction (Restoration) they undertook a test block including a 25 km (2 h) hybrid laboratory/field race walking protocol at ∼75% VO_2 max. Venous blood samples were collected after an overnight fast, 2 h after an energy-matched breakfast based on their diet (immediately pre-exercise), immediately post exercise and after 3 h of passive recovery during which an intervention-matched recovery shake was consumed at 30 min. Blood samples were analyzed for serum concentrations of C-terminal telopeptide of type I collagen (CTX), procollagen 1 N-terminal propeptide (P1NP), and osteocalcin (OC).

TABLE 1 | Dietary intakes in the HCHO and LCHF groups.

	Intervention		Restoration	
	HCHO ($n = 14$)	**LCHF ($n = 18$)**	**HCHO ($n = 8$)**	**LCHF ($n = 10$)**
Energy (kJ· d^{-1})	14,518 ± 2,142	15,138 ± 2,104	13,705 ± 1,948	15,706 ± 1,774
Energy (kJ· kg· d^{-1})	229 ± 13	227 ± 23	219 ± 16	239 ± 27
Protein (g· d^{-1})	133 ± 22	143 ± 19	132 ± 24	151 ± 18
Protein (g· kg· d^{-1})	2.1 ± 0.2	2.1 ± 0.2	2.1 ± 0.2	2.3 ± 0.2
Fat (g· d^{-1})	74 ± 14	318 ± 45***	77 ± 14	95 ± 12**$$$
Fat (g· kg· d^{-1})	1.2 ± 0.1	4.8 ± 0.5***	1.2 ± 0.1	1.4 ± 0.2**$$$
CHO (g· d^{-1})	549 ± 75	35 ± 5***	492 ± 60$	552 ± 62$$$
CHO (g· kg· d^{-1})	8.7 ± 0.4	0.5 ± 0.1***	7.9 ± 0.6$$	8.4 ± 1.0$$$

HCHO, high carbohydrate diet; LCHF, low carbohydrate high fat diet; CHO, carbohydrate.
$^{**}p < 0.01$, $^{***}p < 0.001$ significant difference between diets.
$^{\$}p < 0.05$, $^{\$\$}p < 0.01$, $^{\$\$\$}p < 0.001$ significantly different compared to Intervention.

at around 50 km race pace (75% of maximal oxygen uptake [VO_2 max]) (**Figure 1**). Upon entering the laboratory in an overnight fasted and rested state between 0600 and 0800 in the morning (times were kept consistent within-participant), a cannula was inserted into an antecubital vein for collection of blood samples at rest (Fasting), immediately before exercise (2 h post-meal), immediately after exercise (Post-ex) and 3 h post-exercise (3 h post-ex). Blood was analyzed for concentrations of cross-linked C-terminal telopeptide of type I collagen (CTX), P1NP and total OC to determine the effects of dietary interventions and exercise on bone metabolism. The cannulas were flushed with 3 ml of saline every 30 min throughout the trials. A standardized breakfast (2 g·kg^{-1} CHO for both groups during Baseline and Restoration, or an isocaloric low CHO option for LCHF during Adaptation) was consumed 30 min after the first blood sample, after which the participants rested for 120 min before beginning the session. During the Baseline and Restoration exercise test, both groups ingested glucose (60 g·h^{-1}) throughout the test, while during Adaptation, isocaloric high fat snacks were provided for the LCHF group. Upon completion of the exercise test, the participants rested in the laboratory for a further 3 h, and received a standardized recovery shake (1.5 g·kg^{-1} CHO for both groups during Baseline and Restoration, or an isocaloric low CHO option for LCHF during Adaptation; both shakes included 0.3 g·kg^{-1} protein) at 30 min post-exercise to improve satiety.

Analysis of Serum Bone Modeling/Remodeling Biomarkers

Blood samples were collected into a 3.5 mL EDTA BD Vacutainer Plus SST II tube, and allowed to clot by standing at room temperature for 2 h before centrifuging at 1,000 G for 10 min for subsequent analysis of serum markers of bone resorption (CTX), bone formation (P1NP) and overall bone metabolism (OC). Analysis was undertaken by chemiluminescence on IDS-iSYS (Immunodiagnostic Systems Limited; Boldon, Tyne and Wear, UK). Inter-assay coefficient of variation as reported by the manufacturer was 6.2, 4.6, and 6.1%, respectively. CVs were determined as follows: OC: 6 serum controls were run, using 3 reagents lots, in duplicate twice per day for 20 days, on 2 analyzers; P1NP: 3 serum controls were run, using 3 reagent lots, in quadruplicates once per day for 20 days, on 2 analyzers; CTX: 5 serum controls were run, using 3 reagent lots, in duplicate twice per day for 20 days, on 3 analyzers. In addition to these tests, the laboratory ran quality control samples throughout testing and the results were within the established acceptable manufacturer ranges. The raw data for the analyses of serum bone modeling/remodeling markers are provided in the **Supplementary Table** to this publication.

Statistical Analyses

Statistical analyses were conducted using SPSS Statistics 22 software (INM, New York, USA) and R (R Core Team, 2018) with a significance level set at $p \leq 0.05$. Normality of data was checked with a Shapiro-Wilk test and visual inspection of residual plots. General Linear Mixed models were fitted using the R package lme4 (20) and included random intercepts for Subjects and Camps to account for baseline inter individual heterogeneity and the partial cross-over design. Because the estimated Camp effect variance was 0, this random intercept was subsequently removed to resolve boundary issues in the Restricted Maximum Likelihood estimation. *P*-values were obtained using Type II Wald F tests with Kenward-Roger degrees of freedom. Initial models included all possible interactions but non-significant interaction terms were dropped for ease of interpretation. Fasting values and exercise-related area under curve [AUC; Pre-exercise to 3 h post-exercise (21)] for all markers were compared with a two-way mixed analysis of variance (ANOVA), with *post-hoc* tests of Student's *t*-tests for independent samples (between-groups) and for paired samples (within-groups); where normality was violated, Wilcoxon's test and Mann-Whitney U-test were used. Where a data point was missing, AUC was not calculated; this resulted in exclusion of 1 participant in the CTX AUC calculations, and 2 participants from both P1NP and OC calculations. Effect sizes were calculated based on the Classical Cohen's *d* while accounting for the study design by using the square root of the sum of all the variance components (specified random effects and residual error) in the denominator. Data are presented as means (95% confidence intervals [CI]).

RESULTS

Bone Modeling/Remodeling Biomarkers During Fasting

Compared to Baseline, fasting concentrations of CTX were increased after the LCHF diet (+22% [9, 35]: $p = 0.008$, $d = 0.69$), with a decrease in P1NP (−14% [−19, −9]; $p = 0.001$, $d = 0.99$) and OC (−25% [−35, −14]; $p < 0.001$, $d = 1.39$) levels (**Figure 2**). In addition, the change in fasting P1NP ($p < 0.001$, $d = 1.64$) and OC ($p < 0.001$, $d = 1.78$) after the 3.5-week intervention was significantly different between the diets (**Figure 2**).

Exercise Bone Markers

CTX decreased post-meal independent of dietary intervention (**Figures 3A**, **4A**, $p < 0.001$, $d = 1.63$). At Adaptation, post-exercise CTX concentrations in LCHF increased above Baseline ($p = 0.001$, $d = 1.67$) and HCHO ($p < 0.001$, $d = 0.62$) (**Figure 3A**). LCHF decreased P1NP (**Figure 3B**, $p < 0.001$, $d = 0.85$) and OC across exercise (**Figure 3C**, $p < 0.001$, $d = 0.99$) compared to Baseline. At Restoration, post-exercise CTX returned to Baseline levels for LCHF (**Figure 4A**, $p > 0.05$, $d = 0.20$ compared to Baseline), while concentrations of P1NP (**Figure 4B**, $p < 0.001$, $d = 0.23$) and OC (**Figure 4C**, $p < 0.001$, $d = 0.21$) remained suppressed across exercise.

Bone Marker Exercise Area Under Curve

At Adaptation, LCHF exercise-related AUC for CTX was greater [+81% (54, 109); $p < 0.001$, $d = 1.52$] than Baseline, and higher than HCHO ($p = 0.035$, $d = 0.81$) (**Figure 3D**). Exercise-related AUC for P1NP decreased at Adaptation for LCHF [−19% (−25, −12); $p = 0.003$, $d = 1.27$] compared with Baseline and was lower than HCHO ($p = 0.009$, $d = 1.03$) (**Figure 3E**), with similar outcomes for OC [−29% (−35, −23); $p < 0.001$, $d = 2.0$ and $p < 0.001$, $d = 1.64$, **Figure 3F**]. At Restoration, LCHF experienced a return of exercise-related AUC for CTX back to Baseline values [−43% (−21, 31); $p = 0.003$, $d = 1.08$ compared to Adaptation and no difference compared to HCHO; **Figure 4D**], meanwhile AUC for P1NP [+3% (−17, 48), $p = 1.000$ compared to Adaptation and $p = 0.009$, $d = 1.50$ compared to HCHO; **Figure 4E**], OC [−3% (−19, 14), $p = 1.000$ compared to Adaptation and $p = 0.010$, $d = 1.47$ compared to HCHO; **Figure 4F**] remained suppressed.

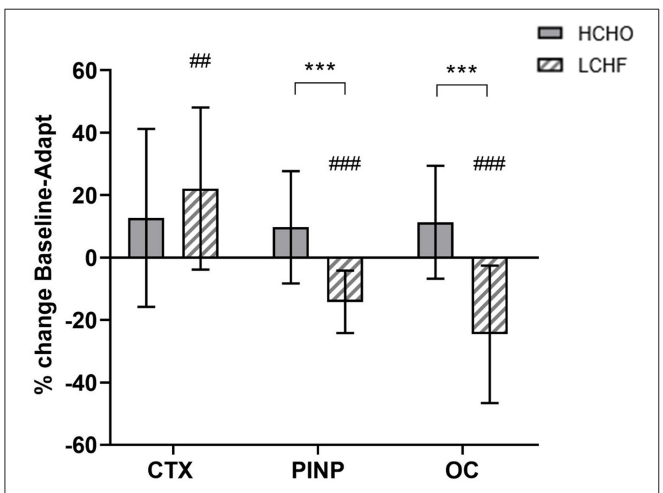

FIGURE 2 | Percentage change in fasting serum C-terminal telopeptide of type I collagen (CTX), procollagen 1 N-terminal propeptide (P1NP) and osteocalcin (OC) for high carbohydrate (HCHO; solid bars) and low CHO high fat (LCHF; striped bars) after the 3.5-week dietary intervention. Data are means ± standard deviations. $^{***}p < 0.001$ Significant between-group difference; $^{\#\#}p < 0.01$; $^{\#\#\#}p < 0.001$ Significant change from Baseline within-group.

DISCUSSION

Our data reveal novel and robust evidence of acute and likely negative effects on the bone modeling/remodeling process in elite athletes after a short-term ketogenic LCHF diet, including increased marker of resorption (at rest and post-exercise) and decreased formation (at rest and across exercise), with only partial recovery of these effects following acute restoration of CHO availability. Long-term effects of such alterations remain unknown, but may be detrimental to bone mineral density (BMD) and bone strength, with major consequences to health and performance. While ketogenic diets are of interest to athletes due to their ability to induce substantial shifts in substrate metabolism, increasing the contribution of fat-based fuels during exercise (11), we have previously reported the downside of a concomitantly greater oxygen cost and reduced performance of sustained high-intensity endurance exercise (19). The current study identifies further complexity in the interaction between the ketogenic diet and exercise with respect to markers of bone modeling/remodeling, in which catabolic processes are augmented and anabolic processes are reduced.

The LCHF diet is also popular within the general community for its purported health benefits, including rapid weight loss and improved glycemic control (22). However, data from animal studies (12, 13) demonstrate that chronic LCHF diets are associated with impaired bone growth, reduced bone mineral content, compromised mechanical properties, and slower fracture healing. Furthermore, increased bone loss has been reported in children with intractable epilepsy placed on a medically supervised LCHF diet for 6 months (14, 15). In contrast, adults with type 2 diabetes mellitus who self-selected to consume a LCHF diet for 2 years experienced no changes in spinal BMD in comparison to a "usual care" group (22). One explanation for these divergent outcomes involves interactions of the LCHF diet with the level of habitual contractile activity. Indeed in mice, a LCHF diet negated the positive benefits of exercise on BMD in trabecular bone (16), while in children with epilepsy, the rate of bone loss was greater in the more active patients (14). Therefore, the hormonal response to exercise undertaken with low CHO availability was of particular interest in our study.

Previous studies involving acute strategies of low CHO availability around exercise have identified effects on bone resorption, as measured by increased blood CTX concentrations. For example, males who undertook 60 min of treadmill running

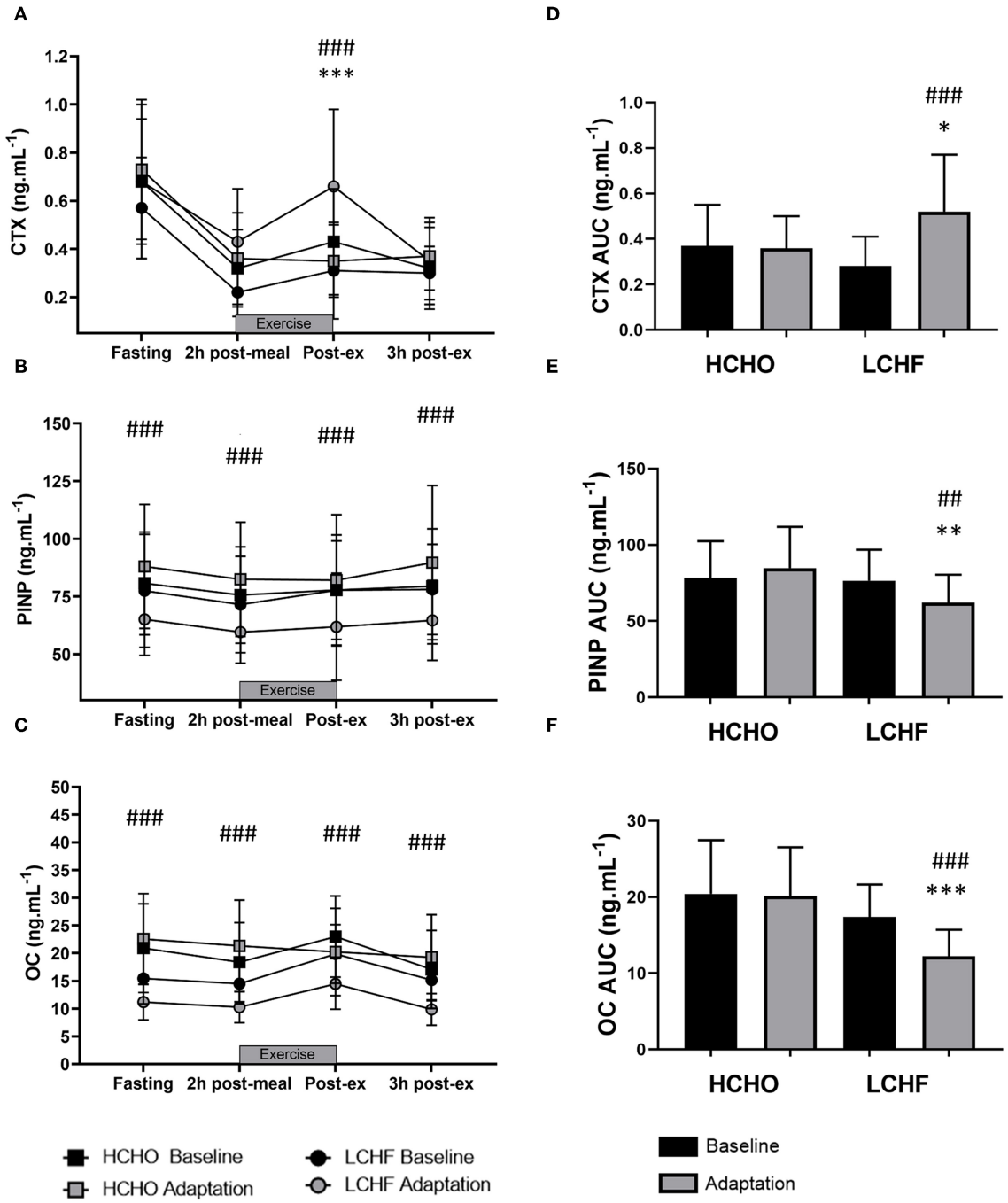

FIGURE 3 | Time course of changes in bone marker concentrations across exercise (left panel) and exercise area under curve (right panel) for serum C-terminal telopeptide of type I collagen (CTX) **(A,D)**, procollagen 1 N-terminal propeptide (P1NP) **(B,E)**, and osteocalcin (OC) **(C,F)** after the 3.5-week dietary intervention. Black bars/symbols represent Baseline, gray bars/symbols represent Adaptation. Squares and circles represent high carbohydrate (HCHO) and low carbohydrate high fat (LCHF), respectively. Gray bars represent a hybrid laboratory/field 19–25 km walk test at ∼75% VO_2 max. Data are means ± standard deviations. $^{\#\#}p < 0.01$; $^{\#\#\#}p < 0.001$ denotes significant differences at time points or tests within diet groups. $^{*}p < 0.05$; $^{**}p < 0.01$; $^{***}p < 0.001$ denotes significant differences between diet groups at a specific time point.

at 65% VO_2 max following a CHO-rich breakfast (∼1 g·kg^{1}) showed small variations in CTX responses, but only around the exercise period, while dietary effects on parathyroid hormone, OC and P1NP were not detected (6). Meanwhile, a more strenuous protocol (120 min at 70% VO_2 max) was associated with an attenuation of acute (pre-exercise to 2 h post-exercise)

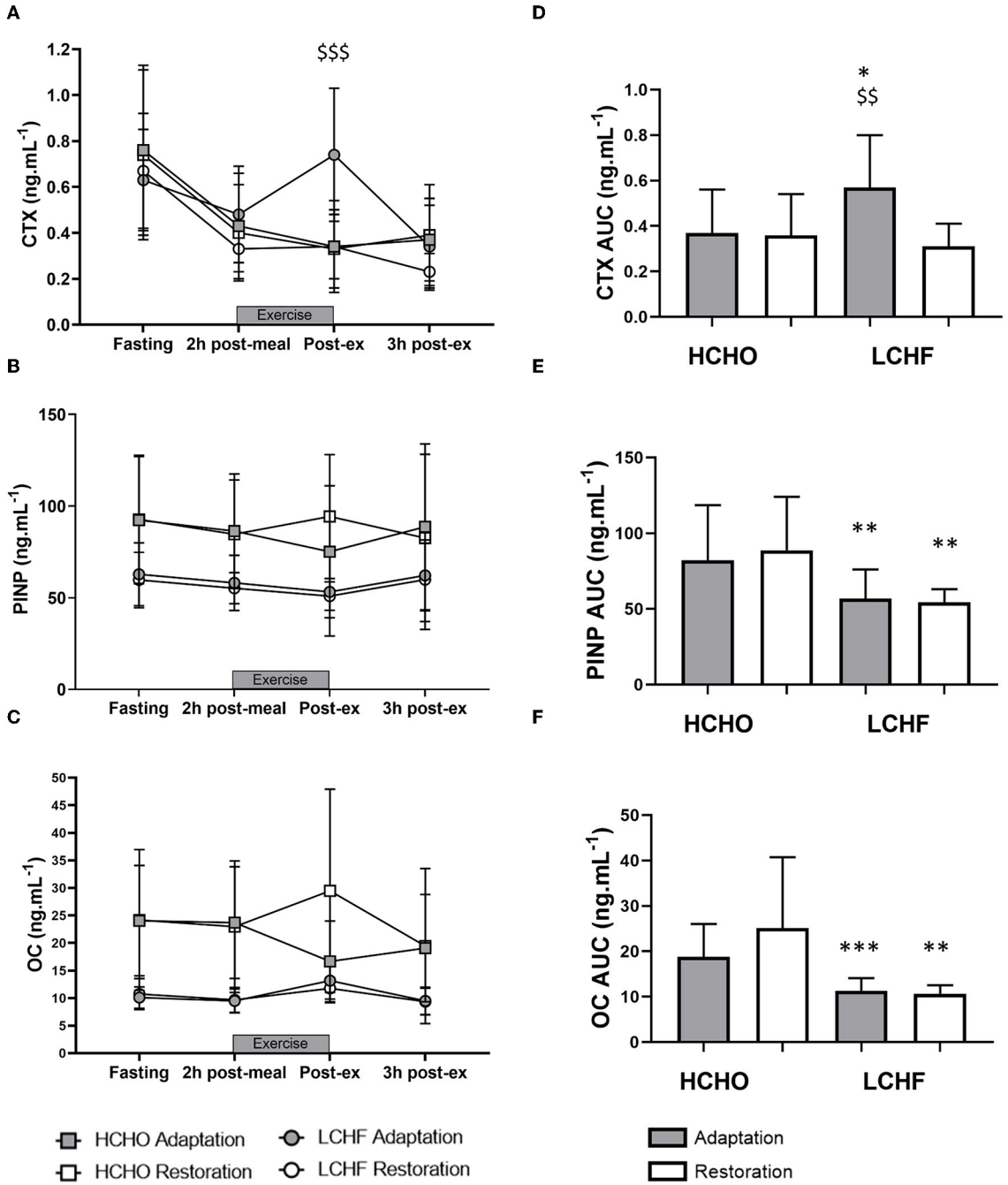

FIGURE 4 | Time course of changes in bone marker concentrations across exercise (left panel) and exercise area under curve (right panel) for serum C-terminal telopeptide of type I collagen (CTX) **(A,D)**, procollagen 1 N-terminal propeptide (P1NP) **(B,E)**, and osteocalcin (OC) **(C,F)** after acute reintroduction of carbohydrate (right panel). Gray bars/symbols represent Adaptation, and white bars/symbols represent Restoration. Squares and circles represent high carbohydrate (HCHO) and low carbohydrate high fat (LCHF), respectively. Gray bars represent a hybrid laboratory/field 19–25 km walk test at ∼75% VO_2 max. Data are means ± standard deviations. $^{\$\$}p < 0.01$; $^{\$\$\$}p > 0.001$ denotes significant within-group difference compared to Restoration. $^{*}p < 0.05$; $^{**}p < 0.01$; $^{***}p < 0.001$ denotes significant differences between diet groups at a specific time point.

concentrations of IL-6, CTX, and P1NP when CHO was consumed (0.7 g·kg·h^{1}) during exercise (7). However, OC was unchanged by diet and no differences in markers of bone metabolism were detected over the subsequent three days, suggesting that these effects are transient and quickly reversed (7). Short-term effects were also reported when 24 elite male runners with energy-matched intake over an 8 d period were divided into a group who consumed CHO before, during, and

immediately after each of their 13 training sessions (additional total CHO) while the others consumed an artificially sweetened placebo (23). Here, CTX concentrations were suppressed at 80 min of recovery following an interval training sessions in the CHO group with no dietary effects on P1NP or OC; furthermore, fasting concentrations of all markers were similar at baseline and on the ninth morning (23). Finally, Hammond and colleagues (9) investigated the independent effects of low CHO availability and acute energy restriction during the recovery from one session of high-intensity interval running and the completion of a subsequent session (3.5 h into recovery). They reported lower CTX concentrations in the high CHO (control) diet compared with both of the other conditions across the various acute responses to exercise-related feeding, while there were no differences between the energy and CHO restricted trials. Meanwhile, only energy restriction produced an increase in IL-6 responses to exercise, and there were no differences in P1NP concentrations between dietary treatments (9). Furthermore, 5 d of low vs. optimal energy availability, which also resulted in a 2-fold difference in CHO availability, was shown to result in a significant difference in the AUC of fasting CTX (+85 vs. +15%, respectively) and P1NP (−60 vs. −25%, respectively) (24). To date, the only study to report an effect of acute manipulations of CHO around exercise on bone formation markers was that of Townsend et al. (8), in which the immediate consumption of a protein-CHO feeding after a run to exhaustion at 75% VO_2 max was associated with a suppression of the post-exercise rise in CTX levels and a higher concentration of P1NP. These authors concluded that immediate post-exercise meal ingestion may benefit bone health compared to delayed feeding, although the effects on CTX concentrations were reversed at 4 h post-exercise and a similar time course of P1NP changes was not provided; therefore, it appears that the overall effect on bone modeling/remodeling processes appears to follow meal ingestion patterns.

The novelty of the current study was the interrogation of the effects of ***prolonged*** adaptation to CHO restriction on bone metabolism. Unlike the previous investigations, we identified clear and consistent effects on bone metabolism at rest and in response to exercise following 3.5-weeks of a ketogenic LCHF diet (**Figures 2–4**), with increases in a marker of bone resorption (CTX) and decreases in markers of bone formation (P1NP) and metabolism (OC). Although some might argue that a complete adaptation to a LCHF diet requires much longer than the 3.5-week period utilized in the current study, it should be noted that adaptations in substrate metabolism and exercise economy have been reported across this (19, 25), and much shorter (26), time periods. Nevertheless, the current study is reflective of a shorter-term adaptation to a LCHF diet and our findings warrant further investigation across longer time periods.

Acute restoration of high CHO availability was only partially effective in reversing these outcomes. Here, marker of bone resorption returned to baseline with high CHO pre-exercise meal and CHO ingestion throughout exercise, while the other markers of bone metabolism remained suppressed, indicating impaired overall balance of bone metabolism. This supports the concept proposed by Hammond et al. (9) that CTX is responsive to acute intake of CHO, possibly mediated through enteric hormone secretion. Meanwhile, differences in muscle glycogen content, which are not addressed by studies of acute feedings, may have a greater effect on OC and P1NP concentrations. Given the serious nature of injury risks and long-term outcomes of poor bone health in later life in endurance athletes, further consideration of the potential effects of the LCHF diet in exacerbating existing risk factors for poor bone health is warranted. In particular, we note that the impairment of bone metabolism around exercise and recovery would involve a significant portion of the day in athletes who undertake multiple training sessions, as well as being superimposed on the changes identified at rest.

The interaction of diet and exercise on bone metabolism is complex and requires more sophisticated investigation including replication of the current findings. Furthermore, evolving knowledge of inter-organ crosstalk suggests that outcomes of altered bone metabolism may be more far-reaching than the fate of the structural integrity of bone. Indeed, we note the recognition of muscle and bone as endocrine organs, with evidence that IL-6 released from contracting muscle has autocrine, paracrine and endocrine effects (27). This includes a purported feed-forward loop in which contraction-induced stimulation of osteocalcin in myofibers promotes the release of IL-6 and enhances muscle adaptation to exercise (27). Results of the current study challenge this synergistic relationship between osteocalcin signaling and IL-6, and remind us of the pleiotropic nature of the molecules stimulated by diet-exercise interactions.

Limitations

The data analysis undertaken in this study was a secondary outcome of our investigations of the ketogenic LCHF diet; these were not specifically powered to optimally address the potential effects on markers of bone modeling/remodeling. However, the detection of changes in the IL-6 response to prolonged exercise in our initial study (12) provided motivation to examine possible downstream effects. Because an identical protocol was undertaken in two separate studies of the LCHF diet, we were able to pool data from these investigations to double the sample size previously known to allow detection of changes in metabolism and performance. Indeed, changes in markers of bone metabolism in the response to the interaction of exercise and the dietary treatments were clearly detected with the pooled data, but were also identifiable in the case of the smaller sample size of the carbohydrate restoration arm of the current dataset. Therefore, we feel confident that our data are robust and warrant further investigation of this theme.

CONCLUSIONS

Despite recent interest in the potential benefits of LCHF diets on endurance performance or metabolic adaptation, the long-term health effects of this dietary intervention are largely unknown. We are the first to show that a 3.5-week ketogenic LCHF diet in elite endurance athletes has negative effects on the markers of bone modeling/remodeling at rest and during a prolonged high

intensity exercise session. We also show only partial recovery of these adaptations with acute restoration of CHO availability. Given the injury risks and long-term outcomes underpinned by poor bone health in later life, in athletes as well as individuals who undertake exercise for health benefits, additional investigations of the ketogenic diet and its role in perturbing bone metabolism are warranted.

DATA AVAILABILITY STATEMENT

The datasets analyzed for this study were harvested from 2 trials registered at Australian New Zealand Clinical Trial Registry (ACTRN12619001015134 and ACTRN12619000794101), found at: http://www.ANZCTR.org.au/ACTRN12619001015134.aspx and http://www.ANZCTR.org.au/ACTRN12619000794101.aspx.

ETHICS STATEMENT

The studies involving human participants were reviewed and approved by Australian Institute of Sport Ethics Committee. The patients/participants provided their written informed consent to participate in this study.

AUTHOR CONTRIBUTIONS

Conception and design of the experiments was undertaken by IH, LB, MR, LG-L, AS, AM, JL, MW, LM, and KA. Collection, assembly, analysis, and interpretation of data was undertaken by IH, LB, MR, LG-L, AS, AM, JL, MW, LM, and KA. Manuscript was prepared by IH, LB, KA, and JH. All authors approved the final version of the manuscript. IH and LB had full access to all the data in the study and take responsibility for the integrity of the data and the accuracy of the data analysis.

FUNDING

This study was funded by a Program Grant from the Australian Catholic University Research Funds to Professor LB (ACURF, 2017000034).

ACKNOWLEDGMENTS

We thank our research colleagues and supporters of the Supernova research series and acknowledge the commitment of the elite race-walking community.

SUPPLEMENTARY MATERIAL

The Supplementary Material for this article can be found online at: https://www.frontiersin.org/articles/10.3389/fendo.2019.00880/full#supplementary-material

Supplementary Table 1 | Individual data for the serum concentrations of bone modeling/remodeling markers (CTX, P1NP and Osteocalcin) in response to strenuous exercise (2 h race walking) and dietary interventions (high carbohydrate and low carbohydrate high fat diets) in elite race walkers.

REFERENCES

1. Mountjoy M, Sundgot-Borgen J, Burke L, Ackerman KE, Blauwet C, Constantini N, et al. International Olympic committee (IOC) consensus statement on relative energy deficiency in sport (RED-S): 2018 update. *Int J Sport Nutr Exerc Metab*. (2018) 28:316–31. doi: 10.1123/ijsnem.2018-0136
2. Scofield KL, Hecht S. Bone health in endurance athletes: runners, cyclists, and swimmers. *Curr Sports Med Rep*. (2012) 11:328–34. doi: 10.1249/JSR.0b013e3182779193
3. Steensberg A, Febbraio MA, Osada T, Schjerling P, van Hall G, Saltin B, et al. Interleukin-6 production in contracting human skeletal muscle is influenced by pre-exercise muscle glycogen content. *J Physiol*. (2001) 537(Pt 2):633–9. doi: 10.1111/j.1469-7793.2001.00633.x
4. Keller C, Steensberg A, Pilegaard H, Osada T, Saltin B, Pedersen BK, et al. Transcriptional activation of the IL-6 gene in human contracting skeletal muscle: influence of muscle glycogen content. *FASEB J*. (2001) 15:2748–50. doi: 10.1096/fj.01-0507fje
5. Lombardi G, Sanchis-Gomar F, Perego S, Sansoni V, Banfi G. Implications of exercise-induced adipo-myokines in bone metabolism. *Endocrine*. (2016) 54:284–305. doi: 10.1007/s12020-015-0834-0
6. Scott JP, Sale C, Greeves JP, Casey A, Dutton J, Fraser WD. Effect of fasting versus feeding on the bone metabolic response to running. *Bone*. (2012) 51:990–9. doi: 10.1016/j.bone.2012.08.128
7. Sale C, Varley I, Jones TW, James RM, Tang JC, Fraser WD, et al. Effect of carbohydrate feeding on the bone metabolic response to running. *J Appl Physiol*. (2015) 119:824–30. doi: 10.1152/japplphysiol.00241.2015
8. Townsend R, Elliott-Sale KJ, Currell K, Tang J, Fraser WD, Sale C. The effect of postexercise carbohydrate and protein ingestion on bone metabolism. *Med Sci Sports Exerc*. (2017) 49:1209–18. doi: 10.1249/MSS.0000000000001211
9. Hammond KM, Sale C, Fraser W, Tang J, Shepherd SO, Strauss JA, et al. Post-exercise carbohydrate and energy availability induce independent effects on skeletal muscle cell signalling and bone turnover: implications for training adaptation. *J Physiol*. (2019) 597:4779–96. doi: 10.1113/JP278209
10. Talbott SM, Shapses SA. Fasting and energy intake influence bone turnover in lightweight male rowers. *Int J Sport Nutr*. (1998) 8:377–87. doi: 10.1123/ijsn.8.4.377
11. Volek JS, Noakes T, Phinney SD. Rethinking fat as a fuel for endurance exercise. *Eur J Sport Sci*. (2015) 15:13–20. doi: 10.1080/17461391.2014.959564
12. Bielohuby M, Matsuura M, Herbach N, Kienzle E, Slawik M, Hoeflich A, et al. Short-term exposure to low-carbohydrate, high-fat diets induces low bone mineral density and reduces bone formation in rats. *J Bone Miner Res*. (2010) 25:275–84. doi: 10.1359/jbmr.090813
13. Scheller EL, Khoury B, Moller KL, Wee NK, Khandaker S, Kozloff KM, et al. Changes in skeletal integrity and marrow adiposity during high-fat diet and after weight loss. *Front Endocrinol*. (2016) 7:102. doi: 10.3389/fendo.2016.00102
14. Simm PJ, Bicknell-Royle J, Lawrie J, Nation J, Draffin K, Stewart KG, et al. The effect of the Ketogenic diet on the developing skeleton. *Epilepsy Res*. (2017) 136:62–6. doi: 10.1016/j.eplepsyres.2017.07.014
15. Bergqvist AG, Schall JI, Stallings VA, Zemel BS. Progressive bone mineral content loss in children with intractable epilepsy treated with the Ketogenic diet. *Am J Clin Nutr*. (2008) 88:1678–84. doi: 10.3945/ajcn.2008.26099
16. Scott MC, Fuller SE, Watt JD, Osborn ML, Johannsen N, Irving BA, et al. Cortical and trabecular bone morpohology in response to exercise and a Ketogenic diet: 2712 Board #4 May 31 1:00 PM - 3:00 PM. *Med Sci Sports Exerc*. (2019) 51:755–6. doi: 10.1249/01.mss.0000562752.04493.10

17. McKay AKA, Peeling P, Pyne DB, Welvaert M, Tee N, Leckey JJ, et al. Chronic adherence to a ketogenic diet modifies iron metabolism in elite athletes. *Med Sci Sports Exerc*. (2019) 51:548–55. doi: 10.1249/MSS.0000000000001816
18. Mirtschin JG, Forbes SF, Cato LE, Heikura IA, Strobel N, Hall R, et al. Organization of dietary control for nutrition-training intervention involving periodized carbohydrate availability and ketogenic low-carbohydrate high-fat diet. *Int J Sport Nutr Exerc Metab*. (2018) 28:480–9. doi: 10.1123/ijsnem.2017-0249
19. Burke LM, Ross ML, Garvican-Lewis LA, Welvaert M, Heikura IA, Forbes SG, et al. Low carbohydrate, high fat diet impairs exercise economy and negates the performance benefit from intensified training in elite race walkers. *J Physiol*. (2017) 595:2785–807. doi: 10.1113/JP273230
20. Bates D, Maechler M, Bolker B, Walker S. Fitting linear mixed-effects models using lme4. *J Stat Softw*. (2015) 67:1–48. doi: 10.18637/jss.v067.i01
21. Matthews JNS, Altman DG, Campbell MJ, Royston P. Analysis of serial measurements in medical research. *Br Med J*. (1990) 300:230–5. doi: 10.1136/bmj.300.6719.230
22. Athinarayanan SJ, Adams RN, Hallberg SJ, McKenzie AL, Bhanpuri NH, Campbell WW, et al. Long-term effects of a novel continuous remote care intervention including nutritional lchfsis for the management of type 2 diabetes: a 2-year non-randomized clinical trial. *Front Endocrinol*. (2019) 10:348. doi: 10.3389/fendo.2019.00348
23. de Sousa MV, Pereira RM, Fukui R, Caparbo VF, da Silva ME. Carbohydrate beverages attenuate bone resorption markers in elite runners. *Metabolism*. (2014) 63:1536–41. doi: 10.1016/j.metabol.2014.08.011
24. Papageorgiou M, Elliott-Sale K, Parsons A, Tang JCY, Greeves JP, Fraser WD, et al. Effects of reduced energy availability on bone metabolism in women and men. *Bone*. (2017) 115:191–9. doi: 10.1016/j.bone.2017.08.019
25. Shaw DM, Merien F, Braakhuis A, Maunder ED, Dulson DK. Effect of a ketogenic diet on submaximal exercise capacity and efficiency in runners. *Med Sci Sports Exerc*. (2019) 51:2135–46. doi: 10.1249/MSS.0000000000002008
26. Burke LM, Angus DJ, Cox GR, Cummings NK, Febbraio MA, Gawthorn K, et al. Effect of fat adaptation and carbohydrate restoration on metabolism and performance during prolonged cycling. *J Appl Physiol*. (2000) 89:2413–21. doi: 10.1152/jappl.2000.89.6.2413
27. Karsenty G, Mera P. Molecular bases of the crosstalk between bone and muscle. *Bone*. (2018) 115:43–9. doi: 10.1016/j.bone.2017.04.006

Conflict of Interest: The authors declare that the research was conducted in the absence of any commercial or financial relationships that could be construed as a potential conflict of interest.

frontiers in Endocrinology

ORIGINAL RESEARCH
published: 28 January 2020
doi: 10.3389/fendo.2019.00922

HIF-1α Regulates Glucocorticoid-Induced Osteoporosis Through PDK1/AKT/mTOR Signaling Pathway

Wen-Ning Xu†, Huo-Liang Zheng†, Run-Ze Yang, Lei-Sheng Jiang and Sheng-Dan Jiang**

Department of Clinic of Spine Center, Xinhua Hospital, Shanghai Jiaotong University School of Medicine, Shanghai, China

Long-term and high dose glucocorticoid treatment can cause decreased viability and function of osteoblasts, which leads to osteoporosis and osteonecrosis. In this study, we investigated the role and mechanism of action of HIF-1α in glucocorticoid-induced osteogenic inhibition in MC3T3-E1 cells. Our results showed that HIF-1α protein expression was reduced when MC3T3-E1 cells were exposed to dexamethasone (Dex) at varying concentrations ranging from 10^{-9} to 10^{-6} M. PDK1 expression was also decreased in MC3T3-E1 cells after dexamethasone treatment. MC3T3-E1 cells when treated with the glucocorticoid receptor antagonist RU486 along with dexamethasone showed enhanced HIF-1α expression. In addition, upregulated expression of HIF-1α was capable of promoting the osteogenic ability of MC3T3-E1 cells and PDK1 expression. However, the HIF-1α antagonist 2-methoxyestradiol (2-ME) had a reverse effect in MC3T3-E1 cells exposed to dexamethasone. Furthermore, the PDK1 antagonist dichloroacetate could repress the osteogenic ability of MC3T3-E1 cells, although HIF-1α was upregulated when transduced with adenovirus-HIF-1α construct. The PDK1 agonist PS48 was able to promote the osteogenic ability of MC3T3-E1 cells treated with dexamethasone. Importantly, the protein levels of p-AKT and p-mTOR were increased in MC3T3-E1 cells treated with dexamethasone after PS48 treatment. *in vivo*, the PDK1 agonist PS48 could maintain the bone mass of mice treated with dexamethasone. This study provides a new understanding of the mechanism of glucocorticoid-induced osteoporosis.

Keywords: glucocorticoid, HIF-1α, PDK1, osteoblast, osteoporosis

OPEN ACCESS

Edited by:
Marco P. Brotto, University of Texas at Arlington, United States

Reviewed by:
Yukiko Kitase, Indiana University, United States
Han Qiao, Shanghai Jiao Tong University, China

****Correspondence:***
Lei-Sheng Jiang
jiangleisheng@xinhuamed.com.cn
Sheng-Dan Jiang
jiangshengdan@xinhuamed.com.cn

†These authors have contributed equally to this work

Specialty section:
This article was submitted to Bone Research, a section of the journal Frontiers in Endocrinology

Received: *20 August 2019*
Accepted: *17 December 2019*
Published: *28 January 2020*

Citation:
Xu W-N, Zheng H-L, Yang R-Z, Jiang L-S and Jiang S-D (2020) HIF-1α Regulates Glucocorticoid-Induced Osteoporosis Through PDK1/AKT/mTOR Signaling Pathway. Front. Endocrinol. 10:922. doi: 10.3389/fendo.2019.00922

INTRODUCTION

Glucocorticoids (GCs), as immunosuppressive and anti-inflammatory drugs, are used extensively to treat various disorders such as autoimmune and inflammatory diseases, among others (1, 2). Patients develop osteoporosis and osteonecrosis due to decreased viability and function of osteoblasts caused by long-term and high dose glucocorticoid treatment (3–5). GCs impair the survival and osteogenic ability of osteoblasts, which is believed to be the main physiopathologic mechanism of GC-induced bone loss (6). Recent studies have reported that apoptosis or autophagy

of osteoblasts are involved in GC-induced osteogenic inhibition in bone cells (3, 7). Glucocorticoids destroy the bone and bone structure by controlling the differentiation of bone marrow-derived stem cells (BMSCs) which differentiate into adipocyte lineage but not osteoblast lineage in bone microenvironments (8). However, the mechanisms of glucocorticoid-induced osteogenic inhibition in osteoblasts remain unknown.

Hypoxia inducible factor-1α (HIF-1α) is highly expressed in hypoxic cells (9, 10). Recent studies have demonstrated that HIF-1α also plays an important role in cell survival in a normoxic environment (11–13). HIF-1α regulates target gene expression to control cell metabolism (14). The bone marrow microenvironment, which affects bone cells including osteoblasts and osteoclasts, and immune cells, is considerably hypoxic by nature (15). Mice with osteoblast-specific deletion of von Hippel-Lindau (VHL) and osteoblast-specific overexpression of HIF-1α show increased bone volume and osteoblast numbers (15, 16). HIF-1α is a transcription factor which regulates the levels of VEGF, resulting in high trabecular bone mass and increased bone vascular density (17–19). HIF-1α has also been reported to regulate PDK1 expression, but not VEGF, resulting in increased bone mass (15). Glucocorticoids suppressed the expression of HIF-1α and VEGF in osteoblasts and osteocytes of mice (20). However, the role of HIF-1α in glucocorticoid-induced osteogenic inhibition of osteoblasts is still unclear.

Pyruvate dehydrogenase kinase (PDK1) suppresses mitochondrial function through antagonizing the function of pyruvate dehydrogenase (PDH), a rate-limiting enzyme involved in the conversion of pyruvate to acetyl-coenzyme A, and entry into the tricarboxylic acid cycle (21). Moreover, PDK1 promotes cell proliferation via activating the AKT pathway (22, 23). Nevertheless, whether PDK1 inhibits osteoblast-induced osteoporosis by regulating glucocorticoid-induced osteoblasts is unclear. In this study, we investigated the role of HIF-1α and PDK1 in regulating glucocorticoid-induced osteogenic inhibition of osteoblasts.

MATERIALS AND METHODS

Cell Culture and Treatments

The pre-osteoblast cell line MC3T3-E1 (subclone 4) was purchased from ATCC (USA) and cultured in α-MEM (#SH30265; Hyclone, GE Healthcare Life Sciences, Pittsburgh, PA, USA) containing 10% fetal bovine serum (FBS, #10099; Gibco, Thermo Fischer Scientific, Bartlesville, OK, USA) in 6 cm plates and incubated at 37°C with 5% CO_2/95% air. Osteogenic differentiation was induced as described in a previous study (24). MC3T3-E1 cells were cultured in an osteogenic differentiation medium containing 4 mM glycerophosphate (#G9891; Sigma-Aldrich, St. Louis, MO, USA) and 25 μg/mL ascorbic acid (#A4403; Sigma-Aldrich) until 70% confluency. Dexamethasone (#D4902; Sigma-Aldrich, final concentration of ethanol, 0.01%, vol/vol) at different concentrations was then added to the osteogenic differentiation medium for 14 days. The culture medium was replaced every two days. MC3T3-E1 cells were cultured in a culture medium containing 10^{-7} M dexamethasone supplemented with or without RU486 (10^{-5} M), 2-ME (20 μM), DCA (10 mM), and PS48 (5 μM).

Animals and Grouping

Fifteen male C57BL/6J mice (8 weeks of age, Shanghai SLAC Laboratory Animal Co., Ltd., Shanghai, China) were randomly assigned into three groups ($n = 5$ per group): control group (injected with empty adenoviral vector and intraperitoneal injection of normal saline), dexamethasone group (injected with empty adenoviral vector and intraperitoneal injection of dexamethasone), and dexamethasone + Ad-PDK1 group (intraperitoneal injection of dexamethasone and bone marrow injection of adenovirus carrying a promoter to overexpress PDK1). Dexamethasone (10 mg/kg bodyweight) was injected intraperitoneally for 21 days, as described in a previous study (25). All mice were euthanized. Bilateral femurs of mice were obtained for subsequent experiments. Male mice were used *in vivo* study in order to rule out the effects of estrogen. All animal care procedures were in accordance with the guidelines of the Ethics Committee of Xinhua Hospital Affiliated to Shanghai Jiao Tong University School of Medicine and were approved by this committee.

Adenoviral Transduction

In vitro, MC3T3-E1 cells were cultured in six-well plates, and adenoviral solution (carrying empty vector or a promoter to overexpress HIF-1α or PDK1) was added into the growth medium. After 48 h, the medium containing adenovirus was removed and osteogenic differentiation medium was added. The target gene and protein expression were confirmed by qRT-PCR and western blotting, respectively. Adenoviral vectors were purchased from Hanbio Biotechnology Co., Ltd. (Shanghai, China).

In vivo, adenoviral particles carrying empty vector or a promoter to overexpress PDK1 were injected into the bone marrow cavity of bilateral femurs, at a dose of 20 μL virus solution (5×10^8 pfu)/limb using a 25 μL microsyringe (Hamilton, 1702RN, Reno, NV, USA) every 2 weeks, as described in a previous study (26).

ALP and Alizarin Red Staining Assay

MC3T3-E1 cells were washed with PBS thrice and fixed with 4% paraformaldehyde for 20 min after induction of osteogenic differentiation. ALP staining was performed for 30 min using the BCIP/NBT reagent kit (Leagene Biotechnology, Beijing, China). Alizarin red staining was performed using the Alizarin working solution (Cyagen Biosciences, Shanghai, China) for 5 min according to the manufacturer's instructions. After washing three times with PBS, the stained MEC3T3-E1 cells in each well were photographed. Each staining experiment was performed at least three times, separately.

Western Blotting

Total protein was isolated from MC3T3-E1 cells using RIPA (Radio-Immunoprecipitation Assay, Beyotime, Shanghai, China) lysis buffer containing 1% PMSF (Phenylmethylsulfonyl fluoride, Beyotime, Shanghai, China). Protein samples were

separated by SDS-PAGE and transferred onto polyvinylidene difluoride (PVDF) membranes. PVDF membranes containing proteins were blocked with 5% non-fat milk for 1 h and then incubated with specific primary antibodies overnight at 4°C. Primary antibodies included HIF-1α (1:1,000, Proteintech, USA), PDK1 (1:1,000, Proteintech, USA), Runx2 (1:1,000, Abcam, UK), OCN (1:1,000, Abcam, UK), ALP (1:1,000, Cell Signaling Technology, USA), total-Akt (1:2,000, Cell Signaling Technology, USA), phospho-Akt (1:1,000, Cell Signaling Technology, USA), total-mTOR (1:2,000, Cell Signaling Technology, USA), phospho-mTOR (1:1,000, Cell Signaling Technology, USA) and GAPDH (1:1,000, Beyotime, Shanghai, China). After washing three times with TBST for 5 min, the PVDF membranes were incubated with horseradish peroxidase-conjugated anti-rabbit secondary antibody for 1 h and target proteins were visualized using the Western Chemiluminescent HRP Substrate Kit (Millipore, Billerica, MA, USA).

Hematoxylin-Eosin and Immunohistochemical Staining

The dissected femurs were fixed in 10% buffered formalin for 3 days, and then decalcified in 10% EDTA (pH = 7.0) at 4°C for 21 days, embedded in paraffin and sectioned for follow-up experiments. For hematoxylin-eosin staining, bone sections were stained with hematoxylin for 5 min and then stained with eosin for 2 min. For immunohistochemical staining, bone sections were incubated with PDK1-specific primary rabbit antibody (1:200 dilution) overnight at 4°C. Isotype control was incubated with rabbit IgG. A horseradish peroxidase-streptavidin detection system (Dako, Glostrup, Sweden) was used to examine the immunoreactivity.

Micro-Computed Tomography Scanning and Quantitative Analysis

The femurs were fixed overnight in 70% ethanol and scanned using Scanco μCT 40 scanner (Scanco Medical AG, Zurich, Switzerland) at a resolution of 18 μm. Two/three dimensional images were obtained and analyzed to evaluate bone mass, bone mineral density (BMD), bone volume/total volume (BV/TV), trabecular thickness (Tb. Th), trabecular number (Tb. N), trabecular separation (Tb. Sp), Medullary area (Ma. Ar), Total area (Tt. Ar), Cortical bone thickness (Ct. Th), and Cortical Area (Ct. Ar) of the distal femur. We set the region of interest (ROI) as trabecular bone of 2-mm length below the epiphyseal growth plate.

Statistical Analysis

All data are presented as the mean ± SD of three independent experiments and quantified relative to control experiments. The differences between multiple groups were analyzed by ANOVA and Tukey *post hoc* analysis. Differences were considered as statistically significant when p value was < 0.05. $^{***}p < 0.001$, $^{**}p < 0.01$, $^{*}p < 0.05$.

RESULTS

Downregulation of HIF-1α and PDK1 by Dexamethasone

To investigate the expression of HIF-1α in glucocorticoid-induced osteogenic inhibition, MC3T3-E1 cells were exposed to dexamethasone at varying concentrations ranging from 10^{-9} to 10^{-6} M. The results of western blotting showed that the protein expression of HIF-1α was decreased (**Figure 1A**). The expression of osteogenic markers such as Runx2 and OCN were also decreased and these results confirmed that dexamethasone could repress the ability and function of osteoblasts. Recent reports have shown that HIF-1α could regulate PDK1 to mediate metabolic effects in different types of cells (15, 27). Therefore, we examined PDK1 expression by western blotting. As shown in **Figure 1A**, PDK1 expression was reduced in MC3T3-E1 cells exposed to dexamethasone. Based on results from a previous study (28) and our findings, we determined that 10^{-6} M of dexamethasone was the most optimal concentration. Treatment of MC3T3-E1 cells with 10^{-6} M dexamethasone for 7 days induced remarkable osteogenic inhibition (**Figure 1B**).

To further confirm whether dexamethasone treatment inhibits osteogenic ability of osteoblasts, MC3T3-E1 cells treated with dexamethasone were exposed to the glucocorticoid antagonist RU486 (10^{-5} M). As shown in **Figure 1C**, RU486 reversed the inhibitory effect of Dex to a similar level as observed in the control cells. These results revealed that dexamethasone inhibited osteogenic ability of osteoblasts through HIF-1α and PDK1. However, whether HIF-1α regulates the osteogenic inhibition induced by dexamethasone via PDK1 is still an unanswered question.

Upregulation of HIF-1α Promotes Osteogenic Function Through Facilitating PDK1 Expression

To test whether overexpression of HIF-1α promotes dexamethasone-induced osteogenic inhibition in MC3T3-E1 cells, we overexpressed HIF-1α by transducing cells with adenoviral plasmid containing HIF-1α construct. As shown in **Figure 2A**, the results of ALP and Alizarin red staining showed that overexpression of HIF-1α led to increased osteogenic function in MC3T3-E1 cells. Western blotting results confirmed the above findings. The expression of the osteogenic marker Runx2 was increased. HIF-1α and PDK1 expression levels were also increased in MC3T3-E1 cells (**Figure 2B**).

To further affirm the role of HIF-1α in MC3T3-E1 cells exposed to dexamethasone, HIF-1α antagonist 2-methoxyestradiol (2-ME, 20 μM) was added to medium containing dexamethasone. The osteogenic inhibition induced by dexamethasone was enhanced in dexamethasone + 2-ME treated cells (**Figure 2C**). Inhibition of HIF-1α expression was also accelerated in dexamethasone + 2-ME treated cells. In addition, 2-ME enhanced the inhibition of PDK1 expression. 2-ME treatment showed increased inhibition of osteogenic markers Runx2 and OCN (**Figure 2D**). These results demonstrated that HIF-1α regulated dexamethasone-induced osteogenic inhibition via PDK1 expression.

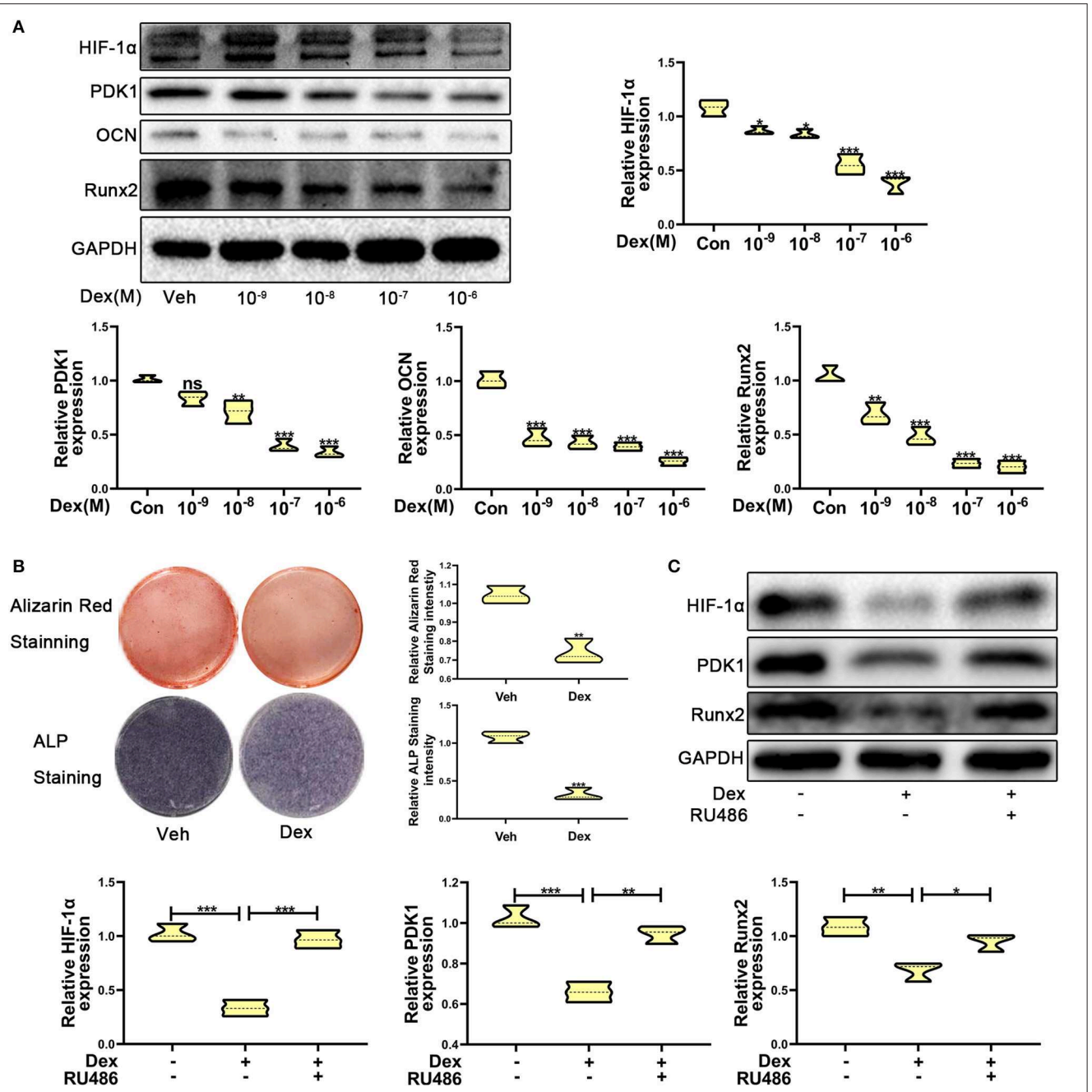

FIGURE 1 | Dexamethasone inhibited the osteogenic function of MC3T3-E1 cells via regulating HIF-1α expression. **(A)** The protein expression levels of HIF-1α, PDK1, OCN, Runx2, and GAPDH were determined by western blotting in MC3T3-E1 cells treated with a varying concentration of dexamethasone for 14 days. **(B)** ALP and Alizarin red staining were performed to detect the osteogenic function of MC3T3-E1 cells treated with vehicle and dexamethasone. **(C)** Western blotting was performed to detect the protein expression levels of HIF-1α, PDK1, Runx2, and GAPDH in MC3T3-E1 cells treated with vehicle, dexamethasone, and dexamethasone + RU486, respectively. Differences were considered as statistically significant when $p < 0.05$. ***$p < 0.001$, **$p < 0.01$, *$p < 0.05$.

Repression of PDK1 Reverses the Protective Effect of HIF-1α on Glucocorticoid-Induced Osteogenic Inhibition

To further confirm whether HIF-1α regulates glucocorticoid-induced osteogenic inhibition via the PDK1 signaling pathway, PDK1 antagonist dichloroacetate (DCA, 10 mM) (29) was added to the medium. As shown in **Figure 3A**, western blotting showed that the expression levels of osteogenic markers such as Runx2, OCN, and ALP were increased in adenovirus- HIF-1α + dexamethasone group compared to adenovirus-NC + dexamethasone group. However, there was decreased expression of Runx2, OCN, and ALP in adenovirus + dexamethasone +

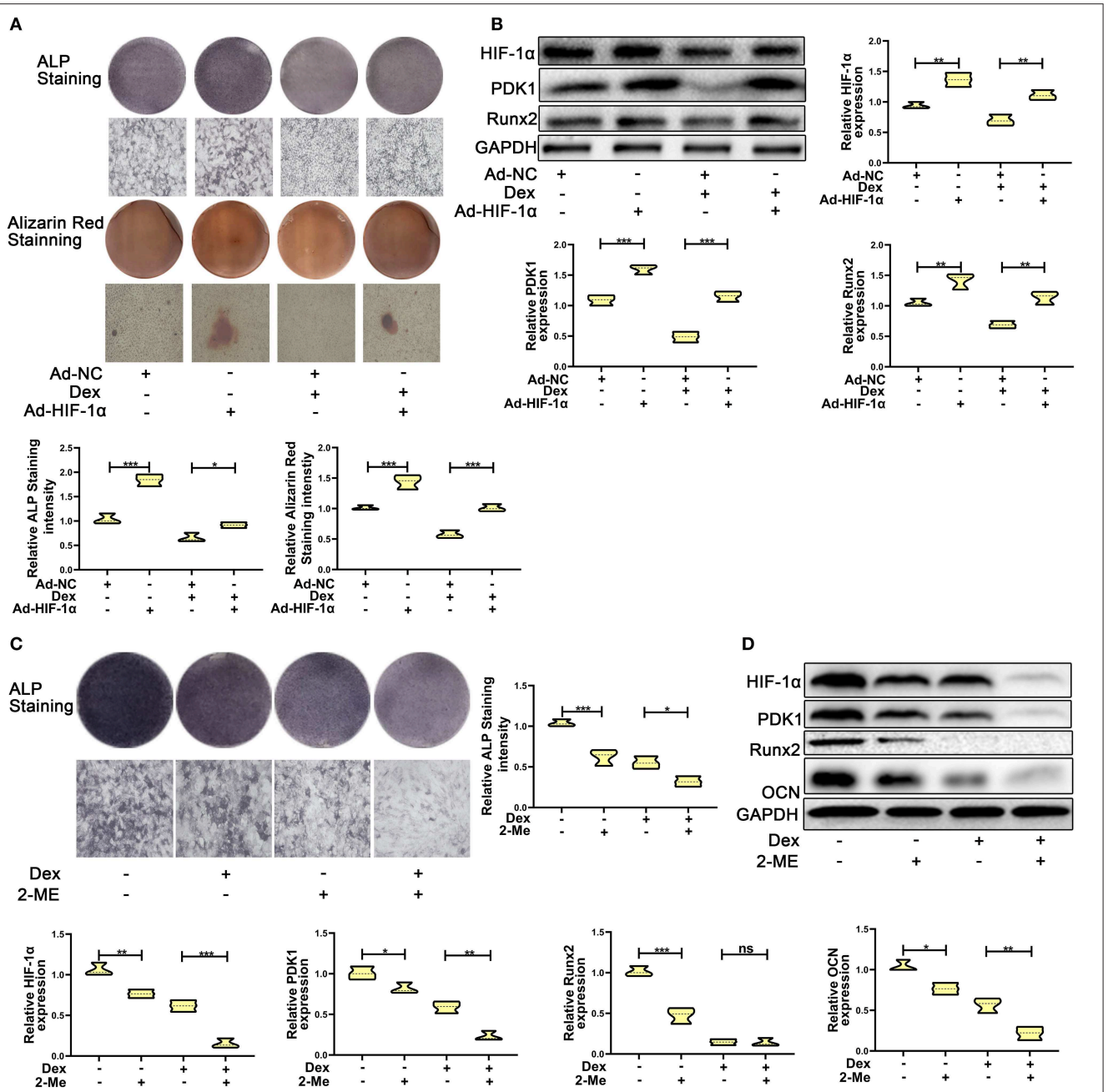

FIGURE 2 | HIF-1α mediated dexamethasone-induced osteogenic inhibition of osteoblasts via regulating PDK1 expression. **(A)** Osteogenic ability was confirmed by ALP and Alizarin red staining in MC3T3-E1 cells treated with Ad-NC, Ad- HIF-1α + dexamethasone, Ad-NC + dexamethasone and Ad-HIF-1α + dexamethasone, respectively. Scale Bar = 20 μm. **(B)** The protein expression levels of HIF-1α, PDK1, Runx2, and GAPDH were detected by western blotting in MC3T3-E1 cells treated with Ad-NC, Ad-HIF-1α + dexamethasone, Ad-NC + dexamethasone and Ad-HIF-1α + dexamethasone, respectively. **(C)** Osteogenic ability was confirmed by ALP staining in MC3T3-E1 cells treated with empty vector, dexamethasone, 2-ME and dexamethasone + 2-ME, respectively. Scale Bar = 20 μm. **(D)** The protein expression levels of HIF-1α, PDK1, Runx2, OCN, and GAPDH were detected by western blotting in MC3T3-E1 cells treated with empty vector, dexamethasone, 2-ME and dexamethasone + 2-ME, respectively. Differences were considered as statistically significant when $p < 0.05$. ***$p < 0.001$, **$p < 0.01$, *$p < 0.05$.

DCA group compared to adenovirus-HIF-1α + dexamethasone group. The results of ALP and Alizarin red staining demonstrated that osteogenic ability of MC3T3-E1 cells was reduced in the adenovirus- HIF-1α + dexamethasone + DCA group compared to adenovirus-HIF-1α + dexamethasone group (**Figure 3B**). These results suggested that HIF-1α promoted the osteogenic ability of MC3T3-E1 cells treated with dexamethasone, by regulating PDK1 expression.

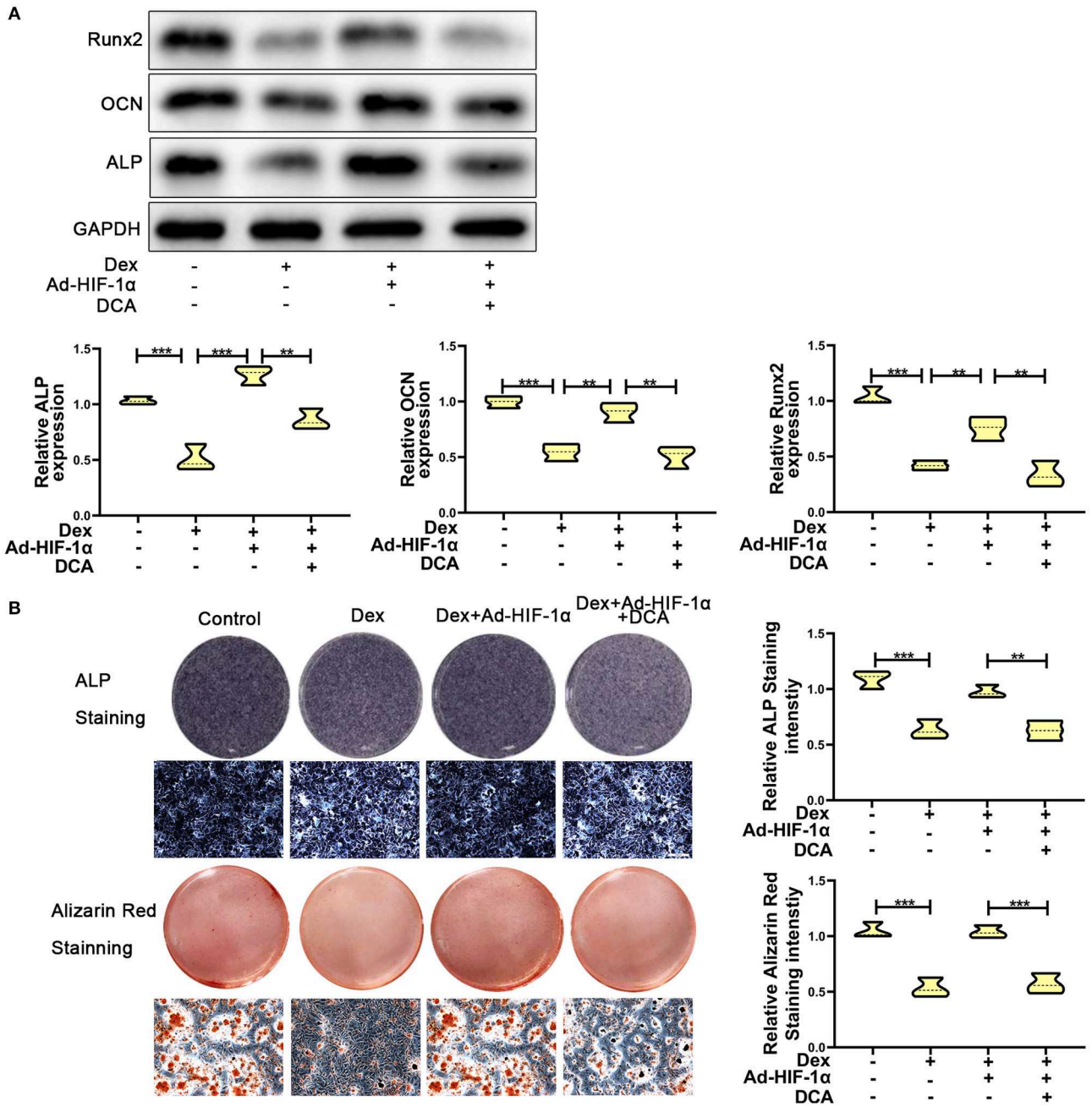

FIGURE 3 | Repression of PDK1 reversed the protective effect of Adenovirus-HIF-1α on glucocorticoid-induced osteogenic inhibition in MC3T3-E1 cells. **(A)** The protein expression levels of osteogenic markers Runx2, OCN, ALP, and GAPDH were determined by western Blotting in MC3T3-E1 cells exposed to empty vector, dexamethasone, dexamethasone + Ad-HIF-1α, and dexamethasone + Ad-HIF-1α+ DCA, respectively. **(B)** ALP and Alizarin red Staining were performed to determine the osteogenic ability of MC3T3-E1 cells exposed to empty vector, dexamethasone, dexamethasone + Ad-HIF-1α, dexamethasone + Ad-HIF-1α+ DCA, respectively. Scale Bar = 20 μm. Differences were considered as statistically significant when $p < 0.05$. ***$p < 0.001$, **$p < 0.01$, *$p < 0.05$.

Upregulation of PDK1 Facilitated the Osteogenic Ability of Osteoblasts After Glucocorticoid Treatment via the AKT/mTOR Pathway

To verify the role of PDK1 in osteoblasts, we treated MC3T3-E1 cells with the PDK1 activator PS48 (5 μM) (30). PS48 promoted the expression levels of PDK1 in addition to osteogenic markers Runx2, OCN and ALP (**Figure 4A**). ALP and Alizarin red staining suggested that the osteogenic function of MC3T3-E1 cells treated with dexamethasone was enhanced by PS48 (**Figure 4B**). These results indicated that PDK1 was able to regulate glucocorticoid-induced osteogenic inhibition.

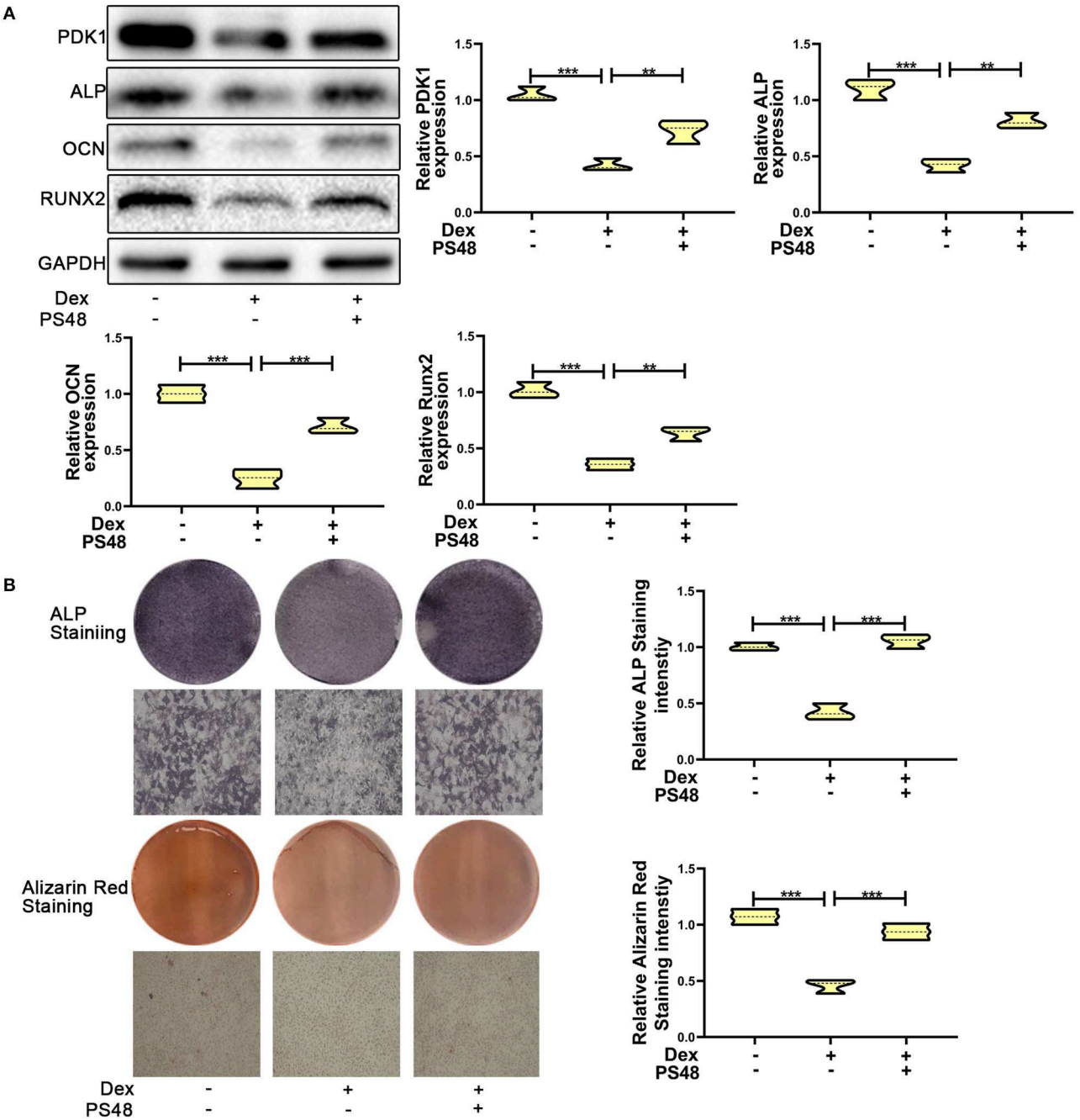

FIGURE 4 | Upregulation of PDK1 promoted the osteogenic ability of MC3T3-E1 cells. **(A)** Western blotting was performed to detect the protein expression levels of PDK1 and osteogenic markers Runx2, OCN, ALP, PDK1, and GAPDH in MC3T3-E1 cells exposed to empty vector, dexamethasone, and dexamethasone + PS48, respectively. **(B)** ALP and Alizarin red staining were performed to determine the osteogenic ability of MC3T3-E1 cells exposed to empty vector, dexamethasone, and dexamethasone + PS48, respectively. Scale Bar = 20 μm. Differences were considered as statistically significant when $p < 0.05$. ***$p < 0.001$, **$p < 0.01$, *$p < 0.05$.

Several studies have reported that PDK1 regulates cellular metabolism by activating the AKT/mTOR pathway (30–32). Adenoviral -PDK1 construct or adenoviral -NC construct was transduced into MC3T3-E1 cells before exposure to dexamethasone. As shown in **Figures 5A,B**, the mRNA and protein expression of PDK1 was increased significantly in MC3T3-E1 cells after transduction with the adenoviral-PDK1 construct. Upregulation of PDK1 enhanced the ratio of p-AKT and p-mTOR in adenovirus-PDK1 + dexamethasone group compared to adenovirus-NC + dexamethasone group

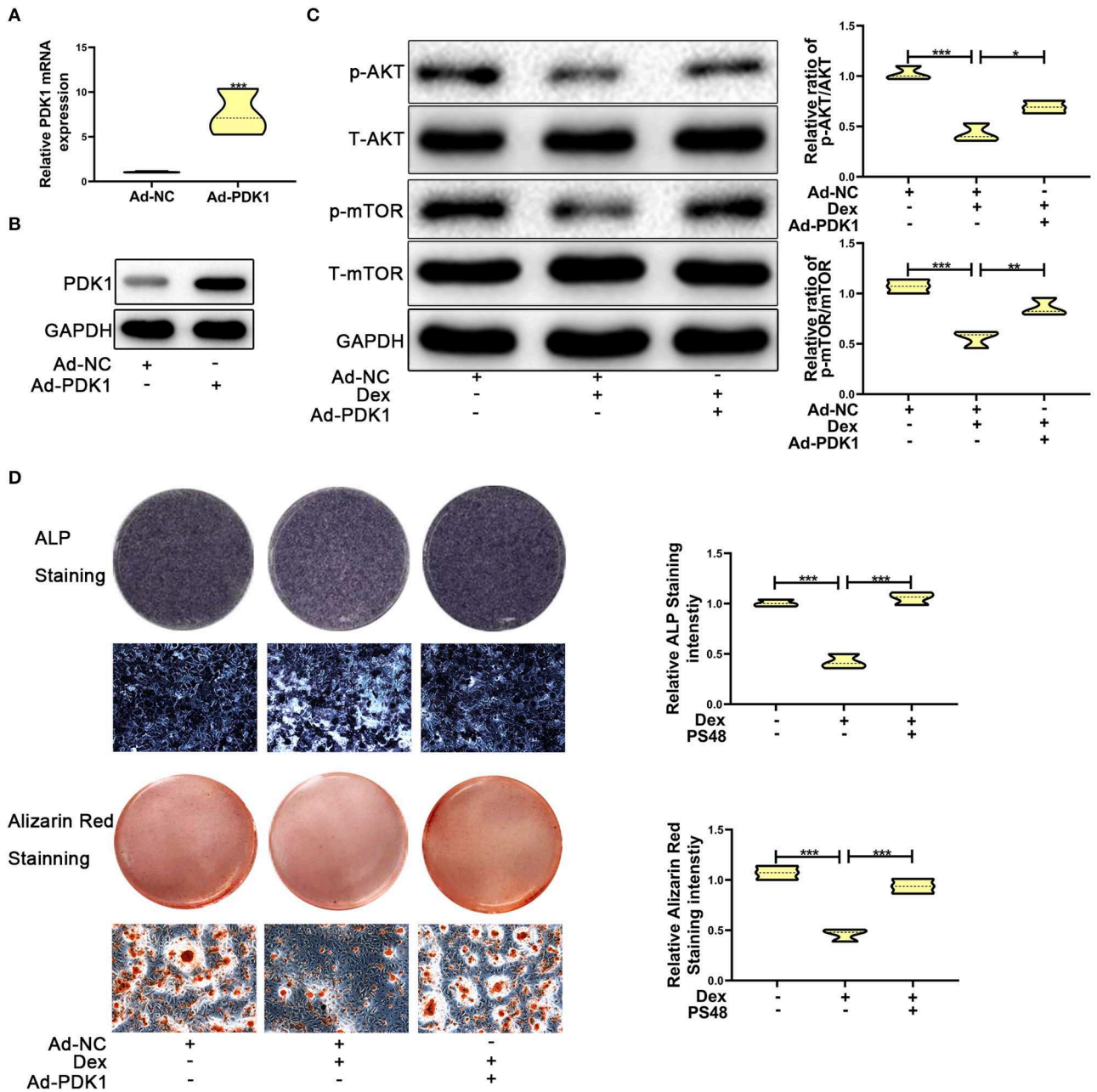

FIGURE 5 | Upregulation of PDK1 by Adenovirus-PDK1 promoted the osteogenic ability of MC3T3-E1 cells by activating the AKT/mTOR pathway. **(A)** The expression of Adenovirus-PDK1 was confirmed by qRT-PCR. **(B)** The effect of Adenovirus-PDK1 was confirmed by qRT-PCR. **(C)** Western blotting was performed to detect the protein expression levels of p-AKT, total-AKT, p-mTOR, total-mTOR, and GAPDH in MC3T3-E1 cells exposed to empty vector, dexamethasone, and dexamethasone + Adenovirus-PDK1, respectively. **(D)** ALP and Alizarin red staining were performed to determine the osteogenic ability of MC3T3-E1 cells treated with empty vector, dexamethasone, and dexamethasone + Adenovirus-PDK1, respectively. Scale Bar = 20 μm. Differences were considered as statistically significant when $p < 0.05$. $^{***}p < 0.001$, $^{**}p < 0.01$, $^{*}p < 0.05$.

(**Figure 5C**). ALP and Alizarin red staining showed that upregulation of PDK1 could enhance the osteogenic ability of MC3T3-E1 cells (**Figure 5D**). These results revealed that PDK1 was able to regulate glucocorticoid-induced osteogenic inhibition of osteoblasts.

Adenovirus-Mediated Delivery of PDK1 Increased the Bone Mass of Mice Treated With Glucocorticoid

To confirm the protective effect of PDK1 *in vivo*, we evaluated the effect of adenovirus-mediated delivery of PDK1 (Ad-PDK1)

in a mouse model of glucocorticoid-induced osteoporosis. When PDK1 was upregulated, the femur BMD and BV/TV in glucocorticoid-treated mice were significantly increased, as indicated by μCT analysis. However, there was no change in Tb. N, Tb. Pf, Tb. Sp, and Tb. Th (**Figure 6A**). Interestingly, marrow area (Ma. Ar) was increased after treatment with Dex and was reduced after upregulation of PDK1. Dex treatment reduced cortical bone thickness (Ct. Th), total area (Tt. Ar), and cortical area (Ct. Ar), but upregulation of PDK1 enhanced both these parameters. The femur trabecular number was not altered while the thickness of cortical bone was reduced. Hematoxylin-eosin staining of femur confirmed the results of μCT analysis (**Figure 6B**). PDK1 expression as determined by immunohistochemical staining was reduced in the cortical bone but not in the trabecular bone after treatment with dexamethasone (**Figure 6C**). Upregulation of PDK1 could improve the thickness of the cortical bone. We speculated that dexamethasone mainly affected the cortical bone. The mechanism of this phenomenon needs to be further studied.

DISCUSSION

In this study, we found that decreased HIF-1α expression was associated with dexamethasone-induced osteogenic suppression of osteoblasts in MC3T3-E1 cells. Excessive and long-term administration of glucocorticoids disturbed the osteogenic function of bone cells (3, 6). It has been reported that HIF-1α plays a positive role in the process of bone remodeling and osteoblast function (33–35). A recent study has demonstrated that HIF-1α was linked to glucocorticoid-induced osteoporosis in mice (20). HIF-1α is highly expressed in osteoblasts and osteocytes in a hypoxic environment and is involved in the process of bone metabolism (16, 36). However, the mechanism of HIF-1α in the regulation of glucocorticoid-induced osteogenic differentiation has not been studied adequately. Here, our results revealed for the first time that, the expression levels of HIF-1α and PDK1 were suppressed by dexamethasone treatment in MC3T3-E1 cells. Furthermore, HIF-1α regulated the negative effects of glucocorticoid on osteogenic function via the PDK1/AKT/mTOR signaling pathway.

MC3T3-E1 cells derived from C57/BL mouse calvaria are pre-osteoblasts possessing the ability to differentiate into osteoblasts and generate mineralized matrix in differentiation medium. Dexamethasone, a synthetic glucocorticoid, is used widely in clinical therapy, but excessive and long-term administration has a deleterious effect on bone formation. Increased concentration of dexamethasone ($>10^{-8}$ M) significantly suppresses osteogenic differentiation and mineralization ability in osteoblasts (28). Inhibition of osteoblast proliferation and differentiation is considered to be the main reason for glucocorticoid-induced osteoporosis (4). However, the molecular mechanisms of glucocorticoid-induced osteogenic inhibition of osteoblasts are still unclear.

A previous study has demonstrated that HIF-1α regulated bone formation via improving VEGF-A levels (33). Glucocorticoids could suppress HIF-1α protein expression (20). In this study, the expression of HIF-1α was decreased in MC3T3-E1 cells treated with different concentrations of dexamethasone. The administration of glucocorticoid receptor (GR) blocker RU486 promoted osteogenic ability and decreased the expression of HIF-1α in MC3T3-E1 cells after dexamethasone exposure. These results demonstrated that glucocorticoid inhibited osteogenic function via the glucocorticoid receptor (28, 37). Upregulation of HIF-1α by transduction with adenoviral- HIF-1α construct could inhibit the deleterious effects of dexamethasone on osteogenic function in MC3T3-E1 cells, while downregulation of HIF-1α by antagonist 2-ME enhanced the negative effects of dexamethasone. Importantly, upregulation of HIF-1α could improve the decreased expression of PDK1, while suppression of HIF-1α accelerated decreased PDK1 expression. These results reveal that HIF-1α might antagonize glucocorticoid-induced osteogenic inhibition of osteoblasts via PDK1 signaling pathway.

To further confirm the mechanism by which PDK1 counteracts glucocorticoid-induced inhibition of osteogenesis, MC3T3-E1 cells transduced with adenoviral-HIF-1α construct were cultured in differentiation medium containing dexamethasone and DCA. DCA could reverse the protective effects of HIF-1α on glucocorticoid-induced osteogenic inhibition of osteoblasts. Moreover, the PDK1 activator PS48 was capable of repressing the deleterious effects of glucocorticoid treatment. These results proved that HIF-1α reduced glucocorticoid-induced osteogenic inhibition of osteoblasts via the PDK1 signaling pathway (15).

To explore the specific molecular mechanisms by which PDK1 reversed glucocorticoid-induced osteogenic inhibition, we investigated the response of AKT/mTOR signaling pathway. Recent studies have demonstrated that the AKT/mTOR signaling pathway regulates various biological activities in osteoblasts (38, 39). Hypoxia was reported to induce osteogenic differentiation via ILK, AKT, mTOR, and HIF-1α pathways (19). In addition, PDK1 has been reported to regulate various cellular metabolic processes via the AKT/mTOR signaling pathway (30, 40, 41). Therefore, we presumed that PDK1 reversed the glucocorticoid-induced osteogenic inhibition of osteoblasts via the AKT/mTOR signaling pathway. In this study, PDK1 adenoviral construct was transduced into MC3T3-E1 cells and the results showed that upregulation of PDK1 promoted the osteogenic function of osteoblasts. To further confirm the effect of PDK1 *in vivo*, PDK1 adenovirus was injected into the bone marrow cavity of femurs of mice. Overexpression of PDK1 reduced the marrow area (Ma. Ar) and increased the cortical bone thickness (Ct. Th), total area (Tt. Ar) and cortical area (CT. Ar). Upregulation of PDK1 significantly promoted the bone mass of mice treated with dexamethasone. The above results revealed that HIF-1α/PDK1 axis reversed the glucocorticoid-induced osteogenic inhibition of osteoblasts via activating the AKT/mTOR signaling pathway.

Our study presents two questions. First, although it has been reported that HIF-1α could mediate the osteogenic ability of osteoblasts, and improve bone mass (33), the role of VEGF-A in glucocorticoid-induced osteogenic inhibition of osteoblasts has not been confirmed yet. Second, whether PDK1 mediates glucocorticoid-induced osteogenic inhibition

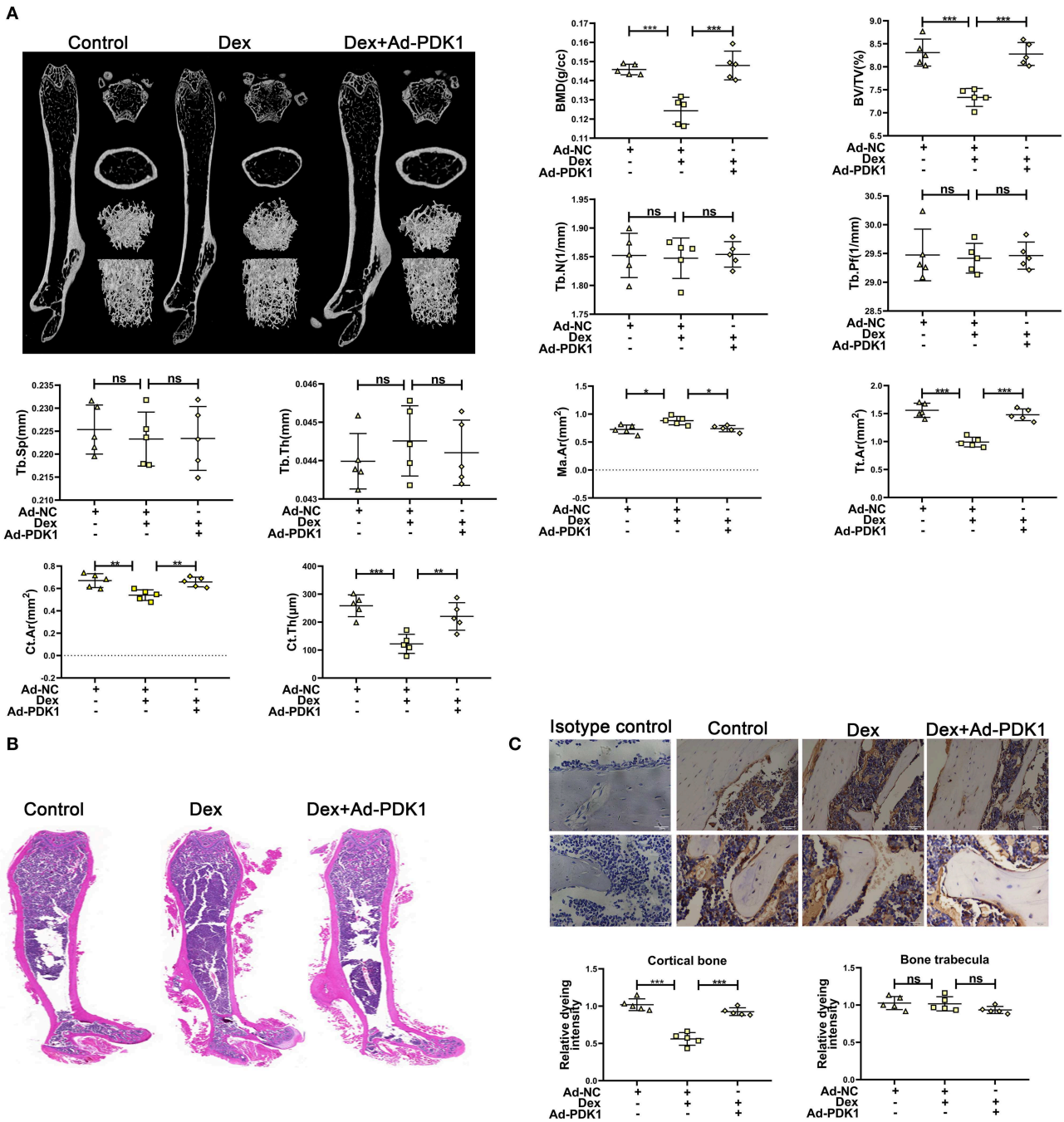

FIGURE 6 | Upregulation of PDK1 improved the bone mass of mice treated with dexamethasone. **(A)** Representative μCT images and quantification analysis of bone parameters in femurs of control, dexamethasone and dexamethasone + Adenovirus-PDK1 mice. **(B)** Representative images of HE staining to examine the structure of femurs. **(C)** Immunohistochemical staining for detecting the protein expression of PDK1 in femurs of mice. Isotype control showed that the binding of the primary antibody was specific. Scale Bar = 5 μm. BMD, Bone Mineral Density; BV/TV, bone volume over total volume; Tb. Th, trabecular thickness; Tb. N, trabecular number; Tb. Sp, trabecular separation, Tt. Ar, Total area; Ma. Ar, Marrow area; Ct. Ar, Cortical area, Cortical bone thickness (Ct. Th) Differences were considered as statistically significant when $p < 0.05$. ***$p < 0.001$, **$p < 0.01$, *$p < 0.05$.

of osteoblasts via regulating mitochondrial metabolism remains to be studied. Future studies are required to resolve these questions.

In conclusion, we demonstrated that HIF-1α antagonized glucocorticoid-induced osteogenic suppression of osteoblasts via the PDK1/AKT/mTOR signaling pathway. Our

findings provide novel insights to further understand the molecular mechanisms of glucocorticoid-induced osteogenic inhibition of osteoblasts. Specific overexpression of PDK1 could be an alternative method to alleviate glucocorticoid-induced osteoporosis.

DATA AVAILABILITY STATEMENT

Publicly available datasets were analyzed in this study. This data can be found here: winningxu@sjtu.edu.cn.

ETHICS STATEMENT

The animal study was reviewed and approved by Ethics Committee of Xinhua Hospital Affiliated to Shanghai Jiao Tong University School of Medicine.

AUTHOR CONTRIBUTIONS

W-NX, S-DJ, and L-SJ conceived and designed the experiments. W-NX and H-LZ performed the experiments. W-NX and R-ZY acquired and analyzed the data. W-NX drafted the manuscript. S-DJ and L-SJ helped perform the analysis with constructive discussions and revised the manuscript.

FUNDING

This research was supported by the National Natural Science Foundation of China (No. 81672206).

ACKNOWLEDGMENTS

We would like to thank our colleagues in the lab for their assistance.

REFERENCES

1. Compston J. Management of glucocorticoid-induced osteoporosis. *Nat Rev Rheumatol*. (2010) 6:82–8. doi: 10.1038/nrrheum.2009.259
2. Tait AS, Butts CL, Sternberg EM. The role of glucocorticoids and progestins in inflammatory, autoimmune, and infectious disease. *J Leukocyte Biol*. (2008) 84:924–31. doi: 10.1189/jlb.0208104
3. Weinstein RS, Jilka RL, Parfitt AM, Manolagas SC. Inhibition of osteoblastogenesis and promotion of apoptosis of osteoblasts and osteocytes by glucocorticoids. Potential mechanisms of their deleterious effects on bone. *J Clin Invest*. (1998) 102:274–82. doi: 10.1172/JCI2799
4. Migliaccio S, Brama M, Fornari R, Greco EA, Spera G, Malavolta N. Glucocorticoid-induced osteoporosis: an osteoblastic disease. *Aging Clin Exp Res*. (2007) 19(3 Suppl):5–10.
5. Zaidi M, Sun L, Robinson LJ, Tourkova IL, Liu L, Wang Y, et al. ACTH protects against glucocorticoid-induced osteonecrosis of bone. *Proc Natl Acad Sci USA*. (2010) 107:8782–7. doi: 10.1073/pnas.0912176107
6. Henneicke H, Gasparini SJ, Brennan-Speranza TC, Zhou H, Seibel MJ. Glucocorticoids and bone: local effects and systemic implications. *Trends Endocrinol Metabol*. (2014) 25:197–211. doi: 10.1016/j.tem.2013.12.006
7. Xia X, Kar R, Gluhak-Heinrich J, Yao W, Lane NE, Bonewald LF, et al. Glucocorticoid-induced autophagy in osteocytes. *J Bone Mineral Res*. (2010) 25:2479–88. doi: 10.1002/jbmr.160
8. Li J, Zhang N, Huang X, Xu J, Fernandes JC, Dai K, et al. Dexamethasone shifts bone marrow stromal cells from osteoblasts to adipocytes by C/EBPalpha promoter methylation. *Cell Death Dis*. (2013) 4:e832. doi: 10.1038/cddis.2013.348
9. Semenza GL. Hypoxia-inducible factors: mediators of cancer progression and targets for cancer therapy. *Trends Pharmacol Sci*. (2012) 33:207–14. doi: 10.1016/j.tips.2012.01.005
10. Semenza GL. Oxygen sensing, hypoxia-inducible factors, and disease pathophysiology. *Annual Rev Pathol*. (2014) 9:47–71. doi: 10.1146/annurev-pathol-012513-104720
11. Ke Q, Costa M. Hypoxia-inducible factor-1 (HIF-1). *Mol Pharmacol*. (2006) 70:1469–80. doi: 10.1124/mol.106.027029
12. Lee JW, Bae SH, Jeong JW, Kim SH, Kim KW. Hypoxia-inducible factor (HIF-1)alpha: its protein stability and biological functions. *Exp Mol Med*. (2004) 36:1–12. doi: 10.1038/emm.2004.1
13. Rabinowitz MH. Inhibition of hypoxia-inducible factor prolyl hydroxylase domain oxygen sensors: tricking the body into mounting orchestrated survival and repair responses. *J Med Chem*. (2013) 56:9369–402. doi: 10.1021/jm400386j
14. Marinho HS, Real C, Cyrne L, Soares H, Antunes F. Hydrogen peroxide sensing, signaling and regulation of transcription factors. *Redox Biol*. (2014) 2:535–62. doi: 10.1016/j.redox.2014.02.006
15. Regan JN, Lim J, Shi Y, Joeng KS, Arbeit JM, Shohet RV, et al. Up-regulation of glycolytic metabolism is required for HIF1α-driven bone formation. *Proc Natl Acad Sci USA*. (2014) 111:8673–8. doi: 10.1073/pnas.1324290111
16. Rankin EB, Wu C, Khatri R, Wilson TL, Andersen R, Araldi E, et al. The HIF signaling pathway in osteoblasts directly modulates erythropoiesis through the production of EPO. *Cell*. (2012) 149:63–74. doi: 10.1016/j.cell.2012.01.051
17. Wan C, Gilbert SR, Wang Y, Cao X, Shen X, Ramaswamy G, et al. Activation of the hypoxia-inducible factor-1alpha pathway accelerates bone regeneration. *Proc Natl Acad Sci USA*. (2008) 105:686–91. doi: 10.1073/pnas.0708474105
18. Wan C, Shao J, Gilbert SR, Riddle RC, Long F, Johnson RS, et al. Role of HIF-1alpha in skeletal development. *Ann N Y Acad Sci*. (2010) 1192:322–6. doi: 10.1111/j.1749-6632.2009.05238.x
19. Tseng WP, Yang SN, Lai CH, Tang CH. Hypoxia induces BMP-2 expression via ILK, Akt, mTOR, and HIF-1 pathways in osteoblasts. *J Cell Physiol*. (2010) 223:810–8. doi: 10.1002/jcp.22104
20. Weinstein RS, Wan C, Liu Q, Wang Y, Almeida M, O'Brien CA, et al. Endogenous glucocorticoids decrease skeletal angiogenesis, vascularity, hydration, and strength in aged mice. *Aging cell*. (2010) 9:147–61. doi: 10.1111/j.1474-9726.2009.00545.x
21. Papandreou I, Cairns RA, Fontana L, Lim AL, Denko NC. HIF-1 mediates adaptation to hypoxia by actively downregulating mitochondrial oxygen consumption. *Cell Metabol*. (2006) 3:187–97. doi: 10.1016/j.cmet.2006.01.012
22. Primo L, di Blasio L, Roca C, Droetto S, Piva R, Schaffhausen B, et al. Essential role of PDK1 in regulating endothelial cell migration. *J Cell Biol*. (2007) 176:1035–47. doi: 10.1083/jcb.200607053
23. Liu Y, Wang J, Wu M, Wan W, Sun R, Yang D, et al. Down-regulation of 3-phosphoinositide-dependent protein kinase-1 levels inhibits migration and experimental metastasis of human breast cancer cells. *Mol Cancer Res*. (2009) 7:944–54. doi: 10.1158/1541-7786.MCR-08-0368
24. Zhu C, Zheng XF, Yang YH, Li B, Wang YR, Jiang SD, et al. LGR4 acts as a key receptor for R-spondin 2 to promote osteogenesis through Wnt signaling pathway. *Cell Signal*. (2016) 28:989–1000. doi: 10.1016/j.cellsig.2016.04.010
25. McLaughlin F, Mackintosh J, Hayes BP, McLaren A, Uings IJ, Salmon P, et al. Glucocorticoid-induced osteopenia in the mouse as assessed by histomorphometry, microcomputed tomography, and biochemical markers. *Bone*. (2002) 30:924–30. doi: 10.1016/S8756-3282(02)00737-8
26. Zhou Z, Shi G, Zheng X, Jiang S, Jiang L. Autophagy activation facilitates mechanical stimulation-promoted osteoblast differentiation and ameliorates hindlimb unloading-induced bone loss. *Biochem Biophys Res Commun*. (2018) 498:667–73. doi: 10.1016/j.bbrc.2018.03.040
27. Vogel J, Thiel CS, Tauber S, Stockmann C, Gassmann M, Ullrich O. Expression of hypoxia-inducible factor 1α (HIF-1α) and genes of related

pathways in altered gravity. *Int J Mol Sci*. (2019) 20:436. doi: 10.3390/ijms20020436
28. Rauch A, Seitz S, Baschant U, Schilling AF, Illing A, Stride B, et al. Glucocorticoids suppress bone formation by attenuating osteoblast differentiation via the monomeric glucocorticoid receptor. *Cell Metabol*. (2010) 11:517–31. doi: 10.1016/j.cmet.2010.05.005
29. Li B, Zhu Y, Sun Q, Yu C, Chen L, Tian Y, et al. Reversal of the warburg effect with DCA in PDGFtreated human PASMC is potentiated by pyruvate dehydrogenase kinase1 inhibition mediated through blocking Akt/GSK3β signalling. *Int J Mol Med*. (2018) 42:1391–400. doi: 10.3892/ijmm.2018.3745
30. Han F, Xue M, Chang Y, Li X, Yang Y, Sun B, et al. Triptolide suppresses glomerular mesangial cell proliferation in diabetic nephropathy is associated with inhibition of PDK1/Akt/mTOR pathway. *Int J Biol Sci*. (2017) 13:1266–75. doi: 10.7150/ijbs.20485
31. Liu R, Chen Z, Yi X, Huang F, Hu G, Liu D, et al. 9za plays cytotoxic and proapoptotic roles and induces cytoprotective autophagy through the PDK1/Akt/mTOR axis in non-small-cell lung cancer. *J Cell Physiol*. (2019) 76:2329–48. doi: 10.1002/jcp.28679
32. Liu C, Mu X, Wang X, Zhang C, Zhang L, Yu B, et al. Ponatinib inhibits proliferation and induces apoptosis of liver cancer cells, but its efficacy is compromised by its activation on PDK1/Akt/mTOR signaling. *Molecules*. (2019) 24:1363. doi: 10.3390/molecules24071363
33. Wang Y, Wan C, Deng L, Liu X, Cao X, Gilbert SR, et al. The hypoxia-inducible factor alpha pathway couples angiogenesis to osteogenesis during skeletal development. *J Clin Invest*. (2007) 117:1616–26. doi: 10.1172/JCI31581
34. Hiraga T. Hypoxic microenvironment and metastatic bone disease. *Int J Mol Sci*. (2018) 19:3523. doi: 10.3390/ijms19113523
35. Niu X, Chen Y, Qi L, Liang G, Wang Y, Zhang L, et al. Hypoxia regulates angeogenic-osteogenic coupling process via up-regulating IL-6 and IL-8 in human osteoblastic cells through hypoxia-inducible factor-1α pathway. *Cytokine*. (2019) 113:117–27. doi: 10.1016/j.cyto.2018.06.022
36. Yang DC, Yang MH, Tsai CC, Huang TF, Chen YH, Hung SC. Hypoxia inhibits osteogenesis in human mesenchymal stem cells through direct regulation of RUNX2 by TWIST. *PLoS ONE*. (2011) 6:e23965. doi: 10.1371/journal.pone.0023965
37. Heitzer MD, Wolf IM, Sanchez ER, Witchel SF, DeFranco DB. Glucocorticoid receptor physiology. *Rev Endocrine Metabol Disord*. (2007) 8:321–30. doi: 10.1007/s11154-007-9059-8
38. Ford-Hutchinson AF, Ali Z, Lines SE, Hallgrimsson B, Boyd SK, Jirik FR. Inactivation of Pten in osteo-chondroprogenitor cells leads to epiphyseal growth plate abnormalities and skeletal overgrowth. *J Bone Mineral Res*. (2007) 22:1245–59. doi: 10.1359/jbmr.070420
39. Xi JC, Zang HY, Guo LX, Xue HB, Liu XD, Bai YB, et al. The PI3K/AKT cell signaling pathway is involved in regulation of osteoporosis. *J Receptor Signal Transduction Res*. (2015) 35:640–5. doi: 10.3109/10799893.2015.1041647
40. Sarbassov DD, Guertin DA, Ali SM, Sabatini DM. Phosphorylation and regulation of Akt/PKB by the rictor-mTOR complex. *Science*. (2005) 307:1098–101. doi: 10.1126/science.1106148
41. Chen L, Xu B, Liu L, Luo Y, Yin J, Zhou H, et al. Hydrogen peroxide inhibits mTOR signaling by activation of AMPKalpha leading to apoptosis of neuronal cells. *Lab Invest*. (2010) 90:762–73. doi: 10.1038/labinvest.2010.36

Conflict of Interest: The authors declare that the research was conducted in the absence of any commercial or financial relationships that could be construed as a potential conflict of interest.

The reviewer HQ declared a shared affiliation, with no collaboration, with the authors to the handling editor at the time of the review.

frontiers in Endocrinology

REVIEW
published: 15 April 2020
doi: 10.3389/fendo.2020.00204

Spinal Cord Injury as a Model of Bone-Muscle Interactions: Therapeutic Implications From *in vitro* and *in vivo* Studies

Marco Invernizzi[1]*, *Alessandro de Sire*[1,2], *Filippo Renò*[3], *Carlo Cisari*[1,4], *Letterio Runza*[5], *Alessio Baricich*[1,4], *Stefano Carda*[6] and *Nicola Fusco*[7,8]

[1] Physical and Rehabilitative Medicine, Department of Health Sciences, University of Eastern Piedmont, Novara, Italy, [2] Rehabilitation Unit, "Mons. L. Novarese" Hospital, Vercelli, Italy, [3] Innovative Research Laboratory for Wound Healing, Department of Health Sciences, University of Eastern Piedmont, Novara, Italy, [4] Physical Medicine and Rehabilitation Unit, University Hospital "Maggiore della Carità", Novara, Italy, [5] Division of Pathology, Fondazione IRCCS Ca' Granda, Ospedale Maggiore Policlinico, Milan, Italy, [6] Neuropsychology and Neurorehabilitation Service, Department of Clinical Neuroscience. Lausanne University Hospital (CHUV), Lausanne, Switzerland, [7] Division of Pathology, IEO - European Institute of Oncology IRCCS, Milan, Italy, [8] Department of Oncology and Hemato-Oncology, University of Milan, Milan, Italy

Spinal cord injuries (SCIs) represent a variety of conditions related to the damage of the spinal cord with consequent musculoskeletal repercussions. The bone and muscle tissues share several catabolic pathways that lead to variable degrees of disability in SCI patients. In this review article, we provide a comprehensive characterization of the available treatment options targeting the skeleton and the bone in the setting of SCI. Among the pharmacological intervention, bisphosphonates, anti-sclerostin monoclonal antibodies, hydrogen sulfide, parathyroid hormone, and RANKL pathway inhibitors represent valuable options for treating bone alterations. Loss phenomena at the level of the muscle can be counteracted with testosterone, anabolic-androgenic steroids, and selective androgen receptor modulators. Exercise and physical therapy are valuable strategies to increase bone and muscle mass. Nutritional interventions could enhance SCI treatment, particularly in the setting of synergistic and multidisciplinary interventions, but there are no specific guidelines available to date. The development of multidisciplinary recommendations is required for a proper clinical management of SCI patients.

Keywords: spinal cord injury, bone, muscle, bone loss, osteoporosis, sarcopenia, rehabilitation

OPEN ACCESS

Edited by:
Giacomina Brunetti,
University of Bari Aldo Moro, Italy

Reviewed by:
Luca Pietrogrande,
University of Milan, Italy
Daniela Merlotti,
University of Siena, Italy

***Correspondence:**
Marco Invernizzi
marco.invernizzi@med.uniupo.it

Specialty section:
This article was submitted to Bone Research, a section of the journal Frontiers in Endocrinology

Received: *15 December 2019*
Accepted: *23 March 2020*
Published: *15 April 2020*

Citation:
Invernizzi M, de Sire A, Renò F, Cisari C, Runza L, Baricich A, Carda S and Fusco N (2020) Spinal Cord Injury as a Model of Bone-Muscle Interactions: Therapeutic Implications From in vitro and in vivo Studies. Front. Endocrinol. 11:204. doi: 10.3389/fendo.2020.00204

INTRODUCTION

Spinal cord injuries (SCIs) encompass a spectrum of conditions associated with modifications in the function of both central and peripheral nervous systems. Due to the crucial role of the spinal cord in linking the brain with the body, these alterations may lead to dramatic consequences in terms of motor, sensitive, and visceral controls (1).

A complex variety of biological pathways arising in both bone and muscle tissues plays a clinically relevant role in SCIs. Hence, these patients experience important changes in the bones (e.g., osteoporosis) that cause a significantly increased risk of fractures, even after minor traumas (e.g., transferring or sitting) (2, 3). These clinical conditions lead to further immobilization of the patient, increased spasticity, pressure ulcers, and in general worsened disability (3). Bone tissue

loss after SCIs starts rapidly and grows in the first 2 years after the injury (4). In chronic SCIs, the skeleton of the lower third of the femur and upper third of the tibia may be subjected to 70% of decreased mineral density (5, 6). Muscle modifications further increase the patients' fragility because they lead to immobilization, increased fracture risk, pressure sores, thrombosis, overpressure, chronic pain, and psychosocial issues (7). The loss of mass in the muscles below the SCI is remarkable, reaching up to 40% in the first 2 years after the injury (8). Regrettably, despite muscle atrophy is macroscopically more evident than osteoporosis, this phenomenon is often underestimated (7).

In this scenario, understanding the biological interplay of the bone and muscle tissues is crucial for proper clinical management of SCIs. Here, we sought to provide a comprehensive portrait of the potentials and limitations of the various treatment options available (or proposed) to date for both osteoporosis and muscle atrophy occurring after SCIs.

PHARMACOLOGICAL APPROACHES TO BONE ALTERATIONS

The use of single, combination, or sequential therapy protocols in the management of bone alterations in SCI is a matter of controversy. After the achievement of clinical benefits, the discontinuation of osteoanabolic treatments could result in a rapid loss of the newly gained bone (9–12). For this reason, clinicians are recommended to promptly start other anti-resorptive therapies after osteoanabolic interventions discontinuation. At present, there are no widely adopted guidelines about the most reliable pharmacological strategy.

Bisphosphonates

Bisphosphonates are the most used class of drugs in the prevention and treatment of osteoporosis (13). Several studies have assessed the efficacy of these anti-resorptive drugs in acute and chronic SCIs. A meta-analysis provided circumstantial evidence to suggest that the early administration of bisphosphonates can reduce SCI-related osteoporosis (13). It should be taken into account, however, that this hypothesis is biased by the small sample size of the few clinical trials available to date (14). Moreover, despite many groups showed that bisphosphonates may be particularly effective at the hip level, only a few information is currently available on their role at the distal third of the femur and/or at the proximal third of the tibia. A recent, non-randomized study on the yearly administration of zoledronic acid failed to show an improvement in the bone mass density (BMD) at this level, being associated, on the contrary, with a reduction in bone mass (15). Therefore, several doubts exist about the efficacy and the safety profile of bisphosphonates in patients with SCI. Due to these issues, at the present time, prophylaxis of osteoporosis with bisphosphonates in SCI remains an interesting area of research but it is not yet ready for prime time (16). On the other hand, alendronate showed significant results in maintaining or even increase BMD after previous osteoanabolic interventions (9, 10, 17). These observations suggest that a sequential therapy scheme with alendronate after teriparatide treatment is likely to prevent bone loss, increase bone mass, and preserve bone strength at the spine and hip in SCI patients.

Anti-sclerostin Antibodies

Murine SCI models showed that anti-sclerostin antibodies could preserve the osteocyte morphology and structure, blocking the skeletal deterioration after either motor-incomplete (18) or motor-complete SCI (15). A recent study assessed the efficacy of these antibodies in reversing the bone loss in a rodent model after motor-complete SCI (19). Animals treated with 25 mg/kg/week for 8 weeks (starting at 12 weeks after SCI) showed a significant increase in BMD, structure, and mechanical strength. Anti-sclerostin antibodies acted in the case group through osteoclastogenesis inhibition and concomitant osteoblastogenesis stimulation. Untreated SCI mice showed a significant reduction in BMD and the deterioration of bone structure at the distal femoral metaphysis. These data suggest that sclerostin antagonism might be a viable therapeutic option not only to prevent bone loss after acute SCI but also in the chronic setting (19).

Hydrogen Sulfide

Hydrogen sulfide (H2S) is a colorless and poisonous gas acting as a gas transmitter to regulate different signaling pathways (20). It has been recently hypothesized that abnormal H2S metabolism could be linked to defects in bone homeostasis (21). Treatment with an H2S donor (GYY4137) increase bone formation, preventing the loss of trabecular bone in case of estrogen deficiency (21). Whether H2S might have anti-osteoporosis effectiveness in motor-complete SCI models has recently been investigated (22). Rats were treated with an intraperitoneal injection of 0.1 ml/kg/day of 0.28 mol/l NaHS (a donor of H2S) for 2 weeks. They showed an increase of femoral and tibial BMD, bone volume fraction (bone volume/total, BV/TV), trabecular thickness and number, and a concomitant reduction of trabecular separation in proximal tibiae. Furthermore, rats treated with NaHS showed an increased mineral apposition rate (MAR), bone formation rate (BFR), and osteoblast proliferation (22). Given that an increased ROS production is one of the main mechanisms related to bone and muscle modifications after SCI, all these results suggest a potential role of H2S treatment in SCI-related bone loss.

Parathyroid Hormone

Parathyroid hormone (PTH) is a well-known player in calcium metabolism. The subcutaneous intermittent administration of PTH has been used for two decades as a valid anabolic therapeutic agent for osteoporosis treatment (23, 24). A recent study investigated whether PTH administration might reduce bone loss in SCI female mice (25). PTH (80 mg/kg) or vehicle was injected subcutaneously daily for 35 days. Isolated tibias and femurs were assessed through microcomputed tomography scanning (micro-CT), histology, and serum bone turnover markers. SCI-vehicle animals reported a 49% reduction in fractional trabecular bone

volume and 18% in trabecular thickness compared to sham-vehicle controls. Moreover, the authors found 15% lower femoral cortical thickness and 16% higher cortical porosity in SCI-vehicle animals compared to sham ones. PTH treatment restored 78% of bone volume in SCI animals. In addition, histomorphometry showed a marked decline in osteoblast and osteoclast number and a 35% reduction in bone formation rate. On the other hand, in SCI-PTH animals the number of osteoblasts and osteoclasts was preserved, and the bone formation rate was enhanced. These results suggest a potential therapeutic role of subcutaneous intermittent PTH treatment in acute SCI patients, however to date, data in humans are lacking. Recently, abaloparatide, a parathyroid hormone-related protein (PTHrP), was approved by Food and Drug Administration (FDA) for the treatment of severe post-menopausal osteoporosis (26). A recent study performed by Sahbani et al. compared abaloparatide to teriparatide on bone structure, turnover, and levels of RANKL and OPG on wild-type female mice (27). The authors showed that 20–80 μg/kg/day of abaloparatide for 30 days resulted in a significant increase (13%) in trabecular bone thickness and lowered the RANKL/OPG ratio. In light of these results, abaloparatide could be a promising therapeutic agent to counter osteoporosis, and future studies could investigate its efficacy also in SCI patients.

Denosumab

The receptor activator of nuclear factor-kB ligand (RANKL)/osteoprotegerin (OPG) system is one of the main regulators of bone remodeling (28). Denosumab, a RANKL pathway inhibitor monoclonal antibody, has been widely used in the treatment of osteoporosis (29–33). Increased osteoblast expression of RANKL has been previously observed in unloading conditions, such as SCI, resulting in an increased RANKL/OPG ratio (34–38). These observations have suggested a potential therapeutic role of denosumab in SCI-induced bone loss. Only one work investigated the effects of denosumab on acute SCI in humans, with promising results (33). Compared to RANKLS-positive patients with detectable RANKL, those with undetectable RANKL levels showed better responses both in terms of femoral BMD increase and bone reabsorption markers decrease. Therefore, denosumab has been regarded as a drug potentially able to prevent SCI-related bone loss (38).

PHARMACOLOGICAL APPROACHES TO MUSCLE ALTERATIONS

To date, there is no robust evidence about local pharmacological agents that can be used to counteract the muscle loss after SCI. Most data currently available are derived from studies on healthy subjects or patients with chronic conditions of which some (e.g., cachexia and wasting) share some pathophysiological pathways with SCI. In this setting, androgens have been extensively studied, either in animal models and in humans. Particularly, testosterone and anabolic-androgenic steroids (AAS) such as nandrolone, as well as the selective androgen receptor modulators (SARMs), have been proposed as pharmacological strategies to hinder the loss phenomena at the musculoskeletal level in different chronic illnesses, such as immunodeficiency, long term glucocorticoid treatment, and aging (39, 40). Data about safety and efficacy on the lean mass increase are available in healthy subjects, aged women, and men and in cancer-related cachexia (40–42). The main factor supporting the use of SARMs instead of testosterone is the tissue selectivity and good tolerability with negligible adverse events. The evidence emerging from cancer cachexia patients suggests a theoretical use of SARMs also in SCI-induced atrophy. The observation that a substantial proportion of male and female individuals experience hypogonadism after acute or chronic SCI represents the rationale of using testosterone and AAS in these patients (43, 44). Several studies have shown a significant effect of testosterone and nandrolone against muscle atrophy in rodents (45, 46). These results have been partially replicated in a small trial on SCI patients, in which the Authors showed that the correction of hypogonadism by 12 months of testosterone therapy can increase lean tissue mass for the whole body, leg, and arm (47). A recent randomized clinical trial showed that the combination of electrical stimulation exercise training and testosterone replacement therapy can increase muscle mass in the lower extremities of SCI patients (48). This effect was not present in patients only treated with testosterone without exercise.

EXERCISE AND PHYSICAL THERAPY

Exercise is the first treatment to increase muscle mass and there is growing evidence that the basic mechanisms that regulate muscle hypertrophy can be used to counteract disuse atrophy (40). The mechanisms by which physical exercise induce muscle hypertrophy have not been completely elucidated. The IGF-1/PIP3K/Akt pathway, even if it is considered a key mediator of normal muscle development, is not able to explain alone the exercise-induced muscle hypertrophy (49). On the other hand, mTORC1 appears to be crucial in load-induced muscle growth (50), as phospholipase D and phosphatidic acid that active mTORC1 (51). In a rodent model, exercise can protect the skeletal muscle against oxidative stress and proteolysis (52). Eccentric contractions can increase phosphatidic acid levels and induce muscle growth on mice, confirming the importance of this mechanism (53).

Physical Exercise and Treadmill

A recent study performed on 42 male Wistar rats showed that stretching is helpful for the correction of contractures after SCI (54). In addition, the Authors observed that heat is more beneficial than cold to increase the effectiveness of stretching in terms of restoring range of motion and decreasing muscle contractures. Lately, it has been demonstrated that 9-week treadmill training in mice affected by incomplete SCI is effective in preventing atrophy of fast-twitch muscles, with limited effects on slow-twitch muscles and muscle fiber type composition of medial gastrocnemius, soleus, and tibialis anterior (55). In healthy humans, several studies have shown that eccentric training (i.e., motion of a muscle while it is lengthening under load) can increase muscle mass and muscle strength more than

concentric exercise [i.e., shortening of a muscle while it is contracting; (56)]. Exercise can also reduce the expression and production of myostatin (57–59).

Functional Electrical Stimulation Rowing Exercise

In the early 1990s, functional electrical stimulation (FES) rowing exercise has been developed as an aerobic training program for SCI patients (60, 61). This approach consists of coordinated voluntary upper body exercise combined with electrical stimulation of the leg large muscle groups to produce a near-full-body exercise. Recently Lambach et al. (62) performed a study on four adults with recent (<2 years) traumatic, motor complete SCI, undergoing a 90-session FES rowing exercise program, and attending 30-min FES training sessions for 3 times/week. They showed that trabecular BMD in the femur and tibia decreased for all participants after 30 sessions, with a rate of loss slowed or reversed between the 30th and 60th sessions, with the little-to-no bone loss for most participants during the period intercurrent from 60th and 90th sessions. However, further studies with larger cohorts of participants are needed to confirm the observation of FES rowing exercise in SCI individuals.

Whole-Body Vibration

In the recent past, whole-body vibration (WBV) effects on bone architecture after SCI have been investigated with inconsistent results. In 2016, Dudley-Javoroski et al. showed that 12 months of vibration training did not preserve BMD or trabecular architecture in subjects affected by chronic SCI, showing bone tissue insensitivity to mechanical loading interventions (63). These results are not in line with the previous studies performed on rats, where WBV seemed to attenuate the bone loss that commonly occurs during the early acute stages after SCI (64). On the other hand, WBV seems to have a positive role in ankle spasticity, balance, and walking ability in patients with incomplete SCI at the cervical level (65), suggesting a potential synergistic role with other therapeutic interventions. Only a handful of studies investigated the use of WBV to improve muscle function in patients with SCI (66). Among them, a single study evaluated functional parameters such as walking speed (67), whereas the others took into account only evaluated electrophysiological data. One study failed to show any modifications in muscle cross-sectional area or muscle density after 40 weeks of treatment (68). It should be noted that available studies have been conducted on small sample sizes, with heterogeneous protocols (intensity, duration, frequencies). Therefore, no strong conclusions can be drawn at present time.

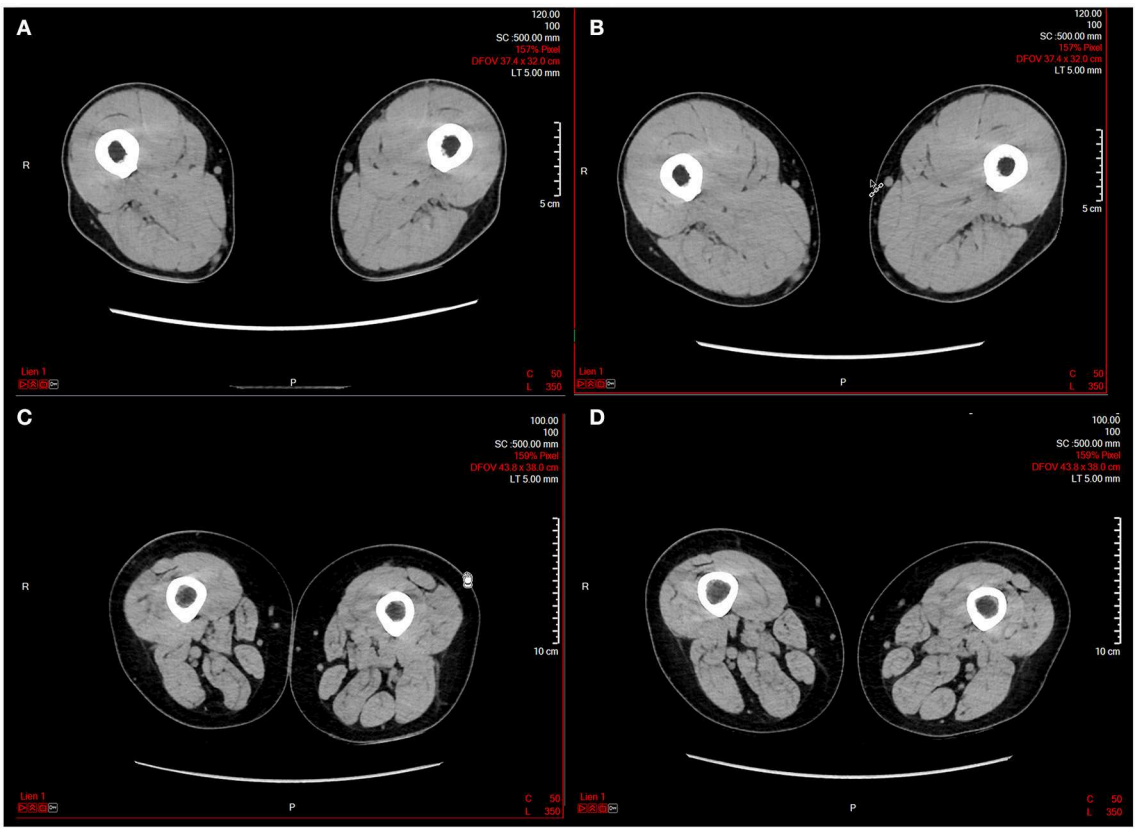

FIGURE 1 | Representative computed tomography (CT) scans before and after a 16 weeks epidural electrical stimulation (EES) protocol in two patients with spinal cord injury. **(A)** Patient 1 before EES; **(B)** patient 1 after EES; **(C)** patient 2 before EES; **(D)** patient 2 after EES. The images have been kindly provided by Prof. G. Courtine and J. Bloch.

Epidural Electrical Stimulation

Epidural electrical stimulation (ESS) is a promising technique for improving motor recovery in chronic patients with SCI (69, 70). Preliminary results showed that the application of ESS improving both motor control and muscle mass in the lower extremity of patients with severe paralysis or plegia (**Figure 1**). This effect could be ascribed to the stimulation of the posterior roots, enabling muscle contraction (69). This mechanism is different from that obtained by FES since muscle contraction is mainly indirect. Interestingly, spasticity, which is another indirect, reflex activity in patients with SCI, is associated with partially preserved muscle mass (70).

NUTRITIONAL INTERVENTIONS

Despite a healthy diet is recommended in SCI individuals, there is a substantial lack of nutritional guidelines for these patients (71–73). In addition, their altered body composition limits the accurate measurement of the energy intake and the need (74, 75). A recent systematic review and meta-analysis investigated the nutritional status of adult subjects with chronic SCI (76, 77). The authors showed that mean total energy (1,876 kcal/day), fiber intake (17 g/day), vitamins A, B5, B7, B9, D, E, potassium, and calcium were below the levels recommended by the United States Department of Agriculture (USDA). On the other hand, protein (319 kcal/day) and carbohydrate (969 kcal/day) intake and vitamins B1, B2, B3, B12, C, K, sodium, phosphorus, copper, and zinc exceeded the USDA recommendation. Of note, the fat intake (663 kcal/day), vitamin B6, iron, and magnesium were within limits (77). Supplementation with creatine to improve muscle strength in patients with chronic SCI has been also evaluated, with conflicting results. Two studies found no effect of creatine supplementation either on hand strength (78) or wheelchair performance (79), while two studies found some positive effects on upper extremity strength and function (80, 81). All these diverse correlations highlight the need for a prompt and precise nutritional assessment in SCI patients, focusing on correct daily energy intake and a higher fiber and micronutrient intake (i.e., vitamin D and calcium). Future studies are required to investigate not only the nutritional health status but also the adequate nutritional supplementation and its synergism with other interventions in SCI patients.

SYNERGISTIC AND MULTIDISCIPLINARY INTERVENTIONS

There is no unequivocal evidence about the superiority of a single therapeutic intervention to counteract the modifications in bone and muscle tissues after SCI. Given the complex and multifaceted nature of these conditions, it is conceivable that the best therapeutic strategy consists of the synergistic use of several different interventions in order to optimize the outcome at bone and muscle level in SCI patients.

Zoledronic Acid Plus FES Rowing Exercise

Considering the promising role of FES rowing exercise in promoting muscle contraction with combined mechanical loading of lower limb long bones in SCI patients, a therapeutic synergism with drugs acting at the bone level has been proposed (82). This combined strategy could induce both bone resorption inhibition and bone neoformation stimulation. A randomized clinical trial comparing FES-rowing alone with FES-rowing plus zoledronic acid (a powerful bone anti-resorptive drug), have been carried out to investigate the impact of bone health in SCI (82). The latter group had significantly greater cortical bone volume (CBV) and cortical thickness index (CTI) at both distal femoral and proximal tibial metaphyses, compared to the FES-rowing-only group. In the rowing-only group of patients, the cortical compressive strength index (CSI) at the tibial metaphysis showed significant variations based on the amount of exercise performed. These data showed that a combined antiresorptive and FES rowing exercise therapy might improve bone quality and geometry, suggesting that multimodal therapeutic interventions could be beneficial in counteracting the bone and muscle modifications.

Teriparatide and Whole-Body Vibration

Teriparatide, a 34 amino acid peptide representing the N-terminal bioactive portion of human PTH, is the only anabolic agent approved to enhance bone mass and prevent fragility fractures (83, 84). A recent randomized, double-blind, multi-center, parallel-group clinical trial on 61 individuals with chronic SCI and low bone mass showed that patients treated with teriparatide 20 μg/day showed a significant increase in areal BMD (aBMD) at the spine level after the first 12 months in both groups treated (4.8–5.5%) regardless of the simultaneous administration of WBV or sham WBV (85). This observation is consistent with a marked response in serum markers of bone metabolism. On the other hand, the magnitude of the objective response rate was not significantly related to the treatment strategy. Furthermore, patients treated by teriparatide in the 12-month extension study showed further improvement in terms of spine aBMD (total increase from baseline 7.1–14.4%), which was higher in those initially randomized to teriparatide. Taken together, teriparatide administration is related to an increased spine aBMD skeletal activity and its activity is not increased by vibration stimulation in chronic SCI individuals.

FUTURE PERSPECTIVES

Despite the progress that has been made in the field of regenerative spinal cord medicine, the majority of SCI patients continue to experience not only the direct neurological damage but also the clinically relevant secondary complications affecting the muscle and bone tissues. Due to the scarcity of available data, attention should be paid in making strong statements or recommendations for the management of these patients. However, it is anyway possible to translate some of the existing information into real-life clinical practice and to outline the future directions for primary research and clinical studies. The

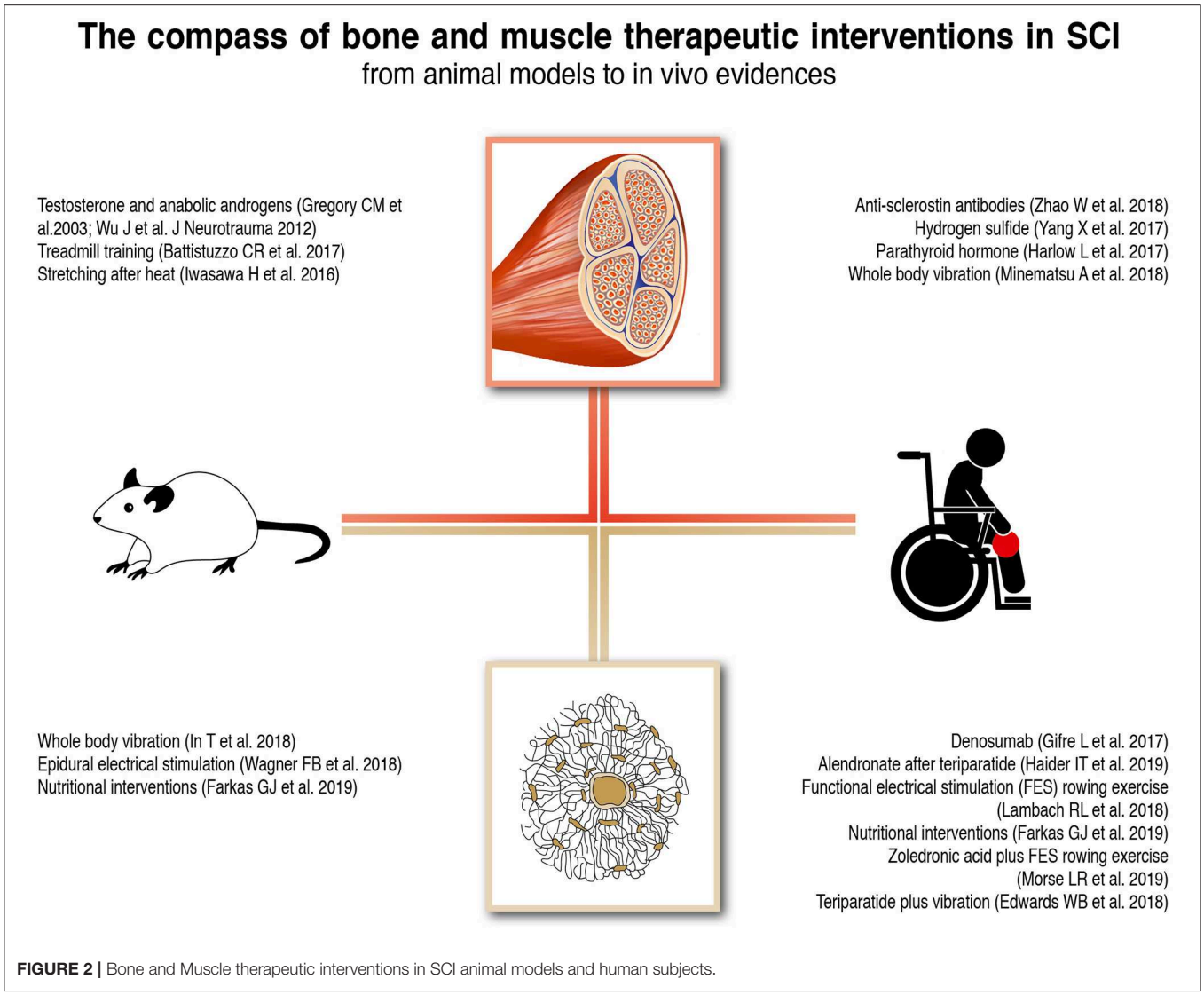

FIGURE 2 | Bone and Muscle therapeutic interventions in SCI animal models and human subjects.

main bone and muscle therapeutic interventions in SCI animal models and human subjects are outlined in (**Figure 2**).

Given that the bone and muscle tissues share not only their origin from the mesenchymal multipotent stem cell but also important signaling pathways, response to mechanical stimulation, and complications, it is reasonable to conceive that treatments should ideally target both tissues. From this perspective, physical exercise, nutrition, and electrical stimulation seem to be the most promising and rational way of treating both muscle atrophy and osteoporosis. In particular, the epidural electrical stimulation has the interesting potential of fostering both the neurological recovery and the increase of the muscle mass. Hormonal treatments represent another valuable option but their safety profile needs to be investigated in the long term.

Another future therapeutic option might be the modulation of microRNAs (miRNAs) which are non-coding RNA molecules involved in transcriptional regulation that target pathways of human diseases. They might be considered not only a target to prevent bone and muscle modifications but also a potential powerful therapeutic intervention in improving the functional recovery after SCI. In this regard, it has been recently showed how miRNA-411 and miRNA-340-5p increase could reduce apoptosis, gliosis and glial scar formation, and all the inflammators in SCI rats (86, 87).

CONCLUSIONS

SCIs encompass a wide variety of abnormal conditions that reverberate at the musculoskeletal level. Many secondary modifications show similarities and shared pathophysiological patterns to both muscle and bone tissues. The limited evidences in the literature summarized in this review suggests the need of an early start of any therapeutic intervention. However, clear evidence about the most effective treatment to counter bone and muscle modifications after SCI is missing.

A deeper understanding of the bone and muscle interactions would improve the outcome of the patients affected by several conditions related to musculoskeletal changes, such as SCI, aging, space travels, and prolonged immobility. Additional insights in bone and muscle interactions will be germane for the development of multitargeted specific therapeutic and preventive strategies acting on both bone and muscle tissue. The development of multidisciplinary recommendations is required for the clinical management of these patients at an individualized level.

AUTHOR CONTRIBUTIONS

MI and SC designed the study. MI, AS, SC, AB, FR, and LR reviewed the literature. MI, AS, NF, SC wrote the manuscript. All authors revised the paper and approved the final edition.

ACKNOWLEDGMENTS

The authors would like to thank Mrs. Erika Pizzo for the graphical development of the Figures and G. Courtine and J. Bloch for kindly providing images contained in **Figure 1**.

REFERENCES

1. Ding Y, Kastin AJ, Pan W. Neural plasticity after spinal cord injury. *Curr Pharm Des.* (2005) 11:1441–50. doi: 10.2174/1381612053507855
2. Lazo MG, Shirazi P, Sam M, Giobbie-Hurder A, Blacconiere MJ, Muppidi M. Osteoporosis and risk of fracture in men with spinal cord injury. *Spinal Cord.* (2001) 39:208–14. doi: 10.1038/sj.sc.3101139
3. Frisbie JH. Fractures after myelopathy: the risk quantified. *J Spinal Cord Med.* (1997) 20:66–9. doi: 10.1080/10790268.1997.11719458
4. Warden SJ, Bennell KL, Matthews B, Brown DJ, McMeeken JM, Wark JD. Quantitative ultrasound assessment of acute bone loss following spinal cord injury: a longitudinal pilot study. *Osteoporos Int.* (2002) 13:586–92. doi: 10.1007/s001980200077
5. Maïmoun L, Fattal C, Micallef JP, Peruchon E, Rabischong P. Bone loss in spinal cord-injured patients: from physiopathology to therapy. *Spinal Cord.* (2006) 44:203–10. doi: 10.1038/sj.sc.3101832
6. Dauty M, Perrouin Verbe B, Maugars Y, Dubois C, Mathe JF. Supralesional and sublesional bone mineral density in spinal cord-injured patients. *Bone.* (2000) 27:305–9. doi: 10.1016/S8756-3282(00)00326-4
7. Pelletier CA, Miyatani M, Giangregorio L, Craven BC. Sarcopenic obesity in adults with spinal cord injury: a cross-sectional study. *Arch Phys Med Rehabil.* (2016) 97:1931–7. doi: 10.1016/j.apmr.2016.04.026
8. Moore CD, Craven BC, Thabane L, Laing AC, Frank-Wilson AW, Kontulainen SA, et al. Lower-extremity muscle atrophy and fat infiltration after chronic spinal cord injury. *J Musculoskelet Neuronal Interact.* (2015) 15:32–41.
9. Black DM, Bilezikian JP, Ensrud KE, Greenspan SL, Palermo L, Hue T, et al. One year of alendronate after one year of parathyroid hormone (1-84) for osteoporosis. *N Engl J Med.* (2005) 353:555–65. doi: 10.1056/NEJMoa050336
10. Prince R, Sipos A, Hossain A, Syversen U, Ish-Shalom S, Marcinowska E, et al. Sustained nonvertebral fragility fracture risk reduction after discontinuation of teriparatide treatment. *J Bone Min Res.* (2005) 20:1507–13. doi: 10.1359/JBMR.050501
11. Leder BZ, Neer RM, Wyland JJ, Lee HW, Burnett-Bowie SM, Finkelstein JS. Effects of teriparatide treatment and discontinuation in postmenopausal women and eugonadal men with osteoporosis. *J Clin Endocrinol Metab.* (2009) 94:2915–21. doi: 10.1210/jc.2008-2630
12. Cohen A, Kamanda-Kosseh M, Recker RR, Lappe JM, Dempster DW, Zhou H, et al. Bone density after teriparatide discontinuation in premenopausal idiopathic osteoporosis. *J Clin Endocrinol Metab.* (2015) 100:4208–14. doi: 10.1210/jc.2015-2829
13. Chang KV, Hung CY, Chen WS, Lai MS, Chien KL, Han DS. Effectiveness of bisphosphonate analogues and functional electrical stimulation on attenuating post-injury osteoporosis in spinal cord injury patients-a systematic review and meta-analysis. *PLoS ONE.* (2013) 8:e81124. doi: 10.1371/journal.pone.0081124
14. Soleyman-Jahi S, Yousefian A, Maheronnaghsh R, Shokraneh F, Zadegan SA, Soltani A, et al. Evidence-based prevention and treatment of osteoporosis after spinal cord injury: a systematic review. *Eur Spine J.* (2018) 27:1798–814. doi: 10.1007/s00586-017-5114-7
15. Qin W, Li X, Peng Y, Harlow LM, Ren Y, Wu Y, et al. Sclerostin antibody preserves the morphology and structure of osteocytes and blocks the severe skeletal deterioration after motor-complete spinal cord injury in rats. *J Bone Miner Res.* (2015) 30:1994–2004. doi: 10.1002/jbmr.2549
16. Anderson D, Park AJ. Prophylactic treatment of osteoporosis after SCI: promising research, but not yet indicated. *Spinal Cord Ser Cases.* (2019) 5:25. doi: 10.1038/s41394-019-0166-z
17. Haider IT, Simonian N, Saini AS, Leung FM, Edwards WB, Schnitzer TJ. Open-label clinical trial of alendronate after teriparatide therapy in people with spinal cord injury and low bone mineral density. *Spinal Cord.* (2019) 57:832–42. doi: 10.1038/s41393-019-0303-3
18. Beggs LA, Ye F, Ghosh P, Beck DT, Conover CF, Balaez A, et al. Sclerostin inhibition prevents spinal cord injury-induced cancellous bone loss. *J Bone Miner Res.* (2015) 30:681–9. doi: 10.1002/jbmr.2396
19. Zhao W, Li X, Peng Y, Qin Y, Pan J, Li J, et al. Sclerostin antibody reverses the severe sublesional bone loss in rats after chronic spinal cord injury. *Calcif Tissue Int.* (2018). 103:443–54. doi: 10.1007/s00223-018-0439-8
20. Wang R. The gasotransmitter role of hydrogen sulfide. *Antioxid Redox Signal.* (2003) 5:493–501. doi: 10.1089/152308603768295249
21. Grassi F, Tyagi AM, Calvert JW, Gambari L, Walker LD, Yu M, et al. Hydrogen sulfide is a novel regulator of bone formation implicated in the bone loss induced by estrogen deficiency. *J Bone Miner Res.* (2016) 31:949–63. doi: 10.1002/jbmr.2757
22. Yang X, Hao D, Zhang H, Liu B, Yang M, He B. Treatment with hydrogen sulfide attenuates sublesional skeletal deterioration following motor complete spinal cord injury in rats. *Osteoporos Int.* (2017) 28:687–95. doi: 10.1007/s00198-016-3756-7
23. Lindsay R, Nieves J, Formica C, Henneman E, Woelfert L, Shen V, et al. Randomised controlled study of effect of parathyroid hormone on vertebral-bone mass and fracture incidence among postmenopausal women on oestrogen with osteoporosis. *Lancet.* (1997) 350:550–5. doi: 10.1016/S0140-6736(97)02342-8
24. Lindsay R, Krege JH, Marin F, Jin L, Stepan JJ. Teriparatide for osteoporosis: importance of the full course. *Osteoporos Int.* (2016) 27:2395–410. doi: 10.1007/s00198-016-3534-6
25. Harlow L, Sahbani K, Nyman JS, Cardozo CP, Bauman WA, Tawfeek HA. Daily parathyroid hormone administration enhances bone turnover and preserves bone structure after severe immobilization-induced bone loss. *Physiol Rep.* (2017) 5:e13446. doi: 10.14814/phy2.13446
26. Miller PD, Hattersley G, Riis BJ, Williams GC, Lau E, Russo LA, et al. Effect of abaloparatide vs placebo on new vertebral fractures in postmenopausal women with osteoporosis: a randomized clinical trial. *JAMA.* (2016). 316:722-33. doi: 10.1001/jama.2016.11136
27. Sahbani K, Cardozo CP, Bauman WA, Tawfeek HA. Abaloparatide exhibits greater osteoanabolic response and higher cAMP stimulation and β-arrestin recruitment than teriparatide. *Physiol Rep.* (2019) 7:e14225. doi: 10.14814/phy2.14225
28. Simonet WS, Lacey DL, Dunstan CR, Kelley M, Chang MS, Lüthy R, et al. Osteoprotegerin: a novel secreted protein involved in the regulation of bone density. *Cell.* (1997) 89:309–19. doi: 10.1016/S0092-8674(00)80209-3

29. Bilezikian JP, Lin CJF, Brown JP, Wang AT, Yin X, Ebeling PR, et al. Long-term denosumab treatment restores cortical bone loss and reduces fracture risk at the forearm and humerus: analyses from the FREEDOM extension cross-over group. *Osteoporos Int.* (2019) 30:1855–64. doi: 10.1007/s00198-019-05020-8
30. Cummings SR, San Martin J, McClung MR, Siris ES, Eastell R, Reid IR, et al. Denosumab for prevention of fractures in postmenopausal women with osteoporosis. *N Engl J Med.* (2009) 361:756–65. doi: 10.1056/NEJMoa0809493
31. Migliaccio S, Francomano D, Romagnoli E, Marocco C, Fornari R, Resmini G, et al. Persistence with_denosumab_therapy in women affected by osteoporosis with fragility fractures: a multicenter observational real practice study in Italy. *J Endocrinol Invest.* (2017) 40:1321–6. doi: 10.1007/s40618-017-0701-3
32. Moretti A, de Sire A, Curci C, Toro G, Gimigliano F, Iolascon G. Effectiveness of denosumab on back pain-related disability and quality-of-life in patients with vertebral fragility fractures. *Curr Med Res Opin.* (2018) 8:1–5. doi: 10.1080/03007995.2018.1545636
33. Ferrari S, Butler PW, Kendler DL, Miller PD, Roux C, Wang AT, et al. Further nonvertebral fracture reduction beyond 3 years for up to 10 years of_denosumab treatment. *J Clin Endocrinol Metab.* (2019) 104:3450–61. doi: 10.1210/jc.2019-00271
34. Jiang SD, Jiang LS, Dai LY. Effects of spinal cord injury on osteoblastogenesis, osteoclastogenesis and gene expression profiling in osteoblasts in young rats. *Osteoporos Int.* (2007) 18:339–49. doi: 10.1007/s00198-006-0229-4
35. Moriishi T, Fukuyama R, Ito M, Miyazaki T, Maeno T, Kawai Y, et al. Osteocyte network; a negative regulatory system for bone mass augmented by the induction of Rankl in osteoblasts and Sost in osteocytes at unloading. *PLoS ONE.* (2012) 7:e40143. doi: 10.1371/journal.pone.0040143
36. Qin W, Sun L, Cao J, Peng Y, Collier L, Wu Y, et al. The central nervous system (CNS)-independent anti-bone-resorptive activity of muscle contraction and the underlying molecular and cellular signatures. *J Biol Chem.* (2013) 288:13511–21. doi: 10.1074/jbc.M113.454892
37. Spatz JM, Wein MN, Gooi JH, Qu Y, Garr JL, Liu S, et al. The Wnt inhibitor sclerostin is up-regulated by mechanical unloading in osteocytes *in vitro*. *J Biol Chem.* (2015) 290:16744–58. doi: 10.1074/jbc.M114.628313
38. Gifre L, Vidal J, Carrasco JL, Muxi A, Portell E, Monegal A, et al. Denosumab increases sublesional bone mass in osteoporotic individuals with recent spinal cord injury. *Osteoporos Int.* (2016) 27:405–10. doi: 10.1007/s00198-015-3333-5
39. Bhasin S, Calof OM, Storer TW, Lee ML, Mazer NA, Jasuja R, et al. Drug insight: Testosterone and selective an- drogen receptor modulators as anabolic therapies for chronic illness and aging. *Nat Clin Pract Endocrinol Metab.* (2006) 2:146–59. doi: 10.1038/ncpendmet0120
40. Iolascon G, Moretti A, de Sire A, Liguori S, Toro G, Gimigliano F. Pharmacological therapy of sarcopenia: past, present and future. *Clin Cases Miner Bone Metab.* (2018) 15:407–15.
41. Basaria S, Collins L, Dillon EL, Orwoll K, Storer TW, Miciek R, et al. The safety, pharmacokinetics, and effects of LGD-4033, a novel nonsteroidal oral selective androgen receptor modulator, in healthy young men. *J Gerontol A Biol Sci Med Sci.* (2013) 68:87–95. doi: 10.1093/gerona/gls078
42. Neil D, Clark RV, Magee M, Billiard J, Chan A, Xue Z, et al. GSK2881078, a SARM, produces dose-dependent increases in lean mass in healthy older men and women. *J Clin Endocrinol Metab.* (2018) 103:3215–24. doi: 10.1210/jc.2017-02644
43. Schopp LH, Clark M, Mazurek MO, Hagglund KJ, Acuff ME, Sherman AK et al. Testosterone levels among men with spinal cord injury admitted to inpatient rehabilitation. *Am J Phys Med Rehabil.* (2006) 85:678–84. doi: 10.1097/01.phm.0000228617.94079.4a
44. Tsitouras PD, Zhong YG, Spungen AM, Bauman WA. Serum testosterone and growth hormone/insulin-like growth factor-I in adults with spinal cord injury. *Horm Metab Res.* (1995) 27:287–92. doi: 10.1055/s-2007-979961
45. Gregory CM, Vandenborne K, Huang HF, Ottenweller JE, Dudley GA. Effects of testosterone replacement therapy on skeletal muscle after spinal cord injury. *Spinal Cord.* (2003) 41:23–8. doi: 10.1038/sj.sc.3101370
46. Wu Y, Zhao J, Zhao W, Pan J, Bauman WA, Cardozo CP. Nandrolone normalizes determinants of muscle mass and fiber type after spinal cord injury. *J Neurotrauma.* (2012) 29:1663–75. doi: 10.1089/neu.2011.2203
47. Bauman WA, Cirnigliaro CM, La Fountaine MF, Jensen AM, Wecht JM, Kirshblum SC, et al. A small-scale clinical trial to determine the safety and efficacy of testosterone replacement therapy in hypogonadal men with spinal cord injury. *Horm Metab Res.* (2011) 43:574–9. doi: 10.1055/s-0031-1280797
48. Gorgey AS, Khalil RE, Gill R, Gater DR, Lavis TD, Cardozo CP et al. Low-dose testosterone and evoked resistance exercise after spinal cord injury on cardio-metabolic risk factors: an open-label randomized clinical trial. *J Neurotrauma.* (2019) 36:2631–45. doi: 10.1089/neu.2018.6136
49. Spangenburg EE, Le Roith D, Ward CW, Bodine SC. A function- al insulin-like growth factor receptor is not necessary for load- induced skeletal muscle hypertrophy. *J Physiol.* (2008) 586:283–91. doi: 10.1113/jphysiol.2007.141507
50. Bodine SC, Latres E, Baumhueter S, Lai VK, Nunez L, Clarke BA et al. Identification of ubiquitin ligases required for skeletal muscle atrophy. *Science.* (2001) 294:1704–8. doi: 10.1126/science.1065874
51. Hornberger TA, Chu WK, Mak YW, Hsiung JW, Huang SA, Chien S. The role of phospholipase D and phosphatidic acid in the mechanical activation of mTOR signaling in skeletal muscle. *Proc Natl Acad Sci USA.* (2006) 103:4741–6. doi: 10.1073/pnas.0600678103
52. Smuder AJ, Kavazis AN, Min K, Powers SK. Exercise protects against doxorubicin-induced oxidative stress and proteolysis in skeletal muscle. *J Appl Physiol.* (2011) 110:935–42. doi: 10.1152/japplphysiol.00677.2010
53. O'Neil TK, Duffy LR, Frey JW, Hornberger TA. The role of phosphoinositide 3-kinase and phosphatidic acid in the regulation of mammalian target of rapamycin following eccentric contractions. *J Physiol.* (2009) 587:3691–701. doi: 10.1113/jphysiol.2009.173609
54. Iwasawa H, Nomura M, Sakitani N, Watanabe K, Watanabe D, Moriyama H. Stretching after heabut not after cold decreases contractures after spinal cord injury in rats. *Clin Orthop Relat Res.* (2016) 474:2692–701. doi: 10.1007/s11999-016-5030-x
55. Battistuzzo CR, Rank MM, Flynn JR, Morgan DL, Callister R, Callister RJ, et al. Effects of treadmill training on hindlimb muscles of spinal cord-injured mice. *Muscle Nerve.* (2017) 55:232–42. doi: 10.1002/mus.25211
56. Roig M, O'Brien K, Kirk G, Murray R, McKinnon P, Shadgan B et al. The effects of eccentric versus concentric resistance training on muscle strength and mass in healthy adults: a systematic review with meta-analysis. *Br J Sports Med.* (2009) 43:556–68. doi: 10.1136/bjsm.2008.051417
57. Kim JS, Cross JM, Bamman MM. Impact of resistance loading on myostatin expression and cell cycle regulation in young and older men and women. *Am J Physiol Endocrinol Metab.* (2005) 288:E1110–9. doi: 10.1152/ajpendo.00464.2004
58. de Sire A, Baricich A, Renò F, Cisari C, Fusco N, Invernizzi M. Myostatin as a potential biomarker to monitor sarcopenia in hip fracture patients undergoing a multidisciplinary rehabilitation and nutritional treatment: a preliminary study. *Aging Clin Exp Res.* (2019) 14. doi: 10.1007/s40520-019-01436-8
59. Ryan AS, Ivey FM, Prior S, Li G, Hafer-Macko C. Skeletal muscle hypertrophy and muscle myostatin reduction after resistive training in stroke survivors. *Stroke.* (2011) 42:416–20. doi: 10.1161/STROKEAHA.110.602441
60. Andrews B, Gibbons R, Wheeler G. Development of functional electrical stimulation rowing: the rowstim series. *Artif Organs.* (2017) 41:E203–12. doi: 10.1111/aor.13053
61. Laskin JJ, Ashley EA, Olenik LM, Burnham R, Cumming DC, Steadward RD, et al. Electrical stimulation-assisted rowing exercise in spinal cord injured people. A pilot study. *Paraplegia.* (1993) 31:534–41. doi: 10.1038/sc.1993.87
62. Lambach RL, Stafford NE, Kolesar JA, Kiratli BJ, Creasey GH, Gibbons RS, et al. Bone changes in the lower limbs from participation in an FES rowing exercise program implemented within two years after traumatic spinal cord injury. *J Spinal Cord Med.* (2018) 26:1–9. doi: 10.1080/10790268.2018.1544879
63. Dudley-Javoroski S, Petrie MA, McHenry CL, Amelon RE, Saha PK, Shields RK. Bone architecture adaptations after spinal cord injury: impact of long-term vibration of a constrained lower limb. *Osteoporos Int.* (2016) 27:1149–60. doi: 10.1007/s00198-015-3326-4
64. Minematsu A, Nishii Y, Imagita H, Takeshita D, Sakata S. Whole-body vibration can attenuate the deterioration of bone mass and trabecular bone microstructure in rats with spinal cord injury. *Spinal Cord.* (2016) 54:597–603. doi: 10.1038/sc.2015.220
65. In T, Jung K, Lee MG, Cho HY. Whole-body vibration improves ankle spasticity, balance, and walking ability in individuals with incomplete cervical spinal cord injury. *NeuroRehabilitation.* (2018) 42:491–7. doi: 10.3233/NRE-172333

66. Ji Q, He H, Zhang C, Lu C, Zheng Y, Luo XT, et al. Effects of whole-body vibration on neuromuscular performance in individuals with spinal cord injury: a systematic review. *Clin Rehabil.* (2017) 31:1279–91. doi: 10.1177/0269215516671014
67. Ness LL, Field-Fote EC. Whole-body vibration improves walking function in individuals with spinal cord injury: a pilot study. *Gait Posture.* (2009) 30:436–40. doi: 10.1016/j.gaitpost.2009.06.016
68. Masani K, Alizadeh-Meghrazi M, Sayenko DG, Zariffa J, Moore C, Giangregorio L, et al. Muscle activity, cross-sectional area, and density following passive standing and whole body vibration: A case series. *J Spinal Cord Med.* (2014) 37:575–81. doi: 10.1179/2045772314Y.0000000255
69. Wagner FB, Mignardot JB, Le Goff-Mignardot CG, Demesmaeker R, Komi S, Capogrosso M, et al. Targeted neurotechnology restores walking in humans with spinal cord injury. *Nature.* (2018) 563:65–71. doi: 10.1038/s41586-018-0649-2
70. Cha S, Yun JH, Myong Y, Shin HI. Spasticity and preservation of skeletal muscle mass in people with spinal cord injury. *Spinal Cord.* (2019) 57:317–23. doi: 10.1038/s41393-018-0228-2
71. Bigford G, Nash MS. Nutritional health considerations for persons with spinal cord injury. *Top Spinal Cord Inj Rehabil.* (2017) 23:188–206. doi: 10.1310/sci2303-188
72. Khalil RE, Gorgey AS, Janisko M, Dolbow DR, Moore JR, Gater DR. The role of nutrition in health status after spinal cord injury. *Aging Dis.* (2012) 4:14–22.
73. Dionyssiotis Y. Malnutrition in spinal cord injury: more than nutritional deficiency. *J Clin Med Res.* (2012) 4:227–36. doi: 10.4021/jocmr924w
74. Lieberman J, Goff D Jr, Hammond F, Schreiner P, Norton HJ, Dulin M, et al. Dietary intake and adherence to the 2010 dietary guidelines for Americans among individuals with chronic spinal cord injury: a pilot study. *J Spinal Cord Med.* (2014) 37:751–7. doi: 10.1179/2045772313Y.0000000180
75. Groah SL, Nash MS, Ljungberg IH, Libin A, Hamm LF, Ward E, et al. Nutrient intake and body habitus after spinal cord injury: an analysis by sex and level of injury. *J Spinal Cord Med.* (2009) 32:25–33. doi: 10.1080/10790268.2009.11760749
76. Farkas GJ, Pitot MA, Berg AS, Gater DR. Nutritional status in chronic spinal cord injury: a systematic review and meta-analysis. *Spinal Cord.* (2019) 57:3–17. doi: 10.1038/s41393-018-0218-4
77. *2015-2020 Dietary Guidelines for Americans*. Washington, DC: U.S. Department of Health and Human Services and U.S. Department of Agriculture (2015).
78. Kendall RW, Jacquemin G, Frost R, Burns SP. Creatine supplementation for weak muscles in persons with chronic tetraplegia: a randomized double-blind placebo-controlled crossover trial. *J Spinal Cord Med.* (2005) 28:208–13. doi: 10.1080/10790268.2005.11753814
79. Perret C, Mueller G, Knecht H. Influence of creatine supplementation on 800 m wheelchair performance: a pilot study. *Spinal Cord.* (2006) 44:275–9. doi: 10.1038/sj.sc.3101840
80. Jacobs PL, Mahoney ET, Cohn KA, Sheradsky LF, Green BA. Oral creatine supplementation enhances upper extremity work capacity in persons with cervical-level spinal cord injury. *Arch Phys Med Rehabil.* (2002) 83:19–23. doi: 10.1053/apmr.2002.26829
81. Amorim S, Teixeira VH, Corredeira R, Cunha M, Maia B, Margalho P, et al. Creatine or vitamin D supplementation in individuals with a spinal cord injury undergoing resistance training: a double-blinded, randomized pilot trial. *J Spinal Cord Med.* (2018) 41:471–8. doi: 10.1080/10790268.2017.1372058
82. Morse LR, Troy KL, Fang Y, Nguyen N, Battaglino R, Goldstein RF, et al. Combination therapy with zoledronic acid and FES-row training mitigates bone loss in paralyzed legs: results of a randomized comparative clinical trial. *JBMR Plus.* (2019) 3:e10167. doi: 10.1002/jbm4.10167
83. Cosman F. Parathyroid hormone treatment for osteoporosis. *Curr Opin Endocrinol Diabetes Obes.* (2008) 15:495–501. doi: 10.1097/MED.0b013e32831a46d6
84. Whitfield JF, Morley P, Willick GE. Parathyroid hormone, its fragments and their analogs for the treatment of osteoporosis. *Treat Endocrinol.* (2002) 1:175–90. doi: 10.2165/00024677-200201030-00005
85. Edwards WB, Simonian N, Haider IT, Anschel AS, Chen D, Gordon KE, et al. Effects of teriparatide and vibration on bone mass and bone strength in people with bone loss and spinal cord injury: a randomized, controlled trial. *J Bone Miner Res.* (2018) 33:1729–40. doi: 10.1002/jbmr.3525
86. Sun F, Li SG, Zhang HW, Hua FW, Sun GZ, Huang Z. MiRNA-411 attenuates inflammatory damage and apoptosis following spinal cord injury. *Eur Rev Med Pharmacol Sci.* (2020) 24:491–8. doi: 10.26355/eurrev_202001_20022
87. Qian Z, Chang J, Jiang F, Ge D, Yang L, Li Y, et al. Excess administration of miR-340-5p ameliorates spinal cord injury-induced neuroinflammation and apoptosis by modulating the P38-MAPK signaling pathway. *Brain Behav Immun.* (2020) 31. doi: 10.1016/j.bbi.2020.01.025

Conflict of Interest: The reviewer LP declared a shared affiliation, with no collaboration with one of the authors NF, to the handling editor at time of review.

The remaining authors declare that the research was conducted in the absence of any commercial or financial relationships that could be construed as a potential conflict of interest.

frontiers in Endocrinology

ORIGINAL RESEARCH
published: 11 August 2020
doi: 10.3389/fendo.2020.00484

New Surgical Model for Bone–Muscle Injury Reveals Age and Gender-Related Healing Patterns in the 5 Lipoxygenase (5LO) Knockout Mouse

Claudia Cristina Biguetti[1,2], Maira Cristina Rondina Couto[3,4], Ana Claudia Rodrigues Silva[1], João Vitor Tadashi Cosin Shindo[4], Vinicius Mateus Rosa[1], André Luis Shinohara[4], Jesus Carlos Andreo[4], Marco Antonio Hungaro Duarte[4], Zhiying Wang[2], Marco Brotto[2] and Mariza Akemi Matsumoto[1]*

[1] Department of Basic Sciences, School of Dentistry, São Paulo State University (UNESP), Araçatuba, Brazil, [2] Bone-Muscle Research Center, College of Nursing and Health Innovation, University of Texas at Arlington, Arlington, TX, United States, [3] Department of Health Sciences, Universidade Do Sagrado Coração, Bauru, Brazil, [4] Bauru School of Dentistry, University of São Paulo, FOB-USP, São Paulo, Brazil

OPEN ACCESS

Edited by:
Giacomina Brunetti,
University of Bari Aldo Moro, Italy

Reviewed by:
Michaël R. Laurent,
University Hospitals Leuven, Belgium
Michaela Tencerova,
Institute of Physiology (ASCR), Czechia

***Correspondence:**
Claudia Cristina Biguetti
claudia.biguetti@uta.edu

Specialty section:
This article was submitted to Bone Research, a section of the journal Frontiers in Endocrinology

Received: 19 March 2020
Accepted: 22 June 2020
Published: 11 August 2020

Citation:
Biguetti CC, Couto MCR, Silva ACR, Shindo JVTC, Rosa VM, Shinohara AL, Andreo JC, Duarte MAH, Wang Z, Brotto M and Matsumoto MA (2020) New Surgical Model for Bone–Muscle Injury Reveals Age and Gender-Related Healing Patterns in the 5 Lipoxygenase (5LO) Knockout Mouse. Front. Endocrinol. 11:484. doi: 10.3389/fendo.2020.00484

Signaling lipid mediators released from 5 lipoxygenase (5LO) pathways influence both bone and muscle cells, interfering in their proliferation and differentiation capacities. A major limitation to studying inflammatory signaling pathways in bone and muscle healing is the inadequacy of available animal models. We developed a surgical injury model in the *vastus lateralis* (VL) muscle and femur in 129/SvEv littermates mice to study simultaneous musculoskeletal (MSK) healing in male and female, young (3 months) and aged (18 months) WT mice compared to mice lacking 5LO (5LOKO). MSK defects were surgically created using a 1-mm punch device in the VA muscle followed by a 0.5-mm round defect in the femur. After days 7 and 14 post-surgery, the specimens were removed for microtomography (microCT), histopathology, and immunohistochemistry analyses. In addition, non-injured control skeletal muscles along with femur and L5 vertebrae were analyzed. Bones were microCT phenotyped, revealing that aged female WT mice presented reduced BV/TV and trabecular parameters compared to aged males and aged female 5LOKO mice. Skeletal muscles underwent a customized targeted lipidomics investigation for profiling and quantification of lipid signaling mediators (LMs), evidencing age, and gender related-differences in aged female 5LOKO mice compared to matched WT. Histological analysis revealed a suitable bone-healing process with osteoid deposition at day 7 post-surgery, followed by woven bone at day 14 post-surgery, observed in all young mice. Aged WT females displayed increased inflammatory response at day 7 post-surgery, delayed bone matrix maturation, and increased TRAP immunolabeling at day 14 post-surgery compared to 5LOKO females. Skeletal muscles of aged animals showed higher levels of inflammation in comparison to young controls at day 14 post-surgery; however, inflammatory process was attenuated in aged 5LOKO

mice compared to aged WT. In conclusion, this new model shows that MSK healing is influenced by age, gender, and the 5LO pathway, which might serve as a potential target to investigate therapeutic interventions and age-related MSK diseases. Our new model is suitable for bone–muscle crosstalk studies.

Keywords: 5 lipoxygenase, bone, lipid mediators, aging, muscle, tissue healing

INTRODUCTION

Investigation of bone and muscle homeostasis has in recent years expanded to biochemical crosstalk via the secretion of different molecules, such as signaling lipid mediators (LMs) derived from essential polyunsaturated fatty acids (PUFA), with potential implications on aging, inflammation, and tissue healing (1–4). In this context, although skeletal muscle possesses great plasticity in response to physiologic stimuli (5, 6), its capacity for adaptation/regeneration is dependent on many different factors, such as the nature and extent of the stimulus (7), viability of satellite cells, aging, and inflammation (7–9). Indeed, higher inflammatory marker levels in elderly populations are directly associated with loss of muscle mass and strength (10), as well with the reduced capacity for bone healing, decreasing in the viability of osteoprogenitor cells (11). As observed in mice, aging also causes changes in skeletal muscle in a variable range of LM (12), such as AA-derived eicosanoids, eicosapentaenoic acid (EPA), as well as Omega 3 (ω-3) PUFA derivatives [e.g., docosahexaenoic acid [DHA]], in an age- and gender-dependent manner. In the face of these multiple factors (inflammation, aging, and gender), healing outcomes on the MSK system can vary from complete tissue regeneration to fibrosis, affecting the functional recovery of these tissues with important clinical implications (11). However, investigations are still ongoing on the specific cellular and molecular factors involved in the interconnected and interdependent healing of bone and muscle.

Due to the close anatomical relationship of bone and muscle, traumatic bone injuries (open bone fractures or surgical trauma) involve damage to the adjacent muscles, requiring simultaneous tissue healing of both compartments (1, 2, 13). Skeletal muscle assists bone healing, not only when it is used as a flap (or a second periosteum) for improving bone defect vascularization (14–16), but also the osteogenic potential of satellite cells (13). *In vitro* studies have suggested that osteocytes can enhance *in vitro* myogenesis and *ex vivo* muscle contractility by different mechanisms, such as through the Wnt/β-Catenin pathway (3) and the secretion of prostaglandin E_2 (PGE_2) key LM, which has a positive impact in the myogenic differentiation of primary mouse myoblasts/myotubes (4).

Skeletal muscle is mainly composed by muscle fibers surrounded by myogenic progenitors (satellite cells) with the capacity to proliferate and induce new fiber formation to restore injured tissue, followed by the upregulation and expression of Myoblast Determination Protein 1 (MyoD), as demonstrated in murine models of muscle regeneration (7, 17). MyoD is a quintessential protein in mammals that belongs to the Muscle Regulatory Family of proteins and is necessary for myoblast differentiation into myotubes (18). While new myotubes are formed, other injured muscle fibers undergo to degeneration/atrophy due to injuries followed by the upregulation and expression of Muscle Ring Finger-1 (MuRF1) (7, 17, 19). MuRF1 belongs to the family of ubiquitin ligases, is proposed to trigger muscle protein degradation via ubiquitination, serving as a marker for fiber degeneration/atrophy (19). MyoD and MuRF1 are both suitable markers for models of muscle regeneration/remodeling in skeletal muscle post-surgery. At the same time, bone has mesenchymal cell-derived osteoblasts, which can transfer from a quiescent stage into rapid proliferation and differentiation after certain stimuli and expression of Runt-related Transcription Factor-2 (Runx-2) (20). After new bone deposition, hematopoietic-derived osteoclasts regulated by osteoblasts, and inflammatory mediators contribute to bone maturation by a coordinated resorption of new bone matrix, followed by expression of different markers, such as Tartrate Resistant Acid Phosphatase (TRAP) (21).

Apart from the specificity of each cell type involved in skeletal muscle and/or bone regeneration, general tissue healing post-injury requires an initial and transient inflammatory phase, with release of several cytokines and inflammatory mediators, such as AA-derived signaling lipid mediators released from ciclooxigenase-2 (COX2) and 5-Lipoxygenase (5LO) pathways (22–24). These processes inherent to the inflammatory response are essential in directing vascular events and leukocytes migration, through the release of PGs and LTs (LTB4 and/or CysLTs), respectively (25, 26). In addition, evidence from other studies have also supported a crucial modulatory role of COXs and 5LO pathways and their products, PGs and LTs, on bone and muscle cells in different models of tissue repair/regeneration (4, 27–31).

While COX2 seems to affect bone healing in a positive manner by inducing new bone formation and angiogenesis (27, 32, 33), the 5LO pathway and its final products are supposed to contribute to osteoclastic differentiation and consequent bone resorption (29, 34–36) and inhibited bone formation *in vitro* (37). Male mice genetically deficient (knockout) for COX2 expression (COX2 KO mice), presented delayed bone formation in femur fractures, but with significant rescue after periosteal injection of the prostaglandin E2 receptor 4 (EP4) agonist (33). On the other hand, male young mice lacking 5LO expression presented increased cortical thickness (36) and accelerated fracture healing in endochondral bones (28). Previous studies comparing 129 SvEv WT with homozygous KO for 5LO have also shown a relevant role of 5LO activity in periodontal inflammation and bone resorption (35, 38). Furthermore, the pharmacological

inhibition of 5LO (39) or antagonism of CysLT1-receptor also enhanced endochondral bone healing in rats (40). In skeletal muscle, LTB4 contributes to muscle regeneration by enhancing the proliferation and differentiation of satellite cells (41). *In vitro* studies revealed that the 5LO pathway is one of the major sources of extracellular ROS release in skeletal muscle (42). Significant upregulation of LTB4 pathway has been particularly found in muscle tissue in chronic inflammatory conditions (polymyositis or dermatomyositis) and seems to be associated with muscle weakness (43). However, the role of 5LO on muscle healing remains elusive, and no previous studies have addressed the effects of 5LO inhibition or its complete deletion in animal models.

Finally, it is important to mention that 5LO activity measured by the amount of LTs are significantly higher in females than in males, in humans (44, 45), and rodents (46–48). These differences in gender generally associate with a higher incidence and severity of inflammatory chronic conditions and autoimmune diseases in females than males, such as rheumatoid arthritis and asthma, and positively associate with increased levels of LTs (49). Thus, it is reasonable to hypothesize that gender is an important factor that can modulate the action of lipid mediators on the MSK system-healing capacity.

Therefore, efforts on development/characterization of animal models of simultaneous bone–muscle healing might support a comprehensive understanding on the role of lipid mediators in this process to provide insights that could lead to the identification of potential targets for the treatment and/or new interventions (e.g., specific diets/exercises) of MSK injuries. Our primary objective was to develop a new surgical mouse model that better represents the pathophysiological conditions for the simultaneous injury of bone and muscle without major catastrophic failure. As a secondary objective, we then utilized this model to investigate healing patterns during aging. We further studied the influence of gender and 5LO using the 5LOKO mouse. Our key findings revealed that aging delayed both muscle and bone healing in mice, with bones recovering faster than muscles, maybe indicating a role of muscles, to act as bone sentinels. We observed the major negative effects in aged WT females. Importantly, despite the aging negative effects, 5LOKO aged females presented an improved skeletal phenotype and healing outcomes compared to the young WT mice.

MATERIALS AND METHODS

Animals

In this study, we utilized 129/SvEv wild type (WT) and 5LO (homozygous knockout for 5LO^{tm1Fun}, designated here as 5LOKO). Littermate controls 129/SvEv and 5LOKO mice were used as previously described by other studies using this strain of 5LOKO mice (35, 38) and from the same source (38). Mice were obtained from Central Animal Facility for Special Mice of the School of Medicine of Ribeirão Preto—University of São Paulo, Brazil (CCCE-FMRP-USP) and were housed in the Central Animal Facility of Universidade Sagrado Coração (USC), Bauru, São Paulo, Brazil, under the approval of IACUC protocol #9589271017 (from Institutional Ethic Committee on Animal Use) and following the normative regulations provided by the National Council for the Control of Animal Experimentation in Brazil (CONCEA). Our design included four experimental groups, each containing 20 mice: 3-month old (young) males and females, and 18-month old (aged) males and females. The mice received sterile water and sterile standard solid mice chow (Nuvital, Curitiba, PR, Brazil) *ad libitum* and were housed at temperature-controlled rooms (22–25°C). We conducted estrus cycle analysis (Toluine blue O vaginal smears) to determine post-menopausal stage in all aged female mice (50, 51). All animal procedures were cared for in accordance with the CONCEA and following the Guide for the Care and Use of Laboratory Animals of the National Institutes of Health (Institute of Laboratory Animal Resources (U.S.), as well as the ARRIVE guidelines recommendations (52). Experimental groups for bone–muscle surgical injury model were comprised of five animals per group/time point (7 and 14 days) and used for microtomography (microCT), histological, and immunohistochemical analysis. Prior and during the experimental protocol, animals from each group were allocated in groups of five mice per cage and the cages were codified by the researcher supervisor and technician in order to minimize bias. Naïve bones (left femur and L5 vertebrae) were used for skeletal phenotyping by microCT analysis. One 129SvEv WT aged and one young female were additionally used for pilot studies for the surgical model. Naïve gastrocnemius muscles were collected for lipidomics analyses at the Bone–Muscle Research Center, https://www.uta.edu/conhi/research/bmrc/index.php, University of Texas–Arlington.

Experimental Protocol for Surgical Muscle and Bone Injury

We developed a new surgical model for the simultaneous injury of bone and muscle to simulate conditions of trauma and/or surgeries in a controlled and reproducible manner, where both tissues are damaged, but without catastrophic damage, such as an injury that occurs in automobile accidents or with military personnel. Mice were anesthetized with intraperitoneal injection of 80 mg/kg ketamine chloride (Dopalen, Agribrands Brasil, Paulínia, SP, Brazil) and 160 mg/kg xylazine chloride (Anasedan, Agribrands Brasil, Paulínia, SP, Brazil). Additional local anesthesia was provided by using 5 μL of intramuscular injection of Mepivacaine Hydrochloride 2% with Epinephrine 1:100,000 (Mepiadre®, DFL, Rio de Janeiro, Brazil) vasoconstrictor, to provide hemostasis and additional comfort in the first hours after surgery. All animals were measured in relation to body weight (BW) and rostrocaudal (RC) length before the experimental procedures. Then, mice were positioned in lateral decubitus under a stereomicroscope providing 5× magnification (DF Vasconcellos, São Paulo, SP, Brazil). The right lower limb was gently shaved, disinfected with polyvinylpyrrolidone prior to a 10-mm vertical incision to expose the Vastus Lateralis (VL) underlying muscle. A 1-mm micro-punch device for rodents (Härte Instrumentos Cirúrgicos, Ribeirao Preto, Brazil) was used to create a muscle defect to a depth of 1.5 mm until it reached the femoral bone. To produce a subjacent monocortical bone defect in the femur, midshaft femoral bone was drilled using a 0.50-mm

pilot drill (NTI-Kahla GmbH Rotary Dental Instruments, Kahla, Thüringen, Germany) to a maximum depth of 1 mm at 600 rpm, using a surgical motor (NSK-Nakanishi International, Kanuma, Tochigi, Japan). Bone defects were created under cold saline solution irrigation to avoid thermal necrosis in bone and surrounding tissues. Only subcutaneous tissue (not muscle) was sutured with 5–0 silk suture (Ethicon, © Johnson & Johnson, São Paulo, Brazil). All groups of animals were submitted to surgery, and the actual surgical procedure (creation of defects) was performed by a single trained, expert surgeon (CCB), who was blinded at this point of the experiment. No antibiotics and anti-inflammatory drugs were administered to the animals after the MSK-injury so as not to interfere with experimental design. At the first 72 h after surgery, the feed was supplied from the bottom compartment of the cage to prevent, but not impede, the recovering mice from getting up in the cage, which could result in additional unintended damage. The suture naturally fell off 3–4 days post-surgery when the skin was clinically healed. Mice were provided sterile water *ad libitum* and were fed with sterile standard solid mice chow (Nuvital, Curitiba, PR, Brazil) throughout all experimental periods of this study.

Sample Collection

At the end of experimental time points, mice were euthanized for sample collection. The VL muscle was dissected from the quadriceps femoris muscles, embedded in optimal cutting temperature compound (OCT) (Tissue-Tek, Sakura Finetek, Torrance, CA, USA) and immediately frozen in liquid nitrogen for cryostat sectioning. Gastrocnemius muscle samples were collected and immediately frozen in liquid nitrogen for targeted quantification of LMs via lipidomics, as previously described (12). Injured femurs, as well as femur controls and L5 vertebrae, were fixed in phosphate buffered saline (PBS) buffered formalin (10%) solution (pH 7.2) for 48 h at room temperature. Bone specimens were washed overnight in running water and maintained in 70% hydrous ethanol for microCT scanning. After microCT scanning, bone specimens were decalcified in 4.13% EDTA (pH 7.2) following histological processing protocols, as previously described (53).

Micro CT

Bone specimens (injured, control femurs, and L5 vertebrae) were scanned for qualitative and quantitative analyses by microCT. Controls used for bone phenotyping (10 biological replicates) from each group were pooled (from 7 to 14 days), since they represented controls. Five biological replicates of injured femurs were used from each group. First, specimens were rehydrated in saline solution for 10 min before scanning. Sample scanning was performed by using a Skyscan 1174 System (Skyscan, Kontich, Belgium) at 50 kV, 800 μA, with a 0.5-mm aluminum filter, 180 degrees of rotation and exposure range of 1 degree and a 14-μm-pixel-size resolution, as previously described (21). Briefly, projections were first reconstructed using the NRecon software (Bruker microCT, Kontich, Belgium), realigned in Data Viewer for 2D images. Tridimensional images were obtained by using CTVox (Bruker microCT, Kontich, Belgium). Quantitative parameters were assessed using CTAn (Bruker microCT, Kontich, Belgium), based on previous guidelines and recommendations (54), as well as similar regions of interest (ROI) for L5 vertebrae and femur analysis (55–57). For skeletal phenotype, L5- vertebral body was evaluated considering a ROI, 1.5 mm in diameter and 3 mm in length. Femur was analyzed considering two regions: a 2-mm length of the cortical of mid-diaphysis and a 1.5-mm length of the cancellous compartment of distal metaphysis. Evaluated parameters for skeletal phenotype comprised bone volume (BV, mm^3), fraction of bone volume [Bone Volume/Tissue Volume (BV/TV), %], trabecular number (Tb.N), trabecular thickness (Tb.Th), and trabecular separation (Tb.Sp). Cross-sectional volume (mm^3) was evaluated only for the cortical mid-diaphysis of femur. Bone defects were evaluated for BV/TV (%) by using a cylindrical ROI, 0.5 mm in diameter and 0.5 mm in depth, considering the size of monortical defect.

Histological Processing for Injured Bone

After microCT scanning, femur samples containing the region of defect were washed and immersed in buffered 4.13% EDTA (pH 7.2) for decalcification for 3 weeks. Then, specimens were processed for histological embedding in paraffin blocks. Semi-serial 5-μm histological transversal slices were obtained from the central area of the bone defect and were used for Hematoxylin and Eosin (H&E), modified Goldner's Trichrome/Alcian Blue (58), and Picrosirius red staining for birefringence and immunohistochemistry for 5LO, Runx2, and TRAP.

Histological Processing for Injured Muscles

Muscle samples were processed as previously described (59, 60). VL muscles were embedded in OCT and sectioned at temperature of −20°C (Leica, CM 1850, Nussloch, Germany). Eight semi-serial 8-μm transversal sections were obtained from each specimen separated by at least 40 μm, comprising the area of defect and adjacent areas. Histological sections from days 7- to 14 post-surgery were used for H&E staining. Histological sections from 7 days post-surgery were used for immunohistochemistry for MuRF1 and MyoD.

Histopathological Analysis of Bone and Muscle Healing

Bone and muscle samples stained with H&E were used for histopathological analysis by two blinded examiners (CCB and MAM). Bone healing was evaluated considering the presence of inflammatory infiltration, connective tissue, cartilage, newly formed bone (containing new osteoblasts and osteocytes differentiation), osteoclasts, and blood vessels in remodeling areas. Modified Goldner's Trichrome/Alcian Blue was also used as a complementary approach to identify newly formed bone, cartilage, and connective tissue. Five biological replicates from muscle samples were also used for histomorphometric analysis. The histological region for healing comprised 1 mm^2 in the central area of muscle defect, as well the adjacent region of central damage, for evaluation of cross-sectional area (CSA) of fibers. CSA measurement was performed with two technical replicates from each animal, from which six photomicrographs at 100× magnification (technical replicates) were captured and

evaluated using the software SigmaScan Pro 5.0 (Systat Software Inc., Chicago, USA). Histomorphometric parameters included inflammatory infiltrate in the area of injury and fibers with centralized myonuclei surrounding the region of the defect. We used histological sections (three technical replicates) from five animals (biological replicates) per group. Quantification of histological parameters was performed using four random histological fields from each histological section. Histological fields were captured at 100× using an oil immersion objective (Carl Zeiss Jena GmbH, Jena, Germany). A grid image was superimposed on each histological field containing a total of 100 points in a quadrangular area by using the ImageJ software (Version 1.51, National Institutes of Health, Bethesda, Maryland, USA), as previously described (53). Only the points coincident (considered as the intersection point of the vertical and horizontal lines) with the histological parameters were considered, and the total number of points was obtained to calculate the area density for each healing component in each section. Results were presented as means ± SDs of the area density for each bone and muscle healing parameter.

Birefringence Analysis for Collagenous Content in Bone Defects

Quality and quantity of bone matrix deposition was performed using the Picrosirius-polarization method and birefringence analysis. Two histological fields (two biological replicates) of each femur defects stained with Picrosirius Red were captured with a 10× objective under polarizing lens coupled to a binocular inverted microscope (Leica DM IRB/E) and analyzed as previously described (21, 61). Green birefringence color indicates thin fibers; yellow and red colors at birefringence analysis indicate thick and organized collagen fibers (21, 58). Briefly, spectra of green, yellow, and red colors were defined by RGB values, and the quantity of pixels-squared was calculated for each field by using the AxioVision 4.8 software (CarlZeiss). After calculations of each spectrum fiber, total area was also calculated by the sum of each color spectrum. Means and standard deviation (SD) considering the two technical replicates (histological fields) and five biological replicates (number of animals per group) were calculated for each group, considering strain, gender and age.

Immunohistochemistry

Histological sections from femur defects were used for individual immune detection of TRAP (sc30832), Runx2 (sc8566), and 5LO (sc136195). Muscle samples were used for individual immune detection of MuRF-1 (sc398608) and MyoD (sc377460). All primary antibodies were purchased from Santa Cruz Biotechnology (Santa Cruz Biotechnology, Santa Cruz, CA, USA). Paraffin-embedded histological sections were rehydrated, and antigen retrieval was performed by boiling the slides in 10 mM sodium citrate buffer (pH 6) for 30 min at 100°C. Sections were pre-incubated with 3% Hydrogeroxidase Block (Spring Bioscience Corporation, CA, USA) and then incubated with 7% Non-fat Dry Milk to block serum proteins. Frozen muscles samples were incubated in ice-cold acetone prior to incubation with horse serum for protein blocking. Anti-TRAP, anti-Runx2, Anti-MuRF1, and Anti-MyoD primary antibodies were diluted at 1:100, while 5LO was diluted in 1:200 in diluent solution and then incubated for 1 h at room temperature. Goat-On-Rodent HRP-Polymer PromARM (cat # GHP516G, Biocare Medical, Pacheco, CA) was used as a detection method for TRAP and Runx-2, and sections were incubated for 40 min at room temperature following manufacturer instructions. Anti-Mouse HRP-Polymer made in goat (ImmPRESS, Vector Laboratories, San Diego, CA) was used as a detection method for 5LO, MuRF-1, and MyoD. The identification of antigen–antibody reaction was performed using 3-3′-diaminobenzidine (DAB). Bone samples labeled for TRAP, Runx-2, and 5LO were counterstained with Mayer's hematoxylin. Muscle samples were left without counterstaining to be used for optical density quantification. Negative controls were performed by using only diluents solution instead of primary antibody.

Quantification of Immunohistochemical Markers

Quantification of all markers was performed by using four histological fields from each histological section captured, using a 100× oil immersion objective (Carl Zeiss Jena GmbH, Jena, Germany). Quantification of TRAP was performed at the 14-day time point; most TRAP+ cells were found in areas of bone remodeling. Runx2, MuRF-1, and MyoD labeling were analyzed at the 7-day time point. Pixels quantification was performed with Aperio Image Scope v. 12.3.3 (Leica Biosystems, Buffalo Grove, USA), used for immunohistochemical analysis in pathology (62). Images were analyzed by choosing the algorithm Positive Pixel Count in Aperio Image Scope (Leica Biosystems, Buffalo Grove, USA). Subsequently, all positive pixels were calculated, and the results were expressed as Positivity (number of positive pixels/number total). Negative controls tissues were used for confirmation of negative labeling and detection. Results were presented as the means and SD for each marker.

Targeted Lipidomics

Targeted lipidomics was performed following our previously published quantification method (12) with some modifications. Briefly, aliquoted frozen muscle tissue (50–100 mg) was applied for LC-MS/MS-based lipidomic analysis. All components of LC-MS/MS system are from Shimadzu Scientific Instruments, Inc. (Columbia, MD). The LC system was equipped with four pumps (Pump A/B: LC-30AD, Pump C/D: LC-20AD XR), a SIL-30AC autosampler (AS), and a CTO-30A column oven containing a two-channel, six-port switching valve. The LC separation was conducted on a C8 column (Ultra C8, 150 × 2.1 mm, 3 μm, RESTEK, Manchaca, TX) along with a Halo guard column (Optimize Technologies, Oregon City, OR). The MS/MS analysis was performed on Shimadzu LCMS-8050 triple quadrupole mass spectrometer. The instrument was operated and optimized under both positive and negative electrospray and multiple reaction monitoring modes (± ESI MRM). Standard lipid mediators and corresponding isotope-labeled lipid mediator internal standards (IS) were purchased from Cayman Chemical Co. (Ann Arbor, MI). All analyses and data processing were completed on Shimadzu LabSolutions V5.91 software (Columbia, MD). Four total bioactive lipids [EPA, DHA, AA, 11,12-epoxyeicosatrienoic

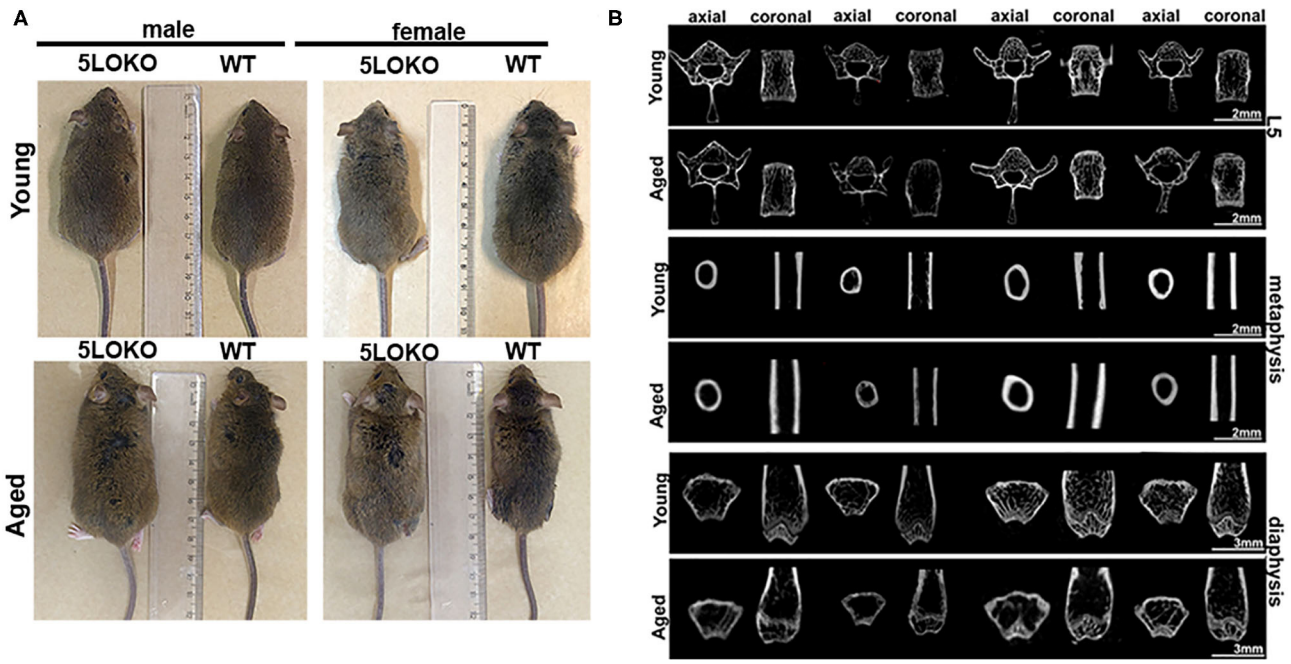

FIGURE 1 | Macroscopic anatomy and skeletal phenotype of young and aged WT and 5LOKO mice: **(A)** Male and female, young (3 months old) and aged (18 months old) 129/SvEv WT and 5LOKO mice. **(B)** Axial and Coronal sections of L5 vertebrae, femur distal metaphysis, and mid-diaphysis. Images were obtained after scanning in Skyscan 1174 System (Skyscan, Kontich, Belgium). Projections were first reconstructed using the NRecon software and realigned in Data Viewer (Bruker, Kontich, Belgium) for 2D images.

acid [11,12-EET], and PGE_2] were quantified from muscle samples in this study. Results were presented quantity of each lipid in muscle (pg/mg muscle).

Statistical Analysis

Quantitative data were first analyzed for distribution of normality using Shapiro-Wilk normality test. Possible outliers were identified using the ROUT method, using the maximum Q of 1% for False Discovery Rate (FDR) (63). The effect of age and/or gender and/or genotype for quantitative parameters were analyzed by two-way ANOVA followed by Bonferroni correction. Values of $p < 0.05$ were considered statistically significant.

RESULTS

Differences in Gross Anatomy and Skeletal Phenotype of 5LOKO Aged Mice

First, we investigated the impact of aging on body weight, RC length, and microtomographic parameters for skeletal phenotype in male and female 129/SvEv WT and 5LOKO mice (**Figure 1**, **Table 1**). Statistically significant differences for the body weight (grams) and RC length (cm) were found between genders in WT groups: higher values for young and aged male compared to female mice. Also, young 5LOKO male presented increased body weight compared to females, and aged 5LOKO male mice presented increased RC length compared to females. Considering differences between genotypes, aged 5LOKO males showed higher RC length compared to aged controls, while no differences were found between aged or young WT vs. 5LOKO females considering these parameters.

We evaluated the cortical diaphysis of femur (BV) and morphological parameters in cancellous compartments of femur (distal metaphysis) and the L5-vertebral body. No statistical differences were found in the cortical diaphysis of femur, considering age, gender, or genotype (**Table 1**); although qualitative differences were observed in the transversal sections of femur diaphysis of aged WT females compared to aged WT males and aged 5LOKO females. Aged WT and aged 5LOKO females displayed increased trabecular spacing (Tb.Sp) in femur metaphysis compared to their young controls ($p < 0.05$), but presented no differences comparing both genotypes. The effect of age led to a reduced BV/TV in femur metaphysis of aged WT females compared to young controls ($p < 0.05$). In a comparison of genotypes, aged female WT mice presented a significantly reduced BV/TV in femur metaphysis in comparison to aged 5LOKO female mice. Major differences were also found in trabecular parameters of L5. The effect of age led to a reduced BV/TV and Tb.N in aged WT female compared to young controls. In comparison of genotypes, aged female WT mice presented a significantly reduced BV/TV and Tb.N in comparison to aged 5LOKO female mice. Both aged male and female WT mice presented an increased Tb.Sp compared to 5LOKO controls. In general, WT mice were most influenced by aging compared to 5LOKO (**Table 1**).

TABLE 1 | Macroscopic features and skeletal phenotyping in WT vs. 5LOKO mice.

Parameters	Sites/Groups	Y WT ♂	Y WT ♀	A WT ♂	A WT ♀	Y KO ♂	Y KO ♀	A KO ♂	A KO ♀
BW (grams)	–	27.97 ± 3.22$^{\&}$	22.54 ± 2.36$^{\&}$	29.06 ± 3.22$^{\&}$	23.96 ± 3.58$^{\&}$	25.90 ± 3.07$^{\&}$	20.61 ± 2.00$^{\&*}$	29.04 ± 2.59	26.07 ± 2.49*
RC (cm)	–	9.07 ± 0.27$^{\&}$	8.43 ± 0.30$^{\&}$	8.66 ± 0.30$^{\#}$	8.51 ± 0.47	9.00 ± 0.23	8.50 ± 0.16	9.37 ± 0.49$^{\&\#}$	8.79 ± 0.42$^{\&}$
BV (mm^3)	Femur diaphysis	1.70 ± 0.09	1.90 ± 0.80	2.22 ± 0.31	1.62 ± 0.32	1.98 ± 0.22	1.59 ± 0.41	1.70 ± 0.26	1.74 ± 0.64
BV/TV (%)	Femur metaphysis	16.98 ± 5.12	23.99 ± 5.81*	19.08 ± 2.87	12.30 ± 2.20$^{*\#}$	28.42 ± 7.00	27.91 ± 54.98	27.30 ± 3.92	21.00 ± 4.19$^{\#}$
	L5 vertebrae	35.88 ± 4.87	44.16 ± 4.35*	33.68 ± 7.45	25.62 ± 6.65$^{*\#}$	40.08 ± 3.28	34.15 ± 5.25	42.63 ± 4.41	42.27 ± 7.06$^{\#}$
Tb.Th (mm)	Femur metaphysis	0.18 ± 0.01	0.19 ± 0.02	0.17 ± 0.02	0.16 ± 0.03	0.19 ± 0.03	0.19 ± 0.04	0.21 ± 0.06	0.21 ± 0.02
	L5 vertebrae	0.09 ± 0.01	0.10 ± 0.01	0.10 ± 0.02	0.10 ± 0.03	0.10 ± 0.01	0.13 ± 0.02	0.12 ± 0.01	0.17 ± 0.03
Tb.Sp (mm)	Femur metaphysis	0.46 ± 0.18	0.33 ± 0.07*	0.53 ± 0.12	0.86 ± 0.39*	0.33 ± 0.09	0.30 ± 0.06*	0.31 ± 0.109$^{\&}$	0.70 ± 0.07$^{*\&}$
	L5 vertebrae	0.29 ± 0.03	0.24 ± 0.02	0.34 ± 0.06$^{\#}$	0.32 ± 0.07$^{\#}$	0.20 ± 0.03	0.21 ± 0.04	0.21 ± 0.01$^{\#}$	0.17 ± 0.03$^{\#}$
Tb.N (1/mm)	Femur metaphysis	1.05 ± 0.16	1.18 ± 0.30	0.99 ± 0.15	0.61 ± 0.11	1.45 ± 0.12	1.67 ± 0.43*	1.53 ± 0.32	0.85 ± 0.26*
	L5 vertebrae	3.22 ± 0.25	3.51 ± 0.34*	2.60 ± 0.66$^{\&}$	1.28 ± 0.36$^{*\#\&}$	3.96 ± 0.39	3.15 ± 0.18	3.07 ± 0.26	2.18 ± 0.28$^{\#}$

Results are presented as the means (± SD) for each parameter.
*In the comparison between columns, symbol *indicates comparison between columns: the effect of age (Y vs. A) in groups of same genotype and gender (e.g., Y ♀ WT vs. A ♀ WT); symbol $^{\#}$indicates the effect of different genotypes (WT vs. KO) in groups of same age and gender (e.g., Y ♀ WT vs. Y ♀ KO); and symbol $^{\&}$indicates the effect of gender (♂ vs. ♀) in the same genotype and age (e.g., Y ♀ WT vs. Y ♂ WT). Statistically significant differences are indicated between groups with equal symbols ($p < 0.05$). Y = 3 months; A = 18 months. BW, Body weight; RC, rostrocaudal length.*

TABLE 2 | Targeted lipidomics of skeletal muscle in WT vs. 5LOKO mice.

Groups Lipids (pg/mg)	Y WT ♂	Y WT ♀	A WT ♂	A WT ♀	Y KO ♂	Y KO ♀	A KO ♂	A KO ♀
AA	4,136 ± 163	4,340 ± 177	3,221 ± 193	3,125 ± 370$^{\#}$	4,652 ± 81	4,473 ± 633	4,481 ± 859	5,288 ± 613$^{\#}$
PGE_2	10.8 ± 3.65	6.9 ± 2.26$^{\#}$	16.77 ± 2.59	15.9 ± 3.06$^{\#}$	12.23 ± 0.64*	20.73 ± 15.22$^{\#}$	10.9 ± 2.78$^{\&*}$	45.87 ± 29$^{\#\&}$
11,12-EET	6 ± 1.37	8 ± 3.36	4 ± 0.70$^{\#\&}$	10 ± 3.28$^{\&}$	9.90 ± 3.36*	5.26 ± 2.08	23.8 ± 8.03$^{\#\&*}$	8.8 ± 1.66$^{\&}$
DHA	8,386 ± 847*	8,899 ± 769*	6,078 ± 586$^{\#*}$	7,333 ± 1,571$^{\#*}$	9,679 ± 643*	11,580 ± 2133*	17,006 ± 1408$^{\#*}$	15,659 ± 2128$^{\#*}$
EPA	197 ± 21	211 ± 24	189 ± 26	172 ± 29$^{\#}$	292 ± 23	325 ± 65$^{\#}$	391 ± 108	401 ± 106$^{\#}$

Results are presented as the means (±SD) for each lipid mediator.
*In the comparison between columns, symbol *indicates comparison between columns: the effect of age (Y vs. A) in groups of same genotype and gender (e.g., Y ♀ WT vs. A ♀ WT); symbol $^{\#}$indicates the effect of different genotypes (WT vs. KO) in groups of same age and gender (e.g., Y ♀ WT vs. Y ♀ KO); and symbol $^{\&}$indicates the effect of gender (♂ vs. ♀) in the same genotype and age (e.g., Y ♀ WT vs. Y ♂ WT). Statistically significant differences are indicated between groups with equal symbols ($p < 0.05$). Y = 3 months; A = 18 months.*

Targeted Lipidomics of Skeletal Muscle

In order to analyze the endogenous quantities of eicosanoid lipid mediators relevant in the inflammatory process of naïve skeletal muscle, we determined the concentration (pg/mg) of PGE_2, 11,12-EET, AA, EPA, and DHA (**Table 2**). Considering the effect of age, WT mice presented a decrease in levels of DHA compared to their young controls, while aged 5LOKO mice presented an increase in this LM when compared with their young controls. Aged WT female mice presented an increase in levels of 11,12-EET compared to young WT female mice and compared to aged WT male mice. Considering the effect of genotype, the amounts of AA, DHA, and EPA were significantly decreased in aged female WT mice compared to aged female KO mice. Levels of 11,12-EET were significantly increased in aged 5LOKO male mice compared to aged WT male mice and also compared to aged female 5LOKO mice. Aged male WT mice also had a decrease in the levels of DHA and EPA compared to aged KO mice. Also, young and aged female WT mice had a decrease in the levels of PGE_2 comparing with 5LOKO matched controls. Considering the effect of gender, levels of PGE_2 were significantly increased in aged female KO mice, with significant differences compared to aged male KO mice.

Development of the Surgical Protocol

For developing the surgical MSK injury, we created a defect in the VA muscle (1-mm in diameter) of the right lower limb, followed by a subjacent monocortical defect (0.5 mm diameter) in the midshaft of femoral bone (**Figure 2A**). After animal anesthesia and preparation under the stereomicroscope, the time of surgical procedure and suture was no longer than 10 min. No fractures or other additional complications were observed following the surgeries. There was no evidence of weight loss, infection, and persistent inflammation in surgical sites. The subcutaneous sutures fell off 3–4 days post-surgery when the skin was clinically healed by day 7 post-surgery. The day after the surgery, animals were able to ambulate properly and presented no major signs of distress. Importantly, of the 80 animals used in this study, two aged 5LOKO female mice died immediately

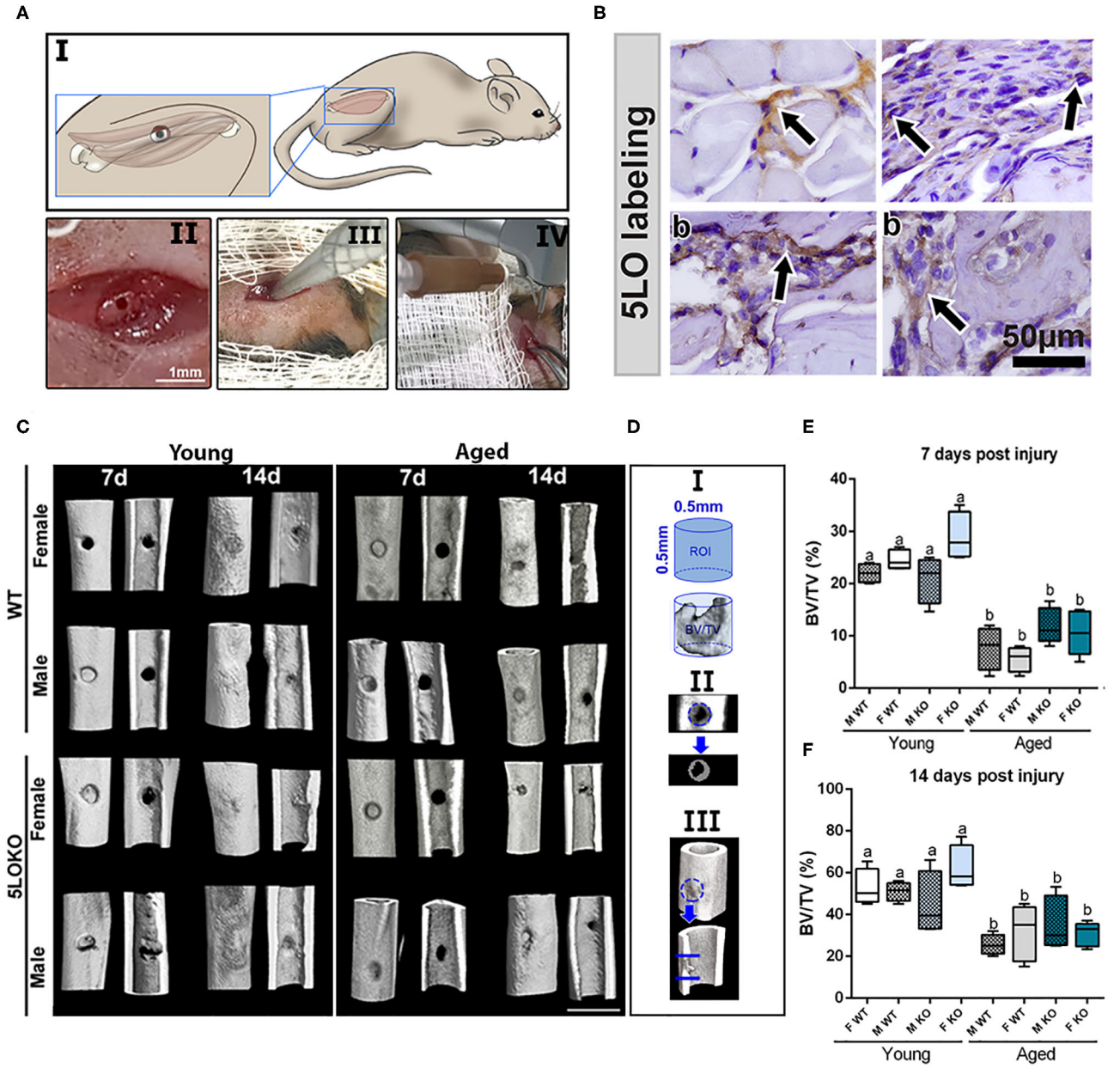

FIGURE 2 | Establishment of the novel surgical bone-muscle model of simultaneous injury: **(A)** Images of the surgical model: I to IV—(I) *vastus lateralis* and femur anatomic localization in mouse and the schematic representation of muscle and bone surgical injury; (II) clinical aspect of muscle and bone injury; (III) 1-mm micro punch created a muscle defect to a depth of 1.5-mm until reaching the femoral bone; (IV) view of the subsequent defect induced by bone drilling using a 0.5-mm pilot drill at 600 rpm under constant irrigation. **(B)** Representative images for the immunolabeling of 5LO (arrows) in bone and muscle of young WT 7 days post-surgery (b), muscle (m), and periosteum (p) surrounding the bone defect. **(C–F)** MicroCT analysis: Femur containing bone defects were scanned with the microCT System (Skyscan 1174; Skyscan, Kontich, Belgium). **(C)** MicroCT 3D qualitative images were obtained from 7 to 14 days post-surgery in young and aged, male and female, and WT and 5LOKO mice. **(D)** ROI determined in the site of femur injury. **(E,F)** Bone Volume Fraction (BV/TV, %) was quantified at days 7 and 14 post-surgery, and results are presented as mean ± SD. Different letters indicate significant differences between young and aged mice for each sex and strain ($p < 0.05$).

after the anesthesia by accidental excess of local anesthesia combined with sedation and were replaced by two other animals. No animals were lost due to the surgical procedure and/or during the recovery phase or up to the 14-day post-surgery period.

5LO Is Detected in WT Mice in Bone- and Muscle-Injured Tissues

Histological slides from young male WT mice at 7 days post-surgery were used for the immunolabeling of 5LO. 5LO-positive cells were found on the cytoplasm

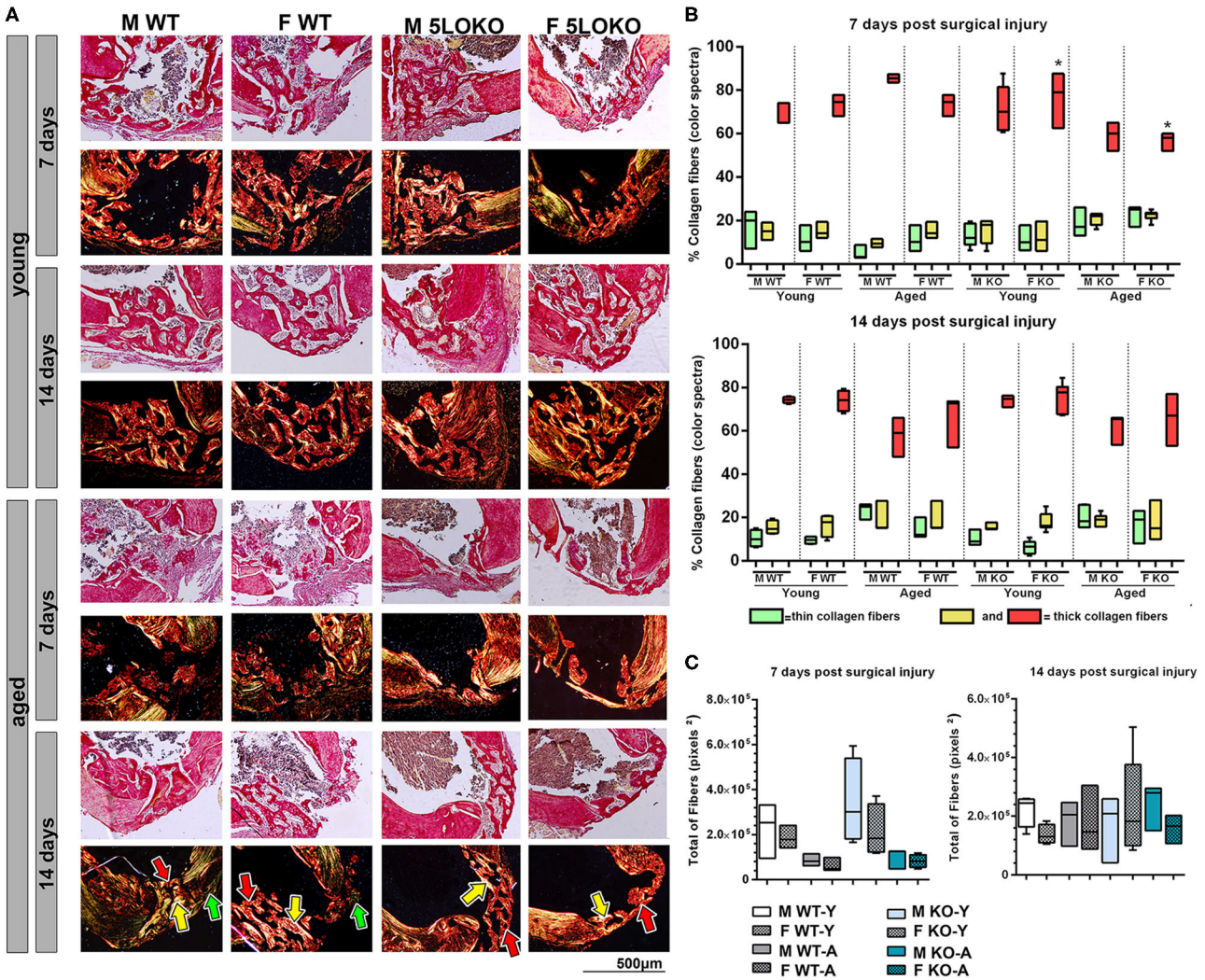

FIGURE 3 | Birefringence analysis of collagen fibers during bone healing in young and aged WT and 5LOKO mice. **(A)** Representative images of the birefringence analysis are seen under polarized light. In the last panel, 14 days post-surgery of aged animals, green, yellow and red fibers bundles are exemplified by arrows in each respective color. Green birefringence color indicates thin fibers, while yellow and red colors indicate thicker collagen fibers, as indicated by arrows and in the **(B)**. **(B)** Proportion of different thickness of collagen fibers (color spectrum) considering the total of collagen in each time point post-surgery (7 and 14 days post-surgery). Slides stained with Picrosirius red and captured at 10× were analyzed in Image-analysis software (AxioVision, v. 4.8, CarlZeiss). **(C)** Total area of collagen fibers (pixel^2) considering the sum of each spectrum of birefringence. Results are presented as mean and SD of pixels^2 for each color in the birefringence analysis. Symbol * indicates statistically significant difference between young female KO and aged female KO ($p < 0.05$).

of inflammatory cells in the granulation tissue of bone healing sites. They were also found in cells of the connective tissue of the periosteum and in the endomysium of VA muscle (**Figure 2B**). Results for negative immunolabeling of 5LO in 5LOKO mouse tissue are found in **Supplementary Figure 1**.

Micro CT and Birefringence Analysis for Bone Healing

The proportion of mineralized bone was measured in sites of bone defect by Micro CT (**Figures 2C–F**). The effect of age was observed in bone healing of all groups at 7 and 14 days post-surgery, with reduced BV/TV (%) in the site of bone defects (**Figures 2D,E**). No significant differences were found for genders and genotypes. Considering the quality and quantity of the new collagen fibers in sites of bone healing, aged female 5LOKO mice presented a significant increase in red spectra fibers 7 days post-surgery compared to young controls (**Figures 3A,B**). After 14 days post-injury, no significant differences were detected in the comparison among both young groups and aged groups at the same time point (**Figures 3A,B**). Despite the difference pointed out at day 7 post-surgery in relation to the red fibers, total collagenous content did not show any significant differences among the groups in both time points (**Figure 3C**).

Histopathological Analysis for Bone Healing

Our histopathological analyses showed that the bone injury site had been filled with woven bone in young female WT mice at day 7 post-surgery, characterized by a maturing process at day 14 post-surgery with osteoclastic resorption of the primary trabeculae and osteoblastic deposition of lamellar bone. In contrast, the aged female WT showed an intense leukocyte infiltration of granulation tissue in the bone defect area at day 7 post-surgery and the presence of primary bone at day 14 post-surgery, predominantly located at the defect walls. The effect of age was also observed in male WT mice. Young male WT mice presented with a similar healing process compared to the young female mice considering the same time points, while in the aged male WT mice, the defect was almost closed by maturing bone at day 14 post-surgery. In 5LOKO animals, female young mice presented a similar healing pattern to their male counterparts 7 days post-surgery, when the defect was filled with primary trabecular bone, and at day 14 post-surgery, when an advanced maturing process was observed by the presence of mature lamellar bone, similarly to the WT genotype. We noted that aged female 5LOKO mice healed the defect with a thin layer of maturing bone filling the bone defect at day 14 post-surgery, while in the aged 5LOKO male mice, it was mostly filled with mature trabecular bone. Comparing the genotypes, we observed major protective effects in aged female 5LOKO compared to aged WT mice, since aged 5LOKO presented an improved bone healing compared to aged WT females, with less inflammation at day 7 post-surgery a more mature bone at day 14 post-surgery in 5LOKO females (**Figure 4**).

Histopathological and Histomorphometric Analysis for Skeletal Muscle Healing

The effects of age were most detrimental regarding the histopathological description of aged WT mice, compared to the controls in both genders. At day 7 post-surgery, a key observation in the site of muscle injury of young WT male mice was the presence of loose connective tissue with eventual mononuclear leukocytes, while aged male WT mice showed a mixture of connective and adipose tissue infiltrated by neutrophils. The same pattern was observed in the group of WT female animals, except that at day 7 post-surgery, the young female mice presented dense connective tissue at the site of muscle injury. In the comparison of different genotypes, 5LOKO young animals, both male and female, showed clear differences as compared to WT mice especially at day 7 post-surgery, when muscle cells with centralized myonuclei could be seen surrounded by connective tissue. However, both male and female aged 5LOKO mice exhibited an injury site filled by connective tissue. Only at day 14 post-surgery, some muscle cells were observed in the injury site in young male and female WT mice, while in the aged mice the site of injury showed a disorganized connective tissue with adipose cells and focal mononuclear and neutrophil leukocytes infiltrate. Nonetheless, at the site of muscle injury in 5LOKO young males, numerous muscle fibers with centralized myonuclei could be seen at day 14 post-surgery. The key difference we found in the site of injury in the aged male 5LOKO animals was that a higher amount of connective tissue could be observed surrounding the muscle fibers. At this same period, female 5LOKO young mice also showed some muscle fibers with centralized myonuclei, but connective tissue was predominant. Muscle fibers with centralized myonuclei were also seen in the defect of 5LOKO aged female mice, but a loose connective tissue highly infiltrated by neutrophils was noted surrounding the muscle fibers (**Figure 5A**). Non-inflammed connective tissue was also observed among muscle fibers in adjacent areas of the injured sites of both WT and 5LOKO female and male aged mice (**Figure 5B**).

From the histomorphometric analysis, the percentage of muscle inflammation did not present significant differences at day 7 post-surgery, but was significantly increased in all aged animals at day 14 post-surgery, evidencing the detrimental effect of aging in muscle healing of both genotypes and genders. When comparing the 5LOKO male and female groups with their matched WT strains, it was detected that muscle inflammation decreased in both male and female aged 5LOKO at day 14 post-surgery. We also determined that aged female WT mice was the only group that showed a significant decrease in muscle fiber CSA when compared to their young WT group at day 14 post-surgery. We also identified an increase in the number of centralized myonuclei in aged 5KOLO female mice between day 7 and 14 post-surgery (**Table 3**).

Immunolabeling and Histomorphometric Analysis of Muscle and Bone Markers of Remodeling

Immunolabeling for both MuRF1 and MyoD was performed at day 7 post-surgery and positive pixel quantification was performed. MuRF1 was predominant in muscle nuclei (**Figure 6AA'**). The effect of age in MuRF1 immunolabeling (e.g., young male WT vs. aged male WT) was observed in both studied strains and genders, with a significant decrease in these markers for all aged animals (**Figure 6B**). No significant differences were obtained for MuRF1 among the genotypes and genders (**Figure 6B**). For MyoD, aged male and female WT mice showed a decreased immunolabeling for MyoD when compared to the matched gender young mice, but no effects of age were observed in 5LOKO mice (**Figure 6C**). No significant differences were found considering the effect of gender and genotype.

Dynamics of bone modeling/remodeling in bone-injured sites were evaluated with anti-Runx-2 and anti-TRAP antibodies (**Figure 7A**). Considering the effect of age for Runx-2, a significant decreased in the area density of positive cells were found in aged 5LOKO male mice compared to young controls. Considering the effect of genotype, both male and female 5LOKO young mice demonstrated an increase in the area density of Runx-2+ cells compared to their matched WT controls at day 7 post-surgery (**Figure 7B**). TRAP immunolabeling was significantly increased in the bone damage sites of female aged WT animals when compared to 5LOKO mice at day 14 post-surgery (**Figures 7A,C**).

DISCUSSION

Aging and inflammation can negatively affect the MSK system of male and females in a different manner and proportion (12,

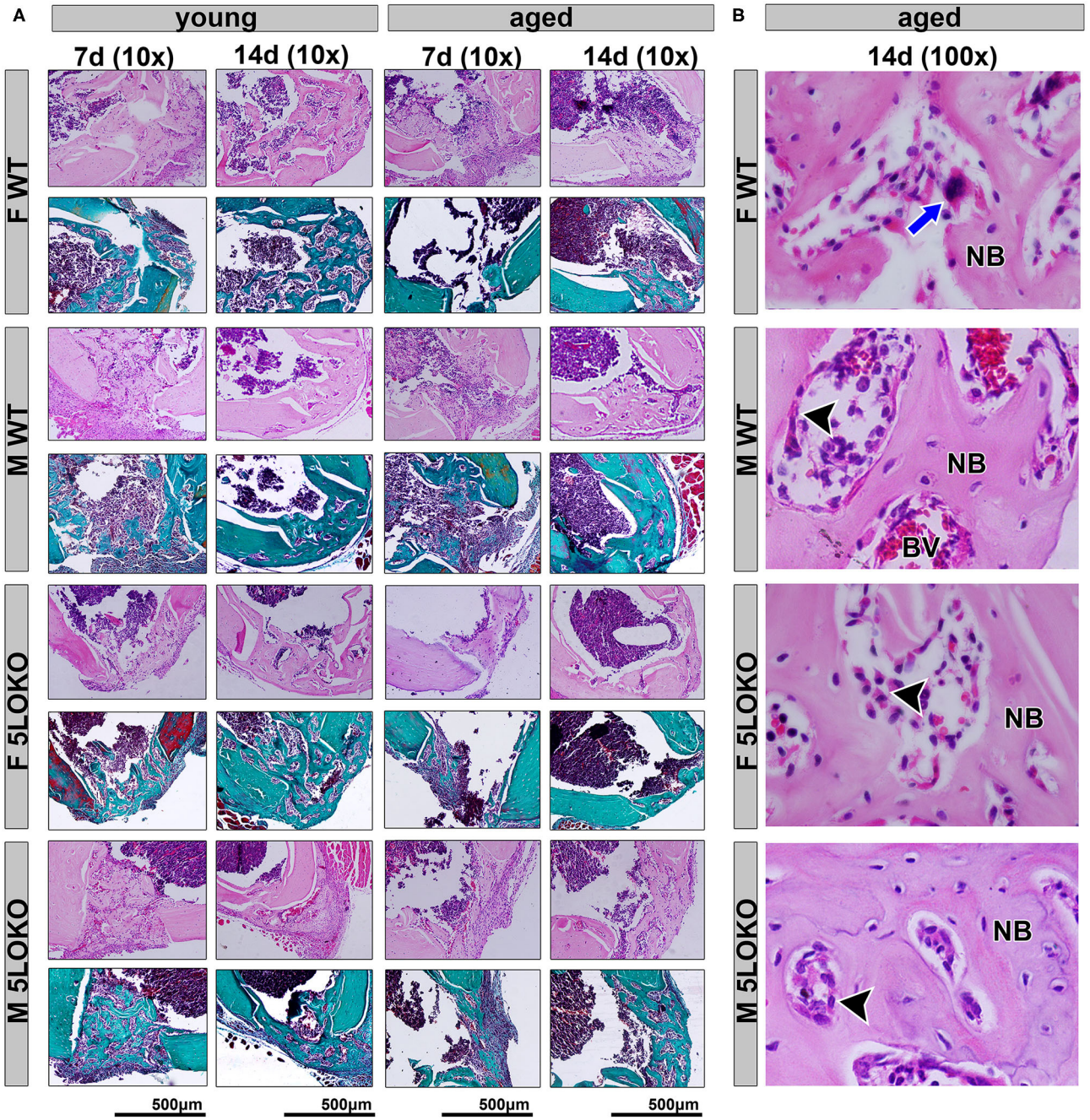

FIGURE 4 | Histopathological characterization of bone healing 7 and 14 days post-surgery: Male and female, young (3 months old), and aged (18 months old) 129/SvEv WT and 5LOKO mice underwent our surgical injury model, and bone specimens were evaluated at 7 and 14 days post-surgery. **(A)** Representative images from young and aged animals (WT and 5LOKO) stained with H&E and Goldner's Trichrome/Alcian Blue. Images were captured at 10× magnification. **(B)** H&E representative images from aged animals at 14 days were captured at 100× magnification. Newly formed bone (NB), Osteoclast (blue arrows), Osteoblast (arrowhead), Blood Vessel (BV).

64, 65). In our results for bone phenotyping, we found significant differences in macroscopic features comparing genders, with higher values (BW and/or RC length) for males compared to females in both genotypes. We observed major detrimental aging effects in female WT mice, with decreased in trabecular bone parameters (BV/TV and Tb.N) in L5 vertebral body compared to aged WT males.

Considering the genotype, aged 5LOKO mice also displayed a higher size compared to aged WT, but additional studies are necessary to observe the proportion of adipose tissue and

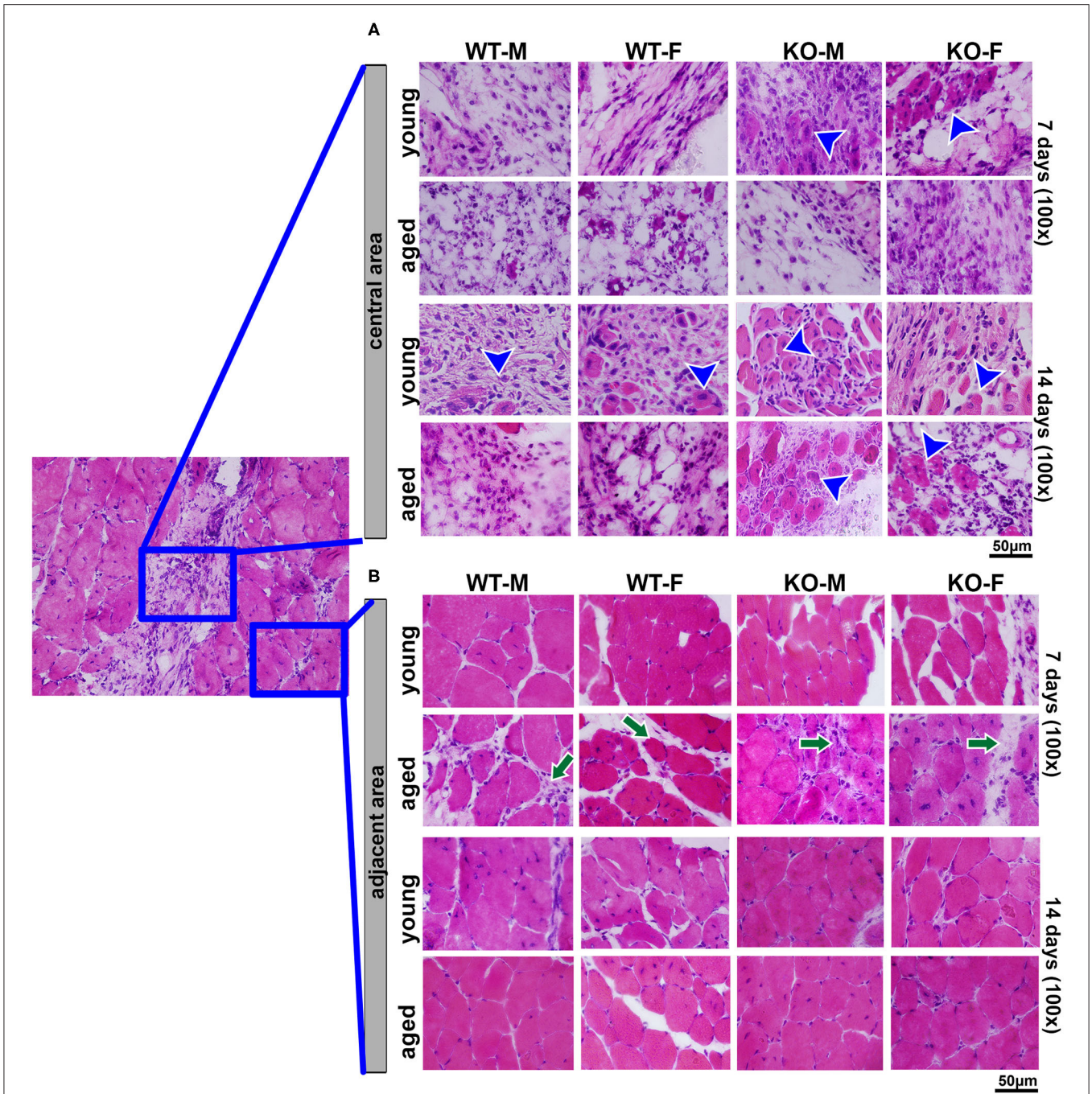

FIGURE 5 | Histopathological analysis during muscle healing in young and aged WT and 5LOKO mice: Male and female, young (3 months old), and aged (18 months old) 129/SvEv WT and 5LOKO mice underwent simultaneous surgical muscle and bone injury, and bone specimens were evaluated at days 7 and 14 post-surgery. **(A)** Representative images from the central area of muscle injury. Blue arrowheads indicate centralized myonuclei in the region of damage. **(B)** Representative images from the adjacent area of injury. Histological transversal sections were stained with H&E. Images were captured at 100× magnification. Green arrows indicate connective tissue among muscle fibers.

muscles in mice lacking 5LOKO. A previous study has associated the 5LO gene (also called Alox5) as a candidate gene for obesity and low bone mass when 5LOKO (in the C57Bl/6 background) is subjected under long-term treatment with high fat diet (containing 45% fat by kcal and 3.0g of AA). Briefly, in this previous study, male and female 5LOKO mice under this treatment presented decrease in Tb.N compared to WT (at final age of 16 weeks, or ∼ 4 months) (66). In our comparisons by

TABLE 3 | Histomorphometry of injured muscles in WT vs. 5LOKO mice.

Parameters	Groups/ Periods	Y WT ♂	Y WT ♀	A WT ♂	A WT ♀	Y KO ♂	Y KO ♀	A KO ♂	A KO ♀
Muscle Inflam (%)	7 days	16 ± 5^{a}	14 ± 2^{a}	14 ± 5^{a}	15 ± 10^{a}	11 ± 3^{a}	13 ± 4^{a}	16 ± 4^{a}	14 ± 7^{a}
	14 days	$14 \pm 6^{a*}$	$18 \pm 9^{a*}$	$43 \pm 8^{b*\#}$	$38 \pm 7^{b*\#}$	$10 \pm 4^{a*}$	$11 \pm 5^{a*}$	$25 \pm 7^{b*\#}$	$22 \pm 4^{b*\#}$
CSA (μm^2)	7 days	$1{,}088 \pm 661^{a}$	977 ± 474^{a}	894 ± 515^{a}	955 ± 424^{a}	$1{,}341 \pm 715^{a}$	1021 ± 516^{a}	994 ± 199^{a}	751 ± 290^{a}
	14 days	$1{,}298 \pm 724^{a}$	$1{,}127 \pm 446^{a*}$	739 ± 94^{a}	$505 \pm 101^{a*}$	$1{,}451 \pm 432^{a}$	$1{,}361 \pm 530^{a}$	869 ± 383^{a}	741 ± 319^{a}
Centralized Myonuclei (%)	7 days	24 ± 18^{a}	26 ± 20^{a}	20 ± 11^{a}	19 ± 10^{a}	37 ± 13^{a}	34 ± 8^{a}	26 ± 4^{a}	24 ± 10^{a}
	14 days	23 ± 16^{a}	28 ± 17^{a}	21 ± 18^{a}	25 ± 11^{a}	39 ± 17^{a}	37 ± 14^{a}	29 ± 15^{a}	37 ± 12^{b}

Results are presented as the means (±SD) for each parameter.

*In the comparison between lines, different letters (a vs. b) indicate significant difference for time points (7 vs. 14 days post-surgery) of the same group in each evaluated parameter ($p < 0.05$). In the comparison between columns, symbol * indicates comparison between columns: the effect of age (Y vs. A) in groups of same genotype and gender (e.g., Y ♀ WT vs. A ♀ WT); symbol # indicates the effect of different genotypes (WT vs. KO) in groups of same age and gender (e.g., Y ♀ WT vs. Y ♀ KO). Statistically significant differences are indicated between groups with equal symbols ($p < 0.05$). Y = 3 months; A = 18 months. No statistical significant differences were found between genders (♂ vs. ♀) in the comparison of the same genotype and age (e.g., Y ♀ WT vs. Y ♂ WT).*

microCT, we observed an increased bone quality in young and aged 5LOKO mice, compared to WT controls. It is also important to emphasize the differences in this particular methodology: 129Sv background, different ages (4 months for young and 18 months for aged mice) and a standard diet. In agreement, a previous study using radiology and bone histomorphometry has shown that both male and female 5LOKO mice, at 7 weeks age, from either 129Sv or mixed C57Bl/6x129sv background, have increased cortical bone compared with WT controls (36). Our study suggested that 5LO knockout protects against age-related bone loss in females, since the effect of aging on 5LOKO females was attenuated and they presented an increased BV/TV and Tb.N in femur and L5 compared to aged WT controls. It is also important to emphasize the differences in this particular methodology: different ages (4 months for young and 18 months for aged mice) and a standard diet.

It has been demonstrated that females have higher 5LO activity and/or higher LT production compared to males which could impact other pathways of the eicosanoid system (46). Using a unique customized approach of targeted lipidomics in gastrocnemius muscles of young and aged C57Bl/6 mice, a previous study has demonstrated lipid signaling is age- and gender-dependent (12). Our results from targeted lipidomics in gastrocnemius muscles demonstrate that the deletion of 5LO in mice significantly impact the profiling and quantities of lipid mediators in skeletal muscles of 5LOKO mice. In accordance, the endogenous levels of AA, EPA, and DHA were significantly decreased in aged female WT mice compared to aged female 5LOKO. Levels of 11,12-EET were significantly increased in aged 5LOKO male mice compared to aged WT mice. Aged male WT mice also presented a decrease in the levels of DHA and EPA compared to aged KO mice. Also, levels of PGE_2 were significantly increased in skeletal muscle of aged female KO mice compared to aged male KO mice. Considering the effect of gender, levels of PGE_2 were significantly increased while 11,12-EET was decreased in aged female KO mice, with significant differences compared to aged male KO mice. It is tempting to postulate that such combination of an elevation of PGE_2, which was demonstrated at nanomolar levels to enhance myogenic differentiation of C2C12 mouse muscle cells and increase *ex vivo* contractile force (3, 4), and the decreased levels in 11,12-EET could combine in the female 5LOKO to promote improved MSK healing. Although AA-derived lipid mediators are known to play a major pro-inflammatory role, PGE_2 can have a dual role, modulating both pro- and anti-inflammatory responses (67). Furthermore, PGE_2 can accelerate myogenesis differentiation (4) and induce osteogenesis (27, 30, 32). EPA and DHA are involved in the lipid-mediator profile switching during resolution of inflammation. In this context, EPA-derived mediators have a low pro-inflammatory potential, whereas DHA is a major source for the final anti-inflammatory products D-series resolvins and protectins required for inflammation resolution without fibrosis (68–70). EET acids, such as 11,12-EET, are generated by the activity of cytochrome p450 (CYP) enzymes on AA (71). 11,12-EET can play a modulatory role on COX-2 activity and attenuate the synthesis of PGE_2 during LPS-induced inflammatory response in rat monocytes (72). Other previous studies have shown that 11,12-EET can play anti-inflammatory activities by inhibition TNFα-induced VCAM-1, E-selectin, and ICAM-1 expression in endothelial cells (73). In our results, aged 5LOKO females presented an increased amount of PGE_2 compared to aged WT females, and conversely, aged 5LOKO females presented a decreased amount of 11,12-EET. An important consideration about the effects of LMs, myokines, osteokines, and secreted factors from bone-muscle and tissues in general is that we should apply accepted knowledge from endocrinology to this growing and fertile field of investigation.

To investigate the role of 5LO in the process of simultaneous bone and muscle healing, we developed a new surgical model of MSK injury in 5LOKO animals. Despite the importance of *in vivo* investigation for the comprehension of bone healing, previous rodent models of bone and muscle damage focus their attention exclusively on bone formation (14, 74), while the majority of studies of the on MSK healing addresses skeletal muscle (23, 75) or bone, but separately (24, 39). In our study, we performed a moderated simultaneous bone and muscle surgical damage, with a 1-mm diameter defect in muscle and a 0.5-mm diameter defect in the subjacent bone (**Figure 2A**), in order to avoid further surgical complications, such as femur fracture in aged animals. Our primary goal was to mirror human conditions

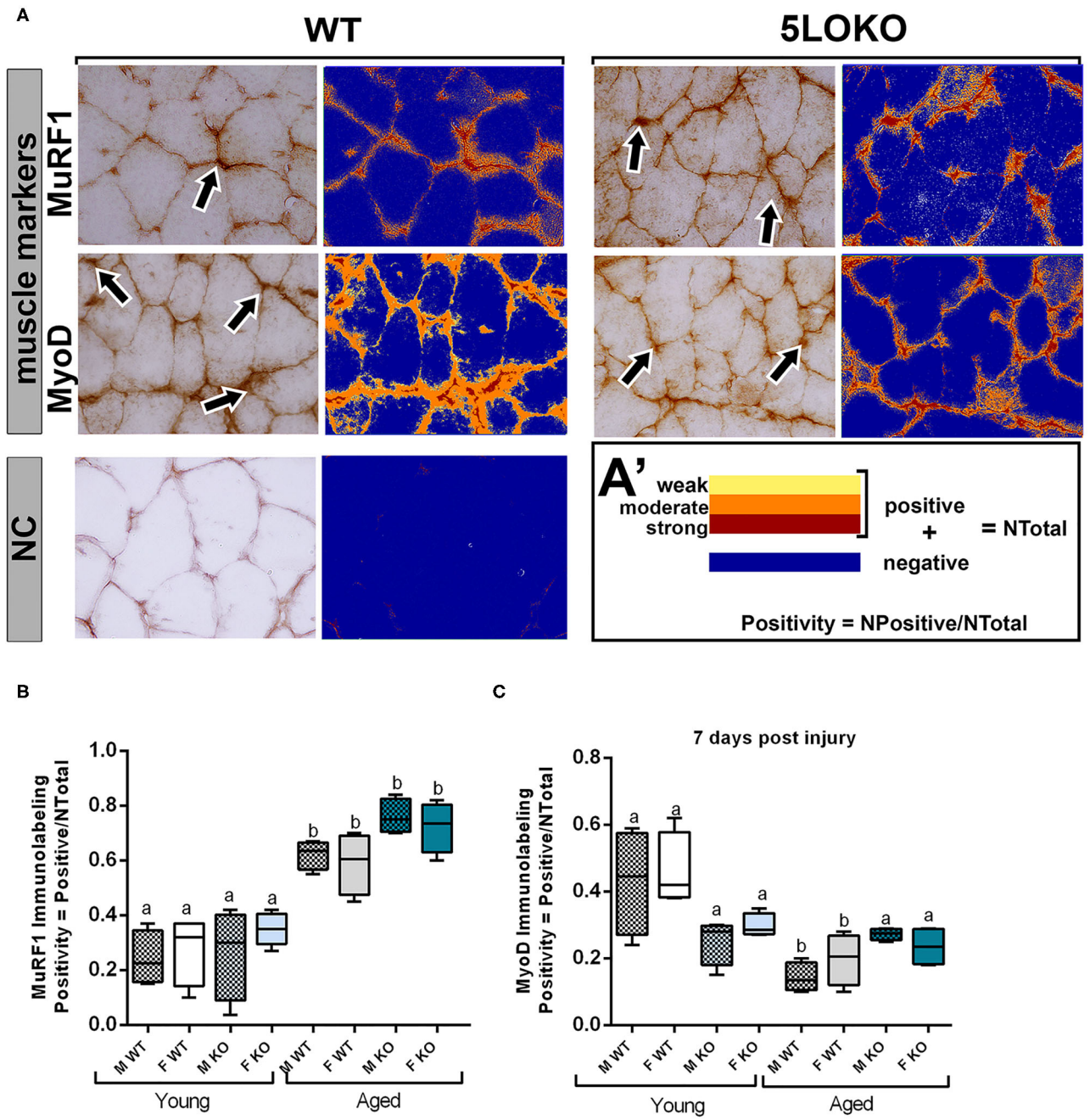

FIGURE 6 | Histomorphometric characterization and Immunolabeling of MuRF1 and MyoD in WT and 5LOKO mice: **(A)** Representative images for MuRF1 immunostaining and MyoD immunostaining (arrows) in male young SvEv WT mice at 7 days post-surgery. DAB was used for the antigen–antibody reaction. Muscle samples were left without counterstaining to be used for optical density quantification. **(A–A')** Positive Pixel quantification was performed by the software Aperio Image Scope v/ 12.3.3 (Leica Biosystems, Buffalo Grove, USA). Images were analyzed with algorithm Positive Pixel Count version 9 and are expressed as Positivity (number of positive pixels/number total). Negative controls (NC) were used for calibration and confirmation. **(B,C)** Results from positive pixel quantification for MuRF1 and MyoD were presented as means ± SD for each marker. Different letters indicate significant differences between young (3 months old) and aged (18 months old) mice for each sex and strain ($p < 0.05$).

of simultaneous tissue damage where recovery is feasible and to avoid any type of major catastrophic failure. Our results revealed a different pattern and timing in bone and muscle healing in WT mice. Interestingly, the bone defects of young male and female mice were completely filled with woven bone by day 7 post-surgery, and maturing by day 14 post-surgery, as

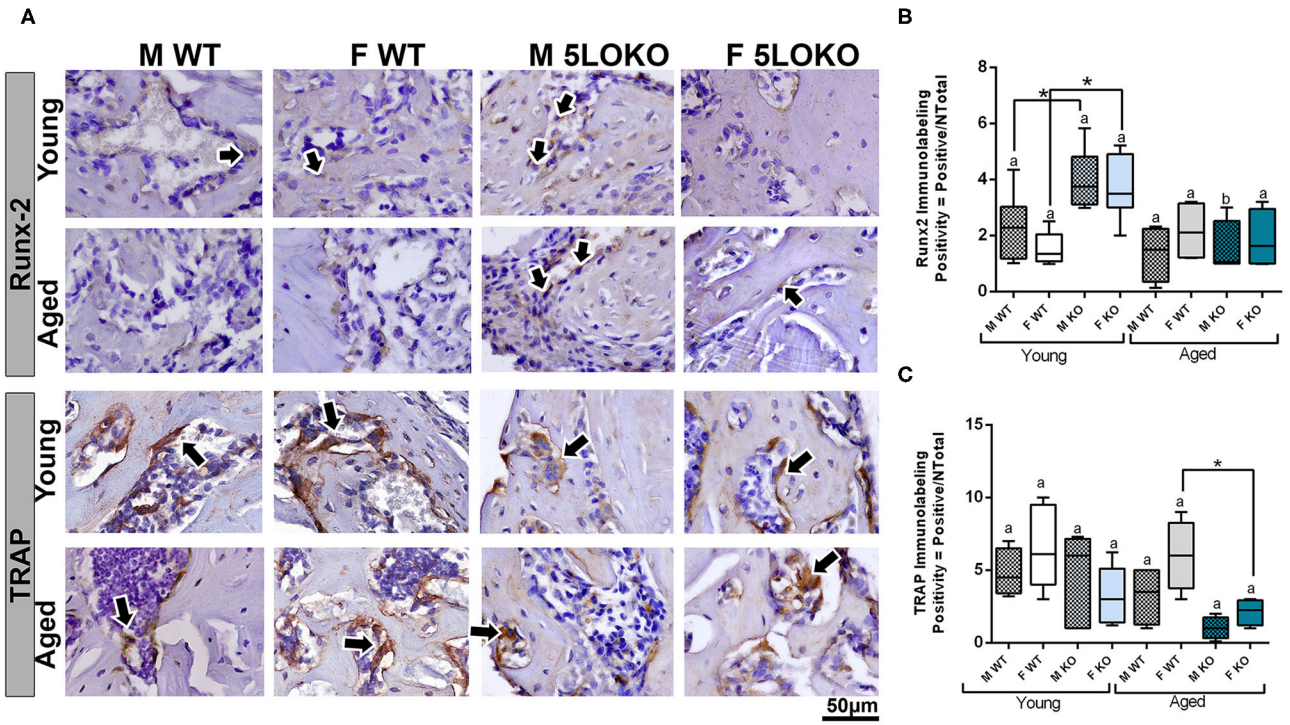

FIGURE 7 | Histomorphometric characterization and Immunolabeling of Runx-2 and TRAP in WT and 5LOKO mice: **(A)** Representative images for Runx2 immunostaining and TRAP immunostaining (arrows) of male and female, young (3 months old), and aged (18 months old) 129/SvEv WT and 5LOKO mice. Identification of antigen–antibody reaction was performed using DAB, counterstained with Mayer's hematoxylin. **(B,C)** Pixels quantification of Runx2 **(B)** and TRAP **(C)** was performed by the software Aperio Image Scope v/ 12.3.3 (Leica Biosystems, Buffalo Grove, USA). Images were analyzed with algorithm Positive Pixel Count version 9 and are expressed as positivity (umber of positive pixels/number total). Negative controls were used for calibration and confirmation. Results were presented as the mean and SD for each marker. Different letters indicate significant differences in between young (3 months old) and aged (18 months old) mice for each sex and strain ($p < 0.05$); symbol * indicates significant differences between WT vs. 5LOKO at the same age.

previously demonstrated for bone healing in the tibia of mice, but in a non-simultaneous muscle defect model (76). On the contrary, muscle healing is clearly delayed in the same animals. In the site of muscle injury of young male and female WT mice there was still connective tissue with eventual mononuclear leukocytes at 7 days post-surgery, with no significant changes in area density of inflammatory infiltrate at 14 days post-surgery. It is important to mention that bone has significant capacity for remodeling/regeneration regarding bone lining cells and/or osteoprogenitors lineages as stable cells, which are found in quiescent stage in physiologic conditions, but can undergo rapid proliferation in response to an injury (20). On the other hand, muscle fibers rapidly undergo degeneration after extensive damage (77, 78), and damaged muscle cells can still be found after 6 days in mouse models of surgical injury (17). Simultaneously and in response to the mediators released to the site of injury, satellite cells can proliferate and differentiate in new myotubes followed by upregulation of MyoD (7). This early process was observed during the first 7 days in mouse models of muscle injury (17, 78). MuRF1 was used in this study as a marker for fiber degeneration as a consequence of the surgical injury, as previously described (79), while MyoD was used as a marker of new fibers. MyoD induces the expression of muscle-specific genes in myoblasts and rapid cell proliferation in models of crush-induced injury, but it may be undetectable in newly formed myotubes (17, 18). We detected both MuRF1 and MyoD 7 days post-injury. An intriguing possibility is that both the degradation of muscle cells and the burst in satellite cell activity and myoblast proliferation could lead to a surge of myokines near the bone damage, which in turn helps bone to accelerate regeneration, and it occurs with muscle flaps, the skeletal muscle functions to assist in the faster recovery of bone tissue.

Other previous models of combined bone and muscle injury have been done using models of volumetric muscle loss injury, and they are more common rats. Usually combined bone and muscle injury models in rodents involve volumetric muscle-loss injuries, followed by endogenously healing osteotomy (80) or severe open fractures (81–83) and non-endogenously healing femur defects (84). Due to the nature of trauma and embryologic origin of femur, bone fractures generally heal throughout a cartilaginous callus formation, previous to woven bone deposition (80), while in our mouse model the bone healing was noted to be predominantly driven by intramembranous healing. Together, these previous studies have also evidenced impaired bone healing related with concomitant muscle trauma and increased levels of inflammatory markers in sites of injury

combined, compared to isolated injuries (80). When muscles are severely traumatized, the sustained inflammation diminishes mechanical bone strength and decreases mineralized matrix in the site of injury (81). Interestingly, these previous studies evaluated bone and muscle defects with or without combination, to permit additional comparisons and better determine the role of muscle in bone healing and *vice versa*. Comparatively, in our study we only produced combined injuries for primary study due the limited number of animals for studying 3 variables (two ages, genders, and genotypes). Additionally, our model does not aim to challenge bone and muscle healing with critical injuries, and it is performed in a very controlled manner, in order to avoid complications related to the surgical procedure. In this way, it is possible to investigate the MKS healing in compromised and fragile animals, such as aged mice.

Considering the advantages of our animal model, we decided by developing this combined defects in mice, considering a number of advantages and the cost–benefit related to mice when comparing with other rodents, such as the possibility to explore genetic approaches (e.g., 5LOKO mouse model utilized in this study); the reduced size compared to rats, which consequently reduces quantities of experimental drugs; and reduced experimental periods (85). In the context of bone–muscle crosstalk field, mouse is a suitable animal model for pharmacological and genetic interventions. Also, while timing of muscle and bone healing ranges from 4 to 12 weeks in rats, this type of MSK injury in mice was evaluated along 14 days. Even including longer time points, it might not exceed 4 weeks due the accelerated mice metabolism compared to other species. Comparing our model with preclinical orthopedic mice models (e.g., closed and open fractures), our study provides a surgical model that can be consistently reproduced with a rapid and simple surgery, minimal timing consuming, improving the animal recovery and avoid the risk of infections (86). On the other hand, since it is a non-critical muscle and bone defect, the present model does not challenge beyond physiological bone-muscle healing mechanisms in non-compromised animals (e.g., young adult and/or health). This is a major advantage in the context of normal aging.

During aging, the MSK system shows a decreased capacity for healing, associated with increased levels of inflammation (7, 11, 87). Our results revealed a significant impairment on both bone and muscle healing in aged mice when compared to the young controls. The fraction of newly formed (BV/TV, %) bone analyzed by microCT was significantly decreased in all aged mice, considering both genotypes and genders (**Figures 2C–F**). Despite increased amount of thicker collagen fibers in young 5LOKO females compared to aged controls, no major differences were found in the collagen content of bone matrix (**Figure 3A**). In skeletal muscles, a significant increase in inflammatory infiltrated in the VL muscles was noted at day 7 and 14 post-surgery (**Table 3**). CSA was also significantly decreased in aged WT females compared to the young controls, while aged 5LOKO females maintained the CSA compared to young 5LOKO females (**Table 3**). Additionally, while MuRF1 immunolabeling was increased in male and female aged mice (both genotypes), decreased immunolabeling for MyoD was observed to the matched young groups (for WT genotype), suggesting a reduced capacity for remodeling and regeneration along aging (**Figure 6**). These observations confirm a detrimental effect of aging in all groups, but with the attenuated effect of the aging effect in 5LOKO mice, especially in histopathological comparisons between aged WT vs. aged 5LOKO females.

After 7 days of surgical trauma, injured muscle, periosteum, and bone of WT mice were assessed for 5LO expression (**Figure 2B**). In support of 5LO roles on inflammation (25), 5LO positive cells were predominantly found in the leucocytes infiltrating bone and muscle healing sites, but also were found in the constitutive cells of connective tissue from the periosteum. In agreement with our findings, a mouse model of femur closed-fracture healing has demonstrated strong positive immunolabeling of 5LO in bone marrow leukocytes, periosteum, osteoclast, muscle interstitial cells, and chondrocytes until 7 days post-injury (27). Given the limitations of immunohistochemistry techniques, future molecular investigation is necessary to explore 5LO in injured and non-injured bone and muscle cells by other approaches.

No previous studies have addressed the effects of 5LO or its metabolites in combined MSK injuries. We next evaluated the influence of 5LO on bone and muscle healing in different ages and gender, by comparing WT vs. 5LOKO. Isolated evaluation of bone injury using bone fracture healing models have previously demonstrated that genetic deletion of 5LO in mice (28) or its pharmacological inhibition (39, 40) accelerate fracture callus formation in young male rodents. An important finding in our studies was that young female and male 5LOKO mice presented significantly increased Runx-2 expression in comparison with matched WT animals at day 7 post-injury, but with no significant differences in BV/TV of newly formed bone. Additionally, genetic deletion of 5LO in females led to attenuated inflammatory response after the simultaneous injury. While an intense inflammatory response in the bone-injury site of aged WT females 7 days post-injury with a delay in healing (14 days) was clear, aged 5LOKO presented less inflammatory infiltration and earlier mature bone (7 days) (**Figure 4**). TRAP-positive osteoclasts were also increased in aged females WT compared to 5LOKO at day 14 post-surgery (**Figure 7**), in agreement with the role of LTs on osteoclast formation in bone resorption and inflamed environments (34, 35). These results suggest that the 5LO signaling pathway may play a negative role on bone healing. Furthermore, young 5LOKO mice displayed advanced healing in VL muscle defects compared to WT mice, with centralized myonuclei surrounded by connective tissue while highly inflamed muscles could be seen in WT animals. Both male and female aged 5LOKO mice exhibited an injury site filled by connective tissue, while aged controls presented connective and adipose tissue (**Figure 4**). Interestingly, the number of positive MyoD cells was already decreased in young 5LOKO mice 7 days post-injury compared to WT (**Figure 6**), but the 5LOKO presented a higher amount of centralized myonuclei indicative of muscle regeneration by day 14 post-surgery (**Table 3**). Furthermore, MyoD positive cells were decreased in aged WT, compared to the young WT mice, but not in aged 5LOKO mice compared to young 5LOKO mice

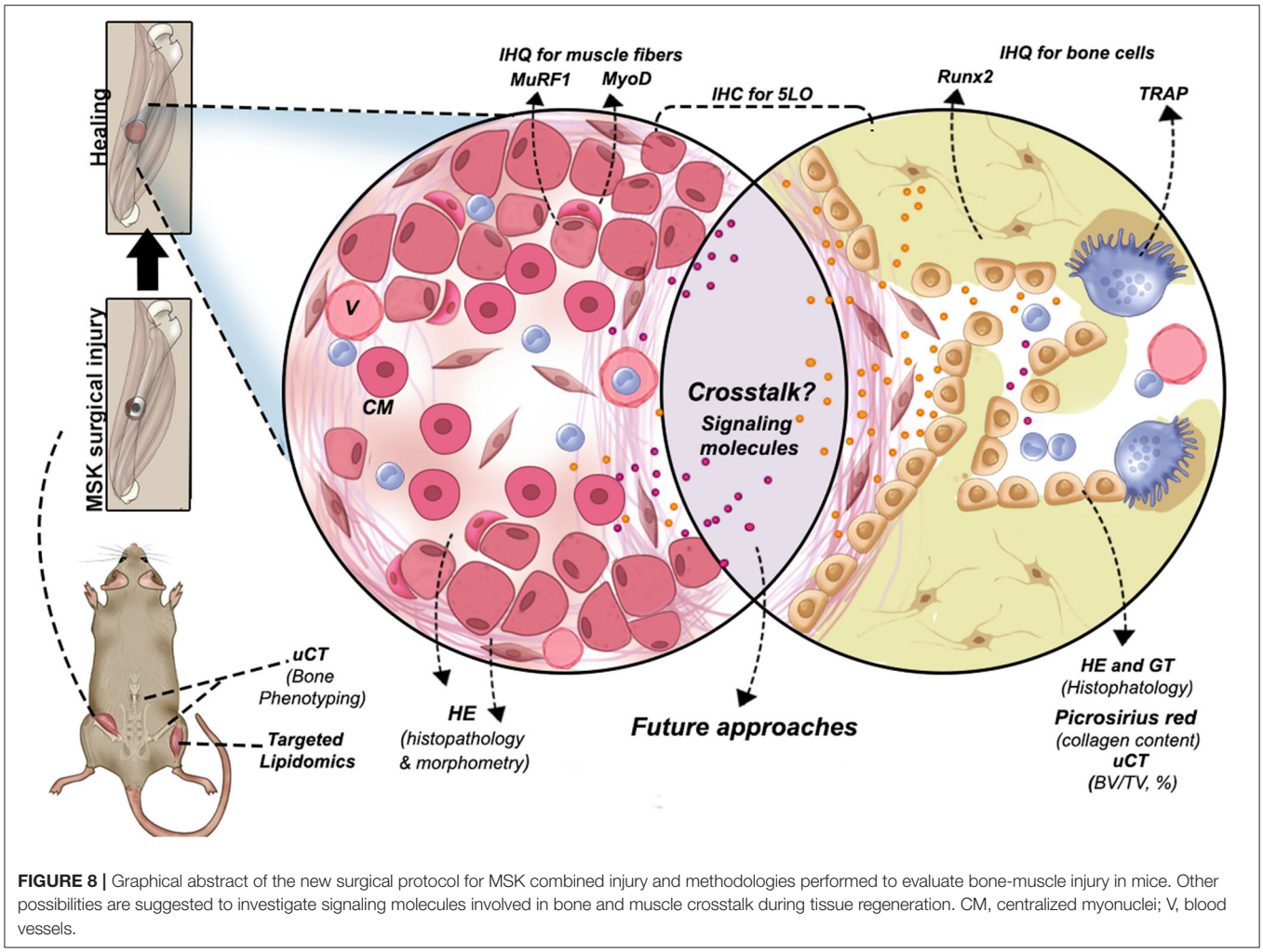

FIGURE 8 | Graphical abstract of the new surgical protocol for MSK combined injury and methodologies performed to evaluate bone-muscle injury in mice. Other possibilities are suggested to investigate signaling molecules involved in bone and muscle crosstalk during tissue regeneration. CM, centralized myonuclei; V, blood vessels.

(**Figure 6**). Future studies could conduct longitudinal studies to help further clarify the roles of 5LO in modulating the levels of muscle regulatory proteins.

In summary, our results demonstrate that 5LOKO mice present important differences in bone phenotyping and lipid profiling and quantification in skeletal muscles. Notably, the deletion of 5LO plays a protective role in bone of aged female 5LOKO mice and significantly impacts the capacity of MSK healing during aging. It is important to emphasize that this study presents some limitations, including detailed functional approaches and molecular quantification of 5LO and its products in both age and genders. However, our detailed lipidomic analyses, along with the bone phenotyping, allowed us to we hypothesize that changes found in skeletal muscle levels of LMs (particularly the intriguing aforementioned combination of elevation of PGE_2 and reduction of 11,12-EET) in 5LOKO may contribute to explain the improved MSK healing in these mice. Reinforcing this hypothesis, aged 5LOKO females mice presented increased amount of anti-inflammatory lipids (EPA and DHA) in comparison to aged WT females. We propose that future studies could investigate the levels of LMs in injured sites as well as expand the investigation on the role of 5LO in the MSK system, by using pharmacological and molecular-genetic approaches. The new model of simultaneous bone-muscle injury is pathophysiologically relevant for future studies in bone–muscle crosstalk, as well as suitable to advance the understanding of MSK healing during aging (**Figure 8**). We finally suggest the 5LO signaling pathway as a potential target for interventions against post-menopausal osteoporosis.

CONCLUSION

This study described a suitable mice model of simultaneous bone–muscle healing in order to contribute to the investigation of future bone–muscle crosstalk studies (**Figure 8**), revealing that simultaneous bone–muscle healing was influenced by aging, gender, and the 5LO pathway. In general, 5LOKO aged female mice presented improved healing capacity when compared to their matched WT groups. Our lipidomic analyses elicited intriguing possibilities for the roles of lipid signaling mediators in skeletal aging and MSK healing. Our studies suggest that

5LO plays a crucial role in both modulation and resolution of inflammation during aging.

DATA AVAILABILITY STATEMENT

The raw data supporting the conclusions of this article will be made available by the authors, without undue reservation.

ETHICS STATEMENT

The animal study was reviewed and approved by Ethic Committee on Animal Use of the Sagrado Coração University (CEUA/USC).

AUTHOR CONTRIBUTIONS

CB and MM contributed to the conception and design, the acquisition, analysis, and interpretation, drafted the manuscript, critically revised the manuscript, gave final approval, and agreed to be accountable for all aspects of work. MB contributed to the analysis and interpretation, drafted the manuscript, critically revised the manuscript, gave final approval, and agreed to be accountable for all aspects of work. MC, ACS, JS, VR, ALS, and ZW contributed to the acquisition, analysis, and interpretation of the manuscript, critically revised the manuscript, gave final approval, and agreed to be accountable for all aspects of work. JA contributed to the conception and design, the interpretation and critically revised the manuscript, gave final approval, and agreed to be accountable for all aspects of work. All authors contributed to the article and approved the submitted version.

FUNDING

This work was supported by grants #2018/08913-9 (CB and MM) from São Paulo Research Foundation (FAPESP). ACS was supported by FAPESP #2018/19406-0. MM was partially supported from FAPESP #13/04714-8. We are grateful for instrumentation support with microCT System from School Bauru of Dentistry, University of São Paulo and additional funding support from USP and UNESP. This work was supported in part by NIH-National Institutes of Aging (NIA) PO1 AG039355 (MB). CB and MB were partially supported by NIA R01AG056504 and R01AG060341 (MB), and the George W. and Hazel M. Jay and Evanston Research Endowments (MB). We are grateful for instrumentation support from Shimadzu Scientific Instruments, Inc.

ACKNOWLEDGMENTS

The authors would like to thank Dr. Lynda Bonewald for her contributions in discussing with the authors important concepts and ideas that helped improve the quality of the manuscript, Rafael Ortiz for his excellent technical assistance with Image Scope Software, and Matthew Fiedler for English revision.

SUPPLEMENTARY MATERIAL

The Supplementary Material for this article can be found online at: https://www.frontiersin.org/articles/10.3389/fendo.2020.00484/full#supplementary-material

REFERENCES

1. Brotto M, Bonewald L. Bone and muscle: interactions beyond mechanical. *Bone.* (2015) 80:109–14. doi: 10.1016/j.bone.2015.02.010
2. Brotto M, Johnson ML. Endocrine crosstalk between muscle and bone. *Curr Osteoporos Rep.* (2014) 12:135–41. doi: 10.1007/s11914-014-0209-0
3. Huang J, Romero-Suarez S, Lara N, Mo C, Kaja S, Brotto L, et al. Crosstalk between MLO-Y4 osteocytes and C2C12 muscle cells is mediated by the Wnt/beta-catenin pathway. *JBMR Plus.* (2017) 1:86–100. doi: 10.1002/jbm4.10015
4. Mo C, Zhao R, Vallejo J, Igwe O, Bonewald L, Wetmore L, et al. Prostaglandin E2 promotes proliferation of skeletal muscle myoblasts via EP4 receptor activation. *Cell Cycle.* (2015) 14:1507–16. doi: 10.1080/15384101.2015.1026520
5. Frontera WR, Ochala J. Skeletal muscle: a brief review of structure and function. *Calcif Tissue Int.* (2015) 96:183–95. doi: 10.1007/s00223-014-9915-y
6. Matsakas A, Patel K. Skeletal muscle fibre plasticity in response to selected environmental and physiological stimuli. *Histol Histopathol.* (2009) 24:611–29. doi: 10.14670/HH-24.611
7. Snijders T, Nederveen JP, McKay BR, Joanisse S, Verdijk LB, van Loon LJC. Satellite cells in human skeletal muscle plasticity. *Front Physiol.* (2015) 6:283. doi: 10.3389/fphys.2015.00283
8. Charge SB, Rudnicki MA. Cellular and molecular regulation of muscle regeneration. *Physiol Rev.* (2004) 84:209–38. doi: 10.1152/physrev.00019.2003
9. Howard EE, Pasiakos SM, Blesso CN, Fussell MA, Rodriguez NR. Divergent roles of inflammation in skeletal muscle recovery from injury. *Front Physiol.* (2020) 11:87. doi: 10.3389/fphys.2020.00087
10. Schaap LA, Pluijm SM, Deeg DJ, Harris TB, Kritchevsky SB, Newman AB, et al. Higher inflammatory marker levels in older persons: associations with 5-year change in muscle mass and muscle strength. *J Gerontol A Biol Sci Med Sci.* (2009) 64:1183–9. doi: 10.1093/gerona/glp097
11. Gibon E, Lu L, Goodman SB. Aging, inflammation, stem cells, and bone healing. *Stem Cell Res Ther.* (2016) 7:44. doi: 10.1186/s13287-016-0300-9
12. Wang Z, Bian L, Mo C, Kukula M, Schug KA, Brotto M. Targeted quantification of lipid mediators in skeletal muscles using restricted access media-based trap-and-elute liquid chromatography-mass spectrometry. *Anal Chim Acta.* (2017) 984:151–61. doi: 10.1016/j.aca.2017.07.024
13. Schindeler A, Liu R, Little DG. The contribution of different cell lineages to bone repair: exploring a role for muscle stem cells. *Differentiation.* (2009) 77:12–8. doi: 10.1016/j.diff.2008.09.007
14. Utvag SE, Iversen KB, Grundnes O, Reikeras O. Poor muscle coverage delays fracture healing in rats. *Acta Orthop Scand.* (2002) 73:471–4. doi: 10.1080/00016470216315
15. Liu R, Schindeler A, Little DG. The potential role of muscle in bone repair. *J Musculoskelet Neuronal Interact.* (2010) 10:71–6.
16. Chan JK, Harry L, Williams G, Nanchahal J. Soft-tissue reconstruction of open fractures of the lower limb: muscle versus fasciocutaneous flaps. *Plast Reconstr Surg.* (2012) 130:284e–95. doi: 10.1097/PRS.0b013e3182589e63
17. Fuchtbauer EM, Westphal H. MyoD and myogenin are coexpressed in regenerating skeletal muscle of the mouse. *Dev Dyn.* (1992) 193:34–9. doi: 10.1002/aja.1001930106
18. Weintraub H, Davis R, Tapscott S, Thayer M, Krause M, Benezra R, et al. The myoD gene family: nodal point during specification of the muscle cell lineage. *Science.* (1991) 251:761–6. doi: 10.1126/science.1846704

19. Koyama S, Hata S, Witt CC, Ono Y, Lerche S, Ojima K, et al. Muscle RING-finger protein-1 (MuRF1) as a connector of muscle energy metabolism and protein synthesis. *J Mol Biol.* (2008) 376:1224–36. doi: 10.1016/j.jmb.2007.11.049
20. Florencio-Silva R, Sasso GR, Sasso-Cerri E, Simoes MJ, Cerri PS. Biology of bone tissue: structure, function, and factors that influence bone cells. *Biomed Res Int.* (2015) 2015:421746. doi: 10.1155/2015/421746
21. Biguetti CC, Vieira AE, Cavalla F, Fonseca AC, Colavite PM, Silva RM, et al. CCR2 contributes to F4/80+ cells migration along intramembranous bone healing in maxilla, but its deficiency does not critically affect the healing outcome. *Front Immunol.* (2018) 9:1804. doi: 10.3389/fimmu.2018.01804
22. Gharaibeh B, Chun-Lansinger Y, Hagen T, Ingham SJ, Wright V, Fu F, et al. Biological approaches to improve skeletal muscle healing after injury and disease. *Birth Defects Res C Embryo Today.* (2012) 96:82–94. doi: 10.1002/bdrc.21005
23. Kim JT, Kasukonis B, Dunlap G, Perry R, Washington T, Wolchok JC. Regenerative repair of volumetric muscle loss injury is sensitive to age. *Tissue Eng A.* (2020) 26:3–14. doi: 10.1089/ten.tea.2019.0034
24. Loi F, Cordova LA, Pajarinen J, Lin TH, Yao Z, Goodman SB. Inflammation, fracture and bone repair. *Bone.* (2016) 86:19–30. doi: 10.1016/j.bone.2016.02.020
25. Bennett M, Gilroy DW. Lipid mediators in inflammation. *Microbiol Spectr.* (2016) 4:343–6. doi: 10.1128/microbiolspec.MCHD-0035-2016
26. Radmark O, Werz O, Steinhilber D, Samuelsson B. 5-Lipoxygenase, a key enzyme for leukotriene biosynthesis in health and disease. *Biochim Biophys Acta.* (2015) 1851:331–9. doi: 10.1016/j.bbalip.2014.08.012
27. Lin HN, O'Connor JP. Immunohistochemical localization of key arachidonic acid metabolism enzymes during fracture healing in mice. *PLoS ONE.* (2014) 9:e88423. doi: 10.1371/journal.pone.0088423
28. Manigrasso MB, O'Connor JP. Accelerated fracture healing in mice lacking the 5-lipoxygenase gene. *Acta Orthop.* (2010) 81:748–55. doi: 10.3109/17453674.2010.533931
29. Martel-Pelletier J, Mineau F, Fahmi H, Laufer S, Reboul P, Boileau C, et al. Regulation of the expression of 5-lipoxygenase-activating protein/5-lipoxygenase and the synthesis of leukotriene B(4) in osteoarthritic chondrocytes: role of transforming growth factor beta and eicosanoids. *Arthritis Rheum.* (2004) 50:3925–33. doi: 10.1002/art.20632
30. O'Connor JP, Manigrasso MB, Kim BD, Subramanian S. Fracture healing and lipid mediators. *Bonekey Rep.* (2014) 3:517. doi: 10.1038/bonekey.2014.12
31. Tagliaferri C, Wittrant Y, Davicco MJ, Walrand S, Coxam V. Muscle and bone, two interconnected tissues. *Ageing Res Rev.* (2015) 21:55–70. doi: 10.1016/j.arr.2015.03.002
32. Simon AM, O'Connor JP. Dose and time-dependent effects of cyclooxygenase-2 inhibition on fracture-healing. *J Bone Joint Surg Am.* (2007) 89:500–11. doi: 10.2106/JBJS.F.00127
33. Xie C, Liang B, Xue M, Lin AS, Loiselle A, Schwarz EM, et al. Rescue of impaired fracture healing in COX-2-/- mice via activation of prostaglandin E2 receptor subtype 4. *Am J Pathol.* (2009) 175:772–85. doi: 10.2353/ajpath.2009.081099
34. Garcia C, Boyce BF, Gilles J, Dallas M, Qiao M, Mundy GR, et al. Leukotriene B4 stimulates osteoclastic bone resorption both *in vitro* and *in vivo*. *J Bone Miner Res.* (1996) 11:1619–27. doi: 10.1002/jbmr.5650111105
35. Moura AP, Taddei SR, Queiroz-Junior CM, Madeira MF, Rodrigues LF, Garlet GP, et al. The relevance of leukotrienes for bone resorption induced by mechanical loading. *Bone.* (2014) 69:133–8. doi: 10.1016/j.bone.2014.09.019
36. Bonewald LF, Flynn M, Qiao M, Dallas MR, Mundy GR, Boyce BF. Mice lacking 5-lipoxygenase have increased cortical bone thickness. *Adv Exp Med Biol.* (1997) 433:299–302. doi: 10.1007/978-1-4899-1810-9_63
37. Traianedes K, Dallas MR, Garrett IR, Mundy GR, Bonewald L. 5-Lipoxygenase metabolites inhibit bone formation *in vitro*. *Endocrinology.* (1998) 139:3178–84. doi: 10.1210/endo.139.7.6115
38. Lopes DEM, Jabr CL, Dejani NN, Saraiva AC, Aquino SG, Medeiros A, et al. Inhibition of 5-Lipoxygenase (5-Lo) attenuates inflammation and bone resorption in Lipopolysaccharide (Lps)-induced periodontal disease. *J Periodontol.* (2017) 91:1–18. doi: 10.1902/jop.2017.170210
39. Cottrell JA, O'Connor JP. Pharmacological inhibition of 5-lipoxygenase accelerates and enhances fracture-healing. *J Bone Joint Surg Am.* (2009) 91:2653–65. doi: 10.2106/JBJS.H.01844
40. Wixted JJ, Fanning PJ, Gaur T, O'Connell SL, Silva J, Mason-Savas A, et al. Enhanced fracture repair by leukotriene antagonism is characterized by increased chondrocyte proliferation and early bone formation: a novel role of the cysteinyl LT-1 receptor. *J Cell Physiol.* (2009) 221:31–9. doi: 10.1002/jcp.21809
41. Sun R, Ba X, Cui L, Xue Y, Zeng X. Leukotriene B4 regulates proliferation and differentiation of cultured rat myoblasts via the BLT1 pathway. *Mol Cells.* (2009) 27:403–8. doi: 10.1007/s10059-009-0053-8
42. Zuo L, Christofi FL, Wright VP, Bao S, Clanton TL. Lipoxygenase-dependent superoxide release in skeletal muscle. *J Appl Physiol.* (1985) 97:661–8. doi: 10.1152/japplphysiol.00096.2004
43. Loell I, Alemo Munters L, Pandya J, Zong M, Alexanderson H, Fasth AE, et al. Activated LTB4 pathway in muscle tissue of patients with polymyositis or dermatomyositis. *Ann Rheum Dis.* (2013) 72:293–9. doi: 10.1136/annrheumdis-2012-201294
44. Pergola C, Dodt G, Rossi A, Neunhoeffer E, Lawrenz B, Northoff H, et al. ERK-mediated regulation of leukotriene biosynthesis by androgens: a molecular basis for gender differences in inflammation and asthma. *Proc Natl Acad Sci USA.* (2008) 105:19881–86. doi: 10.1073/pnas.0809120105
45. Pergola C, Rogge A, Dodt G, Northoff H, Weinigel C, Barz D, et al. Testosterone suppresses phospholipase D, causing sex differences in leukotriene biosynthesis in human monocytes. *FASEB J.* (2011) 25:3377–87. doi: 10.1096/fj.11-182758
46. Pace S, Pergola C, Dehm F, Rossi A, Gerstmeier J, Troisi F, et al. Androgen-mediated sex bias impairs efficiency of leukotriene biosynthesis inhibitors in males. *J Clin Invest.* (2017) 127:3167–76. doi: 10.1172/JCI92885
47. Weinblatt ME, Kremer JM, Coblyn JS, Helfgott S, Maier AL, Petrillo G, et al. Zileuton, a 5-lipoxygenase inhibitor in rheumatoid arthritis. *J Rheumatol.* (1992) 19:1537–41.
48. Savari S, Chandrashekar NK, Osman J, Douglas D, Bellamkonda K, Jonsson G, et al. Cysteinyl leukotriene 1 receptor influences intestinal polyp incidence in a gender-specific manner in the ApcMin/+ mouse model. *Carcinogenesis.* (2016) 37:491–9. doi: 10.1093/carcin/bgw031
49. Pace S, Sautebin L, Werz O. Sex-biased eicosanoid biology: impact for sex differences in inflammation and consequences for pharmacotherapy. *Biochem Pharmacol.* (2017) 145:1–11. doi: 10.1016/j.bcp.2017.06.128
50. Byers SL, Wiles MV, Dunn SL, Taft RA. Mouse estrous cycle identification tool and images. *PLoS ONE.* (2012) 7:e35538. doi: 10.1371/journal.pone.0035538
51. Cora MC, Kooistra L, Travlos G. Vaginal cytology of the laboratory rat and mouse: review and criteria for the staging of the estrous cycle using stained vaginal smears. *Toxicol Pathol.* (2015) 43:776–93. doi: 10.1177/0192623315570339
52. Kilkenny C, Browne WJ, Cuthi I, Emerson M, Altman DG. Improving bioscience research reporting: the ARRIVE guidelines for reporting animal research. *Vet Clin Pathol.* (2012) 41:27–31. doi: 10.1111/j.1939-165X.2012.00418.x
53. Biguetti CC, De Oliva AH, Healy K, Mahmoud RH, Custodio IDC, Constantino DH, et al. Medication-related osteonecrosis of the jaws after tooth extraction in senescent female mice treated with zoledronic acid: microtomographic, histological and immunohistochemical characterization. *PLoS ONE.* (2019) 14:e0214173. doi: 10.1371/journal.pone.0214173
54. Bouxsein ML, Boyd SK, Christiansen BA, Guldberg RE, Jepsen KJ, Muller R. Guidelines for assessment of bone microstructure in rodents using micro-computed tomography. *J Bone Miner Res.* (2010) 25:1468–86. doi: 10.1002/jbmr.141
55. Gao C, Chen BP, Sullivan MB, Hui J, Ouellet JA, Henderson JE, et al. Micro CT analysis of spine architecture in a mouse model of scoliosis. *Front Endocrinol.* (2015) 6:38. doi: 10.3389/fendo.2015.00038
56. Gingery A, Subramaniam M, Pitel KS, Reese JM, Cicek M, Lindenmaier LB, et al. The effects of a novel hormonal breast cancer therapy, endoxifen, on the mouse skeleton. *PLoS ONE.* (2014) 9:e98219. doi: 10.1371/journal.pone.0098219
57. Sheng ZF, Xu K, Ma YL, Liu JH, Dai RC, Zhang YH, et al. Zoledronate reverses mandibular bone loss in osteoprotegerin-deficient mice. *Osteoporos Int.* (2009) 20:151–9. doi: 10.1007/s00198-008-0640-0
58. Thompson J, Mendoza F, Tan E, Bertol JW, Gaggar AS, Jun G, et al. A cleft lip and palate gene, Irf6, is involved in osteoblast differentiation of craniofacial bone. *Dev Dyn.* (2019) 248:221–32. doi: 10.1002/dvdy.13

59. Dare LR, Dias DV, Rosa Junior GM, Bueno CR, Buchaim RL, Rodrigues Ade C, et al. Effect of beta-hydroxy-beta-methylbutyrate in masticatory muscles of rats. *J Anat*. (2015) 226:40–6. doi: 10.1111/joa.12256
60. Krag TO, Pinos T, Nielsen TL, Brull A, Andreu AL, Vissing J. Differential muscle involvement in mice and humans affected by McArdle disease. *J Neuropathol Exp Neurol.* (2016) 75:441–54. doi: 10.1093/jnen/nlw018
61. Biguetti CC, Cavalla F, Silveira EV, Tabanez AP, Francisconi CF, Taga R, et al. HGMB1 and RAGE as essential components of Ti osseointegration process in Mice. *Front Immunol.* (2019) 10:709. doi: 10.3389/fimmu.2019.00709
62. Fonseca FP, de Andrade BA, Rangel AL, Della Coletta R, Lopes MA, de Almeida OP, et al. Tissue microarray is a reliable method for immunohistochemical analysis of pleomorphic adenoma. *Oral Surg Oral Med Oral Pathol Oral Radiol.* (2014) 117:81–8 doi: 10.1016/j.oooo.2013.08.029
63. Motulsky HJ, Brown RE. Detecting outliers when fitting data with nonlinear regression – a new method based on robust nonlinear regression and the false discovery rate. *BMC Bioinformatics.* (2006) 7:123. doi: 10.1186/1471-2105-7-123
64. Elis S, Courtland HW, Wu Y, Rosen CJ, Sun H, Jepsen KJ, et al. Elevated serum levels of IGF-1 are sufficient to establish normal body size and skeletal properties even in the absence of tissue IGF-1. *J Bone Miner Res.* (2010) 25:1257–66. doi: 10.1002/jbmr.20
65. Elis S, Wu Y, Courtland HW, Sun H, Rosen CJ, Adamo ML, et al. Increased serum IGF-1 levels protect the musculoskeletal system but are associated with elevated oxidative stress markers and increased mortality independent of tissue igf1 gene expression. *Aging Cell.* (2011) 10:547–50. doi: 10.1111/j.1474-9726.2011.00683.x
66. Le P, Kawai M, Bornstein S, DeMambro VE, Horowitz MC, Rosen CJ. A high-fat diet induces bone loss in mice lacking the Alox5 gene. *Endocrinology.* (2012) 153:6–16. doi: 10.1210/en.2011-0082
67. Vachier I, Chanez P, Bonnans C, Godard P, Bousquet J, Chavis C. Endogenous anti-inflammatory mediators from arachidonate in human neutrophils. *Biochem Biophys Res Commun.* (2002) 290:219–24. doi: 10.1006/bbrc.2001.6155
68. Calder PC. Omega-3 fatty acids and inflammatory processes. *Nutrients.* (2010) 2:355–74. doi: 10.3390/nu2030355
69. Levy BD, Clish CB, Schmidt B, Gronert K, Serhan CN. Lipid mediator class switching during acute inflammation: signals in resolution. *Nat Immunol.* (2001) 2:612–9. doi: 10.1038/89759
70. Serhan CN. Pro-resolving lipid mediators are leads for resolution physiology. *Nature.* (2014) 510:92–101. doi: 10.1038/nature13479
71. Thomson SJ, Askari A, Bishop-Bailey D. Anti-inflammatory effects of epoxyeicosatrienoic acids. *Int J Vasc Med.* (2012) 2012:605101. doi: 10.1155/2012/605101
72. Kozak W, Aronoff DM, Boutaud O, Kozak A. 11,12-epoxyeicosatrienoic acid attenuates synthesis of prostaglandin E2 in rat monocytes stimulated with lipopolysaccharide. *Exp Biol Med (Maywood).* (2003) 228:786–94. doi: 10.1177/15353702-0322807-03
73. Node K, Huo Y, Ruan X, Yang B, Spiecker M, Ley K, et al. Anti-inflammatory properties of cytochrome P450 epoxygenase-derived eicosanoids. *Science.* (1999) 285:1276–9. doi: 10.1126/science.285.5431.1276
74. Takikawa S, Matsui N, Kokubu T, Tsunoda M, Fujioka H, Mizuno K, et al. Low-intensity pulsed ultrasound initiates bone healing in rat nonunion fracture model. *J Ultrasound Med.* (2001) 20:197–205. doi: 10.7863/jum.2001.20.3.197
75. Kim JT, Kasukonis BM, Brown LA, Washington TA, Wolchok JC. Recovery from volumetric muscle loss injury: a comparison between young and aged rats. *Exp Gerontol.* (2016) 83:37–46. doi: 10.1016/j.exger.2016.07.008
76. Mouraret S, Hunter DJ, Bardet C, Brunski JB, Bouchard P, Helms JA. A pre-clinical murine model of oral implant osseointegration. *Bone.* (2014) 58:177–84. doi: 10.1016/j.bone.2013.07.021
77. Zhao W, Lu H, Wang X, Ransohoff RM, Zhou L. CX3CR1 deficiency delays acute skeletal muscle injury repair by impairing macrophage functions. *FASEB J.* (2016) 30:380–93. doi: 10.1096/fj.14-270090
78. Wang X, Zhao W, Ransohoff RM, Zhou L. Infiltrating macrophages are broadly activated at the early stage to support acute skeletal muscle injury repair. *J Neuroimmunol.* (2018) 317:55–66. doi: 10.1016/j.jneuroim.2018.01.004
79. Moriscot AS, Baptista IL, Bogomolovas J, Witt C, Hirner S, Granzier H, et al. MuRF1 is a muscle fiber-type II associated factor and together with MuRF2 regulates type-II fiber trophicity and maintenance. *J Struct Biol.* (2010) 170:344–53. doi: 10.1016/j.jsb.2010.02.001
80. Hurtgen BJ, Henderson BEP, Ward CL, Goldman SM, Garg K, McKinley T, et al. Impairment of early fracture healing by skeletal muscle trauma is restored by FK506. *BMC Musculosk Disord.* (2017) 18:253. doi: 10.1186/s12891-017-1617-y
81. Hurtgen BJ, Ward Cl, Garg K, Pollot BE, Goldman SM, McKinley TO, et al. Severe muscle trauma triggers heightened and prolonged local musculoskeletal inflammation and impairs adjacent tibia fracture healing. *J Musculoskelet Neuronal Interact.* (2016) 16:122–34.
82. Pollot BE, Goldman SM, Wenke JC, Corona BT. Decellularized extracellular matrix repair of volumetric muscle loss injury impairs adjacent bone healing in a rat model of complex musculoskeletal trauma. *J Trauma Acute Care Surg.* (2016) 81:S184–90. doi: 10.1097/TA.0000000000001212
83. Utvåg SE, Grundnes O, Rindal DB, Reikerås O. Influence of extensive muscle injury on fracture healing in rat tibia. *J Orthop Trauma.* (2003) 17:430–5. doi: 10.1097/00005131-200307000-00007
84. Willett NJ, Li MA, Uhrig BA, Boerckel JD, Huebsch N, Lundgren TL, et al. Attenuated human bone morphogenetic protein-2-mediated bone regeneration in a rat model of composite bone and muscle injury. *Tissue Eng Part C Methods.* (2013) 19:316–25. doi: 10.1089/ten.tec.2012.0290
85. Vandamme TF. Use of rodents as models of human diseases. *J Pharm Bioallied Sci.* (2014) 6:2–9. doi: 10.4103/0975-7406.124301
86. Schindeler A, Mills RJ, Bobyn JD. Little DG preclinical models for orthopedic research and bone tissue engineering. *J Orthop Res.* (2018) 36:832–40. doi: 10.1002/jor.23824
87. Cholok D, Lee E, Lisiecki J, Agarwal S, Loder S, Ranganathan K, et al. Traumatic muscle fibrosis: from pathway to prevention. *J Trauma Acute Care Surg.* (2017) 82:174–84. doi: 10.1097/TA.0000000000001290

Conflict of Interest: The authors declare that the research was conducted in the absence of any commercial or financial relationships that could be construed as a potential conflict of interest.

frontiers | Frontiers in Endocrinology

ORIGINAL RESEARCH
published: 10 May 2022
doi: 10.3389/fendo.2022.844218

Identification of a Potential MiRNA–mRNA Regulatory Network for Osteoporosis by Using Bioinformatics Methods: A Retrospective Study Based on the Gene Expression Omnibus Database

Shi Lin[1], *Jianjun Wu*[1], *Baixing Chen*[2], *Shaoshuo Li*[3] *and Hongxing Huang*[4]*

[1] The Third Clinical Medical College of Guangzhou University of Chinese Medicine, Guangzhou University of Chinese Medicine, Guangdong, China, [2] Department of Development and Regeneration, KU Leuven, University of Leuven, Leuven, Belgium, [3] Laboratory of New Techniques of Restoration and Reconstruction of Orthopedics and Traumatology, Nanjing University of Chinese Medicine, Jiangsu, China, [4] Department of Orthopaedics, The Third Affiliated Hospital of Guangzhou University of Chinese Medicine, Guangdong, China

OPEN ACCESS

Edited by:
Marco Invernizzi,
University of Eastern Piedmont, Italy

Reviewed by:
Lorenzo Lippi,
University of Eastern Piedmont, Italy
Claudio Curci,
Azienda Socio Sanitaria Territoriale di Mantova, Italy

***Correspondence:**
Hongxing Huang
hhx@gzucm.edu.cn

Specialty section:
This article was submitted to Bone Research, a section of the journal Frontiers in Endocrinology

Received: *27 December 2021*
Accepted: *04 April 2022*
Published: *10 May 2022*

Citation:
Lin S, Wu J, Chen B, Li S and Huang H (2022) Identification of a Potential MiRNA–mRNA Regulatory Network for Osteoporosis by Using Bioinformatics Methods: A Retrospective Study Based on the Gene Expression Omnibus Database. Front. Endocrinol. 13:844218. doi: 10.3389/fendo.2022.844218

Introduction: As a systemic skeletal dysfunction, osteoporosis (OP) is characterized by low bone mass, impairment of bone microstructure, and a high global morbidity rate. There is increasing evidence that microRNAs (miRNAs) are associated with the pathogenesis of OP. Weighted gene co-expression network analysis (WGCNA) is a systematic method for identifying clinically relevant genes involved in disease pathogenesis. However, the study of the miRNA–messenger RNA (mRNA) regulatory network in combination with WGCNA in OP is still lacking.

Methods: The GSE93883 and GSE7158 microarray datasets were downloaded from the Gene Expression Omnibus (GEO) database. Differentially expressed miRNAs (DE-miRNAs) and differentially expressed genes (DEGs) were analyzed with the limma package. OP-related miRNAs from the most clinically relevant module were identified by the WGCNA method. The overlap of DE-miRNAs and OP-related miRNAs was identified as OP-related DE-miRNAs. Both upstream transcription factors and downstream targets of OP-related DE-miRNAs were predicted by FunRich. An intersection of predicted target genes and DEGs was confirmed as downstream target genes of OP-related DE-miRNAs. With the use of clusterProfiler in R, Gene Ontology (GO) annotation and Kyoto Encyclopedia of Genes and Genomes (KEGG) pathway enrichment were performed on target genes. Finally, both the protein–protein interaction (PPI) network and miRNA–mRNA network were constructed and analyzed.

Results: A total of 79 OP-related DE-miRNAs were obtained, most of which were predicted to be regulated by specificity protein 1 (SP1). Subsequently, 197 downstream target genes were screened out. The target genes were enriched in multiple pathways, including signaling pathways closely related to the onset of OP, such as Ras, PI3K-Akt,

and ErbB signaling pathways. Through the construction of the OP-related miRNA–mRNA regulatory network, a hub network that may play a prominent role in the formation of OP was documented.

Conclusion: By using WGCNA, we constructed a potential OP-related miRNA–mRNA regulatory network, offering a novel perspective on miRNA regulatory mechanisms in OP.

Keywords: osteoporosis, miRNAs, WGCNA, bioinformatics analysis, miRNA–mRNA regulatory network

INTRODUCTION

As a systemic skeletal dysfunction, osteoporosis (OP) is characterized by low bone mass and impairment of bone microstructure, consequently compromising bone strength and increasing fracture risk (1, 2). During the progression of OP, patients often develop sarcopenia, which leads to frailty syndrome (3). Moreover, OP has a high morbidity rate among the global elderly, especially in postmenopausal women (1, 4). Due to its silent nature, patients suffering from OP often feel no symptoms until the first osteoporotic fracture occurs (1). Annually, over 8.9 million fractures are caused by OP worldwide, which means that an osteoporotic fracture happens every 3 s (5). Among osteoporotic fractures, the spine, hip, distal forearm, and proximal humerus fractures tend to be the most frequent (6, 7). Elderly patients suffering from osteoporotic fractures often require hospitalization, resulting in impaired quality of life, long-lasting medical care, disability, and even death (7, 8). This poses a high economic and social burden worldwide (9) and is a global public health challenge. Hence, a better understanding of the regulatory mechanisms of OP is of great importance, which is conducive to developing novel and effective therapies.

MicroRNAs (miRNAs), commonly 19–23 nt in length, are small non-coding RNAs that are highly conserved and negatively regulate gene expression by transcriptional inhibition through binding to 3′-untranslated regions (3′ UTRs) of target messenger RNAs (mRNAs) (10, 11). With the advances in research, ample evidence indicates that miRNAs regulate a wide range of processes, including proliferation, differentiation, apoptosis, and development (12, 13). Consequently, miRNAs play a crucial role in the pathogenesis of multiple conditions, including inflammation, metabolic disorders, and cancers (12, 14). Studies indicate that miRNAs can maintain the equilibrium of bone resorption and bone formation, a balance that is disturbed in OP. MiR-214-3p derived from osteoclasts inhibits bone formation both *in vivo* and *in vitro* by transferring to osteoblast (15). It is confirmed that elevated miR-214 levels are correlated with reduced bone formation in bone specimens from aged fractured patients, further demonstrating the inhibition of osteoblast proliferation *in vitro* by modulating ATF4 (16). A series of miRNAs were identified to regulate the osteogenic process and bone-forming activity (14, 17, 18). Although the effects of miRNAs on OP have been investigated through various studies, their molecular mechanisms remain to be clarified. Therefore, further in-depth studies of regulatory mechanisms of miRNAs in OP are needed, which may provide a comprehensive understanding of OP development. Meanwhile, potential biomarkers may be identified for OP diagnosis and treatment.

Recent developments in different algorithms and research strategies have contributed to identifying potential mechanisms of gene networks, enabling further understanding of many diseases (19–21). Weighted gene co-expression network analysis (WGCNA) is one of such tools and has been widely applied to identify disease-related biomarkers, such as inflammatory diseases, metabolic diseases, and cancers (22–25). It is a systematical bioinformatics technique for clustering biologically highly-relevant genes into modules, which also defines correlations between modules and clinical traits (25). These modules may contain critical genes that are valuable biomarkers or therapeutic targets for predicting, diagnosing, and treating a specific disease (21). This research conducted a bioinformatics analysis using OP-related transcriptomic profiles from the Gene Expression Omnibus (GEO) database. Key modules of OP-related miRNAs were screened by the WGCNA method. Subsequently, differentially expressed miRNAs (DE-miRNAs) and differentially expressed genes (DEGs) of OP were identified. Transcription factors (TFs) of OP-related DE-miRNAs were specified. Moreover, functional gene annotations were performed to investigate the relevant mechanisms in OP. In order to clarify the miRNA–mRNA regulatory mechanism in OP, we constructed a miRNA–mRNA regulatory network, from which a key subnetwork was identified.

MATERIALS AND METHODS

Microarray Data Collection

The study flowchart is shown in **Figure 1**. Data of miRNAs and mRNAs were acquired from GSE93883 and GSE7158 datasets, respectively. Both datasets were obtained from the GEO database (http://www.ncbi.nlm.nih.gov/geo/). The GSE93883 dataset contains 6 healthy control samples and 12 primary OP samples, using the microarray platform GPL18058.

Abbreviations: Nt, nucleotides; PBM, peak bone mass; EGR1, early growth response 1; SP1, specificity protein 1; SP4, specificity protein 4; POU2F1, POU domain class 2 transcription factor 1; MEF2A, myocyte enhancer factor 2A; NKX6-1, NK6 homeobox 1; NFIC, nuclear factor I-C; ZFP161, zinc finger protein 161; RREB1, Ras-responsive element-binding protein 1; RORA, RAR-related orphan receptor A; FASLG, FAS/FAS ligand; TSC1, tuberous sclerosis complex 1; GO, Gene Ontology; KEGG, Kyoto Encyclopedia of Genes and Genomes; BP, biological process; CC, cellular component; MF, molecular function.

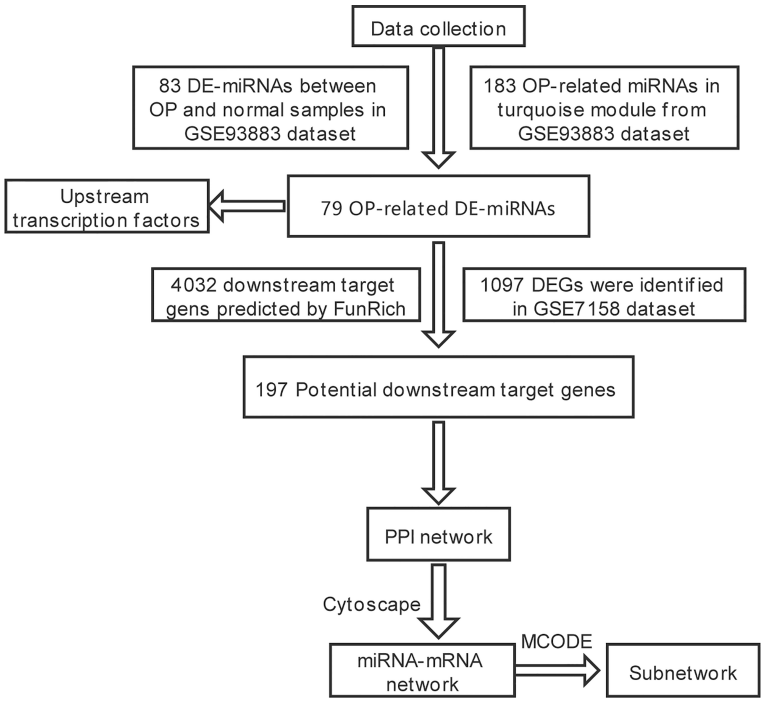

FIGURE 1 | Workflow of research routine to construct the miRNA–mRNA regulatory network in OP. miRNA, microRNA; mRNA, messenger RNA; OP, osteoporosis; DE-miRNAs, differentially expressed miRNAs; DEGs, differentially expressed genes.

The GSE7158 dataset involved 14 high peak bone mass (PBM) and 12 low PBM participants (according to the hip Z-score), using the microarray platform GPL570. The raw data of the GSE93883 dataset were available in GFP format, while those of the GSE7158 dataset were in CEL format.

Data Preprocessing, Differentially Expressed MiRNAs, and Differentially Expressed Genes Screening

The mRNA and miRNA expression matrix was obtained by using Perl script (www.perl.org/). DE-miRNA analysis between OP and normal samples and DEG analysis between low PBM and high PBM samples were performed utilizing the limma (Linear Models for Microarray Data) algorithm. The DEGs meet the criterion $|\log FC| > 2$ and p-value <0.05, while the DE-miRNAs meet the criterion $|\log FC| > 2$ and adjusted p-value <0.05.

Identification of Osteoporosis-Related MiRNAs by Weighted Gene Co-Expression Network Analysis

A weighted gene co-expressed network of miRNAs using the "WGCNA" package in R generates a scale-free weighted gene co-expressed network (26). Co-expressed genes and modules related to clinical traits were identified. A thresholding power β value of 13 was determined for the clustering of data to detect outliers and produce a scale-free network. Subsequently, a hierarchical clustering tree was used to identify gene modules, and the average-linkage hierarchical clustering using topological overlap matrix-based dissimilarity measure was used to detect gene modules (27). MEDissThres was set to 0.25 to automatically combine similar modules. The correlation between modules and clinical traits was confirmed using Pearson's correlation coefficient. Finally, OP-related DE-miRNAs were obtained by overlapping the DE-miRNAs and miRNAs of the most OP-related module.

Screening for Upstream Transcription Factors

The current study screened potential transcription factors of OP-related DE-miRNAs by using FunRich (version 3.1.3) software (http://www.funrich.org), enabling the identification of enriched transcription factors depending on the gene set (28).

Potential Downstream Target Genes

In this study, putative targets genes of OP-related DE-miRNAs were predicted by FunRich. Next, an overlap of predicted target genes and DEGs from the GSE7158 dataset was taken, identifying the potential targets of OP-related DE-miRNAs.

Gene Ontology and Pathways Analysis

Gene Ontology (GO) and Kyoto Encyclopedia of Genes and Genomes (KEGG) pathway analysis were performed *via* the "clusterProfiler" package in R to determine the biological function of potential downstream target genes of OP-related DE-miRNAs. A p-value <0.05 was considered statistically significant.

Construction of Protein–Protein Interaction Network

The protein–protein interaction (PPI) pairs between potential downstream target mRNAs of OP-related DE-miRNAs were identified *via* the String (Search Tool for Retrieval of Interacting Genes; http://string-ab.org/) database, applying high confidence >0.700. Furthermore, the disconnected mRNAs were removed from the PPI network.

Construction and Analysis of MiRNA–mRNA Network

The interactions between OP-related DE-miRNAs and mRNAs from the PPI network were obtained. An OP-related miRNA–mRNA network was then constructed by using Cytoscape v3.7.1. A subnetwork was screened by the MCODE algorithm, which was considered the hub miRNA–mRNA regulatory network of OP.

RESULTS

Identification of Significant Osteoporosis-Related Gene Module

OP samples of miRNAs from the GSE93883 dataset were used for weight gene co-expression network construction, and the pickSoftThreshold function in the WGCNA package was used to determine the value of soft thresholding power β. In the present study, a β value of 13 combined with scale independence reached 0.9, and a high level of mean connectivity was observed (**Figure 2A**). The turquoise module (183 miRNAs) was one of the five clustered co-expressed gene modules and was the most relevant to OP ($R = -0.95$, p-value $\ll 0.05$, **Figures 2B, C**). Furthermore, a strong correlation was detected between the turquoise module and its miRNAs ($R = 0.92$, p-value $\ll 0.05$, **Figure 2D**).

Screening of Differentially Expressed MiRNAs, Differentially Expressed Genes, and Osteoporosis-Related Differentially Expressed MiRNAs

DE-miRNAs in the GSE93883 dataset and DEGs in the GSE7158 dataset were screened *via* the "limma" package in R. The screening results revealed 83 DE-miRNAs, of which 33 were upregulated and 50 were downregulated, meeting the |logFC| > 2 and adjusted p-value <0.05 criterion (**Figures 3A, B**). As a result, 1,097 DEGs in the GSE7158 dataset were screened, fitting the |logFC| > 2, and p-value <0.05 criteria. Among the DEGs, 623 were upregulated and 474 were downregulated (**Figures 3C, D**). Subsequently, 79 OP-related DE-miRNAs were obtained by overlapping DE-miRNAs and miRNAs in the turquoise module (**Figure 3E**).

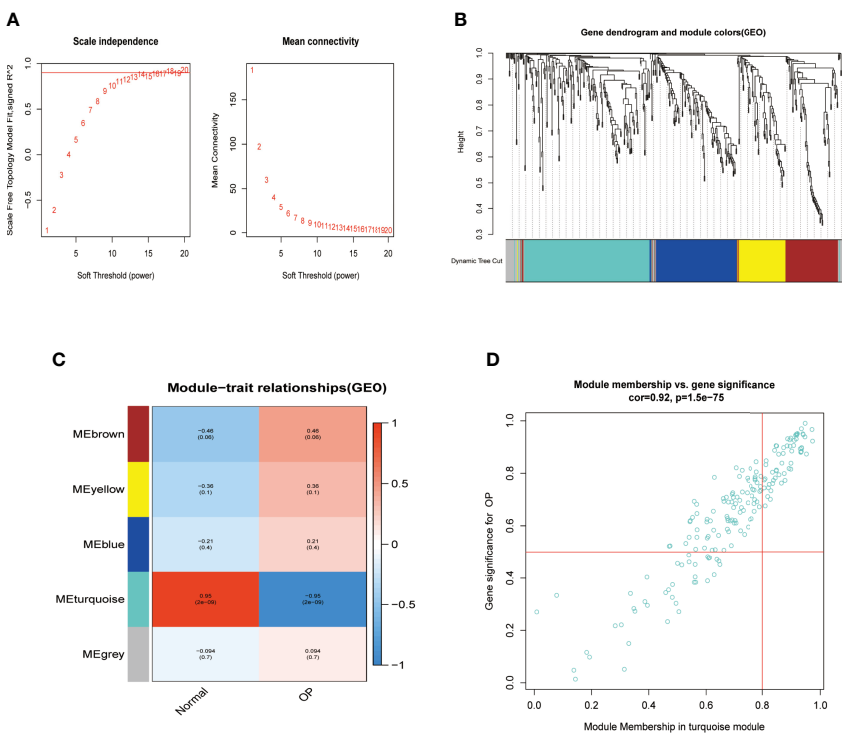

FIGURE 2 | Identifying significant gene modules associated with OP. **(A)** β = 13 was selected to establish a scale-free network in the GSE93883 dataset. **(B)** Gene clustering based on topological dissimilarity and module colors in GSE93883 dataset. **(C)** Correspondence between gene modules with osteoporosis participants or normal ones among the GSE93883 dataset. **(D)** The correlation between gene significance and module membership in the GSE93883 dataset was plotted. OP, osteoporosis.

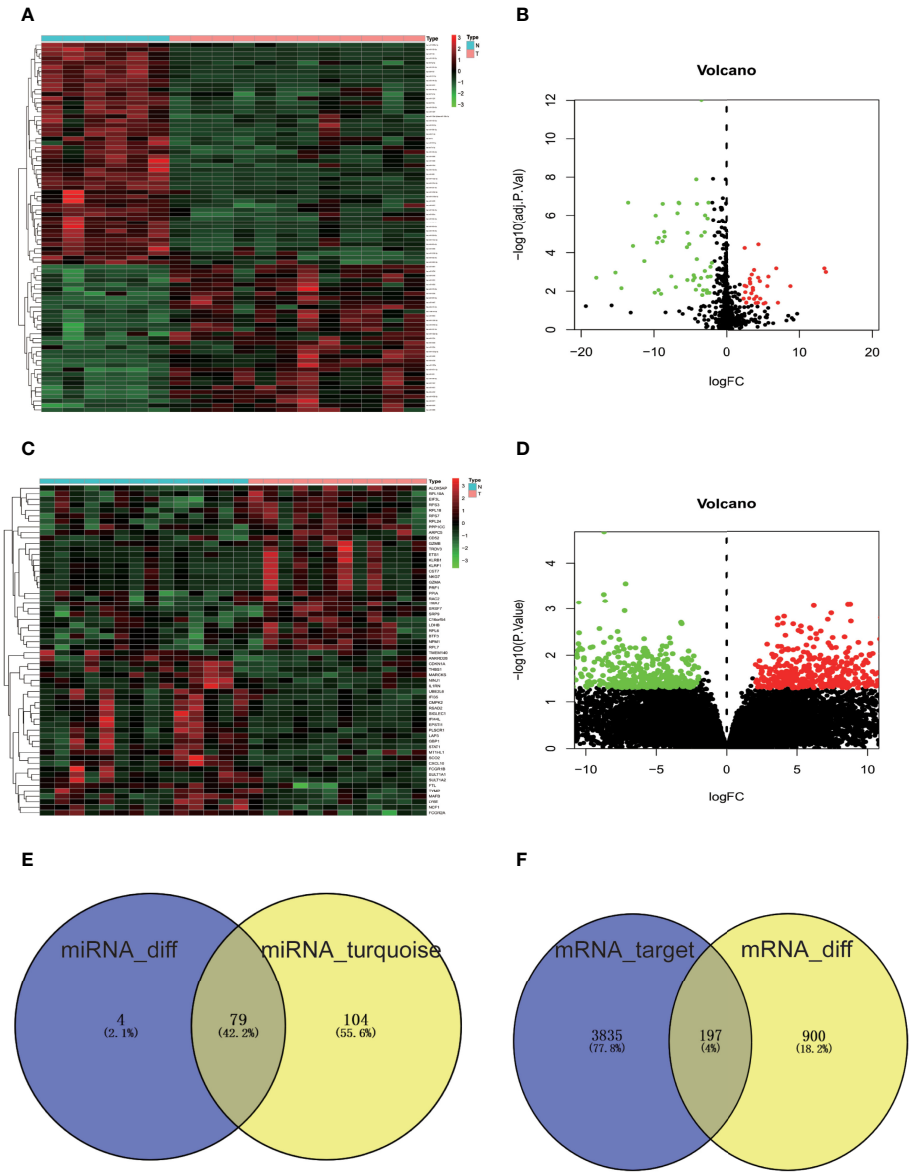

FIGURE 3 | Screening of DE-miRNAs, DEGs, and OP-related DE-miRNAs. **(A)** Heatmap of miRNA expression in GSE93883 dataset. **(B)** GSE93883 miRNA expression volcano plot. **(C)** Gene expression heatmap of GSE7158 dataset. **(D)** GSE7158 gene expression volcano plot. Black color indicates non-significant genes, while red/green color represents upregulated/downregulated DE-miRNAs or DEGs. **(E)** Venn diagram of DE-miRNAs and miRNAs closely related to OP in the turquoise module. **(F)** Venn diagram of predicted targets of OP-related DE-miRNAs and DEGs of GSE7158 dataset. The number of miRNAs or genes in each group is displayed in Venn diagrams. N, normal group; T, osteoporosis group; OP, osteoporosis; miRNA, microRNA; mRNA, messenger RNA; DE-miRNAs, differentially expressed miRNAs; DEGs, differentially expressed genes.

Upstream Transcription Factors for Osteoporosis-Related Differentially Expressed MiRNAs

Furthermore, the upstream transcription factors for OP-related DE-miRNAs were predicted by FunRich (**Figure 4**). The most significant transcription factors were EGR1, SP1, SP4, POU2F1, MEF2A, NKX6-1, NFIC, ZFP161, RREB1, and RORA.

Putative Downstream Targets of Osteoporosis-Related Differentially Expressed MiRNAs

A total of 4,032 genes targeted by OP-related DE-miRNAs were identified by FunRich (**Figure 3F**). In order to refine the results, an intersection (197 genes, **Figure 3F**) of the predicted target genes and DEGs was obtained, identifying the potential downstream target genes of OP-related DE-miRNAs.

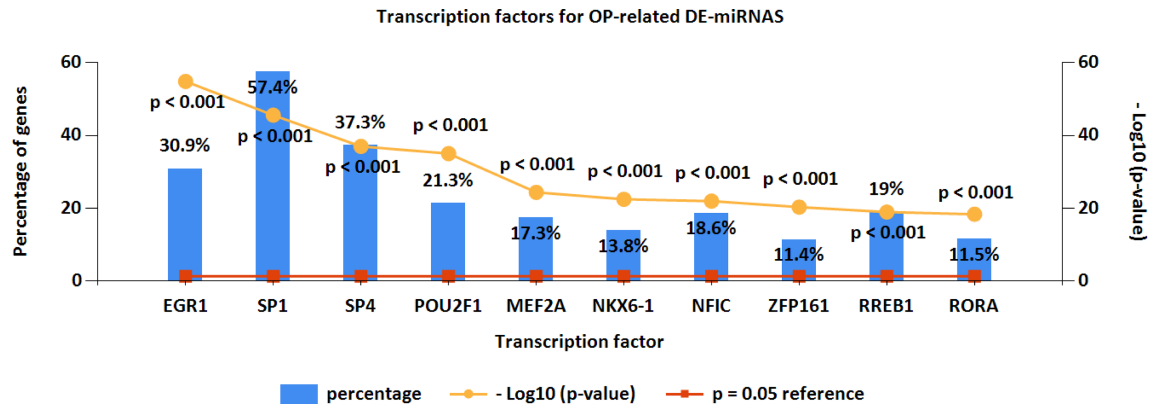

FIGURE 4 | Upstream transcription factors for OP-related DE-miRNAs. OP, osteoporosis; DE-miRNAs, differentially expressed miRNAs.

Gene Ontology and Kyoto Encyclopedia of Genes and Genomes Enrichment

Then, using clusterProfiler in R, GO functional and KEGG enrichment analyses were performed on the downstream target genes to further understand their biological functions. As represented in **Figure 5**, biological process (BP) was significantly enriched in positive regulation of I-kappaB kinase/NF-κB signaling, positive regulation of protein localization to the plasma membrane, and postsynaptic signal transduction; cellular component (CC) was particularly enriched in glutamatergic synapse, cell leading edge, and fibrillar center; molecular function (MF) was mainly enriched in protein phosphatase binding, phosphatase binding, and phosphotyrosine residue binding.

Furthermore, the KEGG pathway analysis of the 197 downstream target genes is shown in **Figure 6**. Among all the pathways enriched, the top 10 most significant pathways were as follows: proteoglycans in cancer, miRNAs in cancer, ubiquitin-

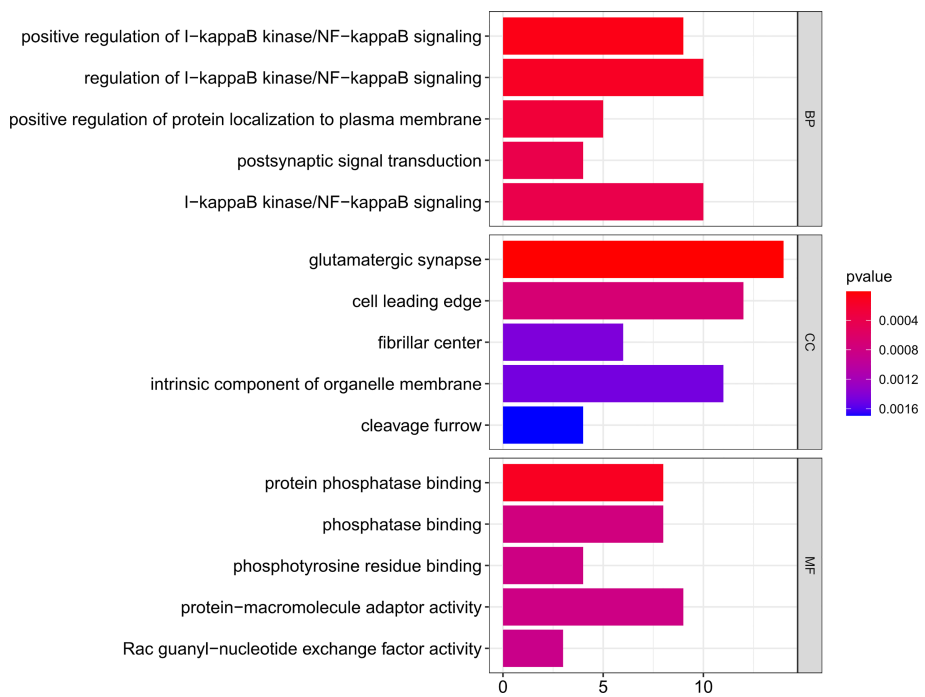

FIGURE 5 | GO functional enrichment of downstream targets of OP-related DE-miRNAs. The x-axis shows enriched gene numbers and the color represents significance. GO terms are shown on the y-axis. $p < 0.05$. OP, osteoporosis; DE-miRNAs, differentially expressed miRNAs; DEGs, differentially expressed genes; GO, Gene Ontology; KEGG, Kyoto Encyclopedia of Genes and Genomes; BP, biological process; CC, cellular component; MF, molecular function.

FIGURE 6 | KEGG pathway enrichment for downstream target genes of OP-related DE-miRNAs. The enriched gene ratio is shown on the x-axis, color represents significance, and the pathway terms are displayed on the y-axis. $p < 0.05$. OP, osteoporosis; DE-miRNAs, differentially expressed miRNAs; KEGG, Kyoto Encyclopedia of Genes and Genomes.

mediated proteolysis, regulation of actin cytoskeleton, Ras signaling pathway, human papillomavirus infection, PI3K-Akt signaling pathway, cellular senescence, ErbB signaling pathway, and insulin resistance (**Figure 6**). Notably, Ras, PI3K-Akt, and ErbB signaling pathway were closely related to the onset of OP.

Protein–Protein Interaction and MiRNA–mRNA Network

The PPI network of downstream targets of OP-related DE-miRNAs was constructed by the STRING online database with a high confidence >0.700 applied (**Figure 7A**). The disconnected nodes (genes) were removed from the PPI network (**Figure 7B**). The interactions between OP-related DE-miRNAs and genes from **Figure 7B** were obtained. A miRNA–mRNA network was then constructed by using Cytoscape (**Figure 8A**), from which the hub miRNA–mRNA regulatory network of OP was identified by the MCODE algorithm (**Figure 8B**), comprising three downregulated miRNAs (has-miR-25-3p, has-miR-92a-3p, and hsa-miR-92b-3p) and two upregulated mRNAs (FASLG and TSC1).

DISCUSSION

Over the past decade, a growing number of studies have focused on OP diagnosis and treatment (29). Patients suffering from OP usually receive treatment based on a lifestyle approach and a precise assessment of the risk of fracture (30–32). Moreover, patients at high risk were treated with pharmacological approaches including bisphosphonates, teriparatide, denosumab, and recently anti-sclerostin antibodies (33). However, concerns about rare side effects of pharmacological treatment, particularly

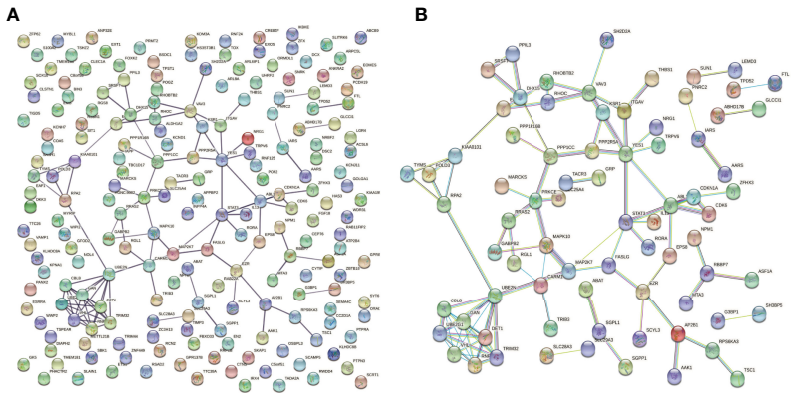

FIGURE 7 | PPI network of downstream targets of OP-related DE-miRNAs. miRNA, microRNA; PPI, protein–protein interaction; OP, osteoporosis; DE-miRNAs, differentially expressed miRNAs.

bisphosphonates, and the absence of clear evidence in support of their long-term efficacy are leading many patients who could benefit from drug therapy to not take these drugs (29), indicating a limited understanding of OP pathogenesis. Therefore, a better understanding of the regulatory mechanism of OP is required to develop new treatments or improve existing therapies for OP. Advances in bioinformatics have facilitated the identification of genetic changes in disease development. The current study detected five modules in GSE93883 data, with the turquoise module being the most correlated with OP. Comparing the DE-miRNAs with miRNAs in the turquoise module (**Figure 3E**), 79 shared miRNAs were identified for further analysis.

In recent years, a growing number of miRNAs have been reported to be involved in diverse biogenesis pathways by mediating gene silencing (11). To better understand the functions of 79 OP-related DE-miRNAs, their downstream target genes were predicted by FunRich. Furthermore, by comparing the predicted genes to DEGs in the GSE7158 dataset, 197 shared genes were screened as downstream targets of OP-related DE-miRNAs (**Figure 3F**). These 197 genes were enriched in a range of functions and pathways based on the GO and KEGG analyses. Evidence suggests that these GO terms and pathways are important in OP. For example, in a high-content imaging-based *in vivo* chemical screen, NF-κB signaling was identified as a cell-autonomous inhibitor of osteoblast differentiation (34). Ras is a crucial regulator of normal bone growth and development (35). During intramembranous osteogenesis induced by tensile force, Ras was proven to promote chemotaxis of chemotaxis in preosteoblasts both *in vivo* and *in vitro* (36). Fisher et al. (37) identified the requirement for ErbB signaling to maintain osteoblast proliferation involved in the timely progression of periosteal osteoblast differentiation. Evidence showed that apoptosis of osteoblasts in OP mice induced by ovariectomy was induced by blockade of the PI3K/AKT signaling (38), while activation of PI3K/AKT signaling pathway facilitated Runx2 and osterix expression in osteoblast (39). In combination with the above evidence, the 197 genes may be involved in the pathogenesis of OP.

Transcription factors can modulate miRNA expression (40). Therefore, transcription factor prediction was performed using

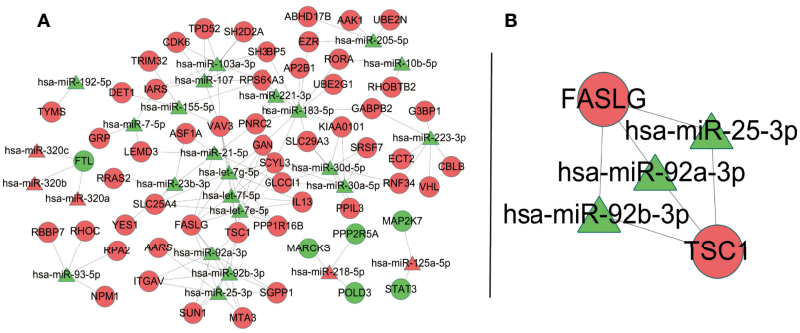

FIGURE 8 | OP-relevant miRNA–mRNA regulatory network. Ellipse represents target genes of miRNAs; triangle represents miRNAs. Red dots represent miRNAs or targets that are upregulated, while green dots represent those that are downregulated. **(A)** MiRNA–mRNA regulatory network of OP. **(B)** A subnetwork identified by the MCODE algorithm in Cytoscape. OP, osteoporosis; miRNA, microRNA; mRNA, messenger RNA.

FunRich to identify potential transcription factors regulating the OP-related DE-miRNAs. As a result, specificity protein 1 (SP1) accounted for the highest percentage of OP-related DE-miRNAs. The C2H2-type zinc-finger transcription factor SP1 has been extensively documented in OP and regulates cell growth, differentiation, apoptosis, and others (41). There is a close relationship between SP1 binding site polymorphism at COL1A1 gene and OP risk among men and women (42). SP1 can also stimulate specific miRNA to inhibit osteogenesis *via* modulating the LRP5/Wnt/β-catenin pathway (43).

The potential regulatory mechanisms of OP were explored by constructing the miRNA–mRNA network of OP, providing further insight into OP. A hub miRNA–mRNA regulatory network, comprising three downregulated miRNAs (has-miR-25-3p, has-miR-92a-3p, and hsa-miR-92b-3p) and two upregulated mRNAs (FASLG and TSC1), was identified. MiR-25-3p can promote osteoclast activity and could be a powerful target for handling skeletal disorders characterized by reduced bone formation (44). TSC1 is a key regulator of mTORC1, and in a RANKL-induced OP mouse model, deletion of Tsc1 in osteoclast lineage cells prevented bone resorption (45). Younes et al. (46) identified FASLG as one of the genetic risk factors that contributed to low bone density in the Qatari population, based on the whole genomes sequenced from 3,000 individuals from the Qatar Biobank. There was no direct evidence that miR-92a-3p and miR-92b-3p were correlated to OP. However, studies have shown that they contributed to different diseases involving different pathways (47–50). Indeed, we provided a reference for OP therapeutic targets, especially those in the hub network. We believe that it may promote the development of new treatments to some extent.

A potential OP-related miRNA–mRNA regulatory network was identified by analyzing microarray profile data and taking clinical traits into consideration using the WGCNA algorithm, providing new insight into OP in terms of biological functions and potential pathophysiological mechanisms. However, the present study has several limitations. The sample size of each GEO dataset in our study was relatively small, and the OP-related miRNA–mRNA interactions were only predicted by public databases, which need further validation through *in vivo* and *in vitro* experiments. Moreover, most proposed pathways (RAS and ERB) are also involved in tumorigenesis, and evidence is only from *in vitro* studies, which limits the results of the present study and the possibility of an intervention. Finally, our study was limited to primary OP.

CONCLUSION

Overall, we established a potential OP-related miRNA–mRNA regulatory network *via* the WGCNA method, offering a novel insight into the regulatory mechanisms of miRNAs in the development of OP. Several key miRNAs and mRNAs, including has-miR-25-3p, has-miR-92a-3p, hsa-miR-92b-3p, FASLG, and TSC1, were identified from the network and may act as key biomarkers or clinical targets for OP. We sincerely hope that our efforts could contribute to future in-depth investigations into OP.

DATA AVAILABILITY STATEMENT

Publicly available datasets were analyzed in this study. This data can be found here: https://www.ncbi.nlm.nih.gov/, GSE93883; GSE7158.

AUTHOR CONTRIBUTIONS

JW and SHL performed the literature search, and HH conceived and designed the project. SL and BC performed the data analysis. SL wrote the paper. HH reviewed and amended the manuscript. The manuscript has been read and approved by all authors.

FUNDING

This work was supported by the National Natural Science Foundation of China (Grant No. 81973886), by Guangzhou University of Chinese Medicine "Double first-class" and High-level University Discipline Collaborative Innovation Team Project (Grant No. 2021XK21), and by the Postgraduate Research and Innovation Project of Guangzhou University of Chinese Medicine in 2021 (Doctoral candidate: Shi Lin).

REFERENCES

1. Johnston CB, Dagar M. Osteoporosis in Older Adults. *Med Clin North Am* (2020) 104(5):873–84. doi: 10.1016/j.mcna.2020.06.004
2. Cauley JA. Osteoporosis: Fracture Epidemiology Update 2016. *Curr Opin Rheumatol* (2017) 29(2):150–6. doi: 10.1097/bor.0000000000000365
3. Greco EA, Pietschmann P, Migliaccio S. Osteoporosis and Sarcopenia Increase Frailty Syndrome in the Elderly. *Front Endocrinol* (2019) 10:255. doi: 10.3389/fendo.2019.00255
4. Hong J, Ye F, Yu B, Gao J, Qi F, Wang W. Identification of the Specific Micrornas and Competitive Endogenous RNA Mechanisms in Osteoporosis. *J Int Med Res* (2020) 48(10):300060520954722. doi: 10.1177/0300060520954722
5. Johnell O, Kanis JA. An Estimate of the Worldwide Prevalence and Disability Associated With Osteoporotic Fractures. *Osteoporos Int* (2006) 17(12):1726–33. doi: 10.1007/s00198-006-0172-4
6. Cosman F, de Beur SJ, LeBoff MS, Lewiecki EM, Tanner B, Randall S, et al. Clinician's Guide to Prevention and Treatment of Osteoporosis. *Osteoporos Int* (2014) 25(10):2359–81. doi: 10.1007/s00198-014-2794-2
7. de Sire A, Invernizzi M, Baricich A, Lippi L, Ammendolia A, Grassi FA, et al. Optimization of Transdisciplinary Management of Elderly With Femur Proximal Extremity Fracture: A Patient-Tailored Plan From Orthopaedics to Rehabilitation. *World J Orthop* (2021) 12(7):456–66. doi: 10.5312/wjo.v12.i7.456
8. Yu F, Xia W. The Epidemiology of Osteoporosis, Associated Fragility Fractures, and Management Gap in China. *Arch Osteoporos* (2019) 14(1):32. doi: 10.1007/s11657-018-0549-y

9. Cui Z, Meng X, Feng H, Zhuang S, Liu Z, Zhu T, et al. Estimation and Projection About the Standardized Prevalence of Osteoporosis in Mainland China. *Arch Osteoporos* (2019) 15(1):2. doi: 10.1007/s11657-019-0670-6
10. Kloosterman WP, Plasterk RH. The Diverse Functions of Micrornas in Animal Development and Disease. *Dev Cell* (2006) 11(4):441–50. doi: 10.1016/j.devcel.2006.09.009
11. Kim VN. Small Rnas: Classification, Biogenesis, and Function. *Mol Cells* (2005) 19(1):1–15.
12. Esteller M. Non-Coding Rnas in Human Disease. *Nat Rev Genet* (2011) 12 (12):861–74. doi: 10.1038/nrg3074
13. Invernizzi M, de Sire A, Renò F, Cisari C, Runza L, Baricich A, et al. Spinal Cord Injury as a Model of Bone-Muscle Interactions: Therapeutic Implications From *in Vitro* and *in Vivo* Studies. *Front Endocrinol* (2020) 11:204. doi: 10.3389/fendo.2020.00204
14. Yang Y, Yujiao W, Fang W, Linhui Y, Ziqi G, Zhichen W, et al. The Roles of Mirna, Lncrna and Circrna in the Development of Osteoporosis. *Biol Res* (2020) 53(1):40. doi: 10.1186/s40659-020-00309-z
15. Li D, Liu J, Guo B, Liang C, Dang L, Lu C, et al. Osteoclast-Derived Exosomal Mir-214-3p Inhibits Osteoblastic Bone Formation. *Nat Commun* (2016) 7:10872. doi: 10.1038/ncomms10872
16. Wang X, Guo B, Li Q, Peng J, Yang Z, Wang A, et al. Mir-214 Targets Atf4 to Inhibit Bone Formation. *Nat Med* (2013) 19(1):93–100. doi: 10.1038/nm.3026
17. Itoh T, Takeda S, Akao Y. Microrna-208 Modulates Bmp-2-Stimulated Mouse Preosteoblast Differentiation by Directly Targeting V-Ets Erythroblastosis Virus E26 Oncogene Homolog 1. *J Biol Chem* (2010) 285(36):27745–52. doi: 10.1074/jbc.M110.105080
18. Inose H, Ochi H, Kimura A, Fujita K, Xu R, Sato S, et al. A Microrna Regulatory Mechanism of Osteoblast Differentiation. *Proc Natl Acad Sci USA* (2009) 106(49):20794–9. doi: 10.1073/pnas.0909311106
19. Dai B, Sun F, Cai X, Li C, Liu H, Shang Y. Significance of RNA N6-Methyladenosine Regulators in the Diagnosis and Subtype Classification of Childhood Asthma Using the Gene Expression Omnibus Database. *Front Genet* (2021) 12. doi: 10.3389/fgene.2021.634162
20. Tang X, Bai Y, Zhang Z, Lu J. A Validated Mirna Signature for the Diagnosis of Osteoporosis Related Fractures Using Svm Algorithm Classification. *Exp Ther Med* (2020) 20(3):2209–17. doi: 10.3892/etm.2020.8928
21. Xiao B, Wang G, Li W. Weighted Gene Correlation Network Analysis Reveals Novel Biomarkers Associated With Mesenchymal Stromal Cell Differentiation in Early Phase. *PeerJ* (2020) 8:e8907. doi: 10.7717/peerj.8907
22. Zhu N, Hou J, Ma G, Guo S, Zhao C, Chen B. Co-Expression Network Analysis Identifies a Gene Signature as a Predictive Biomarker for Energy Metabolism in Osteosarcoma. *Cancer Cell Int* (2020) 20:259. doi: 10.1186/s12935-020-01352-2
23. Hu Y, Tan LJ, Chen XD, Greenbaum J, Deng HW. Identification of Novel Variants Associated With Osteoporosis, Type 2 Diabetes and Potentially Pleiotropic Loci Using Pleiotropic Cfdr Method. *Bone* (2018) 117:6–14. doi: 10.1016/j.bone.2018.08.020
24. Dong L, Li H, Zhang S, Yang G. Mir−148 Family Members Are Putative Biomarkers for Sepsis. *Mol Med Rep* (2019) 19(6):5133–41. doi: 10.3892/mmr.2019.10174
25. Gao X, Sun Y, Li X. Identification of Key Gene Modules and Transcription Factors for Human Osteoarthritis by Weighted Gene Co-Expression Network Analysis. *Exp Ther Med* (2019) 18(4):2479–90. doi: 10.3892/etm.2019.7848
26. Langfelder P, Horvath S. Wgcna: An R Package for Weighted Correlation Network Analysis. *BMC Bioinf* (2008) 9:559. doi: 10.1186/1471-2105-9-559
27. Zheng G, Zhang C, Zhong C. Identification of Potential Prognostic Biomarkers for Breast Cancer Using Wgcna and Ppi Integrated Techniques. *Ann Diagn Pathol* (2021) 50:151675. doi: 10.1016/j.anndiagpath.2020.151675
28. Wang YW, Zhang W, Ma R. Bioinformatic Identification of Chemoresistance-Associated Micrornas in Breast Cancer Based on Microarray Data. *Oncol Rep* (2018) 39(3):1003–10. doi: 10.3892/or.2018.6205
29. Khosla S, Hofbauer LC. Osteoporosis Treatment: Recent Developments and Ongoing Challenges. *Lancet Diabetes Endocrinol* (2017) 5(11):898–907. doi: 10.1016/s2213-8587(17)30188-2
30. Montero-Odasso MM, Kamkar N, Pieruccini-Faria F, Osman A, Sarquis-Adamson Y, Close J, et al. Evaluation of Clinical Practice Guidelines on Fall Prevention and Management for Older Adults: A Systematic Review. *JAMA Netw Open* (2021) 4(12):e2138911. doi: 10.1001/jamanetworkopen.2021.38911
31. Marini S, Barone G, Masini A, Dallolio L, Bragonzoni L, Longobucco Y, et al. The Effect of Physical Activity on Bone Biomarkers in People With Osteoporosis: A Systematic Review. *Front Endocrinol* (2020) 11:585689. doi: 10.3389/fendo.2020.585689
32. Iolascon G, de Sire A, Curci C, Paoletta M, Liguori S, Calafiore D, et al. Osteoporosis Guidelines From a Rehabilitation Perspective: Systematic Analysis and Quality Appraisal Using Agree II. *Eur J Phys Rehabil Med* (2021) 57(2):273–9. doi: 10.23736/s1973-9087.21.06581-3
33. Wu CH, Hung WC, Chang IL, Tsai TT, Chang YF, McCloskey EV, et al. Pharmacologic Intervention for Prevention of Fractures in Osteopenic and Osteoporotic Postmenopausal Women: Systemic Review and Meta-Analysis. *Bone Rep* (2020) 13:100729. doi: 10.1016/j.bonr.2020.100729
34. Mishra R, Sehring I, Cederlund M, Mulaw M, Weidinger G. Nf-Kb Signaling Negatively Regulates Osteoblast Dedifferentiation During Zebrafish Bone Regeneration. *Dev Cell* (2020) 52(2):167–82.e7. doi: 10.1016/j.devcel.2019.11.016
35. Shuai B, Yang YP, Shen L, Zhu R, Xu XJ, Ma C, et al. Local Renin-Angiotensin System Is Associated With Bone Mineral Density of Glucocorticoid-Induced Osteoporosis Patients. *Osteoporos Int* (2015) 26(3):1063–71. doi: 10.1007/s00198-014-2992-y
36. Jiang W, Takeshita N, Maeda T, Sogi C, Oyanagi T, Kimura S, et al. Connective Tissue Growth Factor Promotes Chemotaxis of Preosteoblasts Through Integrin A5 and Ras During Tensile Force-Induced Intramembranous Osteogenesis. *Sci Rep* (2021) 11(1):2368. doi: 10.1038/s41598-021-82246-9
37. Fisher MC, Clinton GM, Maihle NJ, Dealy CN. Requirement for Erbb2/Erbb Signaling in Developing Cartilage and Bone. *Dev Growth differ* (2007) 49 (6):503–13. doi: 10.1111/j.1440-169X.2007.00941.x
38. Zhang Y, Cao X, Li P, Fan Y, Zhang L, Li W, et al. Psmc6 Promotes Osteoblast Apoptosis Through Inhibiting Pi3k/Akt Signaling Pathway Activation in Ovariectomy-Induced Osteoporosis Mouse Model. *J Cell Physiol* (2020) 235 (7-8):5511–24. doi: 10.1002/jcp.29261
39. Chen PC, Liu JF, Fong YC, Huang YL, Chao CC, Tang CH. Ccn3 Facilitates Runx2 and Osterix Expression by Inhibiting Mir-608 Through Pi3k/Akt Signaling in Osteoblasts. *Int J Mol Sci* (2019) 20(13). doi: 10.3390/ijms20133300
40. Zhu M, Ye M, Wang J, Ye L, Jin M. Construction of Potential Mirna-Mrna Regulatory Network in Copd Plasma by Bioinformatics Analysis. *Int J Chron Obstruct Pulmon Dis* (2020) 15:2135–45. doi: 10.2147/copd.S255262
41. Moradifard S, Hoseinbeyki M, Emam MM, Parchiniparchin F, Ebrahimi-Rad M. Association of the Sp1 Binding Site and -1997 Promoter Variations in Col1a1 With Osteoporosis Risk: The Application of Meta-Analysis and Bioinformatics Approaches Offers a New Perspective for Future Research. *Mutat Res Rev Mutat Res* (2020) 786:108339. doi: 10.1016/j.mrrev.2020.108339
42. Soibam D, Singh TA, Nandy P, Dewan SK, Baruah A. Sp1 Binding Site Polymorphism at Col1a1 Gene and Its Relation to Bone Mineral Density for Osteoporosis Risk Factor Among the Sikkimese Men and Women of Northeast India. *Indian J Clin Biochem: IJCB* (2019) 34(2):230–3. doi: 10.1007/s12291-017-0728-4
43. Li L, Qiu X, Sun Y, Zhang N, Wang L. Sp1-Stimulated Mir-545-3p Inhibits Osteogenesis *Via* Targeting Lrp5-Activated Wnt/Beta-Catenin Signaling. *Biochem Biophys Res Commun* (2019) 517(1):103–10. doi: 10.1016/j.bbrc.2019.07.025
44. Huang Y, Ren K, Yao T, Zhu H, Xu Y, Ye H, et al. Microrna-25-3p Regulates Osteoclasts Through Nuclear Factor I X. *Biochem Biophys Res Commun* (2020) 522(1):74–80. doi: 10.1016/j.bbrc.2019.11.043
45. Hiraiwa M, Ozaki K, Yamada T, Iezaki T, Park G, Fukasawa K, et al. Mtorc1 Activation in Osteoclasts Prevents Bone Loss in a Mouse Model of Osteoporosis. *Front Pharmacol* (2019) 10:684. doi: 10.3389/fphar.2019.00684
46. Younes N, Syed N, Yadav SK, Haris M, Abdallah AM, Abu-Madi M. A Whole-Genome Sequencing Association Study of Low Bone Mineral Density Identifies New Susceptibility Loci in the Phase I Qatar Biobank Cohort. *J Pers Med* (2021) 11(1):34. doi: 10.3390/jpm11010034
47. Chen Z, Li Z, Jiang C, Jiang X, Zhang J. Mir-92b-3p Promotes Neurite Growth and Functional Recovery *Via* the Pten/Akt Pathway in Acute Spinal Cord Injury. *J Cell Physiol* (2019) 234(12):23043–52. doi: 10.1002/jcp.28864
48. Sun H, Tian J, Li J. Mir-92b-3p Ameliorates Inflammation and Autophagy by Targeting Traf3 and Suppressing Mkk3-P38 Pathway in Caerulein-Induced Ar42j Cells. *Int Immunopharmacol* (2020) 88:106691. doi: 10.1016/j.intimp.2020.106691

49. Wang L, Cui M, Qu F, Cheng D, Yu J, Tang Z, et al. Mir-92a-3p Promotes the Malignant Progression of Hepatocellular Carcinoma by Mediating the Pi3k/Akt/Mtor Signaling Pathway. *Curr Pharm Des* (2021) 27:3244–50. doi: 10.2174/1381612827666210612054156
50. Xu Y, Miao C, Cui J, Bian X. Mir-92a-3p Promotes Ox-Ldl Induced-Apoptosis in Huvecs *Via* Targeting Sirt6 and Activating Mapk Signaling Pathway. *Braz J Med Biol Res = Rev Bras pesquisas medicas e biologicas* (2021) 54(3):e9386. doi: 10.1590/1414-431x20209386

Conflict of Interest: The authors declare that the research was conducted in the absence of any commercial or financial relationships that could be construed as a potential conflict of interest.

Publisher's Note: All claims expressed in this article are solely those of the authors and do not necessarily represent those of their affiliated organizations, or those of the publisher, the editors and the reviewers. Any product that may be evaluated in this article, or claim that may be made by its manufacturer, is not guaranteed or endorsed by the publisher.

frontiers | Frontiers in Endocrinology

SYSTEMATIC REVIEW
published: 01 June 2022
doi: 10.3389/fendo.2022.863448

Vitamin D Supplementation Improves Handgrip Strength in Postmenopausal Women: A Systematic Review and Meta-Analysis of Randomized Controlled Trials

*Jia-Li Zhang[1,2], Christina Chui-Wa Poon[3], Man-Sau Wong[3], Wen-Xiong Li[1], Yi-Xun Guo[1,2] and Yan Zhang[1,2]**

[1] Spine Disease Research Institute, Longhua Hospital, Shanghai University of Traditional Chinese Medicine, Shanghai, China, [2] Key Laboratory of Theory and Therapy of Muscles and Bones, Ministry of Education, Shanghai, China, [3] Department of Applied Biology and Chemical Technology, The Hong Kong Polytechnic University, Hung Hom, Kowloon, Hong Kong SAR, China

OPEN ACCESS

Edited by:
Alex Ireland,
Manchester Metropolitan University, United Kingdom

Reviewed by:
Alexandra Mavroeidi,
University of Strathclyde, United Kingdom
Khashayar Sakhaee,
University of Texas Southwestern Medical Center, United States

***Correspondence:**
Yan Zhang
medicineyan@aliyun.com

Specialty section:
This article was submitted to Bone Research, a section of the journal Frontiers in Endocrinology

Received: 27 January 2022
Accepted: 19 April 2022
Published: 01 June 2022

Citation:
Zhang J-L, Poon CC-W, Wong M-S, Li W-X, Guo Y-X and Zhang Y (2022) Vitamin D Supplementation Improves Handgrip Strength in Postmenopausal Women: A Systematic Review and Meta-Analysis of Randomized Controlled Trials. Front. Endocrinol. 13:863448. doi: 10.3389/fendo.2022.863448

Introduction: In postmenopausal women, vitamin D deficiency (as defined by the circulating level of 25(OH)D being below 20 ng/ml (50 nmol/L)) is a regular occurrence. The effect of vitamin D supplementation on the muscle function of postmenopausal women has been controversial. This systematic review and meta-analysis of randomized controlled trials (RCTs) examines and summarizes the effects of vitamin D supplementation on the muscular strength and mobility of postmenopausal women.

Methods: RCTs that met the inclusion criteria for this study were identified by searching PubMed, EMBASE, and the Cochrane Library. Postmenopausal women who were included in the study were exposed to RCTs assessing the effectiveness of vitamin D supplements. Meta-analysis data were extracted by two independent reviewers and screened for methodological quality. RCTs that did not meet the minimum requirement for assessment were excluded. In the meta-analysis, the effect size (weighted mean differences, WMD) of handgrip strength (HGS) and timed-up and go test (TUG) with a 95% confidence interval (CI) was obtained to compare reported results across the included RCTs.

Results: A total of 19 trials were included in this systematic review, among which 13 trials were eligible for the meta-analysis. In the 13 included studies, supplementing with vitamin D produced a weighted mean difference of 0.876 kg (95% CI = 0.180 to 1.571, $P = 0.014$, $I^2 = 68.5\%$) for HGS, a measurement of muscle strength. However, an insignificant decrease of 0.044 s was observed after analyzing the TUG (95% CI = -0.979 to 0.892, $P = 0.927$, $I^2 = 95\%$). According to subgroup analysis, vitamin D supplementation increased HGS in patients over the age of 60 ($P = 0.001$), in those without calcium supplementation

(P = 0.032), and in those whose baseline vitamin D level was greater than 75 nmol/L (30 ng/ml) (P = 0.003).

Conclusions: Taking into account the studies in this systematic review, vitamin D supplementation improved muscle strength in postmenopausal women. However, an insignificant result was demonstrated in terms of mobility after vitamin D supplementation.

Keywords: vitamin D, postmenopausal women, handgrip strength, muscle strength, mobility

INTRODUCTION

Postmenopausal women often have osteopenia and osteoporosis, mainly due to advanced age and lack of hormones, and this may cause a high incidence of falls and fractures (1–6). Several recent studies have suggested that muscle mass and bone mineral density (BMD) are linked among postmenopausal women (1–6). Furthermore, the loss of muscular mass and strength seen in postmenopausal women is the most basic symptom of sarcopenia, which is unanimously recognized by the academic consensus of experts from various continents (7–10).

Sarcopenia is caused by nutritional deficiencies, a sedentary lifestyle, decreased protein synthesis and regeneration, inflammation, hormonal and cytokine imbalances, and other factors (10, 11). Among these risk factors, vitamin D deficiency not only receives much attention in the academic medical community but also gradually gains higher awareness in diverse healthcare settings (12, 13).

Vitamin D deficiency is a common health problem among middle-aged people worldwide; it is estimated that more than 1 billion people are vitamin D deficient (6, 14–16). Epidemiological studies and investigations in various countries have revealed that vitamin D deficiency (serum 25(OH)D: less than 50 nmol/L) is common in postmenopausal women (14, 17, 18). Among them, 50.6% of Chinese postmenopausal women are vitamin D-insufficient, while 31.2% are vitamin D-deficient (19). According to compelling data, serum 25(OH)D levels are strongly linked to musculoskeletal function and muscular strength (20–23). Furthermore, multiple *in vivo* and *in vitro* experiments have indicated physiological and histological alterations associated with severe vitamin D deprivation, indicating that vitamin D supplementation has a favorable influence on musculoskeletal health. In detail, vitamin D supplementation is recommended by the Committee Recommendations for people at risk for vitamin D deficiency. They recommended that females who are over 51 years old need 1,500–2,000 IU, but less than 10,000 IU, of daily vitamin D intake (24). Additionally, the vitamin D receptor (VDR) has been identified in skeletal muscle tissue, muscle satellite cells, and myoblasts, which supports the idea that vitamin D might directly affect muscle tissue (25, 26).

International academic consensus emphasizes the importance of vitamin D supplementation or treatment for sarcopenia. Likewise, the impact of vitamin D on muscular function in various populations, namely, adults (27), older people (28–30), athletes (31–33), and patients with chronic diseases (34, 35) has been reported in systematic reviews and meta-analysis. There is, however, a lack of consistency in the results concerning the effect of vitamin D on muscle function in postmenopausal women based on several interventional studies. Vitamin D supplementation, alone or in conjunction with calcium supplements, has been shown in certain studies to enhance muscular strength and reduce the incidence of falls and fractures (36–39). However, several recent randomized controlled trials (RCT) on postmenopausal women with inadequate or deficient vitamin D levels found that vitamin D supplementation had no active effect on muscular strength or the number of falls (40, 41). As a result, there is still a pressing need for studies and academic consensus on postmenopausal women who are at high risk of vitamin D deficiency (7–9).

In this study, the data from the handgrip strength (HGS) and timed up and go test (TUG) are used to calculate the muscle function index, which is used to assess muscular strength and mobility, which are protracted indicators of fracture, osteoporosis, and sarcopenia in postmenopausal women. We conducted a meta-analysis on the efficacy of vitamin D supplementation on muscular strength and mobility in postmenopausal women based on a systematic evaluation of data from the chosen RCTs stated above.

METHODS

The current study was carried out in compliance with PRISMA (Preferred Reporting Items of Systematic Reviews and Meta-Analysis) recommendations (42).

Literature Search

Two independent authors (J-LZ and W-XL) systematically searched PubMed, Embase, and the Cochrane Database from inception dates to January 2021 for randomized controlled trials that investigated the association between vitamin D supplementation and muscle atrophy using a predefined search algorithm using the following search algorithm: "((“muscular atroph*” OR “muscle atroph*” OR “Atroph* Muscular” OR “Atroph* Muscle” OR “sarcopenia*” OR “muscle strength” OR “mobility” OR “handgrip” OR “hand strength” OR “muscle function” OR “myatrophy” OR “myophagism” OR “physical performance”) AND (“postmenopausal women” OR “postmenopausal” OR “postmenopause” OR “PMP”)) AND (“vitamin d” OR “vitamin d” OR “25 hydroxyvitamin d” OR “vitamin d 2” OR “vitamin d 3” OR “calciferol*” OR “ergocalciferol*” OR “eldecalcitol*” OR

"cholecalciferol*" OR "alphacalcidol*" OR "calcitriol*" OR "calcidiol*" OR "calcifediol*" OR "calciferol*" OR "dihydroxycholecalciferol")".

Inclusion and Exclusion Criteria

After screening of titles and abstracts, duplicate studies and those clearly irrelevant were removed. The remaining full-texts of the papers were then retrieved to see if they matched the inclusion criteria for the current meta-analysis. The following are the inclusion criteria: 1) It had to be a human RCT with a cross-over or parallel design, 2) its study population had to be postmenopausal women, and 3) mean difference and standard deviations (SDs), standard error of the mean (SEMs), or 95% confidence intervals (CIs) were provided for the outcomes under consideration. The exclusion criteria are as follows: 1) *in vivo* animal studies, *in vitro* cell research, case reports, and observational studies; 2) any studies conducted in postmenopausal women with other diseases (such as type 2 diabetes, hypertension, trauma, etc.); 3) any studies investigating the effect of vitamin D supplementation combined with other interventions, such as nutrients like amino acid and protein supplements, physical exercise, other medication administration records like insulin, hormone therapy, and etidronate, etc.; 4) studies to be reported in other languages other than English; 5) RCTs that did not fulfill the minimal threshold for methodological quality evaluation.

Data Extraction

The following data were extracted by two independent investigators (J-LZ and W-XL) from each included study: the first author, publication year; sample size (shown as: supplementation/control); age; supplementation; comparator; supplementation duration; presented data. Subgroup analysis was done on the basis of these pre-extracted data. Disagreements were resolved by consensus. Endnote X9 (Clarivate Analytics, Philadelphia, PA, USA) was used to undertake the extraction procedures.

Assessment of the Quality of Included Literature

To estimate the quality of literature, the Jadad scale was used (43). This scale includes the following items: randomization, randomization scheme, double-blinding, double-blinding method, and dropouts and withdrawals in the supplementation and control groups. Each item would get a score from 0 to 1. In terms of quality, studies with scores of 0–2 are considered inferior, and those with scores of 3–5 are considered high quality (**Table 1**).

Data Analysis

The effect sizes were expressed as weighted mean differences (WMDs), and the DerSimonian–Laird approach was used to calculate the 95% confidence interval (CI) from the random effects model. For each clinical study, WMDs were used to examine the effects of vitamin D supplementation on muscle outcomes such as HGS and TUG. The pooled effect sizes for each outcome were estimated using the altered value technique. We also used Cochrane's Q test and I-square (I^2) to assess any existing heterogeneity among the included RCTs. I^2 greater than 50% with P <0.05 was applied to define heterogeneity (57). Furthermore, using the available moderator factors, sensitivity and subgroup analyses were performed to determine the impacts of each research paper on the pooled WMDs and to investigate the source of heterogeneity. Statistical analyses were carried out with STATA software version 15.0 (Stata Corp., College Station, TX) and Review Manager 5.4 software (Cochrane Collaboration, Oxford, UK).

RESULTS

The Description of the Selected RCTs

The first searches yielded a total of 172 potentially suitable documents, with 41 items being eliminated owing to the duplication. The titles and abstracts of the remaining 131 records were screened for inclusion. Then the full texts of 78 records were further estimated, and 19 met the inclusion criteria (36–41, 44–56), of which 13 of those 19 were suitable for meta-analysis. **Figure 1** shows a flowchart of the selection of RCT trials. The main characteristics of the RCTs are summarized in **Table 1**.

The year of publication of the 19 RCT trials included in this review was between 2003 and 2021, with 5,398 participants. The sample size of the RCTs included in multiple countries ranges from 20 (46, 52) to 2,347 (40). Furthermore, the duration of supplementation ranged from 3 (37, 38, 44, 45, 47, 53, 54) to 60 (40) months.

Different analogs of vitamin D_2 (53, 54, 56) or vitamin D_3 (36, 40, 41, 44–50, 52, 55), such as calcitriol (37, 48), alfacalcidol (38, 39, 51), and calcifediol (52), were used with different dosages in the RCT trials. In detail, vitamin D_3 was applied in 12 of the 19 retrieved trials, whose dosages ranged from 400 IU/day (40, 41) to 300,000 IU in a single oral dose (44). Vitamin D_2 was applied in 3 trials of the 19 selected studies at dosages ranging from 1,000 IU/day (56) to 100,000 IU/week (53), and calcitriol, alfacalcidol, and calcifediol were used in 6 trials of the 19 trials.

Study Outcomes

In separate experiments, different approaches for measuring muscle function were used. Twelve (36–41, 45, 47, 49, 53, 48, 54) trials used HGS as a parameter indicating muscle strength. Other measurement methods included back extensor strength (51), low limb muscle strength (56), and leg extensor strength (55). The TUG was used to measure the mobility of subjects in 11 trials (38, 39, 41, 45–47, 49, 50, 53, 55, 56), while the timed walk (40), gait speed (52), walking test (39), etc., were used as the indicator of mobility in the remaining 8 trials.

The authors of 12 studies concluded that vitamin D supplementation with or without calcium played no significant role in the muscle strength and/or mobility of subjects, while 7 studies drew the opposite conclusion.

TABLE 1 | Characteristics of included studies.

First author, year	Sample size (supplementation/ control)	Age (years)	Supplementation	Comparator	Supplementation duration	Presented data	Jadadscore
Apaydin, 2018 (44)	28/32	50–68	300,000 IU D_3/single oral dose	800 IU D_3/ day	3 months	Knee extension; knee flexion	1
Bischoff, 2003 (45)	62/60	63–99	800 IU D_3/day	None	3 months	HGS; TUG; knee flexion; knee extension	5
Bischoff-Ferrari, 2012 (46)	10/10	50–70	20 μg HyD/day; 140 μg HyD/week	800IU(D_3)/ per day; 5600IU(D_3)/ per week	4 months	TUG; knee flexion; knee extension; repeated sit-to-stand test;	4
Bislev, 2018 (47)	40/41	60–80	2,800 IU D_3/day	Placebo	3 months	HGS; TUG; elbow and knee extension flexion; chair raising test	4
Brunner, 2008 (40)	1,185/1,162	50–79	400 IU D_3/day	Placebo	60 months	HGS; chair stand test; time walk	4
Cangussu, 2015 (36)	80/80	50–65	1,000 IU D_3/day	Placebo	9 months	HGS; chair rising test	5
Cheng, 2018 (37)	75/66	58.2 ± 8.1	0.5 μg calcitriol/day	Placebo	3 months	HGS	5
Gao, 2015 (48)	101/109/251	63.44 ± 5.04	800 IU D_3/day; 0.25 μg calcitriol/day	None	24 months	HGS; chair rising test	1
Glendennig, 2012 (49)	353/333	>70	150,000 IU D_3/3 months	Placebo	9 months	HGS; TUG	4
Hansen, 2015 (50)	73/74/73	>60	800 IU D_3/day; 50,000 IU D_3/2 months	Placebo	12 months	TUG; five sit-to-stand test	5
Hara, 2013 (51)	50/44	55–75	1 μg alfacalcidol/day	Placebo	4 months	Back extensor strength	3
Janssen, 2010 (41)	36/34	>65	400 IU D_3/day	Placebo	6 months	HGS; TUG; knee extension strength; leg extension power	5
Meyer, 2015 (52)	10/10	50–70	20 μg calcifediol/day	800 IU D_3/ day	4 months	Gait speed; trunk sway	5
Mueangpaisarn, 2020 (53)	44/41	≥60	100,000 IU D_2/week	40,000 IU D_2/week	3 months	HGS; TUG	4
Setiati, 2018 (38)	46/42	≥60	0.5 μg alphacalcidol/ day	Placebo	3 months	HGS; TUG	5
Suebthawinkul, 2018 (54)	44/44	45–60	40,000 IU D_2/week	Placebo	3 months	HGS; BIA; muscle cross-section area	5
Uusi-Rasi, 2015 (55)	88/96/95/91	70–80	800 IU D_3/day; 800 IU D_3/day +exercise	Placebo; Placebo +exercise	24 months	TUG; leg extensor strength; chair stand time; normal walking speed	5
Verhaar, 2000 (39)	10/14	≥70	0.25 μg alphacalcidol/day*1 month; 0.5 μg alphacalcidol/ day*months	None	6 months	HGS; TUG; knee extension strength; walking test	1
Zhu, 2010 (56)	129/132	70–90	1,000 IU D_2/day	Placebo	12 months	TUG; low limb muscle strength	5

HGS, handgrip strength; TUG, timed up and go test; HyD, 25-hydroxyvitamin D_3; BIA, bioelectrical impedance analysis.

Meta-Analysis

It was challenging to extract and analyze the data uniformly and compare the results since the data on muscular strength and mobility presented in the trials were acquired using a range of assessment methodologies. Additionally, HGS and TUG were the results of the more uniform and published data included in the studies, so we chose HGS as an index to measure the muscle strength of subjects (the best performance of HGS was obtained after three repeated measurements of the standing participants, holding the assessment for at least 5 s during the test with an interval of 30 s between each evaluation), and TUG as the indicator of the mobility measurement for this present meta-analysis.

Handgrip Strength

The meta-analysis of HGS included 9 trials (36–41, 48, 49, 54) with 1,997 participants supplemented with vitamin D and 2,232 participants as the control group (vitamin D in low dosage or placebo). Vitamin D supplementation resulted in considerable improvements in HGS (WMD: 0.876 kg, 95% CI = 0.180 to 1.571, $P = 0.014$), according to the analysis and finding over the

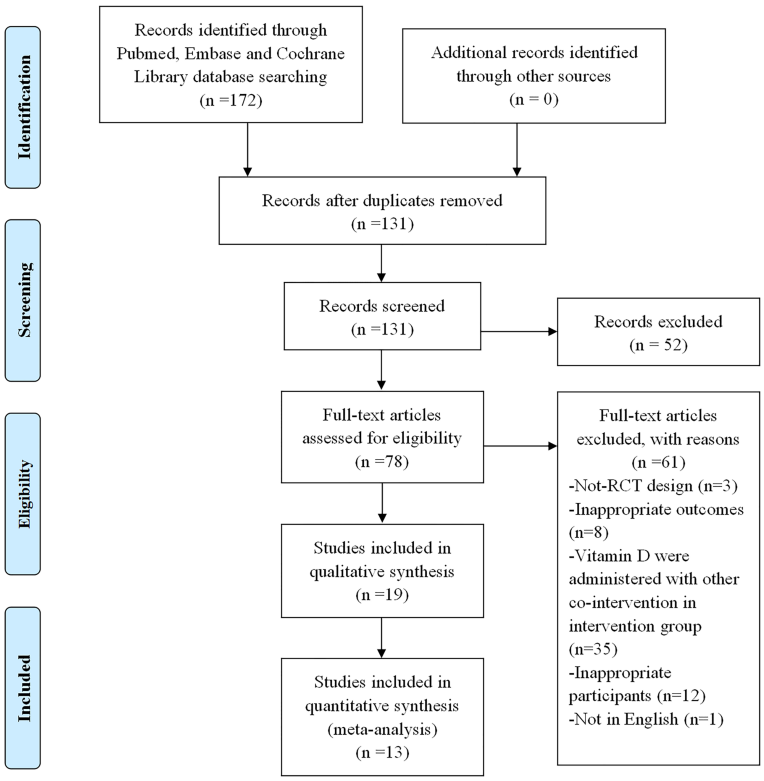

FIGURE 1 | Flowchart of literature search for selection of trials. The selection process of the included trials has been shown in this figure. RCT, randomized controlled trial.

random effects model. There was significant heterogeneity among studies (I^2 = 68.5%, P = 0.001) (**Figure 2**).

Timed Up and Go Test

The meta-analysis of TUG included 8 studies (38, 39, 41, 47, 49, 50, 55, 56) with 937 participants supplemented with vitamin D and 915 participants treated with placebo or a low dose of vitamin D. Using a random effects model, we discovered an insignificant decrease (0.044 s) in the TUG (95% CI = −0.979 to 0.892 s, P = 0.927) after vitamin D supplementation. Furthermore, the meta-analysis manifested a significant heterogeneity among the studies (I^2 = 95.0%, P = 0.000) (**Figure 3**).

Subgroup Analysis

We did the HGS and TUG subgroups analysis based on age, supplementation with calcium or not, vitamin D dosage (IU/day), supplementation duration (month), and baseline vitamin D level.

The scores of the heterogeneity of the HGS subgroups analysis were as follows: without calcium (I^2 = 50.8%, P = 0.107); vitamin D dosage ≥1,000 IU/day (I^2 = 47.0%, P = 0.152); supplementation duration <12 months (I^2 = 74.0%, P = 0.001); baseline vitamin D <75 nmol/L (30 ng/ml) (I^2 = 45.6%, P = 0.102) (**Table 2**).

Meanwhile, the scores of the heterogeneity of the TUG subgroups analysis were as follows: age >60 years old (I^2 = 16.7%, P = 0.308); with calcium (I^2 = 95.6%, P = 0.000); vitamin D dosage ≥1,000 IU/day (I^2 = 57.8%, P = 0.069); supplementation duration <12 months (I^2 = 76.1%, P = 0.002); baseline vitamin D >75 nmol/L (30 ng/ml) (I^2 = 16.9%, P = 0.307) (**Supplementary Table**).

Moreover, according to subgroup analysis, vitamin D supplementation substantially raised HGS when compared to baseline blood vitamin D levels >75 nmol/L (30 ng/ml) (WMD = 0.478 kg, 95% CI = −0.963 to 1.918, P = 0.003), without calcium (WMD = 1.931 kg, 95% CI = 0.166 to 3.697, P = 0.032) and subject to an age of more than 60 (WMD = 1.116 kg, 95% CI = 0.433 to 1.799, P = 0.001).

Publication Bias

Visual inspection of the funnel plot and Egger's linear regression test revealed no indication of publication bias in the meta-analysis of vitamin D supplementation on HGS: P = 0.047 and TUG: P = 0.954.

DISCUSSION

This meta-analysis aimed to see if vitamin D supplementation might enhance the muscular strength and mobility of postmenopausal women. The results of the meta-analysis of the 13 trials included revealed a significant effect of vitamin D

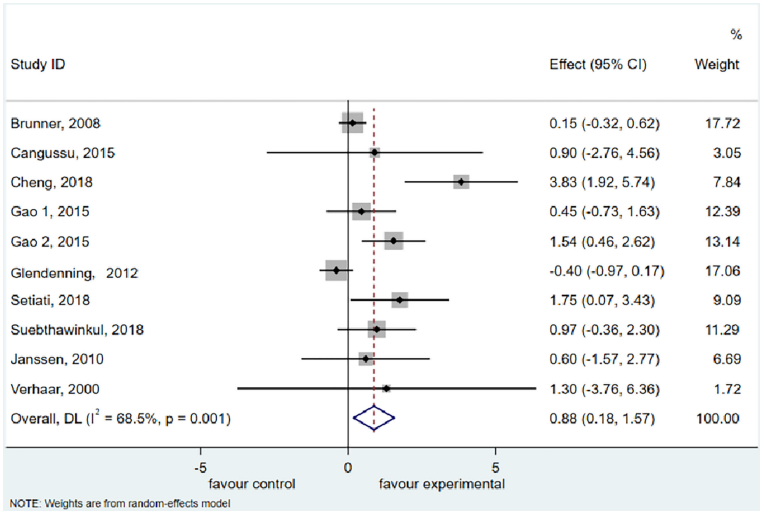

FIGURE 2 | Forest plot displaying the effect of vitamin D supplementation on hand grip strength (HGS) using a random effects model. One study reported results as two intervention groups received two different dosages of vitamin D (Gao 1 and Gao 2). CI, confidence interval.

supplementation on the HGS of postmenopausal women, but not on the TUG. Since the HGS refers to muscle strength while the TUG represents locomotory function, it is considered that vitamin D supplementation could be effective in improving muscle strength in postmenopausal women. Thus, we assume that vitamin D supplementation might first enhance the upper extremities, but it is difficult to improve the strength of the lower limb muscles, which are more used in stance and mobility.

Since the data for men and women were not presented separately, trials that included both males and postmenopausal women were eliminated. Trials for postmenopausal women with diabetes (34), Parkinson's disease (58), chronic kidney disease (35), or other special situations (59, 60) that might affect their mobility were also excluded. Moreover, some studies were considered inappropriate due to the use of combined vitamin D supplementation with other nutrients (61–65). All in all, 19 RCT trials were eventually included, and among them, 13 trials (36–41, 47–50, 54–56) were suitable for meta-analysis. Most of the studies were of medium to high methodological quality as assessed by the Jadad scale.

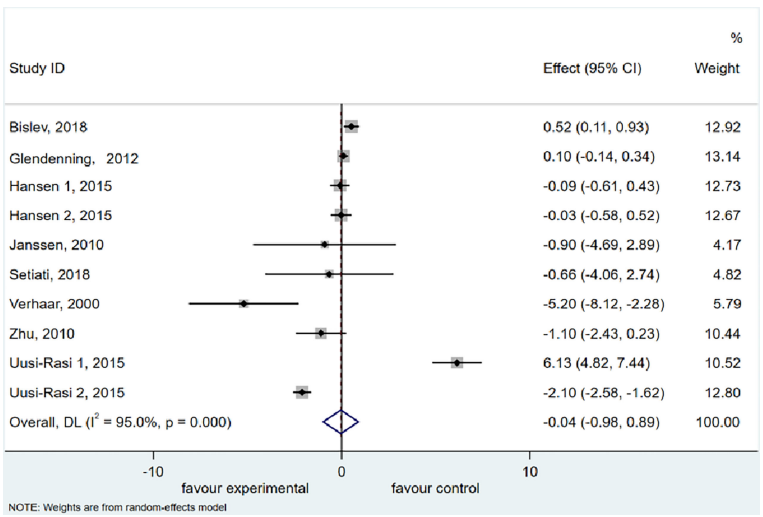

FIGURE 3 | Forest plot displaying the effect of vitamin D supplementation on timed up and go test (TUG) using a random effects model. One study reported results as two intervention groups received two different dose of vitamin D (Hansen 1 and Hansen 2). CI, confidence interval.

TABLE 2 | Subgroup analysis of HGS.

	Subtotal (n)	Number of studies (n)	WMD (95% CI)	*P*-value
Age				
>50	2,736	4	1.353 (–0.238; 2.944)	0.096
>60	870	4	1.116 (0.433; 1.799)	0.001
>70	623	2	–0.379 (–0.944; 0.186)	0.189
With calcium or not				
with calcium	3,816	6	0.478 (–0.165; 1.122)	0.145
without calcium	413	4	1.931 (0.166; 3.697)	0.032
Baseline serum vitamin D level				
<30 ng/ml	1,125	6	1.445 (0.486; 2.403)	0.527
>30 ng/ml	757	3	0.478 (–0.963; 1.918)	0.003
Vitamin D dosage (IU/day)				
<1,000	2,769	3	0.206 (–0.218; 0.630)	0.341
≥1,000	847	3	0.161 (–0.911; 1.234)	0.768
vitamin D analogs	613	4	2.118 (1.024; 3.213)	0
Supplementation duration				
>12	3,059	3	0.621 (–0.219; 1.461)	0.147
<12	1,170	7	1.193 (–0.090; 2.477)	0.068

WMD, weighted mean difference; CI, confidence interval.

Nonetheless, because the studies examined varied in most dimensions, caution should be exercised in determining whether the characteristics of the researched people are consistent. Different techniques for measuring muscle function have been reported by different investigators, and even when measuring comparable parameters, separate methods have been used in different trials, making it even more difficult to compare results directly. For instance, muscle strength was measured in different ways, such as HGS (36–41, 45, 47–49, 53, 54), low limb muscle strength (56), and knee extension strength (39, 41). We used HGS to measure muscular strength, which has recently been proposed as a long-term predictor of fracture and mortality in postmenopausal women (66), and TUG is viewed as an outcome of mobility. Based on the findings of the included trials, taking vitamin D supplements significantly improved the strength of postmenopausal women. The primary outcomes of the quantitative meta-analysis suggested that vitamin D supplementation improved HGS (based on 9 studies) but played an insignificant role in decreasing the time of the TUG (based on 8 RCT studies). As a result, we concluded that vitamin D supplementation had a favorable effect on improving muscular strength in postmenopausal women.

However, the emerging reviews illustrate controversial conclusions about the impact of vitamin D supplementation on muscle function. Tabrizi et al. (67) and Abshirini et al. (68) demonstrated that taking vitamin D supplementation had no effect on markers of muscle function such as HGS and TUG in postmenopausal women, whereas some RCTs suggested a positive effect of vitamin D supplementation on muscle function in postmenopausal women (69–71). In this meta-analysis, however, we found a significant increase in HGS with a non-existent decrease in TUG in postmenopausal women after taking vitamin D supplementation. We assumed that the types of vitamin D, the duration of the supplementation, and the dose of vitamin D might account for the inconsistent conclusions as shown in **Table 1**. Additionally, given that the included RCTs displayed a high degree of heterogeneity, we conducted a subgroup analysis to reveal the potential source of heterogeneity. Following the subgroup analysis, we found that vitamin D supplementation enhanced HGS in participants aged no less than 60 years old, with a baseline level of vitamin D greater than 75 nmol/L (30 ng/ml) and without calcium supplementation during the period of the clinical trial. However, vitamin D supplementation was not found to have a significant effect on TUG from the results of any subgroup.

This study is the first meta-analysis to assess the effects of vitamin D supplementation on muscular health in healthy postmenopausal women enrolled in RCT studies. The strengths of the study are manifest in the fact that the populations studied were healthy postmenopausal women, and that the intervention strategy emphasized vitamin D supplementation or its analogs. However, there are also limitations in this meta-analysis, such as that the stringency of our exclusion criteria resulted in a lack of availability of physical activity, nutritional status, etc., which have the potentially contribute to the lack of change in TUG. Additionally, we also detected substantial heterogeneity between the included trials due to the large number of studies included and the diversity seen across different supplementation techniques. In this meta-analysis, we likewise identified no dose–response effect, which is likely due to the variety of supplementation programs used in the included studies. Furthermore, the limited database we searched was another flaw in this review.

The Asian working group for sarcopenia: 2019 consensus updates on sarcopenia diagnosis and treatment, which were published in JAMDA in 2020, suggested that interventions for patients with sarcopenia should include vitamin D-containing nutritional supplementation in addition to resistance exercise (7). In this review, we could only verify that supplementing with vitamin D is positively associated with muscle strength. This could be explained by the singleness of the supplementation, which we focused on in our review. The supplementation included in this meta-analysis not only excluded interventions such as branched-chain amino acids, whey protein, and other nutritional supplements, but also excluded treatment with

resistance exercise, which is also considered an efficient means of intervention in the consensus.

Additionally, *in vitro* and *in vivo* experimental studies have demonstrated the beneficial effects of vitamin D supplementation on sarcopenia, which could be explained by the fact that vitamin D could bind to the VDR, which has been found in muscle tissue, myoblasts, and muscle satellite cells (25, 26). Moreover, the lack of vitamin D is suspected to cause muscle weakness by reducing the number and size of type II myofibers (72, 73), which are age-related fibers and the first to be recruited for balancing and preventing falls. Those facts might explain the association between circulating levels of 25(OH)D and muscle function in postmenopausal women (74). Thus, future studies that investigate the role of vitamin D supplementation on muscle should include an analysis of muscle composition. Furthermore, a recent study also reported an inverse relationship between skeletal muscle fat and circulating 25(OH)D levels in young women adults (75). Goodpaster et al. (76) and Liu et al. (77) have also found similar results that skeletal muscle attenuation is associated with the lipid content of skeletal muscle, which might thereby emphasize the significance of further research on skeletal muscle fat in postmenopausal women.

The findings of this systematic review and meta-analysis show that although vitamin D supplementation did not improve mobility, it did improve muscle strength, particularly in postmenopausal women over 60 years of age who are without calcium supplementation or whose baseline vitamin D is >75 nmol/L (30 ng/ml). These findings show that future trials should focus on determining the ideal dosage and duration and taking into account the several factors that may impair muscle performance, such as exercise, calcium consumption, frailty, a history of falls or fractures, and baseline vitamin D status, and the relationship between muscle function and/or strength with muscle composition.

DATA AVAILABILITY STATEMENT

The original contributions presented in the study are included in the article/**Supplementary Material**. Further inquiries can be directed to the corresponding author.

AUTHOR CONTRIBUTIONS

J-LZ designed and performed the research, analyzed data and wrote the paper. CP performed the research. M-SW designed and performed the research. W-XL performed the research, statistical analysis, and sample collection. Y-XG performed the research and sample collection. YZ designed and performed the research. All authors listed have made a substantial, direct, and intellectual contribution to the work and approved it for publication.

FUNDING

This study was supported in part by the National Natural Science Foundation of China (82074468), the Science and Technology Commission of Shanghai Municipality (21400760400), the Program of Shanghai Academic Research Leader (19XD1423800), and the Shanghai Collaborative Innovation Center of Industrial Transformation of Hospital TCM Preparation.

SUPPLEMENTARY MATERIAL

The Supplementary Material for this article can be found online at: https://www.frontiersin.org/articles/10.3389/fendo.2022.863448/full#supplementary-material

REFERENCES

1. Muir SW, Montero-Odasso M. Effect of Vitamin D Supplementation on Muscle Strength, Gait and Balance in Older Adults: A Systematic Review and Meta-Analysis. *J Am Geriatr Soc* (2011) 59:2291–300. doi: 10.1111/j.1532-5415.2011.03733.x
2. Kanis JA, Cooper C, Rizzoli R, Reginster JY, Scientific Advisory Board of the European Society for Clinical and Economic Aspects of Osteoporosis (ESCEO) and the Committees of Scientific Advisors and National Societies of the International Osteoporosis Foundation (IOF). European Guidance for the Diagnosis and Management of Osteoporosis in Postmenopausal Women. *Osteoporos Int* (2019) 30:3–44. doi: 10.1007/s00198-018-4704-5
3. Orsatti FL, Nahas EA, Nahas-Neto J, Orsatti CL, Marocolo M, Barbosa-Neto O, et al. Low Appendicular Muscle Mass Is Correlated With Femoral Neck Bone Mineral Density Loss in Postmenopausal Women. *BMC Musculoskelet Disord* (2011) 12:225. doi: 10.1186/1471-2474-12-225
4. Rizzoli R, Bischoff-Ferrari H, Dawson-Hughes B, Weaver C. Nutrition and Bone Health in Women After the Menopause. *Womens Health (Lond)* (2014) 10:599–608. doi: 10.2217/WHE.14.40
5. Yoo JI, Kim H, Ha YC, Kwon HB, Koo KH. Osteosarcopenia in Patients With Hip Fracture Is Related With High Mortality. *J Korean Med Sci* (2018) 33:e27. doi: 10.3346/jkms.2018.33.e27
6. Perez-Lopez FR, Chedraui P, Pilz S. Vitamin D Supplementation After the Menopause. *Ther Adv Endocrinol Metab* (2020) 11:2042018820931291. doi: 10.1177/2042018820931291
7. Chen LK, Woo J, Assantachai P, Auyeung TW, Chou MY, Iijima K, et al. Asian Working Group for Sarcopenia: 2019 Consensus Update on Sarcopenia Diagnosis and Treatment. *J Am Med Dir Assoc* (2020) 21:300–7.e2. doi: 10.1016/j.jamda.2019.12.012
8. Chen LK, Liu LK, Woo J, Assantachai P, Auyeung TW, Bahyah KS, et al. Sarcopenia in Asia: Consensus Report of the Asian Working Group for Sarcopenia. *J Am Med Dir Assoc* (2014) 15:95–101. doi: 10.1016/j.jamda.2013.11.025
9. Fielding RA, Vellas B, Evans WJ, Bhasin S, Morley JE, Newman AB, et al. Sarcopenia: An Undiagnosed Condition in Older Adults. Current Consensus Definition: Prevalence, Etiology, and Consequences. International Working Group on Sarcopenia. *J Am Med Dir Assoc* (2011) 12:249–56. doi: 10.1016/j.jamda.2011.01.003
10. Fuggle N, Shaw S, Dennison E, Cooper C. Sarcopenia. *Best Pract Res Clin Rheumatol* (2017) 31:218–42. doi: 10.1016/j.berh.2017.11.007
11. Bauer J, Morley JE, Schols AMWJ, Ferrucci L, Cruz-Jentoft AJ, Dent E, et al. Sarcopenia: A Time for Action. An SCWD Position Paper. *J Cachexia Sarcopenia Muscle* (2019) 10:956–61. doi: 10.1002/jcsm.12483
12. Abiri B, Vafa M. Nutrition and Sarcopenia: A Review of the Evidence of Nutritional Influences. *Crit Rev Food Sci Nutr* (2019) 59:1456–66. doi: 10.1080/10408398.2017.1412940
13. Cruz-Jentoft AJ, Kiesswetter E, Drey M, Sieber CC. Nutrition, Frailty, and Sarcopenia. *Aging Clin Exp Res* (2017) 29:43–8. doi: 10.1007/s40520-016-0709-0
14. Han W, Fan Z, Zhou M, Guo X, Yan W, Lu X, et al. Low 25-Hydroxyvitamin D Levels in Postmenopausal Female Patients With Benign Paroxysmal

Positional Vertigo. *Acta Otolaryngol* (2018) 138:443–6. doi: 10.1080/00016489.2017.1416168
15. Bilezikian JP. Primary Hyperparathyroidism. *J Clin Endocrinol Metab* (2018) 103:3993–4004. doi: 10.1210/jc.2018-01225
16. Tayem Y, Alotaibi R, Hozayen R, Hassan A. Therapeutic Regimens for Vitamin D Deficiency in Postmenopausal Women: A Systematic Review. *Prz Menopauzalny* (2019) 18:57–62. doi: 10.5114/pm.2019.84159
17. Agarwal K, Sharma M. Association of Hypovitaminosis D With Metabolic Syndrome in Postmenopausal Women. *J Obstet Gynaecol India* (2020) 70:184–8. doi: 10.1007/s13224-020-01314-8
18. Lips P, Hosking D, Lippuner K, Norquist JM, Wehren L, Maalouf G, et al. The Prevalence of Vitamin D Inadequacy Amongst Women With Osteoporosis: An International Epidemiological Investigation. *J Intern Med* (2006) 260:245–54. doi: 10.1111/j.1365-2796.2006.01685.x
19. Huang H, Guo J, Chen Q, Chen X, Yang Y, Zhang W, et al. The Synergistic Effects of Vitamin D and Estradiol Deficiency on Metabolic Syndrome in Chinese Postmenopausal Women. *Menopause* (2019) 26:1171–7. doi: 10.1097/GME.0000000000001370
20. Rinaldi I, Setiati S, Oemardi M, Aries W, Tamin TZ. Correlation Between Serum Vitamin D (25(OH)D) Concentration and Quadriceps Femoris Muscle Strength in Indonesian Elderly Women Living in Three Nursing Homes. *Acta Med Indones* (2007) 39:107–11.
21. Visser M, Deeg DJ, Lips P Longitudinal Aging Study Amsterdam. Low Vitamin D and High Parathyroid Hormone Levels as Determinants of Loss of Muscle Strength and Muscle Mass (Sarcopenia): The Longitudinal Aging Study Amsterdam. *J Clin Endocrinol Metab* (2003) 88:5766–72. doi: 10.1210/jc.2003-030604
22. Bischoff-Ferrari HA, Borchers M, Gudat F, Dürmüller U, Stähelin HB, Dick W. Vitamin D Receptor Expression in Human Muscle Tissue Decreases With Age. *J Bone Miner Res* (2004) 19:265–9. doi: 10.1359/jbmr.2004.19.2.265
23. Michael YL, Smit E, Seguin R, Curb JD, Phillips LS, Manson JE. Serum 25-Hydroxyvitamin D and Physical Performance in Postmenopausal Women. *J Womens Health (Larchmt)* (2011) 20:1603–8. doi: 10.1089/jwh.2010.2606
24. Holick MF, Binkley NC, Bischoff-Ferrari HA, Gordon CM, Hanley DA, Heaney RP, et al. Evaluation, Treatment, and Prevention of Vitamin D Deficiency: An Endocrine Society Clinical Practice Guideline. *J Clin Endocrinol Metab* (2011) 96:1911–30. doi: 10.1210/jc.2011-0385
25. Olsson K, Saini A, Strömberg A, Alam S, Lilja M, Rullman E, et al. Evidence for Vitamin D Receptor Expression and Direct Effects of 1alpha, 25(OH)2D3 in Human Skeletal Muscle Precursor Cells. *Endocrinology* (2016) 157:98–111. doi: 10.1210/en.2015-1685
26. Owens DJ, Sharples AP, Polydorou I, Alwan N, Donovan T, Tang J, et al. A Systems-Based Investigation Into Vitamin D and Skeletal Muscle Repair, Regeneration, and Hypertrophy. *Am J Physiol Endocrinol Metab* (2015) 309:E1019–31. doi: 10.1152/ajpendo.00375.2015
27. Tomlinson PB, Joseph C, Angioi M. Effects of Vitamin D Supplementation on Upper and Lower Body Muscle Strength Levels in Healthy Individuals. A Systematic Review With Meta-Analysis. *J Sci Med Sport* (2015) 18:575–80. doi: 10.1016/j.jsams.2014.07.022
28. Alemán-Mateo H, Macías L, Esparza-Romero J, Astiazaran-García H, Blancas AL. Physiological Effects Beyond the Significant Gain in Muscle Mass in Sarcopenic Elderly Men: Evidence From a Randomized Clinical Trial Using a Protein-Rich Food. *Clin Interv Aging* (2012) 7:225–34. doi: 10.2147/CIA.S32356
29. Moreira-Pfrimer LD, Pedrosa MA, Teixeira L, Lazaretti-Castro M. Treatment of Vitamin D Deficiency Increases Lower Limb Muscle Strength in Institutionalized Older People Independently of Regular Physical Activity: A Randomized Double-Blind Controlled Trial. *Ann Nutr Metab* (2009) 54:291–300. doi: 10.1159/000235874
30. Scanlon TC, Fragala MS, Stout JR, Emerson NS, Beyer KS, Oliveira LP, et al. Muscle Architecture and Strength: Adaptations to Short-Term Resistance Training in Older Adults. *Muscle Nerve* (2014) 49:584–92. doi: 10.1002/mus.23969
31. Jastrzebska M, Kaczmarczyk M, Jastrzebski Z. Effect of Vitamin D Supplementation on Training Adaptation in Well-Trained Soccer Players. *J Strength Cond Res* (2016) 30:2648–55. doi: 10.1519/JSC.0000000000001337
32. Shanely RA, Nieman DC, Knab AM, Gillitt ND, Meaney MP, Jin F, et al. Influence of Vitamin D Mushroom Powder Supplementation on Exercise-Induced Muscle Damage in Vitamin D Insufficient High School Athletes. *J Sports Sci* (2014) 32:670–9. doi: 10.1080/02640414.2013.847279
33. Todd JJ, McSorley EM, Pourshahidi LK, Madigan SM, Laird E, Healy M, et al. Vitamin D3 Supplementation Using an Oral Spray Solution Resolves Deficiency But has No Effect on VO2 Max in Gaelic Footballers: Results From a Randomised, Double-Blind, Placebo-Controlled Trial. *Eur J Nutr* (2017) 56:1577–87. doi: 10.1007/s00394-016-1202-4
34. Cavalcante R, Maia J, Mesquita P, Henrique R, Griz L, Bandeira MP, et al. The Effects of Intermittent Vitamin D3 Supplementation on Muscle Strength and Metabolic Parameters in Postmenopausal Women With Type 2 Diabetes: A Randomized Controlled Study. *Ther Adv Endocrinol Metab* (2015) 6:149–54. doi: 10.1177/2042018815578998
35. Gordon PL, Doyle JW, Johansen KL. Association of 1,25-Dihydroxyvitamin D Levels With Physical Performance and Thigh Muscle Cross-Sectional Area in Chronic Kidney Disease Stage 3 and 4. *J Ren Nutr* (2012) 22:423–33. doi: 10.1053/j.jrn.2011.10.006
36. Cangussu LM, Nahas-Neto J, Orsatti CL, Bueloni-Dias FN, Nahas EA. Effect of Vitamin D Supplementation Alone on Muscle Function in Postmenopausal Women: A Randomized, Double-Blind, Placebo-Controlled Clinical Trial. *Osteoporos Int* (2015) 26:2413–21. doi: 10.1007/s00198-015-3151-9
37. Cheng Q, Wu X, Du Y, Hong W, Tang W, Li H, et al. Levels of Serum Sclerostin, FGF-23, and Intact Parathyroid Hormone in Postmenopausal Women Treated With Calcitriol. *Clin Interv Aging* (2018) 13:2367–74. doi: 10.2147/CIA.S186199
38. Setiati S, Anugrahini, Fransiska JE, Tamin TZ, Istanti R. Combination of Alfacalcidol and Calcium Improved Handgrip Strength and Mobility Among Indonesian Older Women: A Randomized Controlled Trial. *Geriatr Gerontol Int* (2018) 18:434–40. doi: 10.1111/ggi.13201
39. Verhaar HJ, Samson MM, Jansen PA, de Vreede PL, Manten JW, Duursma SA. Muscle Strength, Functional Mobility and Vitamin D in Older Women. *Aging (Milano)* (2000) 12:455–60. doi: 10.1007/BF03339877
40. Brunner RL, Cochrane B, Jackson RD, Larson J, Lewis C, Limacher M, et al. Calcium, Vitamin D Supplementation, and Physical Function in the Women's Health Initiative. *J Am Diet Assoc* (2008) 108:1472–9. doi: 10.1016/j.jada.2008.06.432
41. Janssen HC, Samson MM, Verhaar HJ. Muscle Strength and Mobility in Vitamin D-Insufficient Female Geriatric Patients: A Randomized Controlled Trial on Vitamin D and Calcium Supplementation. *Aging Clin Exp Res* (2010) 22:78–84. doi: 10.1007/BF03324819
42. Liberati A, Altman DG, Tetzlaff J, Mulrow C, Gøtzsche PC, Ioannidis JP, et al. The PRISMA Statement for Reporting Systematic Reviews and Meta-Analyses of Studies That Evaluate Health Care Interventions: Explanation and Elaboration. *PloS Med* (2009) 6:e1000100. doi: 10.1371/journal.pmed.1000100
43. Jadad AR, Moore RA, Carroll D, Jenkinson C, Reynolds DJ, Gavaghan DJ, et al. Assessing the Quality of Reports of Randomized Clinical Trials: Is Blinding Necessary? *Control Clin Trials* (1996) 17:1–12. doi: 10.1016/0197-2456(95)00134-4
44. Apaydin M, Can AG, Kizilgul M, Beysel S, Kan S, Caliskan M, et al. The Effects of Single High-Dose or Daily Low-Dosage Oral Colecalciferol Treatment on Vitamin D Levels and Muscle Strength in Postmenopausal Women. *BMC Endocr Disord* (2018) 18:48. doi: 10.1186/s12902-018-0277-8
45. Bischoff HA, Stähelin HB, Dick W, Akos R, Knecht M, Salis C, et al. Effects of Vitamin D and Calcium Supplementation on Falls: A Randomized Controlled Trial. *J Bone Miner Res* (2003) 18:343–51. doi: 10.1359/jbmr.2003.18.2.343
46. Bischoff-Ferrari HA, Dawson-Hughes B, Stocklin E, et al. Oral Supplementation With 25(OH)D3 Versus Vitamin D3: Effects on 25(OH)D Levels, Lower Extremity Function, Blood Pressure, and Markers of Innate Immunity. *J Bone Miner Res* (2012) 27:160–9. doi: 10.1002/jbmr.551
47. Bislev LS, Langagergaard Rødbro L, Rolighed L, Sikjaer T, Rejnmark L. Effects of Vitamin D3 Supplementation on Muscle Strength, Mass, and Physical Performance in Women With Vitamin D Insufficiency: A Randomized Placebo-Controlled Trial. *Calcif Tissue Int* (2018) 103:483–93. doi: 10.1007/s00223-018-0443-z
48. Gao LH, Zhu WJ, Liu YJ, Gu JM, Zhang ZL, Wang O, et al. Physical Performance and Life Quality in Postmenopausal Women Supplemented With Vitamin D: A Two-Year Prospective Study. *Acta Pharmacol Sin* (2015) 36:1065–73. doi: 10.1038/aps.2015.55

49. Glendenning P, Zhu K, Inderjeeth C, Howat P, Lewis JR, Prince RL. Effects of Three-Monthly Oral 150,000 IU Cholecalciferol Supplementation on Falls, Mobility, and Muscle Strength in Older Postmenopausal Women: A Randomized Controlled Trial. *J Bone Miner Res* (2012) 27:170–6. doi: 10.1002/jbmr.524
50. Hansen KE, Johnson RE, Chambers KR, Johnson MG, Lemon CC, Vo TN, et al. Treatment of Vitamin D Insufficiency in Postmenopausal Women: A Randomized Clinical Trial. *JAMA Intern Med* (2015) 175:1612–21. doi: 10.1001/jamainternmed.2015.3874
51. Hara S, Kishimoto KN, Okuno H, Tanaka M, Saito H, Oizumi A, et al. Effects of Alfacalcidol on Back Extensor Strength Gained Through Back Extensor Exercise in Postmenopausal Women With Osteoporosis. *Am J Phys Med Rehabil* (2013) 92:101–10. doi: 10.1097/PHM.0b013e31826ed991
52. Meyer O, Dawson-Hughes B, Sidelnikov E, Egli A, Grob D, Staehelin HB, et al. Calcifediol Versus Vitamin D3 Effects on Gait Speed and Trunk Sway in Young Postmenopausal Women: A Double-Blind Randomized Controlled Trial. *Osteoporos Int* (2015) 26:373–81. doi: 10.1007/s00198-014-2949-1
53. Mueangpaisarn P, Chaiamnuay S. A Randomized Double-Blinded Placebo Controlled Trial of Ergocalciferol 40,000 Versus 100,000 IU Per Week for Vitamin D Inadequacy in Institutionalized Postmenopausal Women. *Aging Clin Exp Res* (2020) 32:41–8. doi: 10.1007/s40520-019-01151-4
54. Suebthawinkul C, Panyakhamlerd K, Yotnuengnit P, Suwan A, Chaiyasit N, Taechakraichana N. The Effect of Vitamin D2 Supplementation on Muscle Strength in Early Postmenopausal Women: A Randomized, Double-Blind, Placebo-Controlled Trial. *Climacteric* (2018) 21:491–7. doi: 10.1080/13697137.2018.1480600
55. Uusi-Rasi K, Patil R, Karinkanta S, Kannus P, Tokola K, Lamberg-Allardt C, et al. Exercise and Vitamin D in Fall Prevention Among Older Women: A Randomized Clinical Trial. *JAMA Intern Med* (2015) 175:703–11. doi: 10.1001/jamainternmed.2015.0225
56. Zhu K, Austin N, Devine A, Bruce D, Prince RL. A Randomized Controlled Trial of the Effects of Vitamin D on Muscle Strength and Mobility in Older Women With Vitamin D Insufficiency. *J Am Geriatr Soc* (2010) 58:2063–8. doi: 10.1111/j.1532-5415.2010.03142.x
57. Higgins JP, Thompson SG, Deeks JJ, Altman DG. Measuring Inconsistency in Meta-Analyses. *BMJ* (2003) 327:557–60. doi: 10.1136/bmj.327.7414.557
58. Barichella M, Cereda E, Pinelli G, Lorio L, Caroli D, Masiero I, et al. Protein, Leucine and Vitamin D Enhancing Rehabilitation (PROLEADER) in Patients With Parkinson's Disease or Parkinsonism: A Rct. *Movement Disord* (2018) 33:S199. doi: 10.1016/j.clnu.2018.06.2101
59. Ceglia L, Niramitmahapanya S, da SilvaMorais M, Rivas DA, Harris SS, Bischoff-Ferrari H, et al. A Randomized Study on the Effect of Vitamin D(3) Supplementation on Skeletal Muscle Morphology and Vitamin D Receptor Concentration in Older Women. *J Clin Endocrinol Metab* (2013) 98:E1927–35. doi: 10.1210/jc.2013-2820
60. Mason C, Tapsoba JD, Duggan C, Imayama I, Wang CY, Korde L, et al. Effects of Vitamin D3 Supplementation on Lean Mass, Muscle Strength, and Bone Mineral Density During Weight Loss: A Double-Blind Randomized Controlled Trial. *J Am Geriatr Soc* (2016) 64:769–78. doi: 10.1111/jgs.14049
61. Bauer JM, Mikušová L, Verlaan S, Bautmans I, Brandt K, Donini LM, et al. Safety and Tolerability of 6-Month Supplementation With a Vitamin D, Calcium and Leucine-Enriched Whey Protein Medical Nutrition Drink in Sarcopenic Older Adults. *Aging Clin Exp Res* (2020) 32:1501–14. doi: 10.1007/s40520-020-01519-x
62. Bell K, Snijders T, Zulyniak M, Kumbhare D, Heisz J, Parise G, et al. A Whey Protein-Based, Multi-Ingredient Supplement Independently Stimulates Gains in Lean Body Mass and Strength, and Enhances Exercise-Induced Adaptations in Older Men. *FASEB J* (2017) 31:139.4. doi: 10.1371/journal.pone.0181387
63. Bo Y, Liu C, Ji Z, Yang R, An Q, Zhang X, et al. A High Whey Protein, Vitamin D and E Supplement Preserves Muscle Mass, Strength, and Quality of Life in Sarcopenic Older Adults: A Double-Blind Randomized Controlled Trial. *Clin Nutr* (2019) 38:159–64. doi: 10.1016/j.clnu.2017.12.020
64. Chanet A, Verlaan S, Salles J, Giraudet C, Patrac V, Pidou V, et al. Supplementing Breakfast With a Vitamin D and Leucine-Enriched Whey Protein Medical Nutrition Drink Enhances Postprandial Muscle Protein Synthesis and Muscle Mass in Healthy Older Men. *J Nutr* (2017) 147:2262–71. doi: 10.3945/jn.117.252510
65. Verlaan S, Bauer JM, Sieber C, Cederholm T. Muscle Mass, Strength, and Function Effects of a High-Whey, Leucine-Enriched Nutritional Intervention in Sarcopenic Elderly in a Double Blind, Randomised Controlled Trial. *Eur Geriatric Med* (2014) 5:S75. doi: 10.1016/S1878-7649(14)70163-9
66. Rikkonen T, Poole K, Sirola J, Sund R, Honkanen R, Kröger H. Long-Term Effects of Functional Impairment on Fracture Risk and Mortality in Postmenopausal Women. *Osteoporos Int* (2018) 29:2111–20. doi: 10.1007/s00198-018-4588-4
67. Tabrizi R, Hallajzadeh J, Mirhosseini N, Lankarani KB, Maharlouei N, Akbari M, et al. The Effects of Vitamin D Supplementation on Muscle Function Among Postmenopausal Women: A Systematic Review and Meta-Analysis of Randomized Controlled Trials. *EXCLI J* (2019) 18:591–603. doi: 10.17179/excli2019-1386
68. Abshirini M, Mozaffari H, Kord-Varkaneh H, Omidian M, Kruger MC. The Effects of Vitamin D Supplementation on Muscle Strength and Mobility in Postmenopausal Women: A Systematic Review and Meta-Analysis of Randomised Controlled Trials. *J Hum Nutr dietetics Off J Br Diet Assoc* (2020) 33:207–21. doi: 10.1111/jhn.12717
69. Yin MT, Bucovsky M, Williams J, Brunjes D, RoyChoudhury A, Colon I, et al. Effect of Vitamin D-3 and Calcium Carbonate Supplementation on Muscle Strength in Postmenopausal Women Living With HIV. *Antiviral Ther* (2020) 25:411–8. doi: 10.3851/IMP3386
70. Kim BJ, Kwak MK, Lee SH, Koh JM. Lack of Association Between Vitamin D and Hand Grip Strength in Asians: A Nationwide Population-Based Study. *Calcified Tissue Int* (2019) 104:152–9. doi: 10.1007/s00223-018-0480-7
71. Bentes CM, Costa PB, Resende M, Netto C, Dias I, da Silveira ALB, et al. Effects of 12 Months of Vitamin D Supplementation on Physical Fitness Levels in Postmenopausal Women With Type 2 Diabetes. *J Funct Morphol Kinesiol* (2021) 6(4):87. doi: 10.3390/jfmk6040087
72. Lexell J, Henriksson-Larsén K, Winblad B, Sjöström M. Distribution of Different Fiber Types in Human Skeletal Muscles: Effects of Aging Studied in Whole Muscle Cross Sections. *Muscle Nerve* (1983) 6:588–95. doi: 10.1002/mus.880060809
73. Lexell J, Taylor CC, Sjöström M. What is the Cause of the Ageing Atrophy? *J Neurol Sci* (1988) 84:275–94. doi: 10.1016/0022-510X(88)90132-3
74. Bischoff-Ferrari HA, Dawson-Hughes B, Willett WC, Staehelin HB, Bazemore MG, Zee RY, et al. Effect of Vitamin D on Falls: A Meta-Analysis. *JAMA* (2004) 291:1999–2006. doi: 10.1001/jama.291.16.1999
75. Gilsanz V, Kremer A, Mo AO, Wren TA, Kremer R. Vitamin D Status and its Relation to Muscle Mass and Muscle Fat in Young Women. *J Clin Endocrinol Metab* (2010) 95:1595–601. doi: 10.1210/jc.2009-2309
76. Goodpaster BH, Kelley DE, Thaete FL, He J, Ross R. Skeletal Muscle Attenuation Determined by Computed Tomography Is Associated With Skeletal Muscle Lipid Content. *J Appl Physiol (1985)* (2000) 89:104–10. doi: 10.1152/jappl.2000.89.1.104
77. Liu M, Chino N, Ishihara T. Muscle Damage Progression in Duchenne Muscular Dystrophy Evaluated by a New Quantitative Computed Tomography Method. *Arch Phys Med Rehabil* (1993) 74:507–14. doi: 10.1016/0003-9993(93)90115-Q

Conflict of Interest: The authors declare that the research was conducted in the absence of any commercial or financial relationships that could be construed as a potential conflict of interest.

Advantages of publishing in Frontiers

OPEN ACCESS
Articles are free to read for greatest visibility and readership

FAST PUBLICATION
Around 90 days from submission to decision

HIGH QUALITY PEER-REVIEW
Rigorous, collaborative, and constructive peer-review

TRANSPARENT PEER-REVIEW
Editors and reviewers acknowledged by name on published articles

Frontiers
Avenue du Tribunal-Fédéral 34
1005 Lausanne | Switzerland

Visit us: www.frontiersin.org
Contact us: frontiersin.org/about/contact

REPRODUCIBILITY OF RESEARCH
Support open data and methods to enhance research reproducibility

DIGITAL PUBLISHING
Articles designed for optimal readership across devices

FOLLOW US
@frontiersin

IMPACT METRICS
Advanced article metrics track visibility across digital media

EXTENSIVE PROMOTION
Marketing and promotion of impactful research

LOOP RESEARCH NETWORK
Our network increases your article's readership